R. E. Abendroth, H. Pratanata, B. A. Singh

Final Report

Composite Precast Prestressed Concrete Bridge Slabs

August 1991

Sponsored by the Iowa Department of Transportation
Highway Division and the Highway Research Advisory Board

Iowa DOT Project HR-310
ISU-ERI-Ames-92028
ERI Project 3052

Department of Civil and Construction Engineering
Engineering Research Institute
Iowa State University, Ames

Iowa Department of Transportation

report

College of Engineering
Iowa State University

R. E. Abendroth, H. Pratanata, B. A. Singh

Composite Precast Prestressed Concrete Bridge Slabs

Sponsored by the Iowa Department of Transportation
Highway Division and the Highway Research Advisory Board

Iowa DOT Project HR-310
ISU-ERI-Ames-92028
ERI Project 3052

engineering research institute
iowa state university

LIST OF FIGURES

LIST OF TABLES

ABSTRACT

Precast prestressed concrete panels have been used as subdecks in bridge construction in Iowa and other states. To investigate the performance of these types of composite slabs at locations adjacent to abutment and pier diaphragms in skewed bridges, a research project which involved surveys of design agencies and precast producers, field inspections of existing bridges, analytical studies, and experimental testing was conducted.

The survey results from the design agencies and panel producers showed that standardization of precast panel construction would be desirable, that additional inspections at the precast plant and at the bridge site would be beneficial, and that some form of economical study should be undertaken to determine actual cost savings associated with composite slab construction.

Three bridges in Hardin County, Iowa were inspected to observe general geometric relationships, construction details, and to note the visual condition of the bridges. Hairline cracks beneath several of the prestressing strands in many of the precast panels were observed, and a slight discoloration of the concrete was seen beneath most of the strands. Also, some rust staining was visible at isolated locations on several panels. Based on the findings of these inspections, future inspections are recommended to monitor the condition of these and other bridges constructed with precast panel subdecks.

Five full-scale composite slab specimens were constructed in the Structural Engineering Laboratory at Iowa State University. One specimen modeled bridge deck conditions which are not adjacent to abutment or pier diaphragms, and the other four specimens represented the geometric conditions which occur for skewed diaphragms of 0, 15, 30, and 40 degrees. The specimens were subjected to wheel loads of service and factored level magnitudes at many locations on the slab surface and to concentrated loads which produced failure of the composite slab. The measured slab deflections and bending strains at both service and factored load levels compared reasonably well with the results predicted by simplified finite element analyses of the specimens. To analytically

evaluate the nominal strength for a composite slab specimen, yield-line and punching shear theories were applied. Yield-line limit loads were computed using the crack patterns generated during an ultimate strength test. In most cases, these analyses indicated that the failure mode was not flexural. Since the punching shear limit loads in most instances were close to the failure loads, and since the failure surfaces immediately adjacent to the wheel load footprint appeared to be a truncated prism shape, the probable failure mode for all of the specimens was punching shear.

The development lengths for the prestressing strands in the rectangular and trapezoidal shaped panels was qualitatively investigated by monitoring strand slippage at the ends of selected prestressing strands. The initial strand transfer length was established experimentally by monitoring concrete strains during strand detensioning, and this length was verified analytically by a finite element analysis. Even though the computed strand embedment lengths in the panels were not sufficient to fully develop the ultimate strand stress, sufficient slab strength existed.

Composite behavior for the slab specimens was evaluated by monitoring slippage between a panel and the topping slab and by computation of the difference in the flexural strains between the top of the precast panel and the underside of the topping slab at various locations. Prior to the failure of a composite slab specimen, a localized loss of composite behavior was detected.

The static load strength performance of the composite slab specimens significantly exceeded the design load requirements. Even with skew angles of up to 40 degrees, the nominal strength of the slabs did not appear to be affected when the ultimate strength test load was positioned on the portion of each slab containing the trapezoidal-shaped panel. At service and factored level loads, the joint between precast panels did not appear to influence the load distribution along the length of the specimens. Based on the static load strength of the composite slab specimens, the continued use of precast panels as subdecks in bridge deck construction is recommended.

NOMENCLATURE

A_c tributary cross-sectional area of the concrete for each prestressing strand

A_s^* cross-sectional area of a prestressing strand

B bond modulus for the elastic portion of the bond stresses (recommended value of 300 psi/in.)

b width of the rectangular cross section for a prestressed member

b_o perimeter of the critical vertical shear section for punching shear strength

b_1 short dimension for the load footprint

b_2 long dimension for the load footprint

CR_c prestress loss due to concrete creep

CR_s prestress loss due to strand relaxation

D nominal diameter of the prestressing strands

d effective depth for a non-prestressed reinforced concrete member

d_p effective depth from the compression face of the cross section to the centroid of the prestressing steel

E_c modulus of elasticity of the concrete

E_{ci} modulus of elasticity of the concrete when the prestress force is applied to the concrete section

E_{cp} modulus of elasticity of the concrete in a precast panel

E_s modulus of elasticity of the prestressing strands

ES prestress loss due to elastic shortening

f'_c concrete compressive strength at 28 days

f_{cds} concrete stress at the centroid of the tendons caused by the superimposed permanent dead loads which are applied to the section

f'_{ci} concrete compressive strength when the prestress force is applied to the concrete section

f_{cir} net compressive stress at the centroid of the tendons immediately after detensioning of the strands

f_r modulus of rupture strength of the concrete

f'_s ultimate strength of the prestressing strands

f_{se} effective strand prestress

f_{si} initial strand prestress

f^*_{su} strand stress at the nominal flexural strength of the member

F.S. factor of safety

g_i dimensions to yield-line intersection points (i=1,13)

L_d strand development length

L_{fb} strand flexural bond length

L_t strand transfer length

L_{ti} initial strand transfer length

ℓ precast panel span

ℓ_x strand embedment length from the end of the prestressing strand to the midspan of the precast deck panel

L.F. load factor

$M\ell_{nn}$ longitudinal nominal negative moment strength of the composite slab

$M\ell_{np}$ longitudinal nominal positive moment strength of the composite slab

M_{tnn} transverse nominal negative moment strength of the composite slab

M_{tnp} transverse nominal positive moment strength of the composite slab

P_e maximum elastic load

P_{cr} load at which the first crack was observed on the top surface of the composite slab

P_{is} load at which interface-slip was detected

P_{ism} miminum P_{is} load

P_n nominal limit load for yield-line analysis

P_{ss} load at which strand-slip was detected

P_{ssm} minimum P_{ss} load

P_{ts} load at which topping slab-slip was detected

P_{tsm} minimum P_{ts} load

P_u ultimate experimental load

P_w HS-20 AASHTO wheel load including 30 percent impact (20.8 kips)

$P_{0.1}$ load corresponding to a deflection equal to 0.10 in.

RH mean ambient relative humidity, expressed in percent

SH prestress loss due to concrete shrinkage

S_x analytical transverse stress at the extreme fibers of the slab

S_y analytical longitudinal stress at the extreme fibers of the slab

s prestressing strand spacing

t composite slab thickness

t_p precast panel thickness

x_{1G}, x_{3G} x_{6G}, x_{7G} x_{9G} x-axis dimensional parameters for yield-line analysis of Pattern G

x_2 x-axis dimensional parameter for yield-line analysis

y_1, y_2 y-axis dimensional parameters for yield-line analysis

y_{1G}, y_{3G} y_{6G}, y_{7G} y_{9G} y-axis dimensional parameters for yield-line analysis of Pattern G

U_d plastic bond stress along the plastic zone of the strand flexural bond length

U'_d non-dimensionalized bond stress along the plastic portion of the strand flexural bond length (recommended value of 1.32 for uncoated strands)

U_t plastic bond stress along the plastic zone of the strand transfer length

U'_t non-dimensionalized bond stress along the plastic portion of the strand transfer length (recommended value of 6.7 for uncoated 7-wire strands)

V_{nc} nominal punching shear strength of the concrete

α longitudinal span for a two-way slab

β transverse span for a two-way slab

β_c ratio of the long dimension to the short dimension of the loaded rectangular area

Δ_e maximum elastic deflection (deflection at the load P_e)

Δ_u deflection at the nominal strength of the slab (deflection at the load P_u)

ε_{cd} precast panel strain induced by the dead loads

ε_{cp} precast panel strain induced by the prestressing strands

ε_{cr} modulus of rupture strain

ε_t maximum panel tensile strain

ρ^* prestressing steel reinforcment ratio

1. INTRODUCTION

1.1. Background and Previous Research

Precast prestressed concrete panels have been used as permanent formwork in bridge deck construction on secondary roads in Iowa, and on both secondary and primary roads in other states. The panels are fabricated to span between the bridge girders and to serve as a permanent form for a poured topping slab. Initially, the panels support the weight of the construction loads, reinforcing bars, and the wet weight of the topping slab. After the topping concrete has cured, both the panels and topping slab become composite to resist the applied live loads. When panels are used, the bottom layer of reinforcement in both the transverse and longitudinal directions that is present in a conventional full-depth reinforced concrete bridge deck is eliminated.

Previous research on these slab systems has involved various aspects of behavior and performance of rectangular shaped precast panels at locations removed from abutment or pier diaphragms. In 1975, Barker [4] presented an overview of research findings involving precast prestressed panel forms in bridge deck construction. During that same year, Kluge and Sawyer [24] performed a feasibility study on using composite decks for slab and girder bridges. They concluded that panels could be used as a composite part of the bridge decks.

Jones and Furr [19] examined prestress strand development length. They also studied the effects of cyclic loading on the development length for strands and panel stiffness. Twenty panels, utilizing two lengths of 68 in. and 108 in., two different sizes of strand, and either light- or normal-weight concrete types were considered. The strands, which were released gradually during detensioning of the panels, were clean and rust free. Test results showed that an average of 22 in. of development length was required for 3/8 in.-diameter, 7-wire strands with the initial stress of 162 ksi. They concluded that the type of concrete used has little effect on the development length. Cyclic loading was found to have negligible effect on strand development length and panel stiffness.

The influence of concrete strength, diameter of strand and effect of time on transfer length of strands in prestressed panels were studied by Kaar, LaFraugh and Mass [22]. They concluded that an initial concrete strength of 5,500 psi or more at the time of detensioning prestressing strands has little influence on the transfer length of clean seven-wire strands of up to and including 1/2 in. diameter. Also, the average increase in transfer length over a period of one year following prestress transfer was about 6% for all sizes of strand tested.

A new equation for transfer and development lengths which accounts for the effects of strand size, initial prestress and concrete type was proposed by Zia and Mostafa [34] based on their literature survey. Those equations differ from equations in the ACI Specification [2] Sec. 12.9.1. and from the AASHTO Specification [1] Eq. (9-32), which are based on Kaar and Hanson's research [21].

The development length for prestressed strands has recently become a subject of controversy [30]. In October of 1988, the Federal Highway Administration (FHWA) issued a memorandum [16] to the Regional Federal Highway Administrators regarding application of revised multiplication factors for the AASHTO development length equation and limitations on strand diameters that were to be applied for federally funded projects. This memorandum revised a previous FHWA directive which had placed even higher safety factors on strand development lengths. The October 1988 memorandum specified that:

"(1) The use of 0.6 inch diameter strand in a pretensioned application shall not be allowed;

(2) Minimum strand spacing (center-to-center of strand) will be four times the nominal strand diameter;

(3) Development length for all strand sizes up to and including 9/16 inch special strand shall be determined as 1.6 times AASHTO equation 9-32; and,

(4) Where strand is debonded (blanketed) at the end of a member, and tension at service load is allowed in the precompressed tensile zone, the development length shall be determined as 2.0 times AASHTO equation 9-32, as currently required by AASHTO article 9.27.3.

Exceptions to the above criteria are as follows:

(1) Development length for prestressed piling subjected to flexural loading shall be determined as indicated above. Development length for embedded piling not subjected to flexural loading shall be determined as per AASHTO equation 9-32, and the use of 0.6 inch strand will be allowed.

(2) Development length for pretensioned precast sub-deck panels or precast pretensioned voided deck plank, shall be determined as outlined above, or alternatively, by utilizing AASHTO equation 9-32 for development length and designing and tensioning on the basis of a guaranteed ultimate tensile strength (GUTS) of 250 ksi and release of prestress at 70 percent of GUTS regardless of the type of strand used (i.e., 250 or 270 ksi strand)."

An article by Lane [25] states that the FHWA's actions were prompted by the fact that the 270 ksi, low-relaxation strands which are now commonly used in construction are not the same type of strands (250 ksi, stress-relieved) which were used in the research projects that lead to the development of the AASHTO development length equation (AASHTO Eq. 9-32). Recent work by Cousins, Johnston, and Zia [13] has shown that the required development length for 270 ksi low-relaxation strands is actually greater than the length predicted by AASHTO Eq. 9-32. According to Lane [25], research on strand development length are currently under investigation by the FHWA, several universities, and the Prestressed Concrete Institute (PCI).

Jones and Furr [20] also studied three existing bridges which are located in Grayson County, Texas. The panels used in those bridges were 6 ft- 9 in. long, varied in width from 1 ft- 5 in. to 5 ft- 2 in., and were 3 in. thick. The study included mapping of crack patterns in the top of the cast-in-place deck, soundings to detect potential delamination between the precast panel and the topping slab, corings and load tests. They recommended that the width of the panels for future bridge construction should be greater than 5 ft- 2 in.

Barnoff and Rainey [5] examined composite behavior between precast panels and topping slabs with and without mechanical shear connector at the interface betwen the two slab elements. Also, various configurations of the longitudinal panel joints perpendicular to the bridge span were tested to compare deck behaviors. They noted that a scored surface on the planks was sufficient to

develop composite action between panel and topping slab, and that all joint configurations behaved similarly in load transfer characteristics.

Testing of a full-scale, two span, non-skewed experimental bridge containing four deck forming methods was conducted by Barnoff et al [6]. The first span involved a conventional cast-in-place slab constructed with removable wood forms for one-half of the span and with permanent steel forms on the other half of the span. The second span involved precast prestressed concrete panels and a cast-in-place reinforced concrete topping slab. The deck panels for one-half of the span had plain butt joints between adjacent panels, while the panels on the remainder of the second span had keyed joints between adjacent panels. The bridge deck, which was supported by precast prestressed concrete girders, was part of a pavement test track. Over one million cycles of an equivalent 18-kip axle load were applied by driving a five-axled vehicle across the bridge at about 45 miles per hour. Other loads included the standard HS20 load produced by an FHWA test vehicle and progressive overloads applied by a trailer. The precast panels, which were 3 in.-thick, 4 ft.-wide, and 6 ft.-2 in. long were reinforced with 11-7/16 in. diameter, 270 ksi, prestressing strands and one layer of 6 x 12 - 3/3 WWF. The spacing of the strands was not uniform across the panel width, and the strands extended beyond the ends of the panels by 6 in. A 4 1/2 in.-thick, reinforced concrete topping slab was cast over the precst panels. Some of the conclusions relating to the precast panels, which were formulated by Barnoff et al., were as follows:

- Composite behavior between the panels and the topping slab can be achieved with scoring the top surface of the panels.
- The type of joint between adjacent panels did not affect behavior, and the longitudinal wheel load distribution was not affected by the panel joints.
- The bridge deck can be assumed to be continuous across the girders.
- A 6-in. strand extension was adequate to anchor the panels to the topping slab and to provide continuity across the girders.

- Composite panel and slab decks are more flexible than conventional bridge decks.
- The composite deck possesses significantly more strength than design calculations indicate.
- A diagonal tension failure of the bridge deck constructed with precast panels occurred at a 60 kip wheel load on tandem axles spaced at 4 ft. on center.

Bieschke and Klingner [7,23] conducted an experimental test of a full-scale bridge with a series of static and fatigue loads. The north half of the single span bridge contained panels having prestressing strand extensions beyond the panel ends. The south half of the bridge span contained panels without any prestressing strand extensions. They concluded that panels without prestressing strand extensions performed similar to those panels having strand extensions.

Buckner and Turner [8,9] examined the performance of precast panels which spanned between bridge substructure elements. The length and width of the panels were 20 ft- 6 in. and 3 ft- 5 1/2 in., respectively. The thickness of the panels varied from 5 1/2 to 10 in. These researchers presented a design procedure for full span precast panels based on the results of their study.

The effect of deck cracking on slab behavior of a specific composite deck bridge has been investigated by Callis, Fagundo and Hays Jr. [10,17]. Field testing of the Peace River Bridge, constructed using 8 ft span panels, was undertaken to determine the structural adequacy and composite behavior of the deck. Also, panels left over from the construction of the bridge were tested in the laboratory using cyclic loads to determine the fatigue shear strength. The shear stresses in the deck were substantially higher than those associated with a conventional bridge deck. The investigators raised serious doubts about the structural adequacy of the bridge due to observed corrosion of the reinforcement in the top of the bridge deck and of the prestressing strands in the panels.

Another experimental field and laboratory testing program involving composite, precast panel subdecks was conducted by Fagundo et al. [14]. These researchers studied the load versus deflection behavior of bridge decks constructed with panels, which were supported on fiberboard as the

permanent bearing material, of bridge decks constructed with panels having strand extensions and supported on a grout bed, and of bridge decks constructed using a conventional cast-in-place slab. Two of their conclusions were that solid bearing for the precast panels and the presence of strand extensions appeared to have improved the performance of the bridge deck.

Ross Bryan Associates, Inc. has presented recommendations [31] on the design, production, handling and shipping, and erection of the panels. A design example using the AASHTO Specifications and several design aids were included in their report.

A recent paper (1990) by Fang et al. [15] describes arching action in bridge decks constructed as conventional full-depth, cast-in-place slabs and as composite slabs involving precast, prestressed concrete panels. Their research included testing of a 40 ft.-span, steel girder bridge. The bridge deck contained the two slab types. The composite slab portion of the deck had 4 in.-thick by 6 ft.-6 in. wide by either 7 or 8 ft.-long prestressed panels, reinforced with 3/8 in. diameter, 270 ksi, 7-wire, stress-relieved prestressing strands. A 3 1/2 in.-thick reinforced concrete topping slab was cast over the panels. Some of the conclusions formulated by Fang et al are:

- The failure mechanisms was punching shear for both a single and tandem wheel load arrangement. The flexural strength for the composite decks was not reached during the load tests, as correctly predicted by yield-line analyses.
- The experimental testing revealed that the bridge deck constructed with precast panels was stronger, stiffer and more crack resistant than the full-depth, cast-in-place slab.

To the authors' knowledge, no studies have been undertaken involving the behavior of the precast, prestressed panels close to abutment or pier diaphragms on non-skewed or skewed bridges.

1.2. Objectives

This report addresses the research performed to evaluate the behavior of composite, bridge deck slabs at locations not adjacent to and adjacent to abutment or pier diaphragms on both non-skewed and skewed bridges. The composite behavior of the precast panels was investigated by

considering five panel configurations, resembling a portion of a bridge deck at various locations. The performance of the deck system was obtained by evaluation of the following items:

1. Transverse strain and displacement distributions along panel length and specimen length.
2. The effect of the longitudinal panel joint on the vertical load transfer between panels.
3. Failure mechanism of the specimens compared to yield-line and punching shear theories.
4. Panel bearing condition of the specimens.
5. Composite behavior of the panel and topping slab.
6. Transfer and flexural bond lengths of the prestressing strands.

1.3. Scope

The research involved four tasks. Task 1 consisted of a review of the literature and surveys of design agencies and panel producers. Field investigations of three bridges constructed with precast panel subdecks in Iowa were contained in Task 2. Task 3 involved an extensive experimental testing program of full-scale specimens, and analytical investigations were contained in Task 4.

2. QUESTIONNAIRES

2.1. Design Agency Questionnaire

A questionnaire was distributed to the 50 state departments of transportation, the District of Columbia, tollway authorities, two United States provinces, and eight Canadian provinces. This survey addressed topics related to general bridge geometry and conditions, general panel geometry and conditions, panel bearing details, prestressing strand description and conditions, design criteria, economy, experiences with panel usage, panel details and specifications. The complete results for this survey are given in Appendix A.

Sixty-nine out of 121 questionnaires that were sent to the design agencies were returned. Twenty-nine of those agencies which returned the survey, or about 42 percent, stated that they allow or have allowed the use of precast panels in bridge deck construction. Many of the remaining 40 design agencies, which have not specified precast panels, provided reasons for not using the subdecks. Concerns about bridge deck and panel performance, economy of panel useage, lack of demand for the product, the AASHTO Specification not providing criteria for composite slab design, and cautions from FHWA Region 10 regarding the serviceability of decks constructed with panels were expressed by design agencies. Twelve design agencies, which had previously permitted precast panel usage, now prohibit or discontinued the use of the subdecks. Some of the reasons for the change in design philosophy included: concerns about panel quality control, occurrence of reflective cracking in the topping slabs, questions about economic benefits with panel-slab systems, completion of an experimental program, and discontinued use on steel girder bridges.

Some of the results from the questionnaire are given in Table 2.1. The number in the parentheses represents the number of design agencies having that particular answer. The total of the responses to a given question may not equal 29, since multiple responses may have been given or the question may have been skipped by some of the respondents. Sixteen out of the 29 design agencies, who at some time permitted the use of prestressed concrete panels, are currently allowing

Table 2.1. Selected survey results from design agencies

1. Is your state or agency currently using or specifying panels for bridge deck construction?

   (16) Yes (13) No

2. What type of panel support is provided for typical panels spanning perpendicular to the bridge span?

   (1) Panels are not used to span in this direction
   (16) Precast prestressed concrete girders only
   (3) Steel girders only
   (9) Either precast concrete or steel girders
   (3) Other

3. Panel construction at skewed abutment or pier locations:

   (8) Panels not used at these locations
   (4) Panels sawn to match the skew only
   (2) Panels cast to match the skew only
   (12) Panels sawn or cast to match the skew
   (4) Other

4. Maximum panel width used:

(3) Not specified	(5) 4 ft.	(0) 6 ft.
(18) 8 ft.	(0) 10 ft.	(4) Other

5. Minimum panel thickness used:

(1) Not specified	(4) 2 1/2 in.	(7) 3 in.
(11) 3 1/2 in.	(3) 4 in.	(1) Other

6. Total diameter of the strand that is used most often:

(0) 1/4 in.	(23) 3/8 in.	(3) 1/2 in.
(0) 5/16 in.	(2) 7/16 in.	(0) Other

7. Are strand extensions used?

   (18) Always (2) Sometimes (8) Never

8. Is the bridge deck designed as a continuous span across the girders when panels are used?

   (24) Always (3) Sometimes (1) Never

Table 2.1. (Continued)

9. Is two-way plate action considered in the design of the deck when the panels are supported along three edges?

   (10) Three edge panel support not permitted (1) Yes (16) No

10. Is fatigue considered in the design of the deck when panels are used?

    (1) Yes (26) No

11. What are the approximate cost savings realized (including costs associated with construction time), when panels are used for subdecks on a typical bridge compared to a conventional full depth bridge deck?

    (18) Cost savings not known
    (6) No cost savings
    (3) \$0 - \$1.00/ft^2 of deck area
    (0) Over \$1.00/ft^2 of deck area

12. Which of the following items related to the performance of the panel and cast top slab bridge deck have your state or agency experienced more than just a few times or occasionally?

    (12) Can not really comment since we have not used panels often enough
    (7) Reflective cracks in the top of the cast-in-place slab above the transverse panel joints
    (7) Reflective cracks in the top of the cast-in-place slab above the longitudinal panel joints
    (3) Cracks in the top of the cast-in-place slab that are not above the panel joints
    (3) Cracks in the top of the cast-in-place slab at the abutment or pier diaphragm
    (3) Cracks in the bottom of the panels parallel to the panel span
    (1) Cracks in the bottom of the panels transverse to the panel span and near the midspan of the panel
    (1) Strand slippage
    (0) Some loss of composite behavior between panels and cast-in-place slab
    (3) Apparent loss of panel bearing at some locations
    (5) Other

13. How does your state or agency classify any problems associated with panel usage for bridge deck construction?

    (12) Can not really comment since we have not used panels often enough
    (1) Non-existent (7) Minor (6) Moderate (6) Significant
    (0) Major

14. Considering all aspects of manufacturing, transportation, erection, and performance of panels for bridge deck construction, how does your state or agency rate panel usage?

    (11) Can not really comment since we have not used panels often enough
    (1) Excellent (3) Very Good (7) Good (5) Fair (5) Poor

panel usage. Considering the bridge girders, 16, 3, and 9 agencies have specified that the panels are to be supported by precast concrete girders only, steel girders only, and either concrete or steel girders, respectively. Eight agencies have stated that they prohibit panels at skewed abutment or pier diaphragm locations. When non-rectangular panels are permitted, 4, 2, and 12 agencies specify that the panels may be sawn to match the skew only, cast to match the skew only, and either sawn or cast to match the skew, respectively.

A majority of the design agencies limit the maximum panel width to 8 ft. The panel thickness varies for the design agencies from a minimum of 2 1/2 in. thick to a maximum of 4 in. thick. The most common strand diameter is 3/8 in., and most agencies required strand extensions.

Regarding the behavior of the composite slab system, most agencies assume that the full-depth bridge deck acts as a continuous slab spanning between the bridge girders. However, the response by most of the design agencies which specify precast panels to the three questions in the survey which followed the continuity question, revealed that special or additional reinforcement is never provided across the girders, beyond the top layer of reinforcement specified for full-depth cast-in-place slabs. Evidently, the assumption made by the designers is that the concrete which is cast between the ends of the panels does not shrink away from the ends of the panels or cracks do not form within this concrete filler. The validity of this assumption may require additional verification, particularly when strand extensions may not be used, or when strand extensions are used but they do not overlap significantly.

When panels are used, 26 of the 27 agencies who specified panels do not consider fatigue in the design of the bridge deck. Also, two-way plate bending is considered only by one design agency and neglected by 16 agencies when panels are supported along three edges. Ten agencies do not permit panels to be supported along three edges.

The survey revealed that five design agencies have performed some form of an economical analysis to evaluate the advantages of using composite, precast panel slabs instead of a conventional

full-depth, reinforced concrete slab. When asked to place an approximate dollar value on any savings, all of the design agencies responded that the cost savings were either unknown or less than $1.00/ft^2 of the bridge deck area.

Each design agency was asked to classify any problems associated with precast panel usage for bridge deck construction. Twelve of the 29 agencies, which had specified panels, responded that they could not really comment on their experiences, since they had not used panels often enough. For those agencies that did reply, cracking in the top of the cast-in-place slab has been experienced by a significant number of design agencies, and several agencies noted cracking in the bottom surface of the precast panels and problems with panel bearing. However, no agency thought that major problems existed with the panels. Twelve agencies categorized problems as either moderate or significant, while 8 agencies classify problems as either non-existent or minor. Another question on the survey asked the respondent to rate panel usage, considering all aspects of manufacturing, transportation, erection, and performance of panels for bridge deck construction. Ten agencies gave panel usage only a fair or poor rating and 11 agencies gave the panels an excellent, very good, or good rating. Another 11 agencies stated that they could not really comment since they had not used panels often enough.

Each design agency was given the opportunity to provide additional comments related to any aspect of precast panel usage. Sixteen agencies provided comments which addressed topics of quality, economy, design limitations, maintenance, and specifications. Both positive and negative comments were expressed, with many agencies expressing caution by implying that evaluation of existing deck panel slabs will establish future use.

2.2. Precaster Questionnaire

Survey questionnaires were distributed to 192 precast prestressed concrete producers who are members of the Prestressed Concrete Institute. This questionnaire addressed topics related to the producers background, general bridge panel conditions and geometry, bridge panel bearing

details, prestressing strand conditions and description for bridge panels, design criteria, economy, inspection, experience with panel usage, and panel details and specifications. The complete results for this survey are given in Appendix B. Seventy-two out of 192 questionnaires that were sent to the precast manufacturers were returned. Twenty-seven of the precasters which returned the survey, or about 38 percent, stated that they have produced precast panels for bridges. Many of the remaining 45 precast concrete manufacturers, which do not produce precast panels, provided reasons for not casting subdecks. Some of the reasons included: no opportunity to bid a panel bridge project, precast panels are not cast by this producer, the department of transportation does not permit bridge deck panels, local preference exists for cast-in-place slabs, panel manufacturing is too hard to control and be profitable, and too many producers are in the market. Eight of the 27 companies which had produced precast panels no longer cast panel subdecks. When asked why panel production was discontinued, some of the reasons stated included: Usage by the state department of transportation has been prohibited, panel production is not economically feasible, casting tolerances required can not be realistically obtained, and panel cracking and poor quality control by some producers has caused panel use to decline.

Some of the results from the questionnaire that was sent to the manufacturers of precast, prestressed concrete panels are given in Table 2.2. The number in the parentheses represents the number of precast panel manufacturers having that particular answer. The total of the responses to a given question may not equal 27, since multiple responses may have been given or a question may have been skipped by some of the respondents. Twenty of the 27 precasters who have manufactured precast panels have provided panels or submitted a bid to provide panels for bridge projects within the last two years (1987 and 1988), which indicates that many designers and bridge contractors believe that precast panels provide a viable option for bridge deck construction. The treatment of the top surface of the precast panels to obtain composite behavior between the panels and the cast-in-place reinforced concrete slab varies amongst the panel producers. A raked finish

Table 2.2. Selected survey results from panel producers

1. Top slab roughness and projection (not including lifting hooks):

   (0) Smooth finish without bar projections
   (0) Smooth finish with U-shaped bars or dowels
   (3) Broom finish without bar projections
   (1) Broom finish with U-shaped bars or dowels
   (14) Raked finish without bar projections
   (17) Raked finish with U-shaped bars or dowels
   (2) Other

2. What is the direction of the raked depression with respect to the panel span?

   (1) Raked depression not used
   (6) Parallel to panel span only
   (17) Transverse to panel span only
   (1) Both parallel and transverse to the panel span
   (2) Diagonal to panel span
   (0) Other

3. Is additional steel provided in the panel ends to prevent splitting due to bond transfer:

   (8) Always (8) Sometimes (11) Never

4. Temporary bearing material used to support panels:

   (2) Temporary bearing material not used
   (3) Unknown
   (18) Fiberboard, neoprene, polystyrene, or similar material only
   (2) Mortar, grout or concrete bed only
   (2) Steel shims only
   (2) Other

5. What is the minimum length of permanent bearing parallel to the panel span?

   (3) Unknown (7) 1 1/2 in. (3) 2 1/2 in.
   (6) 1 in. (3) 2 in. (4) Other

6. What method is used to release the bridge panel prestressing strands?

   (20) Acetylene torches (2) Slow release of hydraulic pressure
   (6) Abrasive saw blades (0) Other
   (3) Wire (bolt) cutters

7. Does the state or agency for which your company is casting panels have a representative at your plant to observe strand detensioning, form stripping, and panel handling and storage?

   (1) Not their responsibility (19) Always (6) Sometimes (0) Never

8. Does your company send a representative to the bridge jobsite to inspect the panels after erection for cracks and proper bearing?

   (5) Not our responsibility (5) Always (12) Sometimes (4) Never

9. Which of the following items of panel damage has your company directly experienced more than just a few times or occasionally?

   (4) Can not really comment since we have not cast panels often enough
   (6) Have not experienced any problems
   (8) Broken corners
   (9) Spalled or chipped edges
   (9) Cracking parallel to strands along a significant portion of the panel length
   (10) Cracking parallel to strands near the ends of the panel only
   (2) Cracking transverse to the strands near panel midspan
   (3) Diagonal cracks across panel surface
   (1) Strand slippage
   (4) Skew panels are difficult to detension properly
   (1) Other

10. Which of the following casting techniques has your company established to minimize problems in panel fabrication?

   (4) Can not really comment since we have not cast panels often enough
   (4) Provide strand tie downs along prestress bed length
   (10) Clean out header strand slots after each casting
   (19) Allow for concrete preset prior to heat application for accelerated curing
   (11) Institute special strand cutting sequence
   (14) Provide steel headers
   (2) Allow strands to oxidize by exposure to the weather for a few days
   (2) Increase concrete release strength above minimum specified
   (4) Increase concrete ultimate strength above minimum specified
   (13) Provide a reinforcing bar transverse to the strands at panel ends
   (0) Apply compressed air when stripping panels
   (2) Cast panels inside a structure to avoid exposure to weather
   (1) Other

11. Considering all aspects of manufacturing, transportation, erection, and performance of panels for bridge deck construction, how does your company rate panel usage?

   (1) Can not really comment since we have not cast panels often enough
   (7) Excellent (7) Very Good (5) Good (3) Fair (2) Poor

is most common with the direction of the raking usually transverse to the panel span. U-shaped bars or dowels across the interface between the two slabs appears to be used about 50% of the time. To prevent splitting of the panels during strand release, some precasters place additional steel in the ends of the panels.

A large majority of the panel producers use a temporary panel bearing material that is somewhat compressible. The length of permanent bearing, measured parallel to the panel span, varied considerably amongst the precasters. Lengths of 1 or 1 1/2 in. were the most common.

Most of the panel producers use acetylene torches to release prestressing strands. Acetylene torches applied at a single point on a strand, abrasive saw blades, and wire cutters are all associated with quick strand release techniques. If the strands are heated along a portion of their length before final torch cutting, the release of the prestress force will not be as sudden. Two producers indicated that they release strands slowly by using hydraulic pressure.

The responses to the two inspection questions listed in Table 2.2 indicate that additional inspection by both design agencies and panel producers may be beneficial.

Experiences with panel usage were addressed by eight questions in the survey. Three of these questions along with the producers responses are given in Table 2.2. The four types of panel damage experienced by the most panel producers were broken corners, spalled or chipped edges, cracking parallel to strands along a significant portion of the panel length, and cracking parallel to the strands near the ends of the panel only. To help eliminate problems with panel manufacturing, a variety of production techniques have been employed by panel producers. The items which received the greatest number of responses were to clean out header strand slots after each casting, allow for concrete preset prior to heat application for accelerated curing, institute special strand cutting sequence, provide steel headers, and provide a reinforcing bar transverse to the strands at panel ends. The manufacturers were also asked to rate panel usage, considering all aspects of

manufacturing, transportation, erection, and performance. Five producers rated precast panel usage as fair or poor, while 19 manufacturers rated panel usage as either excellent, very good or good.

Each precaster had the opportunity to include any additional comments related to precast panel bridge deck construction. Several of these comments strongly address the differences of opinion that exists between inspectors from state departments of transportation and panel producers concerning quality control. For precast panels to become a more economical product, several producers mentioned that standardization of panel configurations and details will be necessary.

3. FIELD INSPECTIONS

3.1. Bridge Descriptions

On October 19, 1989 field inspections of three Iowa bridges located in Hardin County near Eldora, Iowa were performed. All three prestressed concrete girder bridges are on the farm to market system and involve water crossings. The first bridge inspected was Bridge No. 9066 that is located 900 ft. south of the east 1/4 corner of Section 8-87-19 in Eldora Township of Hardin County over the Iowa River. This bridge has a 30 ft. roadway width, three spans (72 ft.-5 in. 81 ft.-6 in., and 72 ft.-5 in.), and no skew. The horizontal alignment is straight and the vertical alignment is at a 0.5% grade. The second bridge inspected was Bridge No. 8401 that is located 140 ft. north of the southwest corner of Section 36-88-19 in Clay Township of Hardin County over Pine Creek. This bridge has a 28 ft. roadway width, a single 80 ft. span, and no skew. The horizontal alignment is straight and the vertical alignment is at a 0.375% grade. The third bridge inspected was Bridge No. 7022 that is located 1320 ft. south and 1320 ft. east center of Section 12-88-20 in Jackson Township of Hardin County over the Iowa River. This bridge has a 30 ft. roadway width, three spans (68 ft.-3 in., 77 ft.-6 in., and 68 ft.-3 in.), and a 30 deg. skew angle. The horizontal alignment is straight and the vertical alignment is on a curve having grades of $\pm$ 1.000%.

The precast prestressed concrete panels for these bridges were cast by Precast Concrete Operations, a Division of Wheeler Consolidated, Inc., Iowa Falls, Iowa. The panels which span between the prestressed girders and extend along the entire length of each bridge were cast during the months of June 1983, March 1983, and June 1982 for Bridge Nos. 9066, 8401, and 7022, respectively. All three bridges have the same type of details for the precast panels. The 2 1/2 in. thick by 8 ft. wide panels were set on 3/4 in. thick by 1 in. wide fiberboard strips to permit the concrete from the topping slab to flow under the panel ends for permanent bearing. The condition and extent of the concrete bearing could not be confirmed since the detail is hidden from view. At the abutment and pier diaphragms, the precast panels are supported along three edges. Steel

channel intermediate diaphragms are provided at approximately the girder midspan locations. These diaphragms are attached to the precast girder webs and do not support the precast panels.

3.2. Inspection Results

The condition of the precast prestressed concrete panels in each of the three bridges is essentially the same. The slope of the grade beneath each bridge, the height of the bridge, and the presence of the waterways prevented inspection of the underside of the panels within the center span and many panels within the end spans of the three span bridges (Bridge Nos. 9066 and 7022) and the panels within about the center third of the single span bridge (Bridge No. 8401). Many of the inspected panels for all three bridges have single and sometimes multiple hairline cracks running parallel to the panel span. These cracks, which are located within the center half of the affected panels, usually extend along the entire panel length and occur below prestress strands. Also, for all three bridges, most of the observed panels had a slight discoloration (darker gray color) beneath the strands. For Bridge No. 9066, rust discoloration on the underside of the panels within the bridge end spans was not observed. For bridge No. 8401, one panel located above the steel channel intermediate diaphragm along the west side of the bridge has rust strains about 3 in. long near the midspan of the panel. In addition, a diagonal crack at the southwest corner of the second panel from the south abutment along the west side of this bridge was observed. For Bridge No. 7022, several panels have rust discoloration about 6 in. to 12 in. long beneath strand locations. Two panels were observed to have significant rust staining. One of these panels, located along the north side of the bridge in the west end span, is the fourth panel from the west bridge abutment. The other panel with significant rust stains is the fourth panel from the east bridge abutment and is located along the south side of the bridge.

The top surface of the cast-in-place reinforced concrete slab for all bridges had been raked parallel to the panel span. The concrete deck on Bridge Nos. 9066, 8401, and 7022 was completely exposed, covered entirely by a sand and gravel layer, and partly covered by sand and gravel,

respectively. The grooves from the raking and the presence of the sand and gravel fill prevented the observation of any reflective cracking in the topping slab.

4. EXPERIMENTAL PROGRAM

4.1. Composite Slab Specimens

4.1.1. Geometric Conditions

An extensive experimental program which involved testing five full-scale composite slab specimens was conducted. These specimens represented different geometric configurations for a portion of a bridge deck.

Specimen No. 1 represented an interior deck condition with the composite slab simply supported at the ends of the panels as shown in Fig. 4.1. Four specimens were constructed to model a composite deck at locations adjacent to an abutment or pier diaphragm. At these locations, one of the precast panels within a specimen was supported along the two ends as well as along one longitudinal panel edge. Specimen Nos. 2, 3, 4, and 5 incorporated a bridge skew angle of 0, 15, 30, and 40 degrees, respectively, as shown in Figs. 4.2, 4.3, 4.4, and 4.5, respectively.

Each of the composite specimens contained two 2 1/2-in. thick, precast, prestressed concrete panels which had a reinforced concrete slab, approximately 5 1/2-in. thick, cast directly on the panels. Figure 4.6 shows a typical section for the composite slabs taken parallel to the panel span. The two concrete supports shown in the figure represent precast concrete bridge girders. To accommodate the geometrical configuration for the five specimens, eight concrete supports were constructed with appropriate angles at the ends to account for the required skew angles, when the supports were assembled in various U-shaped patterns (Figs. 4.1-4.5). The concrete supports forming the bottom of the U-shape represented an abutment or pier diaphragm in the modeled bridge deck construction. All joints between the concrete support segments were located to prevent matching the joint between the two precast panels in a given specimen. The 6′-6" clear span between the faces of the concrete supports matched the maximum clear span permitted when precast panels are used by the Iowa Department of Transportation.

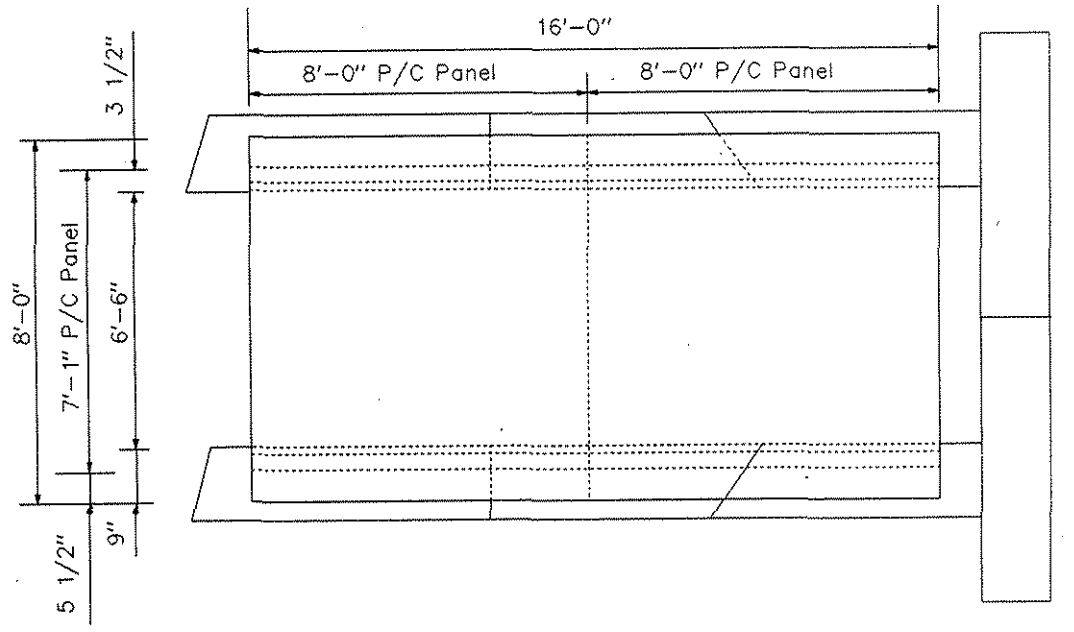

Figure 4.1. Specimen No. 1 configuration.

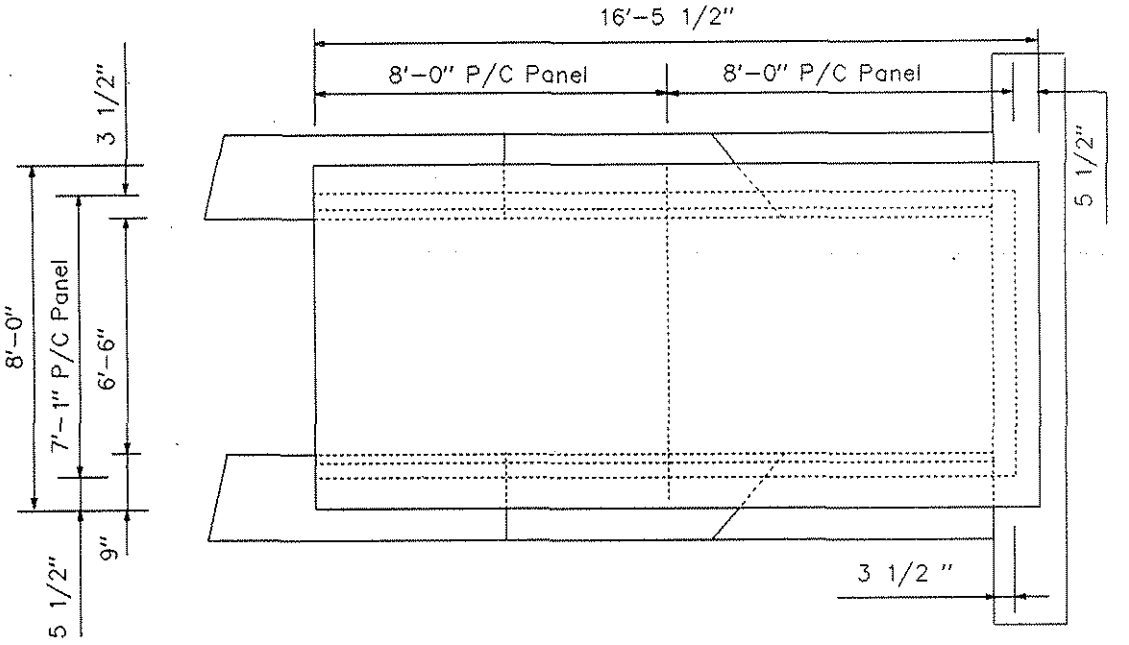

Figure 4.2. Specimen No. 2 configuration.

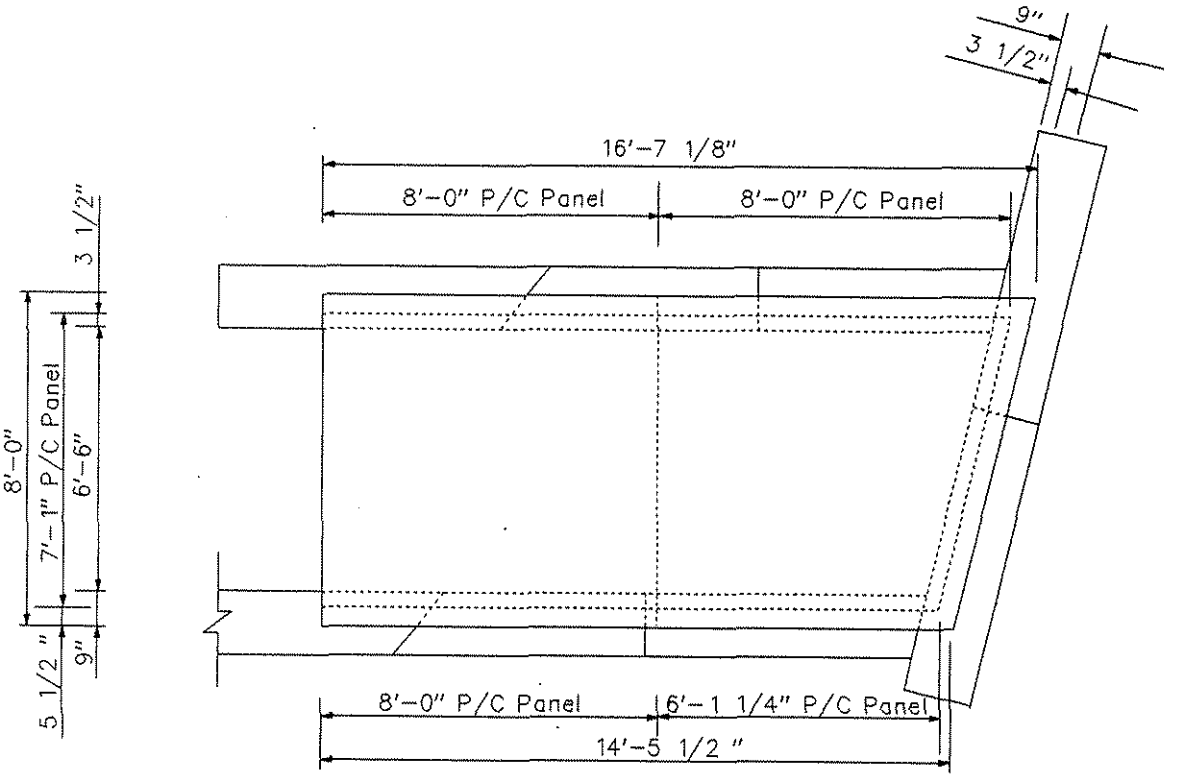

Figure 4.3. Specimen No. 3 configuration.

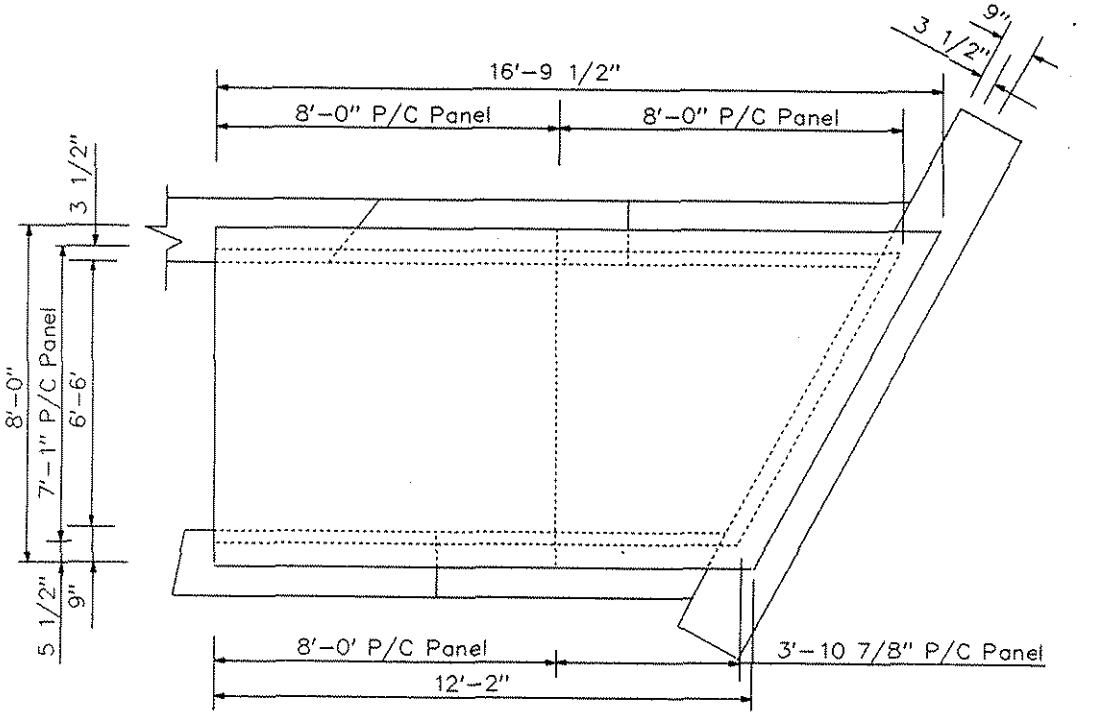

Figure 4.4. Specimen No. 4 configuration.

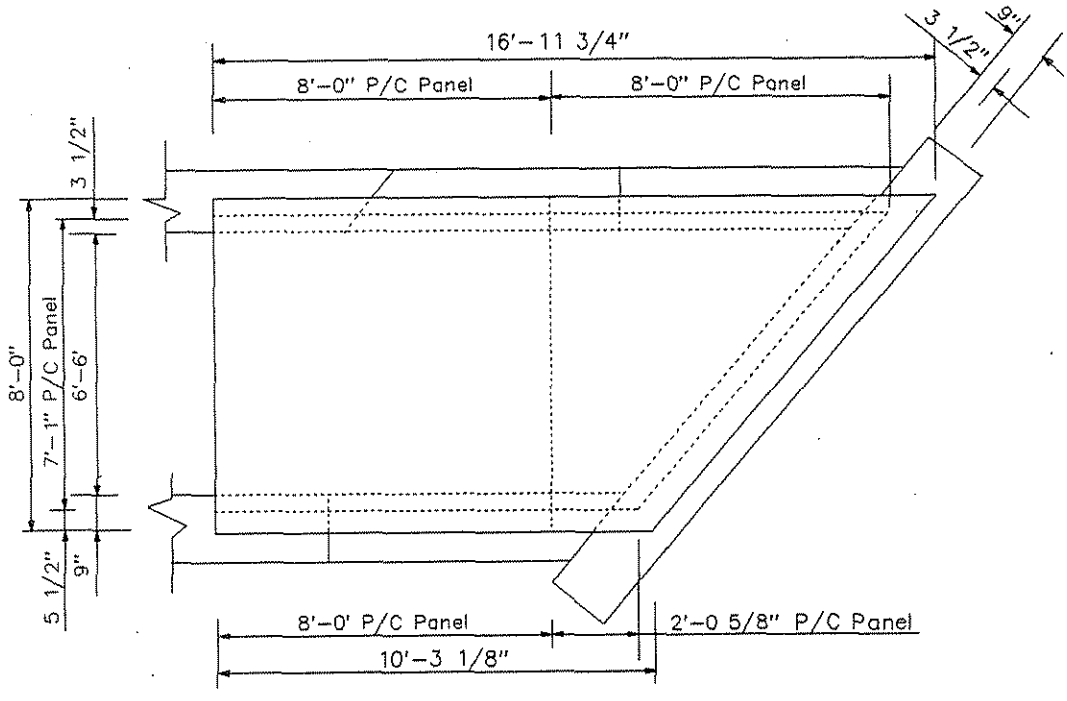

Figure 4.5. Specimen No. 5 configuration.

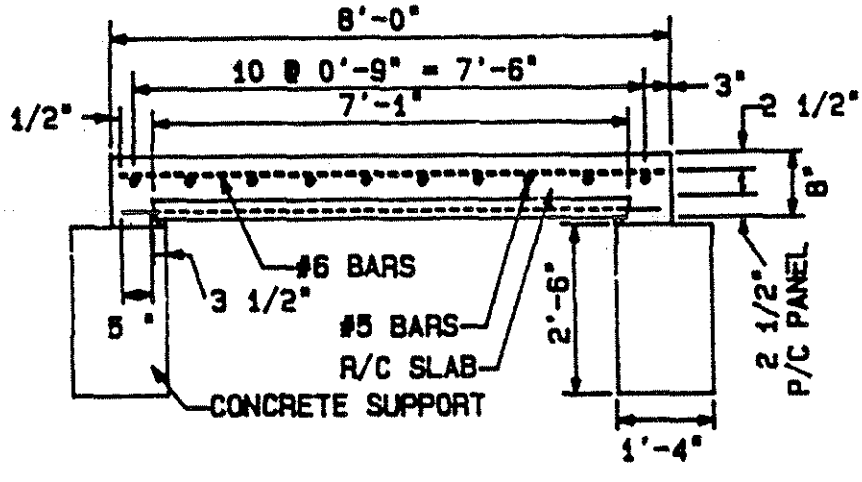

Figure 4.6 Cross section of composite specimen.

To establish a level bearing surface for the panels, a grout bed having a minimum thickness of 1 in. was cast on top of the concrete supports. Temporary bearing for the precast panels consisted of 3/4 in. thick by 1 in. wide fiber-board strips which were glued to the top surface of the grout bed along the inside edges of the concrete supports. Permanent 2 1/2 in. wide bearing for the panels was provided by the concrete from the topping slab which flowed beneath the ends of the panels during the casting of the poured-in-place slab.

4.1.2. Precast Prestressed Concrete Panels

All of the precast panels which were used to construct the test specimens were 2 1/2 in. thick and 7 ft.-1 in. long. As shown in Fig. 4.7, each rectangular shaped panel was 8 ft. wide. The three trapezoidal shaped panels, each represented in Fig. 4.8, varied in width. Each of these panels had a maximum width of 8 ft. The minimum widths were 6 ft.-1 1/4 in., 3 ft.-10 7/8 in., and 2 ft.-0 5/8 in. for the panels associated with bridge skew angles of 15, 30, and 40 deg., respectively. The top surface for all of the panels had a raked finish with the grooves orientated perpendicular to the 7 ft.-1 in. dimension of the panel. The mix quantities per cubid yard of concrete were 705 lb of cement (Portland Cement Type I), 1850 lb of course limestone aggregate with a 1/2 in. maximum size, 1100 lb of fine aggregate (natural sand with a 3/8 in. maximum size), and 300 lb of water. An entrained air content was 6%, and the concrete slump was 4 in. All of the panels contained sixteen 3/8 in. diameter, 7 wire, 270 ksi Grade, low-relaxation prestressing strands positioned at the mid-depth of each panel. The strands, which were spaced at 6 in. on center, extended 5 in. beyond the ends of the panels and extended 6 in. beyond any diagonal edge. Before the concrete was cast, the strands were prestressed to about 17.2 kips, approximately 75% of the strand tensile strength. Each panel had a single layer of 6x6-W5.5xW5.5 welded wire fabric located directly on top of the prestressing strands. The trapezoidal shaped panels had two No. 3 reinforcing bars placed along the diagonal edge of each panel. Some of the short strands in the trapezoidal shaped panels were sleeved along their entire length to prevent bonding with the concrete. For the trapezoidal-shaped

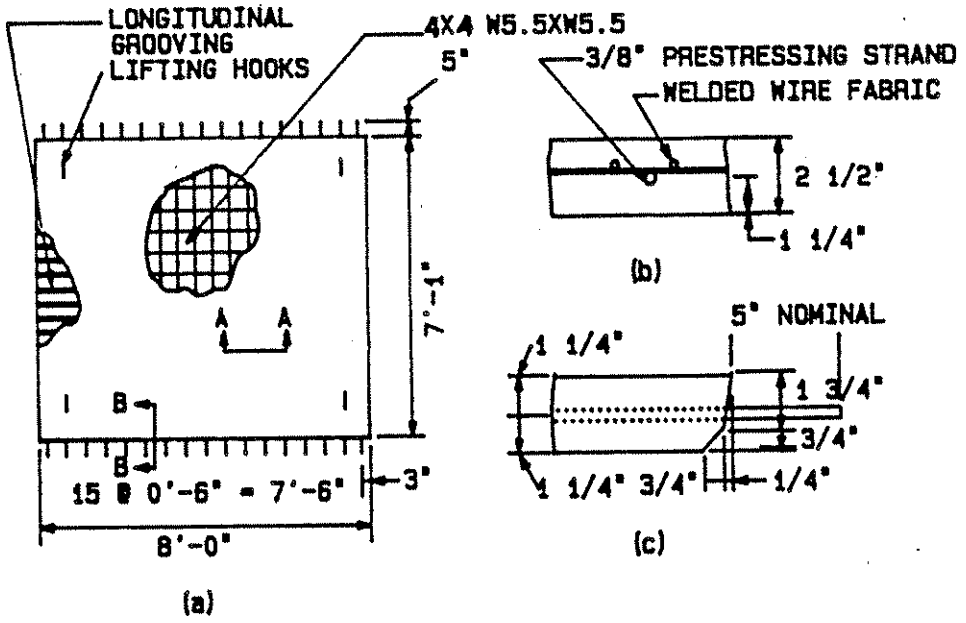

Figure 4.7. Rectangular precast prestressed concrete panel:
(a) Plan view (b) Section A-A (c) Section B-B.

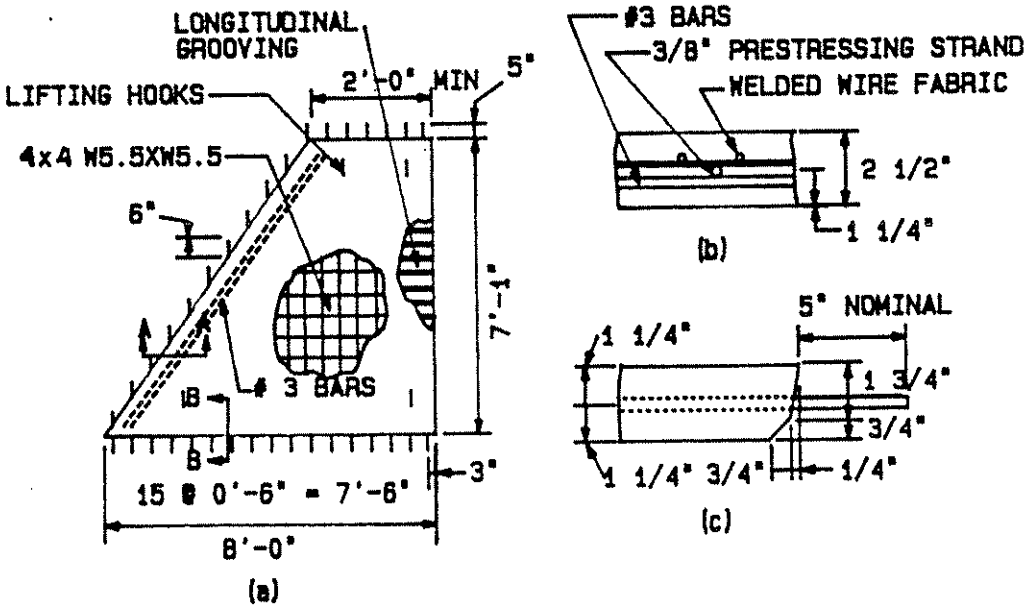

Figure 4.8. Trapezoidal precast prestressed concrete panel:
(a) Plan view (b) Section A-A (c) Section B-B.

panels adjacent to the 15, 30, and 40 degree skewed modeled diaphragms, the two, three, and four shortest strands, respectively, were sleeved. This debonding was done to prevent the triangular shaped corner of a panel from breaking during the detensioning of the prestressing strands. The panels were cast on October 5, 1988 at Precast Concrete Operations, a Division of Wheeler Consolidated, Inc., in Iowa Falls, IA. The concrete compressive strength, f'_c, modulus of elasticity, E_c, and modulus of rupture, f_r, at various ages for the concrete used in the precast panels are given in Section 6.1.1.

4.1.3. Reinforced Concrete Topping Slabs

A reinforced concrete slab approximately 5 1/2-in. thick was cast on top of the 2 1/2-in. thick precast panels for each of the specimens. The total composite slab thicknesses at various locations along the midspan of the panels for each specimen are listed in Table 4.1. These slabs contained

Table 4.1. Composite slab thicknesses.

Location	Total mid-span slab thickness (in.)				
	Specimen No. 1	Specimen No. 2	Specimen No. 3	Specimen No. 4	Specimen No. 5
EE[a]	-	-	8.53	8.37	8.23
EP[b]	8.17	7.51	8.58[f]	8.24	8.15
J[c]	8.08	7.40	8.62	8.45	8.11
WP[d]	8.22	7.47	8.29	8.60	7.93
WE[e]	8.18	7.34	8.30	8.55	7.69

[a]East edge of east panel
[b]Mid-width of east panel
[c]Joint between east and west panels
[d]Mid-width of west panel
[e]West edge of west panel
[f]Average of EE and J

a single layer of reinforcement which had the same bar sizes, bar spacings and locations as the top layer of reinforcement specified for a conventional 8 in.-thick bridge deck. Number 5 bars, which were positioned transverse to the span of the panels were spaced at 9 in. on center and were

supported on 1 1/2 in.-high individual bar chairs spaced at approximately 3 ft. on center in both directions. The bar chairs rested directly on the top surface of the precast panels. Number 6 bars spaced at 10 in. on center were positioned parallel to the span of the panels and were directly above the No. 5 bars. All reinforcing bars were A615 Grade 60 bars. Epoxy coated bars were not used. The concrete cover above the No. 6 bars was about 2 1/2 in. The concrete for the topping slab was the Iowa Department of Transportation Mix No. D57 [18] with the course aggregate satisfying Gradation No. 5 and the fine aggregate satisfying Gradation No. 1. The approximate quantities of dry materials per cubic yard of concrete were 710 lb of cement (Portland Cement Type I), 1413 lb of course aggregate (limestone with a 1" maximum size), 1413 lb of fine aggregate (natural sand with a 3/8 in. maximum size), and 291 lb of water. The amount of air entrainment for the topping slabs was about 6%, and the slump was between 2 and 4 in. The concrete compressive strength, f'_c, modulus of elasticity, E_c, and modulus of rupture, f_r, at various ages for the concrete used in the topping slabs for each of the specimens are given in Section 6.1.1.

4.2. Experimental Testing

4.2.1. Test and Instrumentation Frames

A three-dimensional structural steel test frame was fabricated to load the composite deck specimens. The main elements of the frame consisted of four W30 x 108 columns, two W30 X 108 girders, three W30 x 108 diaphragms, four W21 x 62 tie-down girders, sixteen S15 x 42.9 tie-down beams, a W21 x 62 stiffened load beam, and four S15 x 42.9 diagonal braces. The ends of the test frame were fastened to the floor of the structural laboratory using eight 1 3/8 in.-diameter Dywidag bars which were prestressed to 60 kips each using a hydraulic ram.

A three-dimensional aluminum and steel instrumentation frame was used to support the dial gauges for measuring the vertical deflections of the top surface of the composite deck specimens. Several 2 x 2 x 1/4 steel angles, which held the dial gauge rod attachments, were connected to the frame's aluminum rectangular tubes. These angles could be moved to any position along the alum-

inum tubes, depending on the load position. Steel angle corner bracing in both horizontal and vertical planes provided stability to the frame.

4.2.2. Loads

Initially, all of the composite deck specimens were subjected to a series of service loads positioned at various locations on the slab surface as shown in Figs. 4.9 through 4.13. The number and letter within the rectangularly shaped wheel footprint corresponds to a load or wheel load position number. Both single and double wheel loads were applied to the specimens. When multiple loads were used, the 4 ft. spacing between the two loads is the distance between the wheels on two trucks located adjacent to each other. The maximum magnitude for these service loads was equal to an HS-20 wheel load (16 kips) plus a 30% impact load (4.8 kips). This 20.8 kips load was applied through an AASHTO wheel footprint [1], having a rectangular area equal to 160 $in.^2$ (8 in. by 20 in.). After completion of the service load test series for a particular specimen, factored and/or ultimate load tests were conducted. Specimen Nos. 4 and 5 were subjected to factored loads near the modeled abutment or pier diaphragm. A maximum factored load, equal to 3 times the HS-20 wheel load without impact or 48 kips, was applied through a stronger wheel footprint (9 1/8 in. by 18 1/2 in.) to these specimens. Ultimate strength tests were performed on all five specimens. Except for Specimen No. 1, the ultimate strength tests were conducted using the 9 1/8 in. by 18 1/2 in. footprint. Specimen No. 1 was loaded through the 8 in. by 20 in. footprint. Table 4.2 lists the wheel load positions for each specimen for the three load levels. The numbers in the table correspond to the wheel load positions shown in Figs. 4.9 through 4.13.

All loads were applied by hydraulic rams. For the service load tests, 1 kip load increments were applied until a 6 kip wheel load was reached. After this load, the load increments were about 2 kips until the 20.8 kip wheel load was achieved. Unloading of a specimen involved about 5 kip load decrements. For the factored load tests, 4 kip load increments were applied until a total wheel load equal to 48 kips was reached. Load decrements for the factor load tests equalled 12 kips.

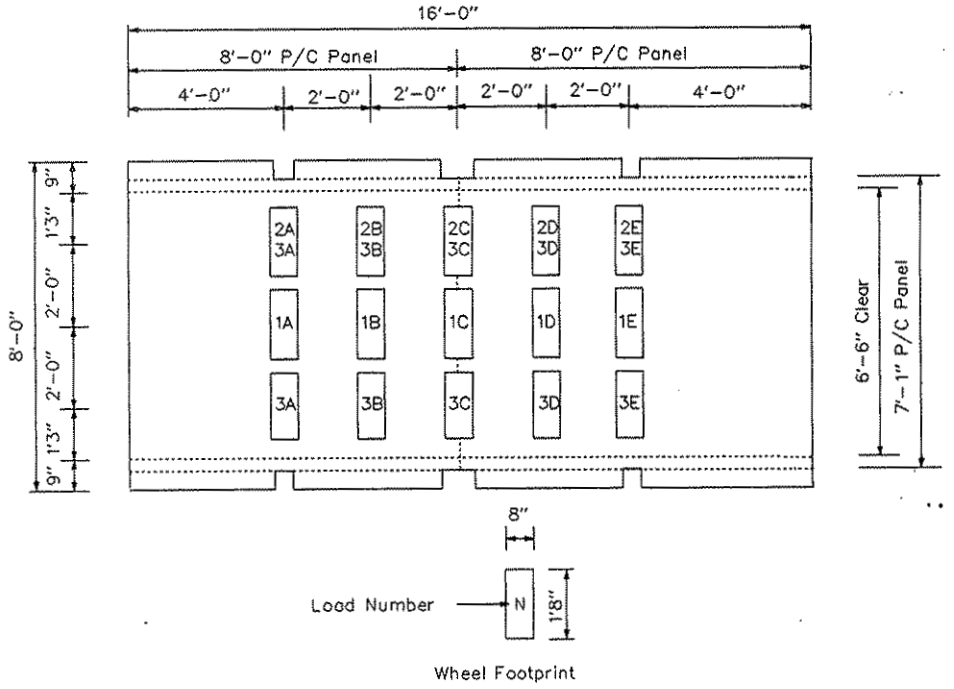

Figure 4.9. Load positions for Specimen No. 1.

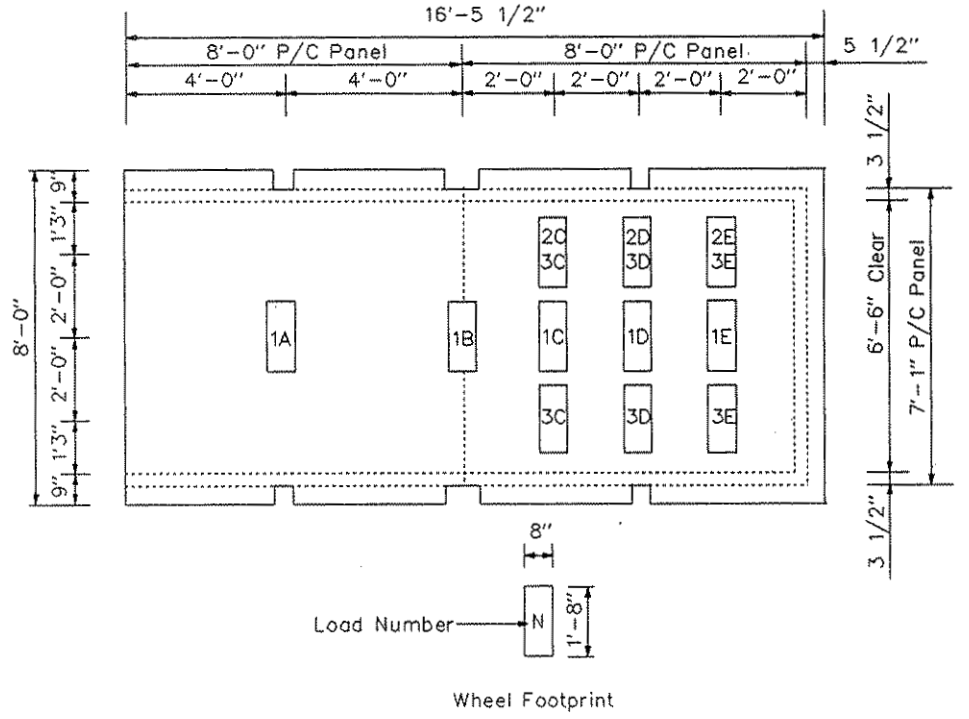

Figure 4.10. Load positions for Specimen No. 2.

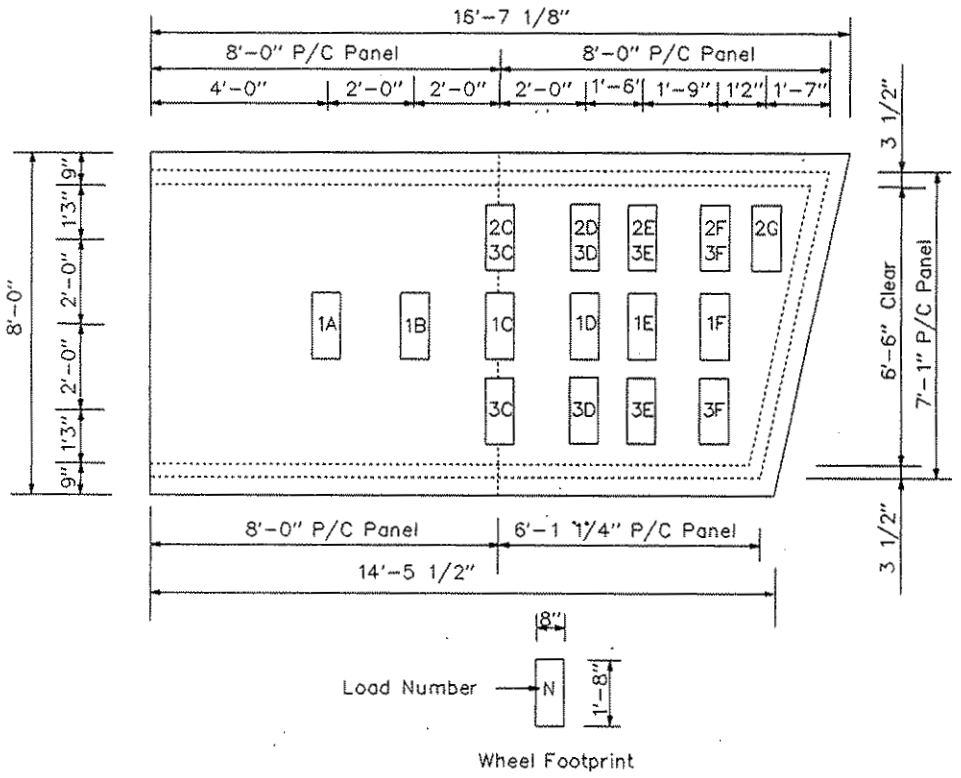

Figure 4.11. Load positions for Specimen No. 3.

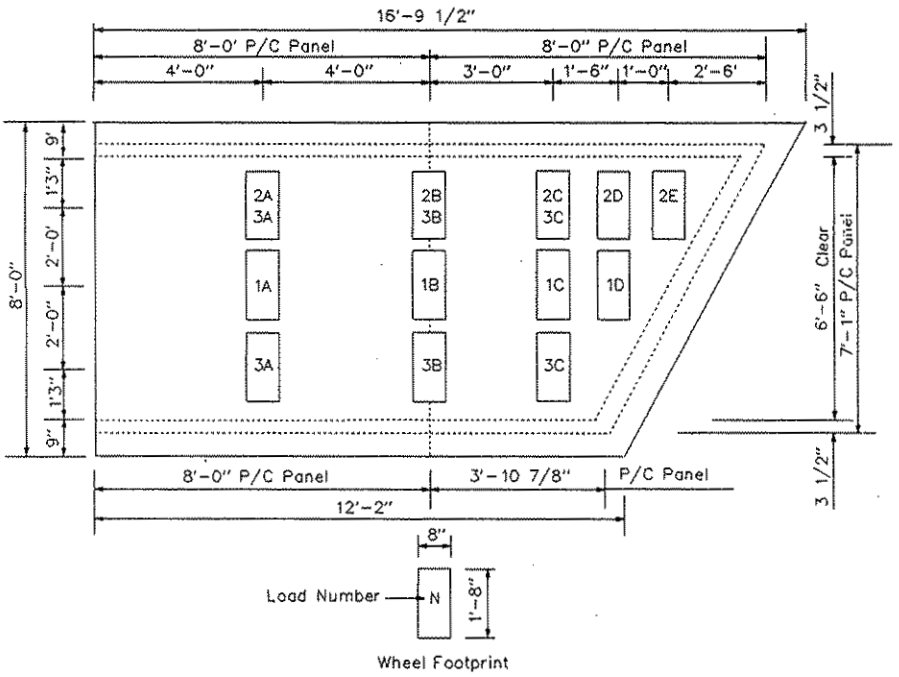

Figure 4.12. Load positions for Specimen No. 4.

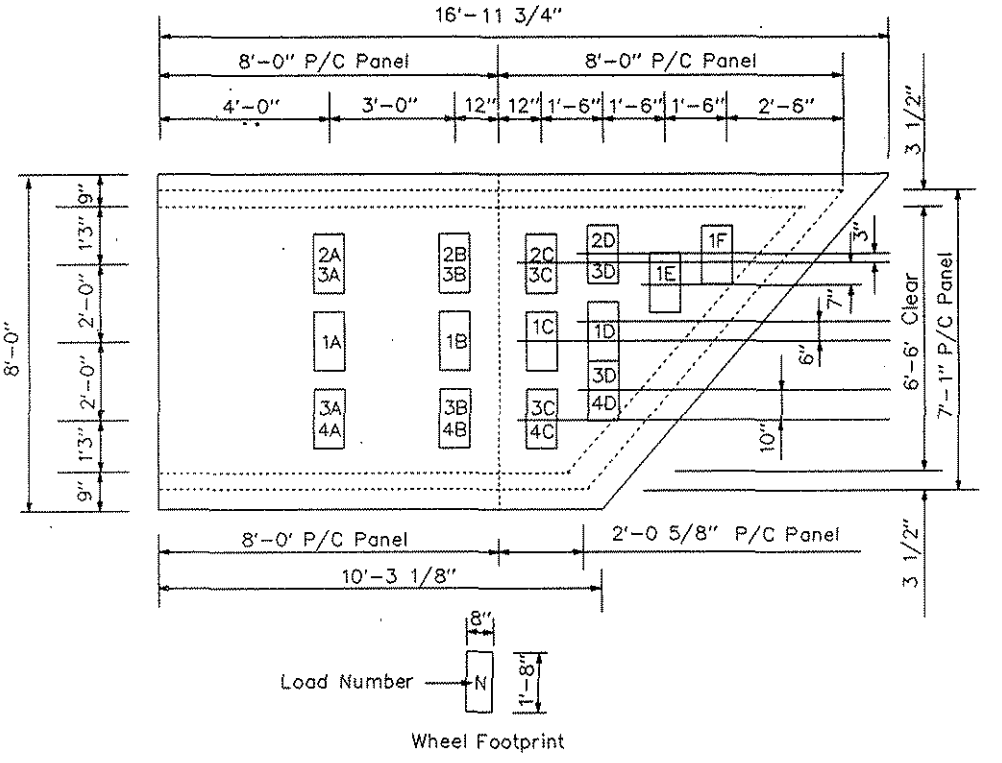

Figure 4.13. Load position for Specimen No. 5.

Except for Specimen No. 1, the ultimate load tests involved 5 kip load increments throughout the entire load range. The load increments for Specimen No. 1 were 5 kips until the first crack appeared in the specimen and 3 kips between the load at initial cracking and failure of the specimen.

Table 4.2. Wheel positions for service, factored and ultimate load levels.

Specimen No.	Service Loads		Factored Loads	Ultimate Loads
	Single	Double		
1	1A-1E 2A-2E	3A-3E	None	1C
2	1A-1E 2C-2E	3C-3E	None	1D 1A
3	1A-1F 2C-2G	3C-3F	None	1E 1′-6" above 1A
4	1A-1D 2A-2E	3A-3C	1C, 1D 2C-2E 3C (Bottom)	1C 1A
5	1A-1F 2A-2D 4A-4D	3A-3D	1A, 1C-1F 2C, 2D 4C, 4D	1D 1′-4" above 1A

4.2.3. Instrumentation

Service and factored loads were monitored with a load cell having a capacity of 50 kips. The loads applied during the ultimate strength tests were measured by a load cell with a capacity of 300 kips.

Several types of displacements were monitored during the testing of a composite slab specimen. Vertical deflections at selected points on the top surface of the slab were measured by dial gauges which were suspended from the instrumentation framework. Potential slip (strand-slip) between selected prestress strands and a precast panel were monitored by dial gauges or direct current displacement transducers (DCDTs) attached to the strand extensions, which were left exposed by block-outs used during casting of the reinforced concrete topping slab. To detect possible slippage (topping-slip) between a precast panel and the topping slab, dial gauges or DCDTs

were mounted on steel rods, which were set in holes drilled into the vertical face of the topping slab within the block-out locations at the bearing ends of the panels. For both types of slip measurement, the instrumentation stem was set against the partially exposed panel end. The displacement devices had an accuracy of 0.001 in. Figures 4.14 through 4.18 show the locations for the vertical displacement gauges for a particular wheel load position, and for the slippage measurement devices. The prefix notations (S) and (T) refer to the devices used to monitor strand-slip and topping-slip, respectively.

For the composite slab specimens, concrete strains were measured by electrical resistance strain gauges which were located at selected points on the top surface of the reinforced concrete slab and on the top and bottom surface of the precast panels. Most of the strain gauges were PL-90 strain gauges having a gauge length of 90 mm; however, some PL-60 strain gauges with a 60 mm gauge length were used when length limitations occurred. Ideally, the gauge length should be at least 3 times the maximum concrete aggregate size. These gauges were standard wire strain gauges utilizing a backing material impregnated with a polyester resin. The location and orientation of the surface mounted strain gauges are shown in Figs. 4.19 through 4.23 for Specimen Nos. 1 through 5, respectively.

Before these gauges were mounted on the concrete surfaces of the slab elements, the cast concrete surface was prepared to provide a smooth surface. At the gauge locations on the top of the reinforced concrete slab and on the bottom of the precast panels, the concrete surface was ground smooth to eliminate any roughness that was present. The surfaces were treated with a conditioner and a neutralizer. An epoxy resin adhesive (M-bond AE 10/15) and its compliment was mixed in a 10 gram to 1.5 gram ratio and spread over the ground concrete surface to fill any voids that were present. Fifty pounds of pressure at each gauge location was applied during the curing of the epoxy glue. After the glue had cured, the hardened epoxy was ground down to the concrete surface, and the smooth surface was treated with a conditioner and neutralizer. Each strain gauge

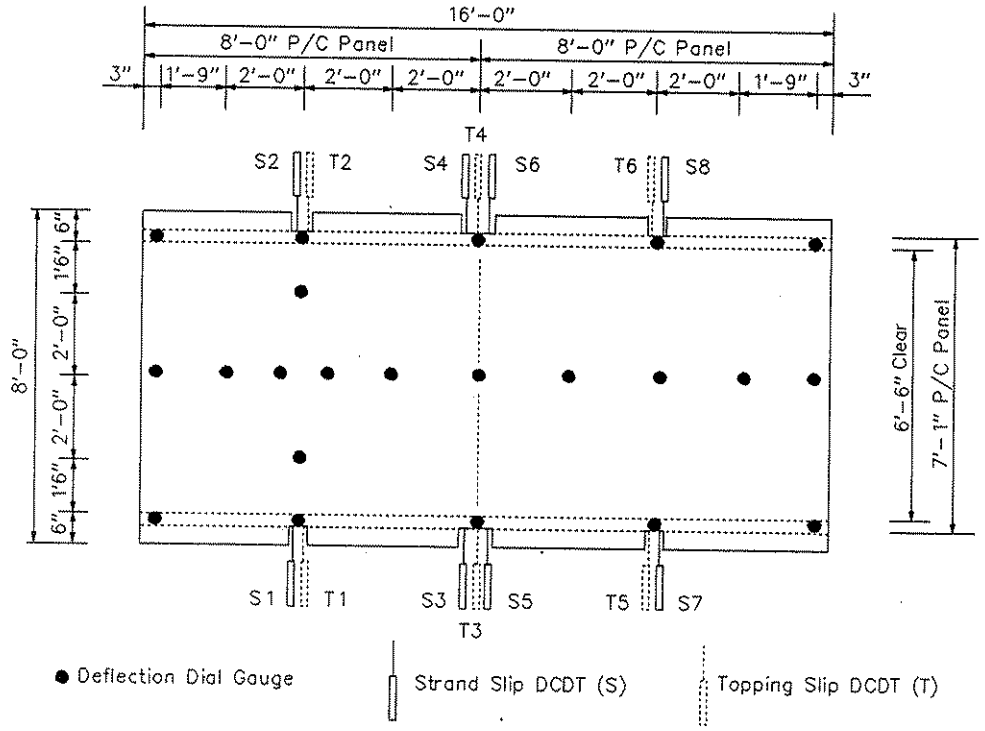

Figure 4.14. Dial gauge and DCDT locations for Specimen No. 1. (Load a Position No. 1A).

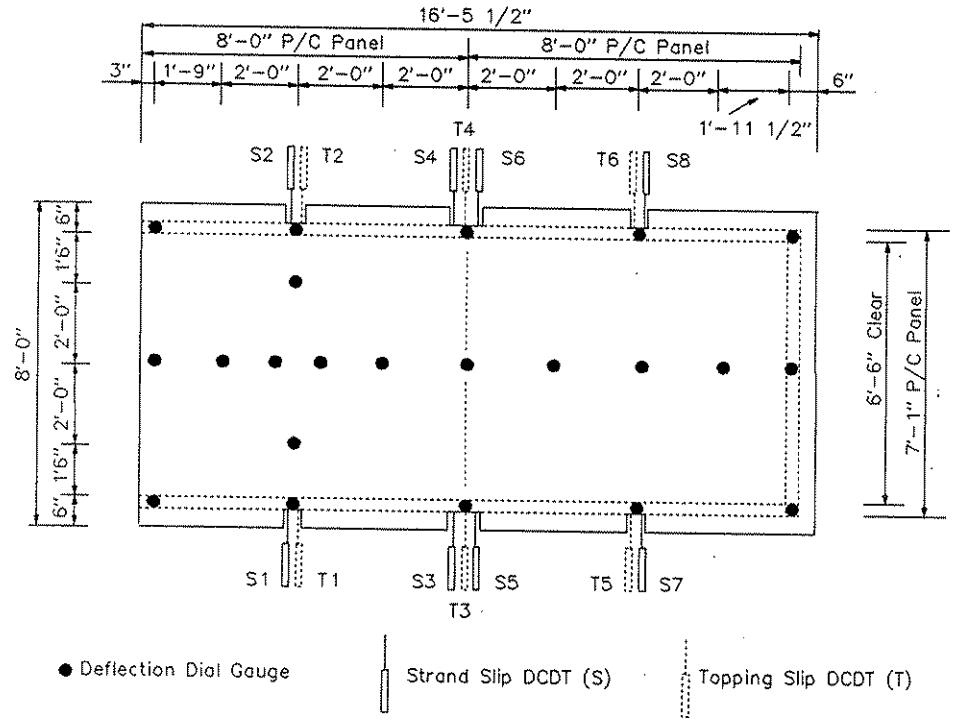

Figure 4.15. Dial gauge and DCDT locations for Specimen No. 2. (Load at Position No. 1A).

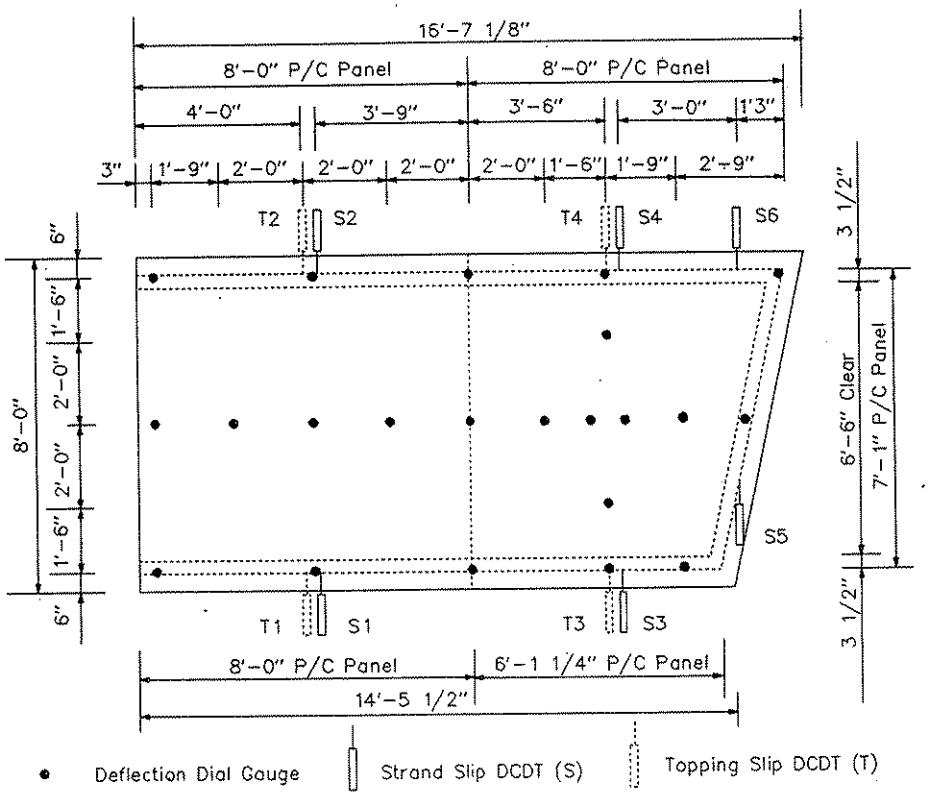

Figure 4.16. Dial gauge and DCDT locations for Specimen No. 3. (Load at Position No. 1E).

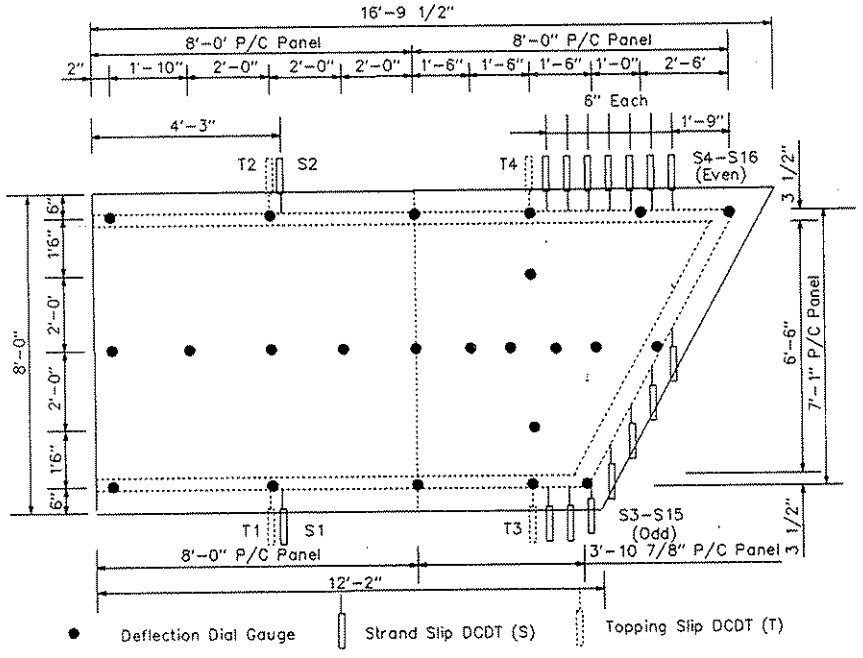

Figure 4.17. Dial gauge and DCDT locations for Specimen No. 4. (Load at Position No. 1C).

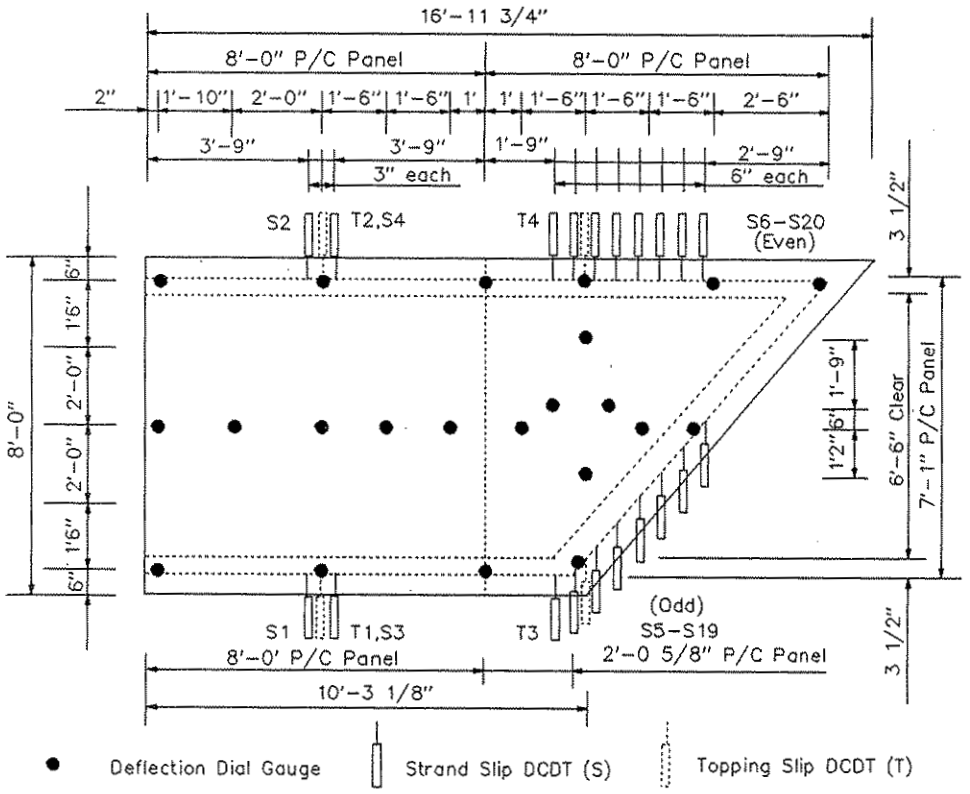

Figure 4.18. Dial gauge and DCDT locations for Specimen No. 5. (Load at Position No. 1D).

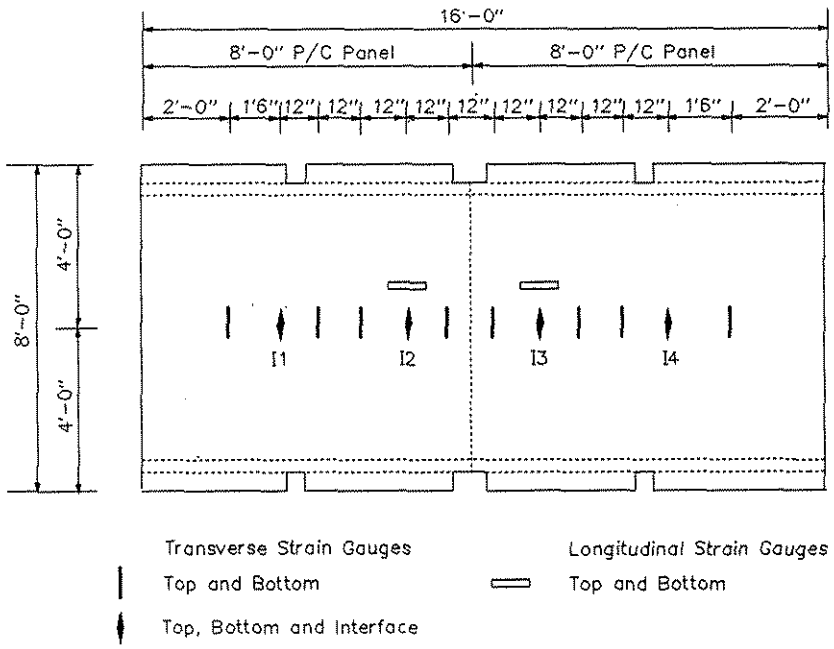

Figure 4.19. Strain gauge locations for Specimen No. 1.

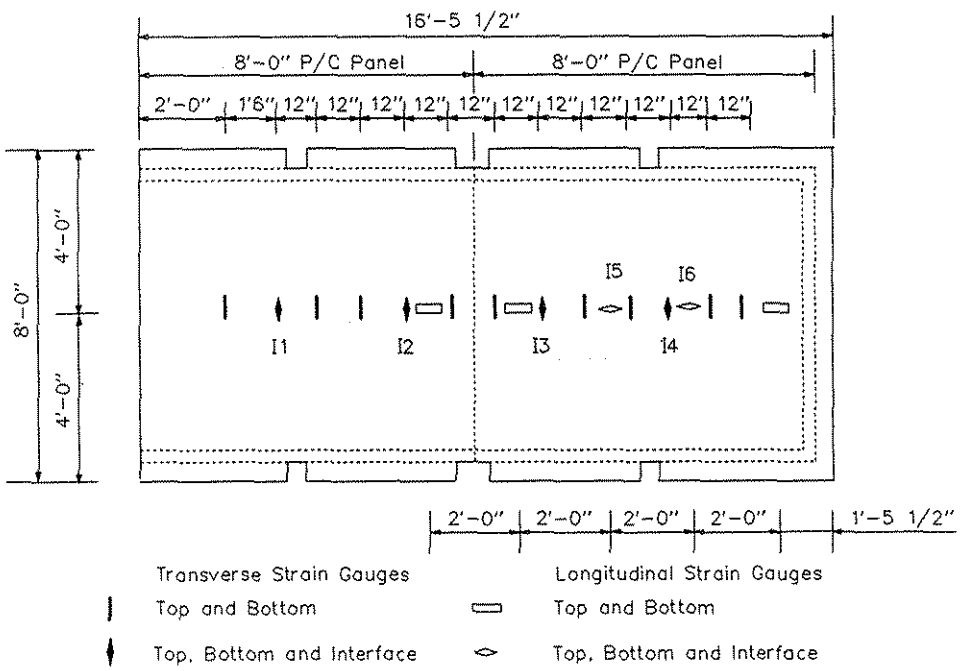

Figure 4.20. Strain gauge locations for Specimen No. 2.

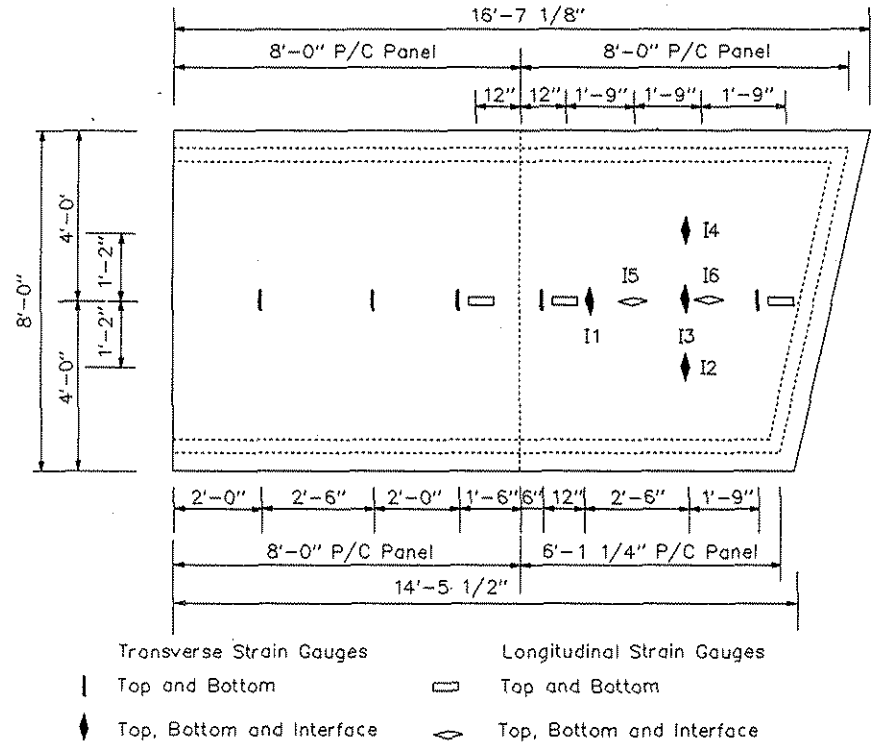

Figure 4.21. Strain gauge locations for Specimen No. 3.

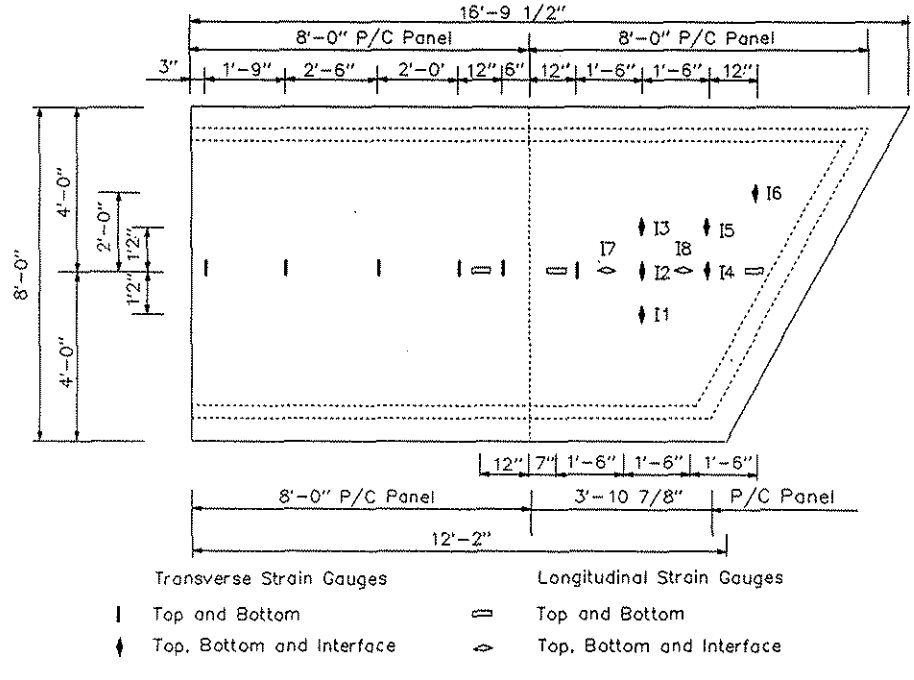

Figure 4.22. Strain gauge locations for Specimen No. 4.

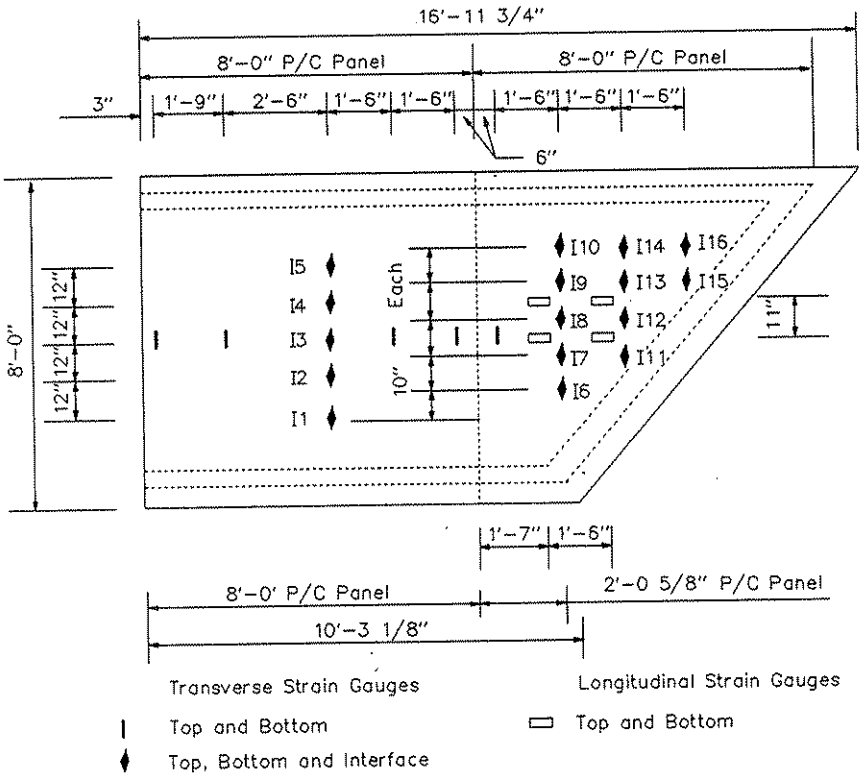

Figure 4.23. Strain gauge locations for Specimen No. 5.

and its solder tab was glued to the prepared surface with an adhesive (RP-2). Again, 50 lb of pressure was applied during the curing of the adhesive. For the strain gauges located on the top of the precast concrete panels, a mortar bed was spread over the raked surface at the gauge locations to fill the deep grooves in the surface. After the grout had cured, gauge installation followed the same procedure as previously described. Since these gauges would be encased in the concrete of the topping slab, moisture and abrasion resistance was provided by a polysulfide coating (M-Coat J).

For monitoring concrete strains within the precast panels during strand detensioning, PML-30 strain gauges were used. These gauges, which had a 30 mm gauge length, were standard wire gauges with wire leads hermetically sealed between thin resin plates. The plates had been coated with a course grit to facilitate bonding with the concrete which enveloped these gauges during casting of the topping slab. The PML gauges were initially wired between adjacent strands to position the gauges at the mid-thickness of the panels and midway between two strands. Figure 4.24 shows the locations for the embeddment gauges in the four precast panels which were used in the construction of Specimen Nos. 2 through 5.

The PL and PML strain gauges and the RP-2 adhesive were manufactured by Tokyo Sokki Kenkyujo Co., Ltd. and distributed by Texas Measurements, Inc. The neutralizer, conditioner, epoxy adhesive, and polysulfide coating were distributed by Measurements Group, Inc. a Division of Micro Measurements, Inc.

During the loading of a test specimen, concrete strains monitored by the PL and PML strain gauges and displacements obtained from the DCDTs were recorded by a Hewlett-Packard (HP) 110 channel data acquisition system (DAS). The displacements measured by the dial gauges were recorded manually.

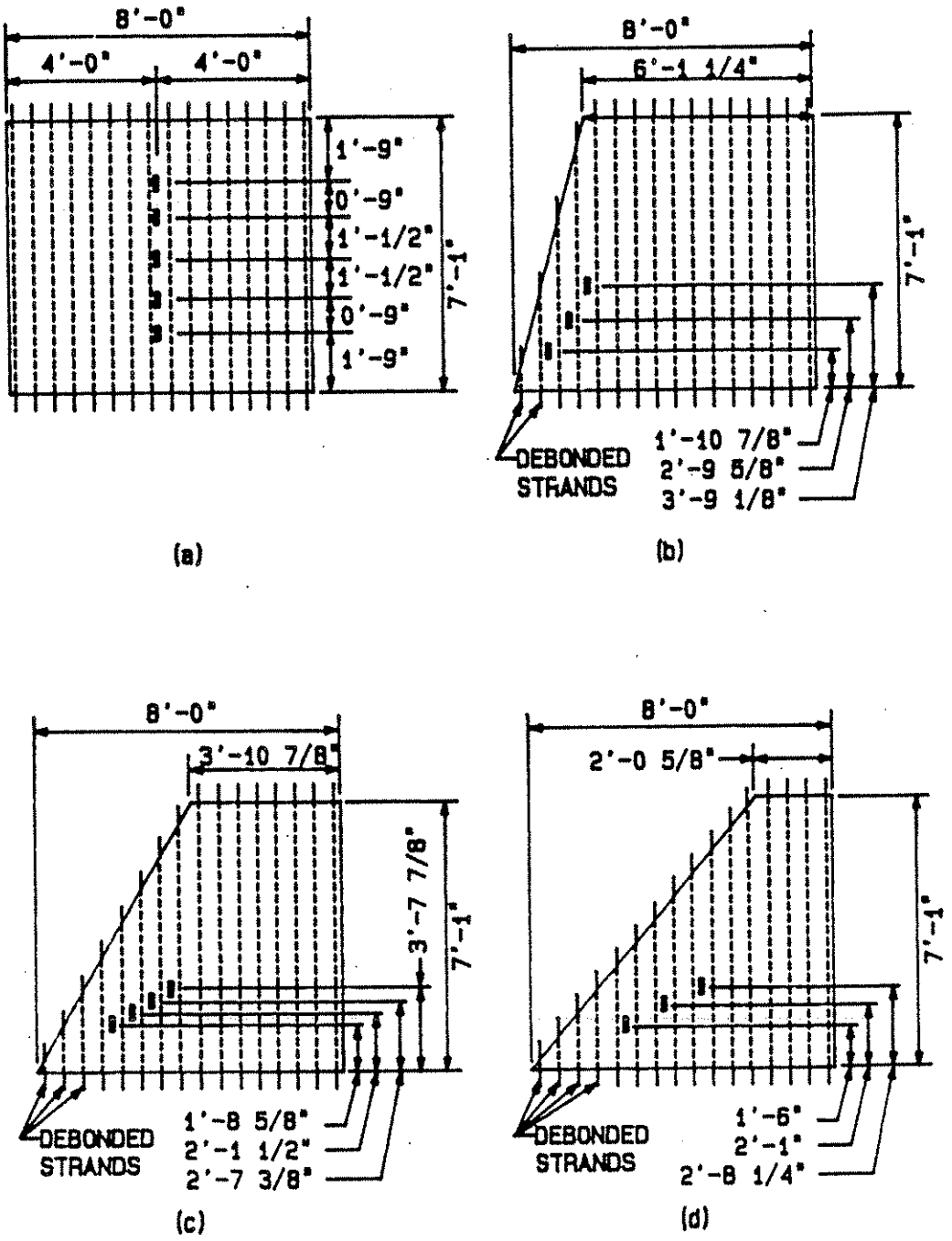

Figure 4.24. Location of panel embeddment gauges:
(a) Rectangular panel (b) 15° skewed panel
(c) 30° skewed panel (d) 40° skewed panel.

5. ANALYTICAL STUDIES

5.1. Strand Embedment Models

5.1.1. Strand Transfer Length

The prestressing strands and the concrete within a member interact through bond stresses that are developed along the interface between the two materials. The basic concepts concerning strand embedment lengths needed for flexural strength are discussed in textbooks on prestressed concrete, such as the book by Lin and Burns [26]. One part of the strand development length is the strand transfer length, L_t, which is the strand embedment length required to develop the effective strand prestress, f_{se}. For a pretensioned bonded tendon, this stress is the stress remaining in a strand after it has been released from the prestressing bed anchorages and after all prestress losses for elastic shortening, ES, creep, CR_c, and shrinkage, SH, of the concrete and relaxation, CR_s, of the strands have occurred. For a low-relaxation prestressing strand, the effective prestress, f_{se}, without considering frictional losses, is given by

$$f_{se} = 0.75 f'_s - (ES + CR_c + SH + CR_s) \tag{5.1}$$

where, f'_s = ultimate strength of the prestressing strands.

In 1979, Zia et al [34] presented emperical expressions for each of these prestress losses. Some of these expressions have been directly adopted, while others have been modified for use in the AASHTO Specification (1985 Interim Supplement) [1]. For members pretensioned with 270 ksi Grade, low-relaxation strands, the concrete elastic shortening loss (AASHTO Eq. 9-6) can be expressed as

$$ES = E_s \left(\frac{f_{cir}}{E_{ci}} \right) \tag{5.2}$$

where, E_s = modulus of elasticity of the prestressing strand, f_{cir} = net compressive stress at the

centroid of the tendons immediately after detensioning of the strands, and E_{ci} = modulus of elasticity of the concrete when the prestress force is applied to the concrete. For low-relaxation strands, the stress f_{cir} has been approximated in the AASHTO Specification as

$$f_{cir} = \frac{0.69\, f_s'\, A_s^*}{A_c} \tag{5.3}$$

where, A^*_s = cross-sectional area of the prestressing strand and A_c = tributary cross-sectional area of the concrete for each prestressing strand. The concrete creep prestress loss (AASHTO Eq. 9-9) is given by

$$CR_c = 12\, f_{cir} - 7\, f_{cds} \tag{5.4}$$

where, f_{cds} = concrete stress at the centroid of the tendons caused by the superimposed permanent dead loads which are applied to the concrete section. For pretensioned members, the concrete shrinkage prestress loss (AASHTO Eq. 9-4) can be expressed as

$$SH = 17{,}000 - 150RH \tag{5.5}$$

where, RH = mean ambient relative humidity, expressed in percent. For low-relaxation prestressing strands in pretensioned members, the strand relaxation prestress loss (AASHTO Eq. 9-10A) is given by

$$CR_s = 5000 - 0.10\, ES - 0.05\, (SH + CR_c) \tag{5.6}$$

Once the effective prestress, f_{se}, has been determined from Eq. (5.1), the transfer length, L_t, can be established from the ACI Code Commentary [3] expression as

$$L_t = \left(\frac{f_{se}}{3}\right) D \tag{5.7}$$

where, D = nominal diameter of the prestressing strand.

Other expressions for the transfer length have been proposed. Cousins et al [11,13] have developed a simple analytical model to represent the mechanics of force transfer between prestressed strands and the surrounding concrete. The model was calibrated by correlations to experimental results conducted by themselves and other researchers. For calculating the transfer length, Cousins et al proposed the expression

$$L_t = \left(\frac{0.5\ U_t' \sqrt{f_{ci}'}}{B} \right) + \left(\frac{f_{se} A_s^*}{\pi D\ U_t' \sqrt{f_{ci}'}} \right) \tag{5.8}$$

with the additional terms defined as: B = bond modulus for the elastic portion of the bond stresses occurring along the transfer length, f_{ci}' = concrete compressive strength when the prestress force is applied to the concrete, and U'_t = non-dimensionalized bond stress along the plastic portion of the transfer length given by

$$U_t' = \frac{U_t}{\sqrt{f_{ci}'}} \tag{5.9}$$

where, U_t = plastic bond stress along the plastic zone of the transfer length. For uncoated seven-wire strands, Cousins et al recommended that B be set equal to 300 psi/in. and that U'_t be set equal to 6.7.

Considering the strand transfer length immediately after the prestress force is applied to the concrete, the only prestress losses which have occurred are due to elastic shortening of the concrete and strand relaxation during the placing and curing of the concrete. Neglecting the prestress loss associated with the relaxation of the tendons, since the time interval involved is extremely short (1 to 2 days), and using an equation similar to Eq. (5.7), the initial transfer length, L_{ti}, can be expressed as

$$L_{ti} = \left(\frac{f_{si}}{3}\right) D \tag{5.10}$$

where, f_{si} = initial strand prestress. For low-relaxation strands, the stress f_{si} can be approximated by

$$f_{si} = 0.75\, f'_s - ES \tag{5.11}$$

Another expression for the initial strand prestress can be developed by equating the changes in length for the concrete and prestressing strand along a unit length of member. Considering the elastic shortening beyond the initial transfer length and applying the statical equilibrium condition which states that the internal concrete compression force equals the internal strand tension force, the initial strand prestress, f_{si}, for low-relaxation strands, can be expressed as

$$f_{si} = \frac{0.75\, f'_s}{\left[1 + \left(\frac{E_s}{E_{ci}}\right)\left(\frac{A_s^*}{A_c}\right)\right]} \tag{5.12}$$

Zia and Mustafa [33] have proposed that the initial strand transfer length should be given by

$$L_{ti} = 1.5 \left(\frac{f_{si}}{f'_{ci}}\right) D - 4.6 \tag{5.13}$$

This expression was obtained from a linear regression analysis of experimentally derived transfer lengths from several researchers.

5.1.2. Strand Flexural Bond Length

The strand flexural bond length, L_{fb}, is the additional embedment length beyond the transfer length, L_t, required to provide for an increase in the prestressing strand stress from the effective prestress, f_{se}, to the stress f^*_{su} associated with the nominal (ultimate) flexural strength of the member.

The ACI Code Commentary [3] discusses the contribution of the flexural bond length to the strand development length. This commentary specifies that the flexural bond length of a prestressing strand is given by

$$L_{fb} = (f_{su}^{*} - f_{se})D \tag{5.14}$$

Even though the AASHTO Specification [1] does not distinguish between the strand transfer or flexural bond lengths within the strand development length, the approach used to establish the relationship between the strand prestress and strand embedment length is similar to the ACI Code method. For bonded tendons, the AASHTO Specification (Eq. 9-16) permits the calculation of the ultimate strand stress, f_{su}^{*}, by the expression

$$f_{su}^{*} = f_{s}^{'}\left(1 - \frac{\rho^{*} f_{s}^{'}}{2 f_{c}^{'}}\right) \tag{5.15}$$

provided that an appropriate stress versus strain relationship exists for the prestressing strands, the effective prestress, f_{se}, is not less than one-half of the ultimate strength, f'_s, of the strand, and sufficient strand development length exists. The term f'_c = concrete compressive strength at 28 days and the prestressing steel ratio, ρ^{*}, is given by

$$\rho^{*} = \frac{A_{s}^{*}}{bd_{p}} \tag{5.16}$$

where, b = width of the rectangular cross-section for the prestressed member and d_p = effective depth from the compression face of the cross section to the centroid of the prestressing steel. To ensure a ductile failure mode, consisting of yielding of the tension reinforcement, AASHTO Eq. (9-20) requires that

$$\rho^{*} < 0.30\,\frac{f_{c}^{'}}{f_{su}^{*}} \tag{5.17}$$

Other expressions for the flexural bond length, L_{fb}, have been proposed by several researchers. Cousins et al [12,13] have suggested that

$$L_{fb} = (f^*_{su} - f_{se}) \left[\frac{A^*_s}{\pi D U'_d \sqrt{f'_c}} \right] \tag{5.18}$$

where, U'_d = non-dimensionalized bond stress along the plastic portion of the flexural bond length is given by

$$U'_d = \frac{U_d}{\sqrt{f'_c}} \tag{5.19}$$

with, U_d = plastic bond stress along the plastic zone of the flexural bond length. For uncoated strands, Cousins et al recommended that U'_d be set equal to 1.32.

Zia and Mostafa [33] have suggested that the flexural bond length, L_{fb}, should be established by the following equation:

$$L_{fb} = 1.25\ (f^*_{su} - f_{se})D \tag{5.20}$$

This expression will provide flexural bond lengths 25 percent greater than the length established by the ACI Code approach (Eq. 5.14).

5.1.3. Strand Development Length

The strand development length, L_d is the prestressing strand embedment length in the concrete required to permit the obtainment of the ultimate strand stress, f^*_{su}, associated with the nominal strength of the precast member. This length is equal to the sum of the transfer length and the flexural bond length, as given by

$$L_d = L_t + L_{fb} \tag{5.21}$$

If the actual strand embedment length from the end of the member to the point of maximum

moment is less than the strand development length, the nominal flexural strength of the member cannot be obtained, since strand slippage would occur due to a bond failure between the strand and the surrounding concrete.

By adding Eqs. (5.7) and (5.14), the ACI Code [2] expression for the strand development length (ACI Sec. 12.9.1) is given as

$$L_d = \left(f_{su}^* - \frac{2 f_{se}}{3}\right) D \tag{5.22}$$

This expression is AASHTO [1] Eq. (9-32) and an alternate form of the AASHTO Eq. (9-19), which expresses the ultimate strand stress as a function of the available embedment length, ℓ_x, measured from the end of the prestressing strand to the center of the precast deck panel, the strand diameter, and the effective stress in the prestressing strand after losses. Rewriting AASHTO Eq. (9-19),

$$f_{su}^* = \frac{l_x}{D} + \frac{2}{3} f_{se} \tag{5.23}$$

If the length ℓ_x in Eq. (5.23) is replaced by the development length, L_d, and if Eq. (5.23) is solved for the length L_d, Eq. (5.22) is obtained. An upper limit on the stress f^*_{su} obtained by applying Eq. (5.23) is established by Eq. (5.15). When sufficient strand embedment length exists ($\ell_x \geq L_d$), the bond resistance between the prestressing strands and the surrounding concrete will not limit the flexural strength of the composite slab.

5.2. Finite Element Models

5.2.1. Trapezoidal Shaped Panel Model

The finite element panel model shown in Fig. 5.1 was developed to analytically establish the concrete strains induced in a trapezoidal shaped panel as a result of prestressing the panel. This model of a panel for a 40° skewed diaphragm condition contains 201 nodes and 180 elements. Node Nos. 79, 95, 110, and 125 shown in Fig. 5.1 represent locations at the mid-length of four strands.

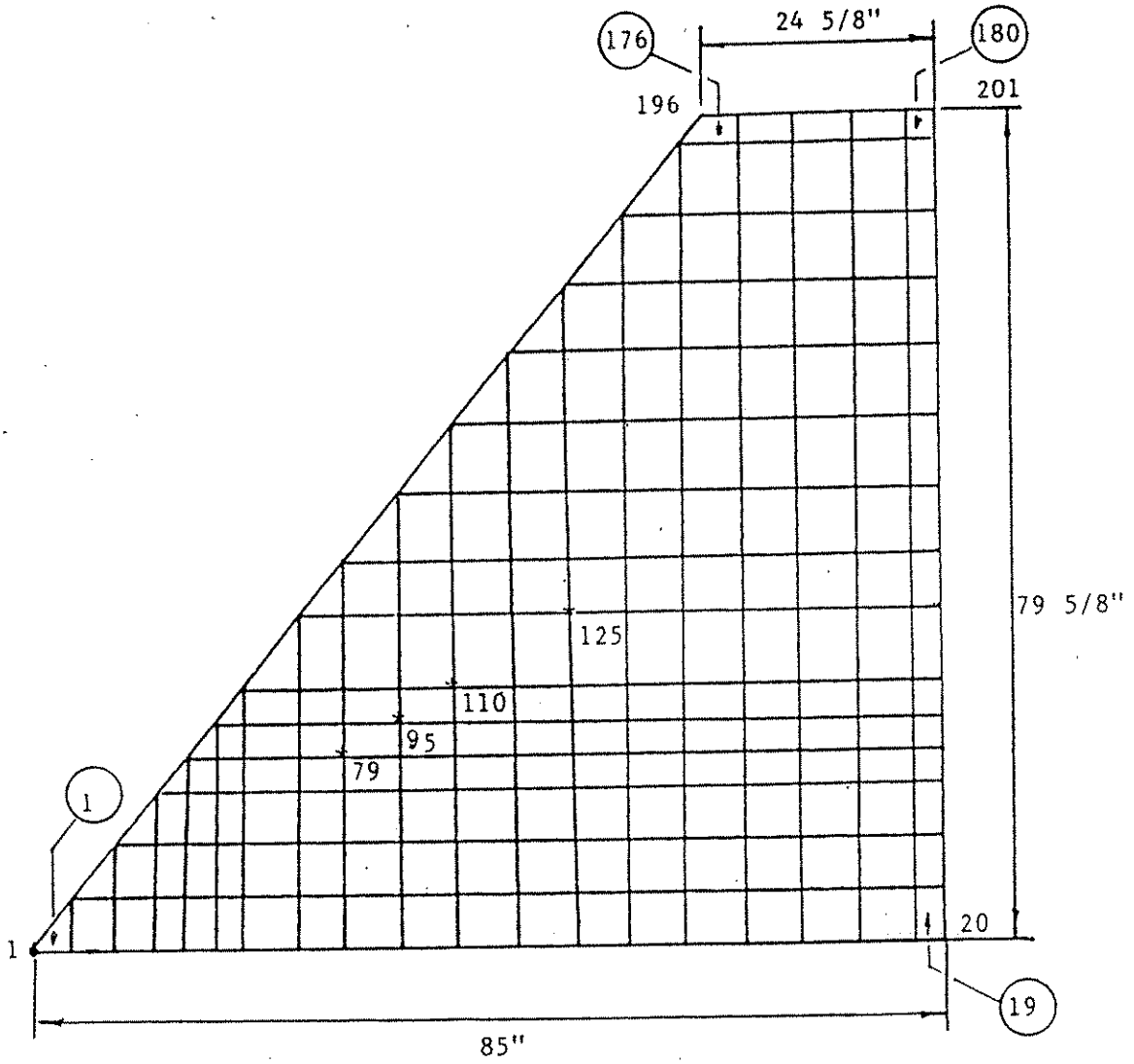

Figure 5.1. Finite element panel model for the 40 degree skewed configuration.

These nodes were used for strain comparisons between the analytical and experimental results which are discussed in Section 6.2.1. Thin plate elements (ANSYS Stiff 63) were used to represent the concrete within the panel. The prestressing strands, welded wire fabric, and the two additional No. 3 reinforcing bars along the diagonal edge of the actual panel were not included in the analytical model. Since the embedment lengths for the strands located within the triangular region of the trapezoidal panel varied, the prestressing forces induced in the panel were not constant across the panel width. To simplify the analytical loading on the trapezoidal panel, loads representing the maximum strand forces, after elastic shortening of the panel but before concrete creep and shrinkage and strand relaxation had occurred, were applied only at the exterior nodes which were in alignment with the strands in the actual panel. The magnitudes for the individual strand forces was based on the transfer length available. Once the required strand transfer length was established from the concrete strains measured with embedded PML-30 polyester mold strain gauges in the four monitored panels during panel prestressing, the strand forces were calculated assuming that the strain in the concrete adjacent to a strand was the same as the strand strain. Analytical and experimental results for the strand transfer length are given in Section 6.2.1.

5.2.2. Bridge deck models

Finite element models were developed to analytically establish displacements and strains in the five configurations of composite bridge decks, each having a different support condition along one of the longitudinal precast panel edges. To simplify each model, the composite slab was approximated as a slab of homogeneous material having the properties of the topping slab cast for the experimental studies. The reinforcing bars, prestressing strands, and welded wire fabric were not included as separate elements in a model. Each slab was modeled by a single layer of thin isotropic plate elements (ANSYS Stiff 63 elements). The thickness of the plate elements was based on the measured thickness of the composite slab specimens.

The minimum number of nodes and elements selected for the bridge deck models were established from a mesh size sensitivity study for an 8 in. thick by 8 ft wide by 16 ft long rectangular shaped slab which was simply supported along the four edges. For this study, several mesh models containing a different number of elements and nodes were generated to represent a homogenous slab. Each of the models were analyzed for a 20.8 kip load distributed over an AASHTO wheel footprint (8 in. by 20 in. area) located at center of the model. Near the wheel footprint, a finer mesh was introduced to improve the accuracy of the analytical solution in the vicinity of the load. The magnitude of the analytical longitudinal stress, S_y, and transverse stress, S_x, at the extreme slab fibers, located at the center of the partial distributed load, were affected by the number of nodes used in the finite element model, as shown in Fig. 5.2. Classical plate theory was also applied to obtain the longitudinal and transverse stresses for the same location. These stresses are shown as dotted lines in the figure. Figure 5.2 shows that convergence of the calculated stress values towards the classical plate solution occurred when the finite element mesh contained between 225 and 250 nodes.

Additional analyses were performed on the rectangular slab model, which contained 231 nodes and 200 elements, to evaluate the accuracy of the computed longitudinal stress, S_y, and transverse stress, S_x at specific locations on the slab surface, when a 20.8 kip wheel load was applied over the AASHTO footprint area and when the load was considered to be concentrated at a point. For both loading conditions the center of the load was located at center of the rectangular slab. The accuracy of the finite element stress results were verified by comparing these computed stresses with the corresponding stresses established by classical plate bending theory. Tables 5.1 and 5.2 list the stresses S_x and S_y, obtained from both the finite element method (FEM) and the classical plate theory (CPT), at various points on the slab surface which were measured from the load position along the longitudinal span, α, at the mid-width of the slab and along the transverse span, β, at the mid-length of the slab. The stresses associated with the partially distributed load induced by the

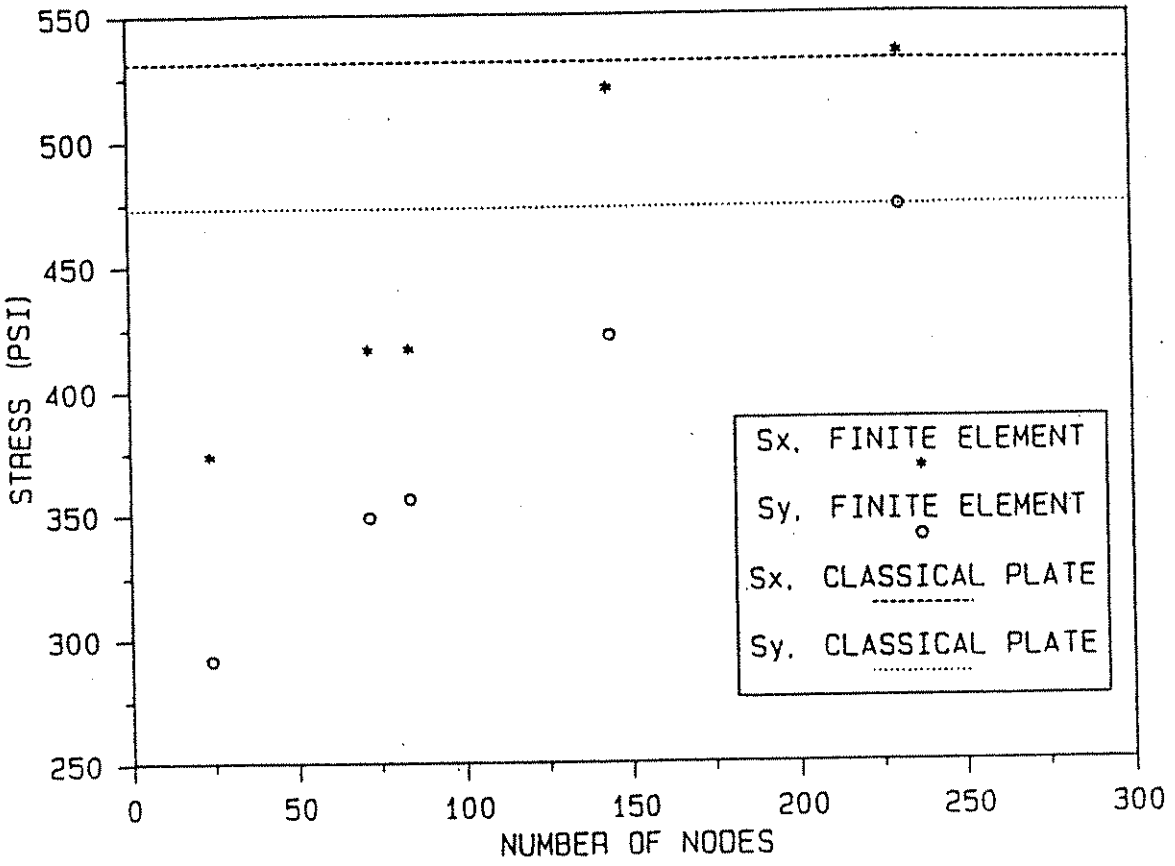

Figure 5.2. Mesh size effects on slab stresses.

Table 5.1. Stresses for partial distributed loading.

Location from the load point	FEM S_x (psi)	CPT S_x (psi)	FEM S_y (psi)	CPT S_y (psi)
Along the longitudinal direction				
0	534	531	473	473
0.1α	425	427	272	275
0.3α	106	106	5	6
Along the transverse direction				
0	534	531	473	473
0.1β	507	505	450	451
0.3β	132	136	137	140

Table 5.2. Stresses for concentrated loading.

Location from the load point	FEM S_x (psi)	CPT S_x (psi)	FEM S_y (psi)	CPT S_y (psi)
Along the longitudinal span direction				
0	899	1083	815	1092
0.1α	465	475	260	272
0.3α	108	109	5	5
Along the transverse span direction				
0	899	1083	815	1092
0.1β	502	502	539	512
0.3β	129	136	136	142

AASHTO wheel footprint are given in Table 5.1 and the stresses caused by a concentrated point load are given in Table 5.2.

The stress results along the longitudinal and transverse axes of a rectangular slab for a finite element model containing 231 nodes and 200 elements that was subjected to a partial distributed load at center of the slab are in close agreement with solutions obtained by classical plate bending theory. The stresses obtained from the finite element solution and from the classical plate theory for the concentrated load case are not in agreement close to the load point. At locations removed from the concentrated load point, the stresses established by the two analytical procedures are almost the same, and these stresses are essentially identical with the calculated stresses obtained when the load was applied through the AASHTO wheel footprint.

Based on the results of the mesh size sensitivity study and on the comparison of the stresses obtained by the finite element method and classical plate theory, a finite element model containing 242 nodes and 200 elements was used to model Specimen Nos. 1 and 2 when a single wheel load was applied to the specimen, as shown in Fig. 5.3. The model for Specimen No. 1 was simply supported along both longitudinal edges, and the model for Specimen No. 2 was simply supported along both longitudinal edges and along one transverse edge. The presence of the skewed end in Specimen Nos. 3, 4, and 5 required a finer mesh for this slab region. Figures 5.4, 5.5, and 5.6 show a typical finite element mesh that was selected for Specimen Nos. 3, 4, and 5, respectively, when a single wheel load was applied to the slab. The models for Specimen Nos. 3 and 4 involved 288 nodes and 255 elements, while the model for Specimen No. 5 required 322 notes and 307 elements. Each of these models was simply supported along both longitudinal edges and along the diagonal edge. When the composite slabs were analyzed for two wheel loads acting simultaneously, additional nodes and elements were required for the models. The largest finite element model, containing up to 488 nodes and 470 elements, was used to analyze the double wheel load conditions on Specimen No. 3. The shaded portion shown in Figs. 5.3 through 5.6 represents the load area associated with the

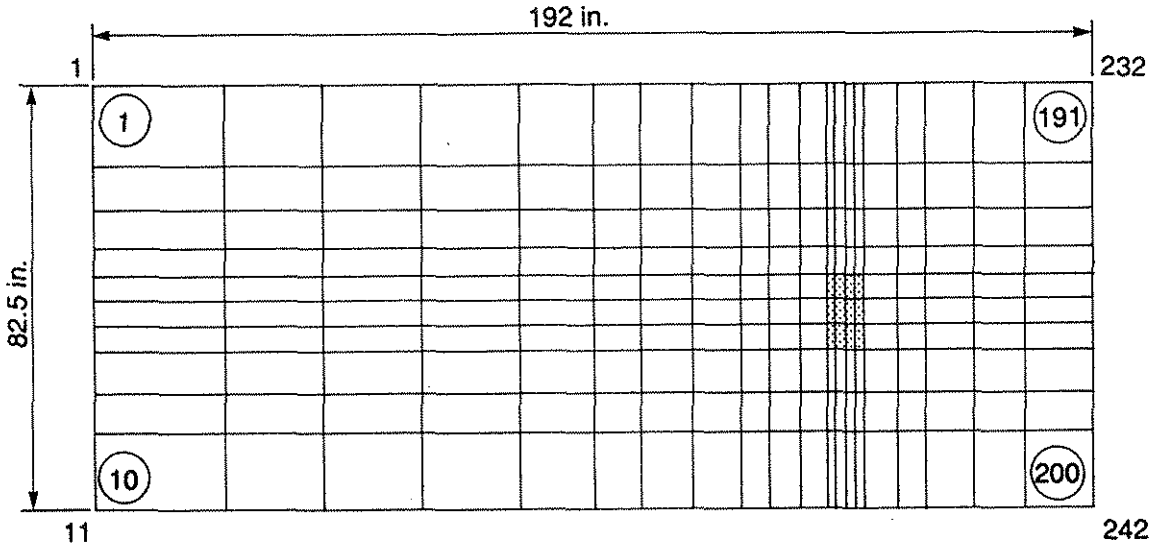

Figure 5.3. Finite element model for wheel load at Position No. 1E on Specimen No. 1 and at Position No. 1D on Specimen No. 2.

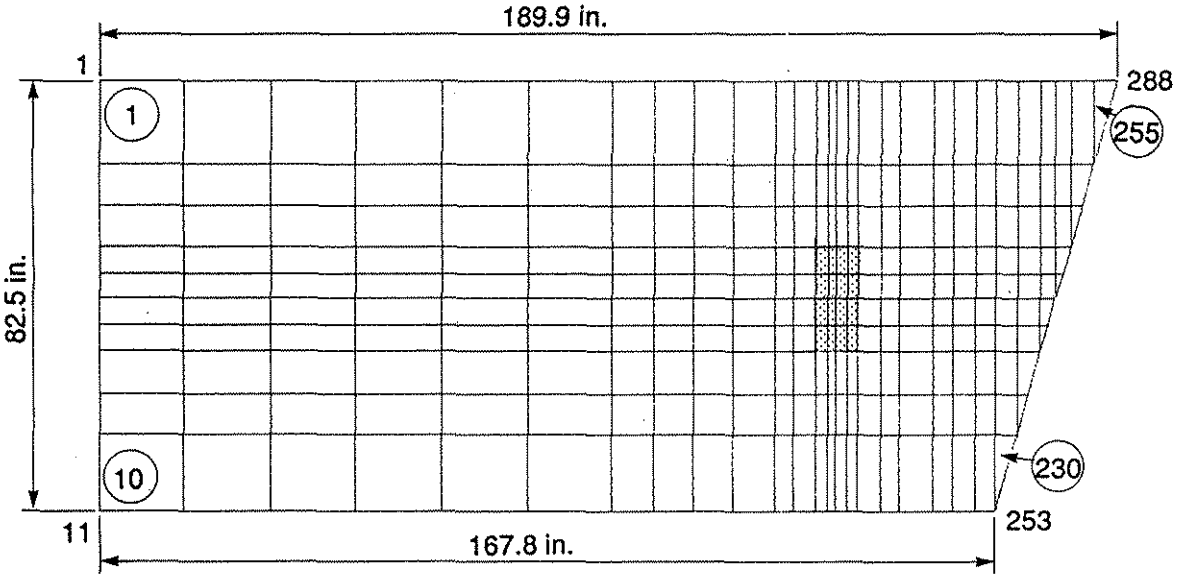

Figure 5.4. Finite element model for wheel load at Position No. 1E on Specimen No. 3.

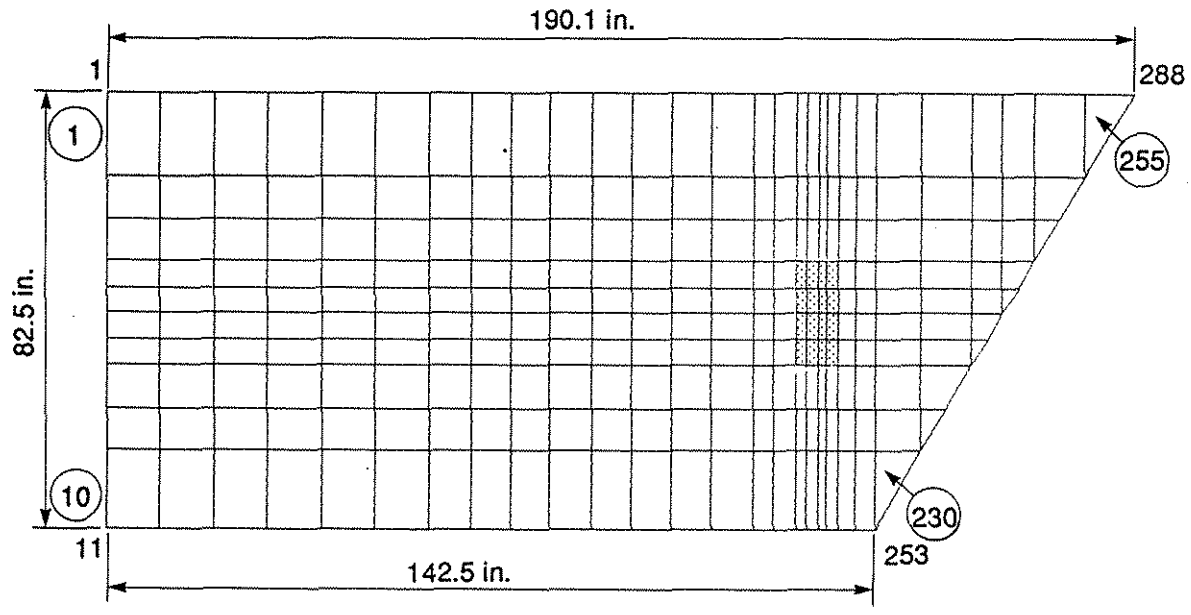

Figure 5.5. Finite element model for wheel load at Position 1C on Specimen No. 4.

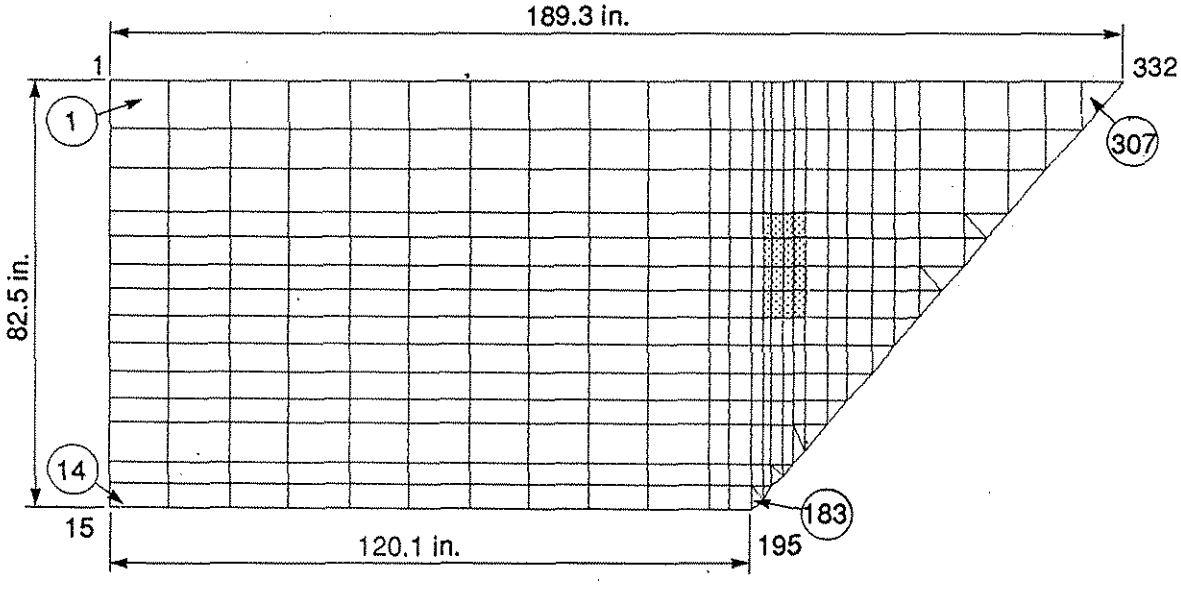

Figure 5.6. Finite element model for wheel load at Position 1D on Specimen No. 5.

AASHTO wheel load. Similar element arrangements were generated for the other wheel load positions on each of the five specimen configurations. Since uplift along the supported edges of the slabs constructed for the experimental testing was not restrained, several nodes along these edges of the finite element models had the vertical restraint released when a significant hold-down reaction occurred. For a rectangular slab configuration, uplift occurred at the corners of the slab when concentrated loads were applied to the specimens. The uplift conditions became more complex as the specimens became more non-rectangular. Several cycles of analysis were required to correctly model the support conditions for the finite element models.

Comparisons of displacement and strain results obtained from the finite element analyses and the experimental testing of the full-scale composite bridge deck specimens are discussed in Sections 6.4 and 6.5.

5.3. Yield-Line Models

A limit load strength for each slab configuration was evaluated by applying yield-line analysis methods. This approach, which is based on flexural strength, involves the following four basic assumptions [32]:

1. The tension steel reinforcement which intersects a yield-line has yielded when the limit load is reached.
2. At failure, the slab behaves plastically along the yield lines, which separate the slab into segments.
3. Bending moments normal to the yield-lines and torsional moments parallel to the yield-lines are uniformly distributed along the yield lines. These moments are statically equivalent to the nominal bending moments for the slab along the directions of orthogonal reinforcement present in a two-way slab.

4. The elastic deformations of the slab are negligible when compared to the plastic deformations; therefore, the slab segments between the yield-lines and axes of rotation are rigid plates that displace as rigid bodies.

Yield-line patterns for the limit load analysis were established from the cracks which occurred in the experimental specimens during the ultimate load tests. The yield-lines chosen for a particular pattern represented either the center of the crack bands when multiple cracks occurred or a single crack. The cracks for the positive and negative moment yield-lines occurred in the bottom and top surfaces, respectively, of a slab specimen. The edge boundaries for the analytical model correspond to the edge conditions which were present in the test specimens. Figures 5.7a through 5.7g show the yield-line patterns (Patterns A through G, respectively) that were selected to mathematically represent the collapse mechanisms associated with a yield-line analyses. Yield-line Patterns A and B were obtained by observing the cracks shown in Fig. 6.37, which shows the top and bottom surfaces of Specimen No. 1. Yield-line Patterns C and D were established to represent the failure mechanism corresponding to the crack patterns which developed in the top and bottom slab surfaces as a result of the ultimate load test on both the east and west panels of Specimen No. 2, as shown in Figs. 6.38 and 6.39, respectively. These two yield-line patterns also provided mechanisms to analyze the flexural limit load for the east panel of Specimen Nos. 3, 4, and 5. The crack patterns for these specimens are shown in Figs. 6.41, 6.43, and 6.45, respectively. Yield-line Pattern E represents another potential collapse mechanism for a concentrated load on the east panel of Specimen Nos. 2 through 5. For this pattern, the negative moment yield-line corresponds to the negative moment resistance at the joint between the two precast panels, while the positive moment yield-lines represent the approximate center of the cracks within a band width as shown in Figs. 6.39b, 6.41b, 6.43b, and 6.45b for the bottom surface of Specimen Nos. 2, 3, 4, and 5, respectively. Yield-line Patterns F and G were selected to evaluate the limit load for the portion of the slabs adjacent to the experimentally modeled abutment or pier diaphragm in skewed and non-skewed

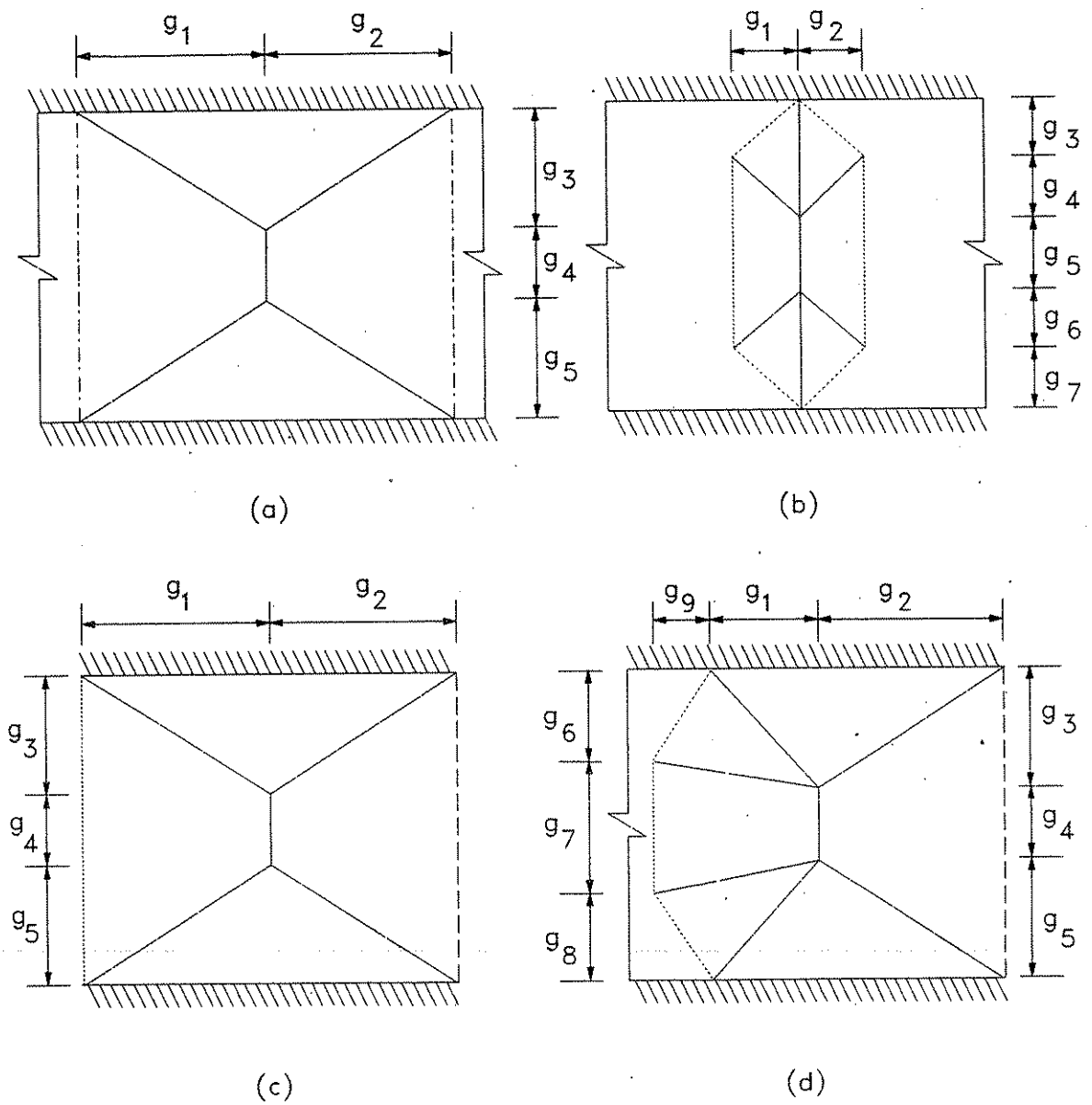

Figure 5.7. Yield-line patterns: (a) Pattern A, (b) Pattern B, (c) Pattern C, (d) Pattern D.

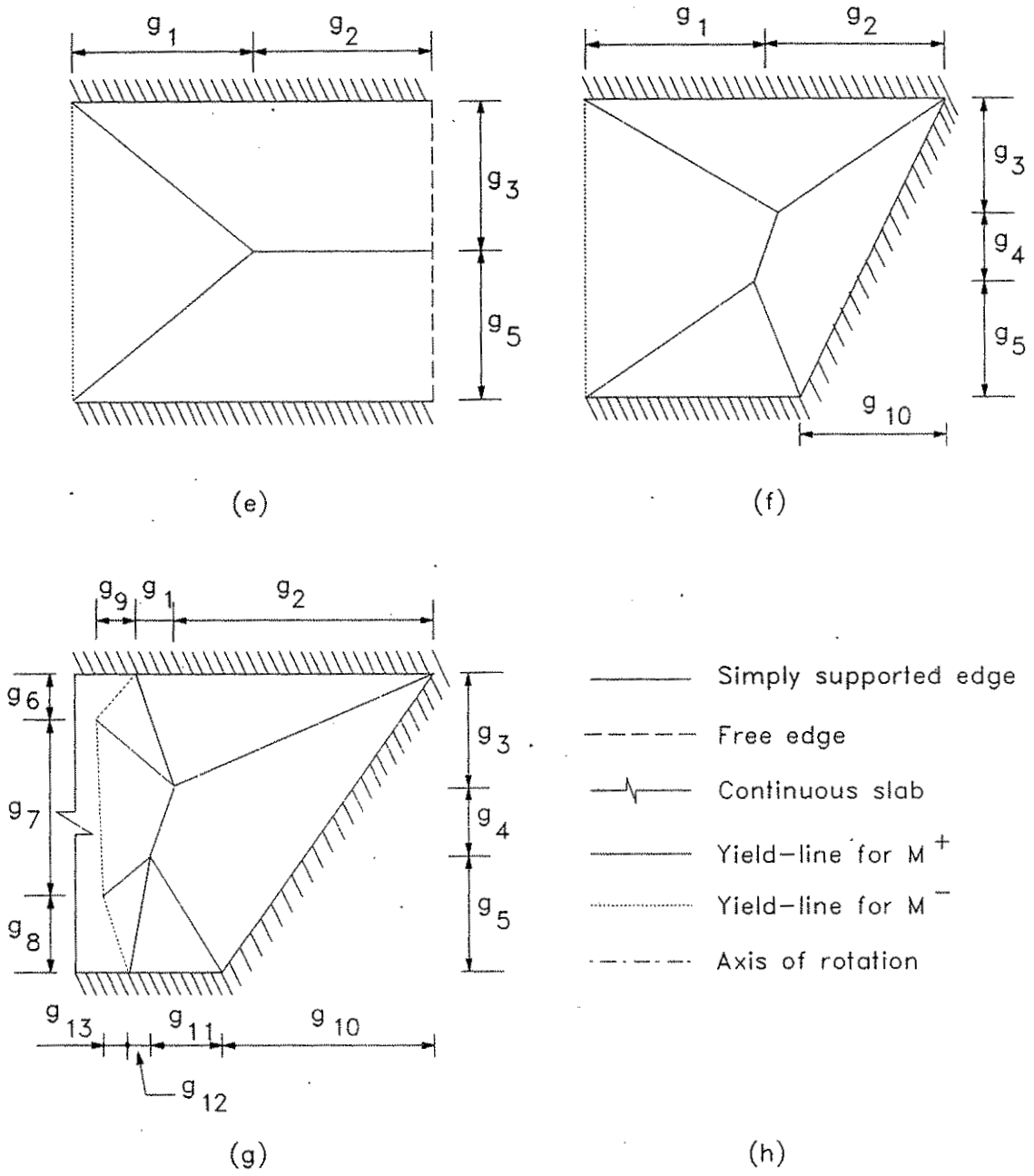

Figure 5.7. Yield-line patterns (continued): (e) Pattern E, (f) Pattern F, (g) Pattern G, (h) Key.

bridges. These two patterns can be visualized from the crack patterns for the top and bottom surfaces of the west panel of Specimen Nos. 3, 4, and 5, as shown in Figs. 6.40 and 6.42 and 6.44, respectively. The dimensions g_i shown in the figures and listed in Table 5.3, locate the yield-line intersection points for the various yield-line patterns. A dash (-) shown in Table 5.3 for a yield-line pattern indicates that the pattern does not contain that particular g-dimension.

Table 5.3. Yield-line dimensions.

Specimen No.	Ultimate test No.	Yield-line pattern	Dimensions (in.)												
			g_1	g_2	g_3	g_4	g_5	g_6	g_7	g_8	g_9	g_{10}	g_{11}	g_{12}	g_{13}
1	1	A	42	30	25	30	25	-	-	-	-	-	-	-	-
		B	24	20	18	13	20	12	19	-	-	-	-	-	-
2	1	C	51	41	31	17	32	-	-	-	-	-	-	-	-
		D	41	41	31	17	32	12	56	12	10	-	-	-	-
	2	A	50	45	32	19	29	-	-	-	-	-	-	-	-
		C	45	50	32	19	29	-	-	-	-	-	-	-	-
		D	21	50	32	19	29	26	39	28	13	-	-	-	-
		E	50	45	38	-	42	-	-	-	-	-	-	-	-
3	1	F	36	60	41	0	41	-	-	-	-	22	-	-	-
	2	C	48	48	20	20	40	-	-	-	-	-	-	-	-
		D	24	48	20	20	40	30	20	30	8	-	-	-	-
		E	48	48	64	-	16	-	-	-	-	-	-	-	-
4	1	F	36	60	35	12	35	-	-	-	-	48	-	-	-
		G	13	60	35	12	35	19	35	28	12	48	13	17	4
	2	C	48	48	35	12	35	-	-	-	-	-	-	-	-
		D	17	48	35	12	35	18	46	18	16	-	-	-	-
		E	48	48	41	-	41	-	-	-	-	-	-	-	-

Table 5.3. Yield-line dimensions (continued).

Specimen No.	Ultimate test No.	Yield-line pattern	Dimensions (in.)												
			g_1	g_2	g_3	g_4	g_5	g_6	g_7	g_8	g_9	g_{10}	g_{11}	g_{12}	g_{13}
5	1	F	30	66	34	0	46	-	-	-	-	67	-	-	-
		G	30	66	34	0	46	24	32	24	16	67	-9	28	20
	2	C	48	48	19	12	49	-	-	-	-	-	-	-	-
		D	48	48	19	12	49	36	20	24	20	-	-	-	-
		E	48	48	55	-	25	-	-	-	-	-	-	-	-

Application of the third yield-line theory assumption requires that the nominal flexural strengths for both positive and negative moments in orthogonal directions be evaluated. Since the composite bridge decks are orthogonally anisotropic slabs (orthotropic slabs), the bending moment strengths are different for the transverse and longitudinal directions of the bridge. The transverse direction was parallel to the precast panel span, while the longitudinal direction was perpendicular to the panel span. The nominal moment resistances were calculated by applying strength design principles. The neutral axis locations for each unit-width cross section was established by considering the effects of all of the reinforcement (prestressing strands, welded wire fabric, and reinforcing bars); the concrete strength of the compression zone; the panel joint, when the yield-line pattern involved this discontinuity; slab thickness; and reinforcement depths. For transverse and longitudinal positive moment strengths (M_{tnp} and $M_{\ell np}$, respectively) the extreme compression fiber of a cross section was the top surface of the topping slab, while for transverse and longitudinal negative moment strengths (M_{tnn} and $M_{\ell nn}$, respectively) the extreme compression fiber was normally the bottom surface of the precast prestressed panel. For Specimen No. 1, the presence of the joint between the two precast panels significantly affected both $M_{\ell np}$ and $M_{\ell nn}$ strengths. Table 5.4 lists the nominal moment resistances which were used for the yield-line analyses of the ultimate load tests.

Table 5.4. Nominal moment resistances.

Specimen no.	Ultimate test no.	Nominal Moments (ft-kips/ft)					
		M_{tnp}	M_{tnn}	M^{a}_{tnp}	M^{a}_{tnn}	M^{b}_{tnp}	M^{b}_{tnn}
1	1	30.14	15.33	7.28	3.40	12.26	9.71
2	1	26.46	15.33	6.41	3.39	10.77	9.71
	2	26.77	15.32			10.83	9.71
3	1	33.03	15.29	6.63	3.40	12.82	9.68
	2	32.22	15.23			12.83	9.67
4	1	32.04	15.28	7.84	3.41	13.02	9.67
	2	31.75	15.30			12.96	9.69
5	1	28.06	15.30	6.63	3.40	11.35	9.68
	2	28.20	15.21			11.38	9.66

[a]Near panel joint
[b]Not near panel joint

The nominal limit load, P_n, for a yield-line analysis was calculated by applying work expressions for the collapse mechanism formed by the various yield-line patterns shown in Fig. 5.7. For each yield-line pattern, the expressions for the limit load were obtained by equating the external work done by the limit load in moving through a virtual displacement to the internal work done by the nominal moment resistances in moving through the inelastic rotations about the yield-lines. Eqs. (5.24) through (5.30) are the expressions for P_n which were derived for yield-line Patterns A through G, respectively.

$$P_n = M_{tnp}\left[\frac{(g_1 + g_2)(g_3 + g_5)}{g_3 g_5}\right] + M_{tnp}\left[\frac{(g_1 + g_2)(g_3 + g_4 + g_5)}{g_1 g_2}\right] \qquad (5.24)$$

$$P_n = (M_{tnp} + M_{tnn}) \left[(g_1 + g_2) \left(\frac{1}{g_3 + g_4} + \frac{1}{g_6 + g_7} \right) \right]$$

$$+ (M_{lnp} + M_{lnn}) \left\{ [g_4 + g_5 + g_6] \left[\frac{1}{g_1} + \frac{1}{g_2} \right] \right.$$

$$+ [g_3^2] \left[\left(\frac{1}{g_2 g_3 + g_2 g_4} \right) + \left(\frac{1}{g_1 g_3 + g_1 g_4} \right) \right]$$

$$\left. + [g_7^2] \left[\left(\frac{1}{g_2 g_6 + g_2 g_7} \right) + \left(\frac{1}{g_1 g_6 + g_1 g_7} \right) \right] \right\} \tag{5.25}$$

$$P_n = [P_n]_{Eq.5.24} + M_{lnn} \left[\frac{g_3 + g_4 + g_5}{g_1} \right] \tag{5.26}$$

$$P_n + (M_{tnp}) \left[(g_1 + g_2) \left(\frac{1}{g_3} + \frac{1}{g_5} \right) \right] + (M_{lnp}) \left[\frac{g_3 + g_4 + g_5}{g_2} \right]$$

$$+ (M_{tnp} + M_{tnn}) \left[\left(\frac{g_9^2}{g_5 g_9 + g_1 g_8} \right) + \left(\frac{g_9^2}{g_3 g_9 + g_1 g_6} \right) \right]$$

$$+ (M_{lnp} + M_{lnn}) \left[\left(\frac{g_8^2}{g_1 g_8 + g_7 g_9 + g_8 g_9} \right) + \left(\frac{g_6^2}{g_1 g_6 + g_3 g_9} \right) + \left(\frac{g_7}{g_1 + g_9} \right) \right] \tag{5.27}$$

$$P_n = (M_{tnp}) \left[(g_1 + g_2) \left(\frac{1}{g_3} + \frac{1}{g_5} \right) \right] + (M_{lnp} + M_{lnn}) \left[\frac{g_3 + g_5}{g_1} \right] \tag{5.28}$$

$$P_n = \left[\frac{2(y_1 + g_4 + g_5)}{2(y_1 + g_5) + g_4}\right]\left\{(M_{tnp})\left[\left(\frac{g_1 + g_2}{g_3}\right) + \left(\frac{y_1 + g_5}{y_1 + g_4 + g_5}\right)\left(\frac{g_1 + g_2 - g_{10}}{g_5}\right) + \left(\frac{2(g_1 + g_2 - g_9) - g_{10}}{y_2 - g_3}\right)\right]\right.$$

$$\left. + (M_{lnp})\left(\frac{g_3 + g_4 + g_5}{g_2 - x_2}\right) + (M_{lnp} + M_{lnn})\left(\frac{g_3 + g_4 + g_5}{g_1}\right)\right\} \qquad (5.29)$$

$$with,\ g_9 = g_1\left(\frac{y_1 + g_5}{y_1 + g_4 + g_5}\right)$$

$$x_2 = g_3\left(\frac{g_{10}}{g_3 + g_4 + g_5}\right)$$

$$y_2 = g_2\left(\frac{g_3 + g_4 + g_5}{g_{10}}\right)$$

$$y_1 = \left(\frac{g_3 + g_4 + g_5}{g_{10}}\right)(g_1 + g_2 - g_{10})$$

$$P_n = \left[\frac{2(y_{1G} + g_4 + g_5)}{2(y_{1G} + g_5) + g_4}\right]\left\{(M_{tnp})\left[\left(\frac{g_1 + g_2}{g_3}\right) + \left(\frac{g_{10}}{y_{3G}}\right) + \left(\frac{g_{11} + g_{12}}{g_5}\right)\left(\frac{y_{1G} + g_5}{y_{1G} + g_4 + g_5}\right)\right]\right.$$

$$\left. + (M_{lnp})\left[\frac{g_3 + g_4 + g_5}{x_{3G}}\right]\right.$$

$$\left. + (M_{tnp} + M_{tnn})\left[\left(\frac{g_{13}(y_{1G} + g_5)}{(g_5 + y_{6G})(y_{1G} + g_4 + g_5)}\right) + \left(\frac{g_9}{y_{9G} + g_3}\right) + \left(\frac{g_1 + g_2 + g_9 - g_{10} - g_{11} - g_{12} - g_{13}}{y_{7G} - g_3 + g_6}\right)\right]\right.$$

$$\left. + (M_{lnp} + M_{lnn})\left[\left(\frac{g_8(y_{16} + g_5)}{(g_{12} + g_{13} + x_{6G})(y_{1G} + g_4 + g_5)}\right) + \left(\frac{g_7}{x_{7G}}\right) + \left(\frac{g_6}{x_{9G}}\right)\right]\right\} \qquad (5.30)$$

with,

$$y_{1G} = \frac{x_{1G}(g_3 + g_4 + g_5)}{g_{10}}$$

$$x_{1G} = \frac{\left[\frac{(g_4)(g_{11})}{g_{10} + g_{11} - g_2}\right] + g_5}{\left(\frac{g_4}{g_{10} + g_{11} - g_2}\right) - \left(\frac{g_3 + g_4 + g_5}{g_{10}}\right)}$$

$$y_{3G} = \frac{x_{3G}(g_3 + g_4 + g_5)}{g_{10}}$$

$$x_{3G} = (y_{1G} + g_4 + g_5)\left[\left(\frac{g_{10}}{g_3 + g_4 + g_5}\right) - \left(\frac{g_{10} + g_{11} - g_2}{g_4}\right)\right]$$

$$y_{6G} = \frac{(g_8)(g_{12})}{g_{13}}$$

$$x_{6G} = \frac{g_{13}(g_5 - g_8)}{g_8}$$

$$y_{7G} = \frac{g_7(g_1 + g_9)}{g_1 + g_2 + g_9 - g_{10} - g_{11} - g_{12} - g_{13}}$$

$$x_{7G} = g_1 + g_2 - \left(\frac{g_3 - g_6}{g_7}\right)(g_1 + g_2 + g_9 - g_{10} - g_{11} - g_{12} - g_{13})$$

$$y_{9G} = \frac{(g_1)(g_6)}{g_9}$$

$$x_{9G} = \frac{(g_1)(g_6) + (g_3)(g_9)}{g_6}$$

5.4. Punching Shear Model

When a reinforced concrete slab is subjected to a concentrated load, a punching shear failure may occur before a yield-line mechanism can become fully developed. According to the AASHTO Specification [1], the nominal punching shear strength of the concrete, V_{nc}, in a non-composite slab is expressed as

Table 6.1. Concrete strengths, modulus of elasticity, and modulus of rupture (continued).

Concrete Element	Age (days)	f'_c (psi)	E_c[a] (ksi)	E_c[b] (ksi)	f_r[c] (psi)	f_r[b] (psi)
Topping	28	6,451	4,530	4,578	-	602
#3 West	85[e]	7,186	5,574	4,832	632	636
Topping	8	5,629	4,213	4,276	-	563
#4 East	21	6,332	4,075	4,536	-	597
	113[e]	7,462	4,665	4,924	608	648
Topping	15	6,624	4,828	4,639	-	610
#4 West	28	7,202	4,437	4,837	-	636
	113[e]	8,165	4,827	5,151	586	678
Topping	7	4,598	3,492	3,865	-	509
#5 East	14	5,949	3,775	4,396	-	578
	21	6,132	4,216	4,464	-	587
	28	6,251	4,196	4,507	-	593
	62	7,197	4,285	4,836	-	636
	88[e]	7,520	4,591	4,943	628	639
Topping	7	4,504	3,864	3,825	-	503
#5 West	14	5,518	4,309	4,234	-	557
	21	6,109	4,012	4,455	-	586
	28	6,447	4,306	4,577	-	602
	62	6,950	4,438	4,752	-	625
	88[e]	7,229	4,533	4,846	668	638

[a]Experimental result.
[b]Computed value.
[c]Topping slab age for the ultimate load test.
[d]Questionable test result.
[e]Precast panel age for the ultimate load test on Specimen No. 1.
[f]Precast panel age for the ultimate load tests on Specimen No. 3.
[g]Precast panel age for the ultimate load tests on Specimen No. 4.
[h]Precast panel age for the ultimate load tests on Specimen No. 5.

Also listed in Table 6.1 are the computed values for the modulus of elasticity and modulus of rupture obtained from the expressions

$$E_c = 57{,}000\sqrt{f'_c} \tag{6.1}$$

$$f_r = 7.5\sqrt{f'_c} \tag{6.2}$$

A dash (-) shown in the table indicates that an experimental test was not conducted to establish that particular parameter for the concrete age listed.

The east and west designations shown in the first column of Table 6.1 corresponds to the directional orientation in the laboratory for the region of the reinforced concrete topping slab where concrete cylinders and prisms were made during the casting of the concrete for the topping slab in Specimen Nos. 2 through 5. For these specimens, the first ultimate strength test was performed on the west end of the composite slab, and the second ultimate strength test was conducted on the east end of the composite slab. Specimen No. 1 was loaded directly over the joint between the two precast panels during the ultimate load test; therefore, an east end or west end designation was not required.

6.1.2. Prestressing Strand Modulus of Elasticity

Modulus of elasticity values for the prestressing strands were determined by performing tensile tests on three segments of strand that were approximately 20 feet long. The tests were conducted in a horizontal test frame. For safety reasons, the strands were tensioned up to a maximum stress of 190 ksi (70% of the ultimate strength). Loads were monitored with a load cell and the displacements at the ends of the strands were measured with displacement transducers. For the three tests, the experimentally based values for the modulus of elasticity, E_s, were 27,955, 27,946, and 29,282 ksi. The average value of E_s, equal to 28,394 ksi, was in good agreement with the published magnitude of 28,000 ksi for 7-wire, low-relaxation, 270 Grade prestressing strand.

6.2. Strand Embedment Lengths

6.2.1. Strand Transfer Lengths

The precast, prestressed, concrete panels were constructed with normal-weight concrete and low-relaxation, 270 Grade, prestressing strands which were prestressed to 0.75 f'_s prior to casting the panels. The material properties and panel cross-sectional parameters described in Section 4.1 are summarized in Table 6.2.

Table 6.2. Panel parameters related to strand transfer length.

Prestressing Strand		Reinforced Concrete	
Parameter	Magnitude	Parameter	Magnitude
f'_s	270 ksi	f'_{ci}	4,810 psi
E_s	28,000 ksi	E_{ci}	3.95×10^6 psi
A_s^*	0.085 in.^{2}	A_c	14.915 in.^{2}
D	0.375 in.		

Substituting the appropriate parameters from Table 6.2 into Eq. (5.3), the computed compressive stress, f_{cir}, at the centroid of the strands and mid-depth of the panels is given by

$$f_{cir} = \frac{0.69(270{,}000)(0.085)}{14.915} = 1{,}062 \ psi$$

The prestress loss, ES, due to elastic shortening of a precast panel can be evaluated by Eq. (5.2) as

$$ES = (28x10^6)\left(\frac{1{,}062}{3.95x10^6}\right) = 7{,}526 \ psi$$

The initial strand prestress, f_{si}, for a panel with an adequate strand transfer length is obtained from Eq. (5.11) as

$$f_{si} = (0.75)(270{,}000) - 7{,}526 = 195{,}000 \ psi$$

Applying an alternate method for evaluating the stress, f_{si}, which is based on equating the change

in lengths of the strands and the concrete panel, the initial strand prestress according to Eq. (5.12) is given by

$$f_{si} = \frac{(0.75)(270{,}000)}{\left[1 + \left(\frac{28x10^6}{3.95x10^6}\right)\left(\frac{0.085}{14.915}\right)\right]} = 194{,}600\ psi$$

Both approaches produced essentially the same strand prestress. Substituting the stress f_{si} equal to 195,000 psi for the 3/8 in. diameter strands into the modified ACI Code Commentary expression Eq. (5.10), the initial strand transfer length, L_{ti}, for the precast panels used in this research was calculated to be

$$L_{ti} = \left[\frac{195{,}000}{3(1{,}000)}\right](0.375) = 24.4\ in.$$

Other analytically derived initial strand transfer lengths can be established from expressions presented in Sec. 5.1. Applying the empirical equation (Eq. 5.13) suggested by Zia and Mustafa [33], the initial strand transfer length can be computed as

$$L_{ti} = (1.5)\left(\frac{195{,}000}{4{,}810}\right)(0.375) - 4.6 = 18.2\ in.$$

Also, by substituting the initial strand prestress, f_{si}, for the effective prestress, f_{se}, in Eq. (5.8), an initial transfer length can be calculated from the expression proposed by Cousins et al [13] as

$$L_{ti} = \left[\frac{(0.5)(6.7)\sqrt{4{,}810}}{300}\right] + \left[\frac{(195{,}000)(0.085)}{\pi(0.375)(6.7)\sqrt{4810}}\right]$$

$$L_{ti} = 30.3\ in.$$

Returning to the modified ACI Code Commentary approach for strand transfer length, Fig. 6.1 illustrates the relationship between the initial strand prestress and the embedment length of a strand

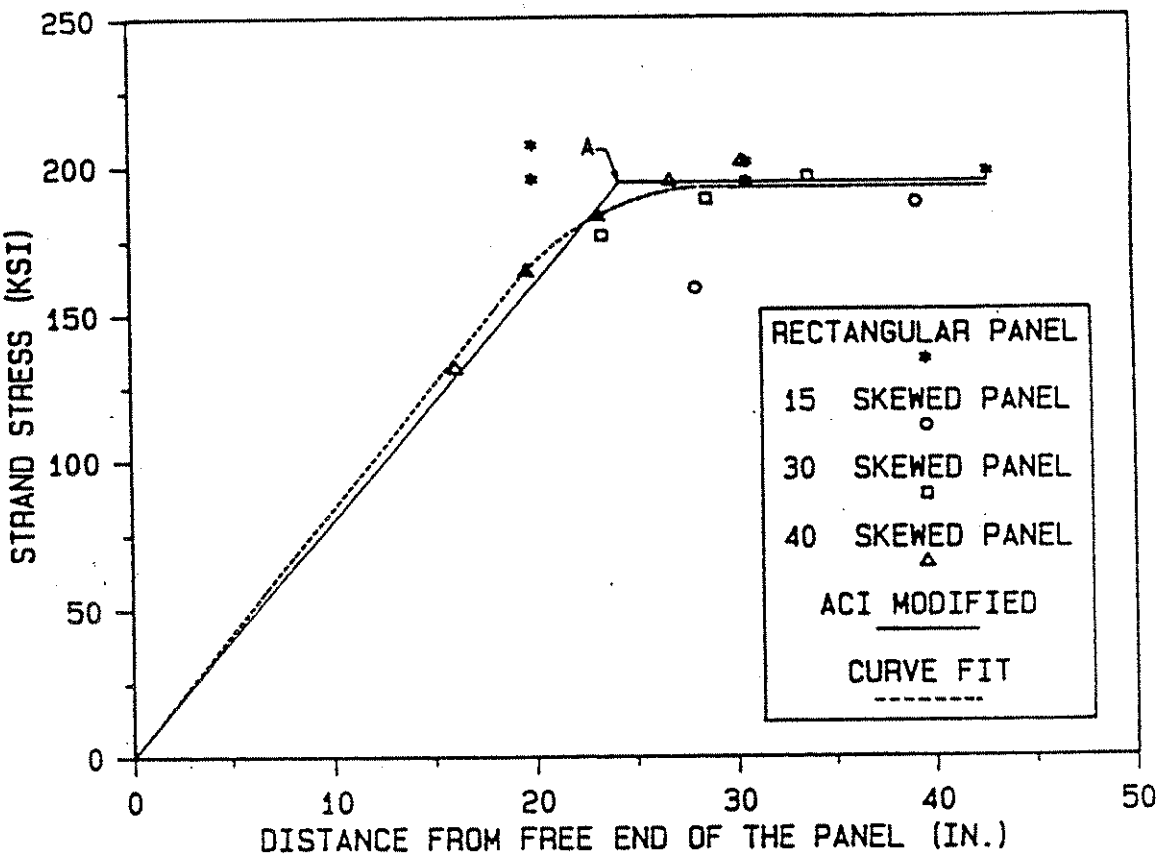

Figure 6.1. Strand embedment versus initial strand prestress.

measured from the end of a precast panel. Point A corresponds to the condition at which the maximum initial prestress of 195 ksi is obtained when the initial strand transfer length is equal to 24.4 in. The bi-linear curve (solid lines) represents the behavior associated with the modified ACI Code Commentary expression in which the initial strand prestress, f_{si}, is substituted for the effective strand prestress, f_{se}. The data points shown in Fig. 6.1 were established from experimentally measured concrete strains at known locations in the four monitored precast panels. The strain readings, obtained from the PML-30 gauges which were embedded in the concrete, were taken before, during, and after the strands were cut at the prestress plant. Since the gauges were positioned between adjacent strands, visual curvalinear interpolations and extrapolations were used to establish concrete strains at the prestressing strand locations. Assuming that strand slippage did not occur between the concrete and the prestressing strands within the interior regions of the panels where the strain gauges were located, the change in the strand stress was evaluated by multiplying the induced concrete strain adjacent to a strand by the modulus of elasticity of the prestressing strand. Knowing the stress in the strands from the strand elongation before the strands were released, the final strand stress after transfer was computed and plotted in Fig. 6.1. The dotted curve shown in Fig. 6.1 was visually established as a "best-fit" curve through the computed data points. The experimental strain obtained from one of the strain gauges in the 15 deg. skewed panel was low, since this gauge was located between a bonded and an unbonded (sleeved) strand. As Fig. 6.1 shows, the correlation between the experimental and analytical behavior was excellent.

An experimentally derived initial strand transfer length, L_{ti}, of about 28.5 in. was established by observing where the dotted curve becomes tangent with the dotted horizontal line, corresponding to an initial prestress of about 193 ksi. To obtain the maximum initial prestress, the total panel length at a strand location would have to be at least twice as long as L_{ti} or about 57 in. If a shorter length of panel along a strand existed, a decrease in the initial strand prestress would occur as shown by the dotted curve in Fig. 6.1.

Other researchers have experimentally established initial strand transfer lengths. Table 6.3 lists experimental results obtained by Kear et al [22], Cousins et al [13], Over and Au [27], and Abendroth et al (reported herein) for 3/8 in. diameter, uncoated, 7-wire prestressing strands.

Table 6.3. Initial strand transfer lengths for 3/8 in. diameter, 7-wire uncoated prestressing strands.

f_{si} (ksi)	f'_{ci} (psi)	L_{ti} (in.)	Researcher
177.1	1,690	24.5	Kear et al
169.7	3,400	28.5	
158.2	5,000	25.5	
164.8	3,250	32.0	
141.5	3,450	26.0	
119.1	3,400	23.0	
146.0	3,150	33.0	
187.0	4,190	26.0	Cousins et al
182.8	4,190	35.0	
183.7	4,190	36.0	
184.2	4,190	42.0	
199.9	4,120	34.0	
194.9	4,120	34.0	
195.9	4,120	38.0	
200.1	4,120	38.0	
199.4	4,120	36.0	
195.9	4,120	38.0	
194.5	4,120	38.0	
194.8	4,120	38.0	
193.9	4,810	30.0	
194.8	4,810	30.0	
194.3	4,810	26.0	

Table 6.3. Initial strand transfer lengths for 3/8 diameter, 7-wire uncoated prestressing strands (continued).

f_{si} (ksi)	f'_{ci} (psi)	L_{ti} (in.)	Researcher
195.5	4,810	26.0	Cousins et al
133.0	4,180	30.0	Over and Au
195.0	4,810	28.5	Abendroth et al

Significant variation occurred for the experimentally derived initial strand transfer lengths shown in Table 6.3. The average transfer length, L_{ti}, for the tests conducted by Kear et al, in which the initial strand stress was larger than 150 ksi and the concrete strength at the time of transfer was greater than 3,000 psi, was equal to 28.7 in. For the lower and higher strength concrete tests performed by Cousins et al, the average transfer lengths were equal to 36.1 in. and 28.0 in., respectively.

The initial strand transfer length of 28.5 in. obtained from the experimental work of this research is in agreement with the lengths obtained by these other researchers. The experimentally established transfer length of 28.5 in. is about 17 and 34 percent larger and 6 percent smaller than the analytically derived transfer lengths predicted by the modified ACI Code [3] Commentary expression, Zia and Mustafa's [33] proposed equation, and Cousins et al's [13] recommended formula, respectively.

A confirmation of the accuracy of the experimentally derived strand prestress versus strand embedment length relationship was obtained from a finite element analysis of the trapezoidal-shaped precast panel which was used in 40 degree skewed specimen configuration. Knowing that the available strand transfer length was equal to one-half of the total strand embedment length, the initial prestress for each bonded strand in the panel was established from the curve (dotted line) shown in Fig. 6.1. The strand prestress forces were obtained by multiplying the initial prestress for each strand by the strand area, A_s^*. These forces were applied to the nodes representing the ends of the strands in the finite element model (Fig. 5.1), and the resulting concrete strains at Nodes 79,

95, 110, and 125 were computed. Table 6.4 shows that excellent correlation occurred between the analytical and experimentally measured strains at these points.

Table 6.4. Concrete strains in 40 degree skewed panel.

Node No.	Analytical Strain (μ in./in.)	Experimental Strain (μ in./in.)
79	-229	-228
95	-260	-254
110	-270	-270
125	-281	-286

To calculate the final transfer length, L_t, the additional prestress loss due to concrete creep, CR_c and shrinkage, SH, and strand relaxation, CR_s, were evaluated. For the precast panels used in this research, these strand stress losses, established from Eqs. (5.4), (5.5) with a 70 percent mean ambient relative humidity, and (5.6), are computed as

$$CR_c = 12(1{,}062) - 7(0) = 12{,}744 \text{ psi}$$

$$SH = 17{,}000 - 150\ (70) = 6{,}500 \text{ psi}$$

$$CR_s = 5{,}000 - (0.10)(7{,}526) - 0.05\ (6{,}500+12{,}744)$$

$$CR_s = 3{,}285 \text{ psi}$$

The total prestress loss ($ES+CR_c+SH+CR_s$), excluding friction, was calculated to be equal to 30,055 psi, which is less than the estimated prestress loss of 45,000 psi listed in the AASHTO Specification [1] Table 9.16.2.2. Once the prestress losses have been established, the effective prestress, f_{se}, can be computed from Eq. (5.1) as

$$f_{se} = 0.75(270{,}000) - 30{,}055 = 172{,}400 \text{ psi}$$

Substituting f_{se} into Eq. (5.7), the transfer length, L_t, becomes

$$L_t = \left[\frac{172{,}400}{3(1000)}\right](0.375) = 21.6\ in.$$

Applying the transfer length expression presented by Cousins et al [13] the transfer length for the prestressing strands in the precast panel used in this research was computed from Eq. (5.8) as

$$L_t = \left[\frac{(0.5)(6.7)\sqrt{4{,}810}}{300}\right] + \left[\frac{(172{,}400)(0.085)}{\pi(0.375)(6.7)\sqrt{4{,}810}}\right] = 27.5\ in.$$

This length is about 27 percent longer than the length obtained by applying the ACI Code [3] Commentary approach.

6.2.2. Strand Flexural Bond Strength

As shown by Eqs. (5.14), (5.18), and (5.20), the flexural bond length is a function of the strand stress, f^*_{su}, corresponding to the nominal flexural strength of the section; the effective strand prestress, f_{se}; the nominal strand diameter, D; the reinforcement ratio, ρ^*, or area, A^*_s, of the prestressing steel within the cross section; and the concrete compressive strength, f'_c, for the cross section. Since each slab specimen tested was a composite deck consisting of two precast prestressed concrete panels and a reinforced concrete topping slab, the parameters f^*_{su}, ρ^*, and f'_c were different for each specimen. The concrete strength, f'_c, should be the strength associated with the topping slab, since positive bending moments place the upper portions of the topping slab in compression. Table 6.5 lists the composite slab parameters needed to calculate the flexural-bond lengths and the lengths L_{fb} computed from Eq's (5.14), (5.18), and (5.20) required to develop the maximum nominal strength for each ultimate load test. The effective depth, d_p, to the centroid of the prestressing strands was obtained by subtracting 1 1/4 in. (one-half of the panel thickness) from the mid-span slab thicknesses listed in Table 4.1.

Table 6.5. Computed flexural-bond lengths.

Specimen No.	Ultimate Test No.	f'_c (psi)	d_p (in.)	ρ^* ($x10^{-3}$)	f^*_{su} (ksi)	L^a_{fb} (in.)	L^b_{fb} (in.)	L^c_{fb} (in.)
1	1	7,346	6.83	2.074	259.7	32.7	55.7	40.9
2	1	6,990	6.22	2.278	258.1	32.1	56.0	40.2
	2	7,596	6.26	2.263	259.1	32.5	54.4	40.6
3	1	7,186	7.04	2.012	259.8	32.8	56.4	41.0
	2	7,257	7.33	1.933	260.3	33.0	56.4	41.2
4	1	8,165	6.99	2.027	261.0	33.2	53.6	41.5
	2	7,462	7.35	1.927	260.6	33.1	55.8	41.3
5	1	7,229	6.68	2.121	259.3	32.6	55.9	40.7
	2	7,520	6.90	2.053	260.0	32.9	55.2	41.1

[a]Computed from Eq. (5.14).
[b]Computed from Eq. (5.18) with $U'_d = 1.32$.
[c]Computed from Eq. (5.20).

6.2.3. Strand Development Length

Analytical solutions for the strand development length, L_d, were obtained by adding together the strand transfer and flexural bond lengths. Table 6.6 lists the development lengths established by applying the ACI Code expression, Eq. (5.22), or the AASHTO Eq. (9-19); the equation proposed by Cousins et al (Eq. (5.8) + Eq. (5.18)); and the formulas suggested by Zia and Mustafa (Eq. (5.13) + Eq. (5.20)).

The development lengths listed in Table 6.6 can be applied to establish the minimum precast panel lengths for midspan wheel loads. Assuming that the 5 in. strand extension length that projects from each end of a precast panel (Fig. 4.6) are fully encased by the concrete from the topping slab and contribute to the total development length of a strand, the minimum precast panel lengths would have to be about 8.2, 13.0, and 9.0 ft, according to ACI or AASHTO Specifications, Cousins et al, and Zia and Mustafa, respectively, to fully develop the nominal flexural stength of the composite deck. If only the strand embedment length within the precast panel are considered effective in

Table 6.6. Computed strand development lengths.

Specimen No.	Ultimate Test No.	Development Lengths (in.)		
		ACI/AASHTO	Cousins et al	Zia and Mustafa
1	1	54.3	83.2	59.1
2	1	53.7	83.5	58.4
	2	54.1	81.9	58.8
3	1	54.4	83.9	59.2
	2	54.5	83.9	59.4
4	1	54.8	81.1	59.7
	2	54.7	83.3	59.5
5	1	54.2	83.4	58.9
	2	54.5	82.7	59.3
Average		54.4	83.0	59.1

developing a strand, the panel lengths would have to be 9.1, 13.8, and 9.9 ft. for the same three approaches. The length established by applying the recommended expressions of Cousins et al are significantly longer than the lengths obtained from the other two methods. If the criteria specified by the Federal Highway Administration memorandum [16] is applied, the development length for the 3/8 in. diameter, 270 Grade, prestressing strand would have to be 1.6 times the length established by AASHTO [1] Eq. (9-32), since the strands used in this research were stressed to 70 percent of their guaranteed ultimate tensile strength of 270 ksi. Then, the minimum precast panel length should not be less than 9.1 ft. times 1.6 or 14.6 ft. This length is close to the minimum panel length established by applying the expressions proposed by Cousins et al. The rectangular panel lengths used in the experimental test specimens were 7.1 ft. The trapezoidal-shaped panels had much shorter concrete lengths available for the strands which intersected the diagonal panel edge. Therefore, based on analytically established development lengths, the full nominal flexural strength

of the composite slab specimens would not be obtainable, since a bond failure between the prestressing strands and the surrounding concrete would occur before the strands would reach the stress f_{su}^*.

6.2.4. Strand-Slip Results

The experimental tests of the composite slab specimens did not provide explicit strand development lengths, due to the three dimensional behavior of the slabs. A qualitative evaluation of the strand development lengths was performed by monitoring the ends of selected strands, as discussed in Section 4.2.3, for movement relative to the ends of the panel. Any relative strand movement would represent strand slippage. Strand slippage can only occur after the actual bond stresses between the strand and the surrounding concrete, along the entire strand embedment length from the point of maximum strand force to the end of the panel, have exceeded the nominal bond stress resistance. If strand slippage occurred, the bond strength at the location of the strand would have been reached.

To establish if slippage of a particular monitored strand occurred, graphs of load versus slip were developed. Due to the sensitivity of the monitored movements, some of the extraneous raw data results were adjusted or eliminated. For the plotted data, "best-fit" curves were drawn to match the experimental results. After the load versus slip relationship had been graphically represented, measurable strand-slip was considered to have occurred when the "best-fit" curve digressed from the initial vertical line that represented no strand-slip. Figures 6.2, 6.3, 6.4, and 6.5 show representative load versus strand-slip relationships for an ultimate strength test on Specimen Nos. 1, 2, 4, and 5, respectively. Strand-slip at the monitored locations did not occur during the service level or factored level load tests.

The slippage characteristics associated with movement of the end of a prestressing strand involved either a sudden slip, as illustrated by the graph of the S3 strand-slip in Fig. 6.4 for Specimen

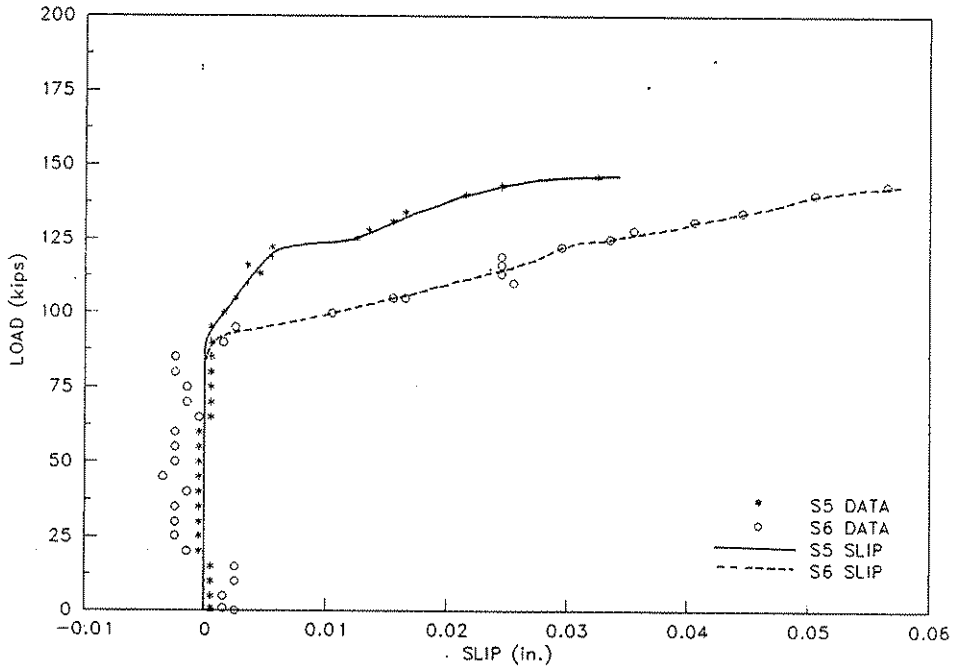

Figure 6.2. Strand-slip at S5 and S6 during ultimate load test on Specimen No. 1.

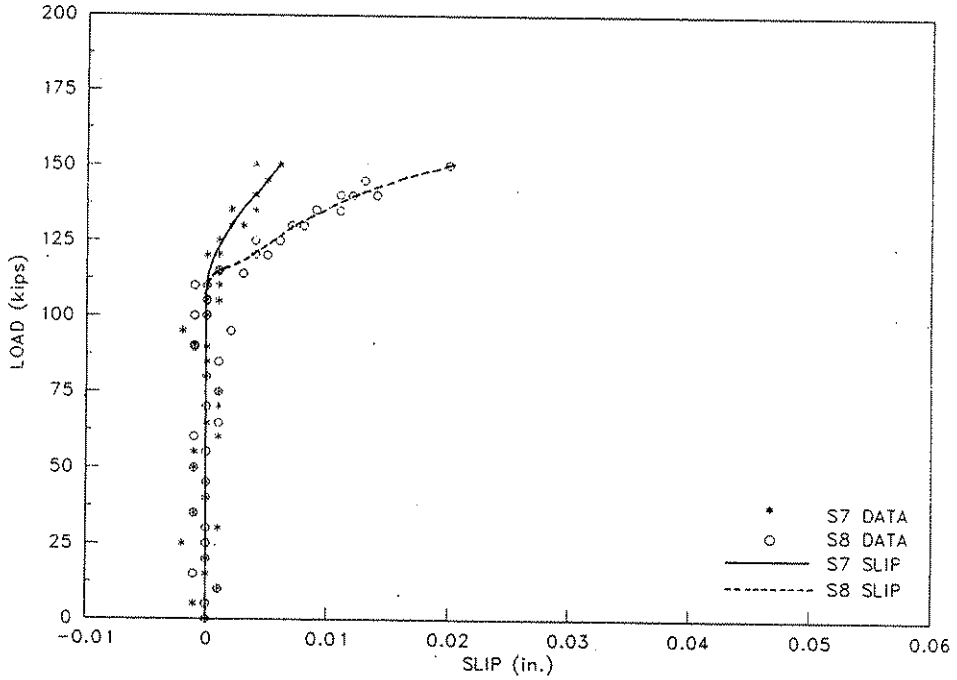

Figure 6.3. Strand-slip at S7 and S8 during ultimate Test No. 1 on Specimen No. 2.

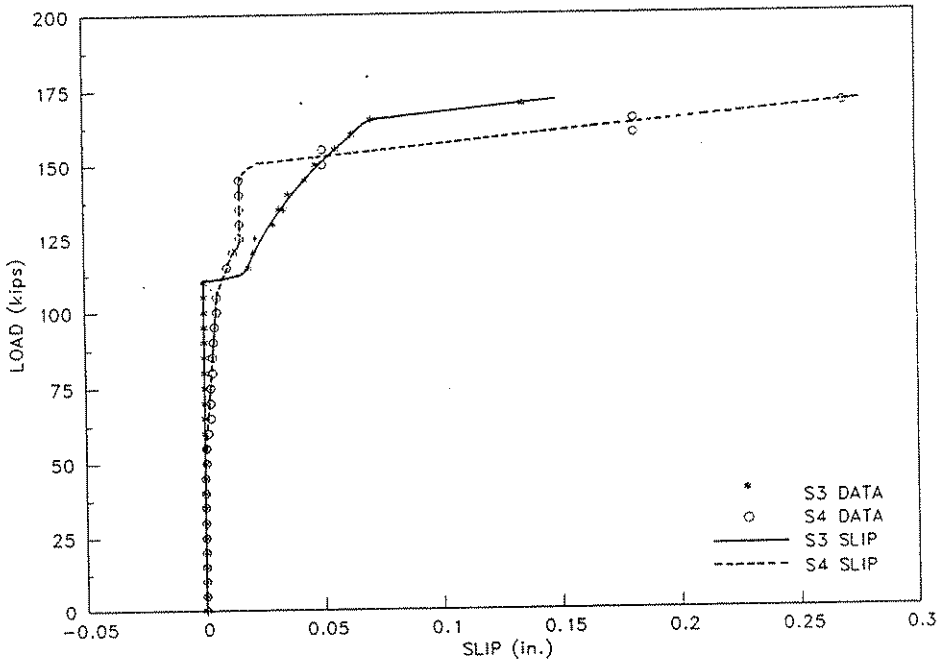

Figure 6.4. Strand-slip at S3 and S4 during Ultimate Test No. 1 on Specimen No. 4.

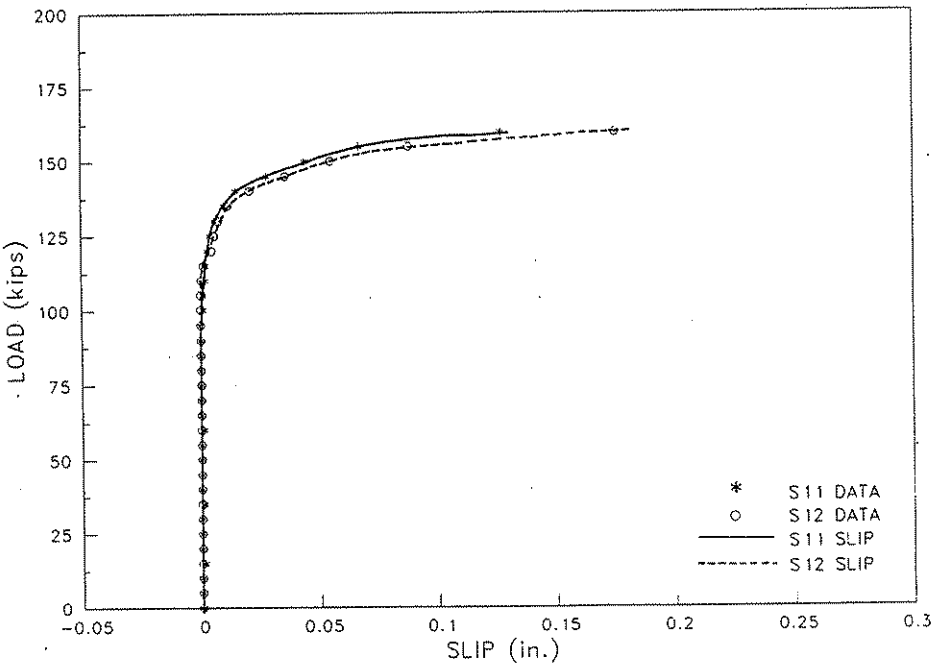

Figure 6.5. Strand-slip at S11 and S12 during Ultimate Test No. 1 on Specimen No. 5.

No. 4, or as a gradual slip, as shown by the S11 or S12 strand-slip curves in Fig. 6.5 for Specimen No. 5. The strand-slip locations S11 and S12 were on opposite ends of the same strand as shown in Fig. 4.18. The magnitudes of an initial strand-slip was normally around a few thousandths of an inch. As the loading continued, the amount of slip increased and in many instantaneous reached well over a tenth of an inch before the slab failed.

Table 6.7 lists the load, P_{ss}, at which strand-slip was initiated at a particular location, based on an interpretation of a graph showing load versus strand movement at the end of a panel, for the five composite slab specimens. The strand-slip location (S1 through S20) refers to the displacement instrumentation designation shown in Figs. 4.14 through 4.18 for Specimen Nos. 1 through 5, respectively. The odd numbers for the strand-slip corresponded to the north end of the strands and the even numbered strand-slip locations were on the south end of the strands. Both ends of the same strand were monitored for movement. A superscript shown in the table designates the location of that particular strand with respect to the wheel load position. A dash (-) indicates that strand-slip at that particular location did not occur during the ultimate load test. The letter "M" shown in the table represents an erratic result attributed to a transducer malfunction.

Listed at the bottom of Table 6.7 are the minimum load, P_{ssm}, causing slip in any of the monitored strands for A particular ultimate load test; the ultimate experimental load, P_u, for the slab; the ratio of P_{ssm} to P_u; and the ratio of P_{ssm} to the HS-20 AASHTO wheel load, P_w, including 30 percent impact. The maximum ratio of P_{ssm} to P_u for all of the slab specimens was 0.73, which indicates that even after strand slippage occurred in the strand(s), a significant reserve strength still existed for these composite slabs. The minimum ratio of P_{ssm} to P_w for all of the slab specimens was 2.64, which indicates that strand-slip did not initiate in any of these slabs until a load equal to approximately two and one-half times the design load, P_w, had been placed on the slab.

Table 6.7. Strand-slip loads (kips).

Specimen No.		1	2		3		4		5	
Ultimate Test No.		1	1	2	1	2	1	2	1	2
Strand - Slip Location	S1	65[i]	-[n]	-[a]	-[m]	125[a]	-[l]	-[a]	-[k]	-[a]
	S2	90[i]	-[n]	105[a]	-[m]	M[a]	-[l]	70[a]	-[k]	105[a]
	S3	90[a]	-[i]	100[h]	135[a]		110[a]		-[j]	-[a]
	S4	90[a]	-[i]	100[h]	-[a]		55[a]		-[j]	105[a]
	S5	90[a]	115[h]	110[i]	165[g]		125[b]		-[b]	
	S6	85[a]	-[h]		115[g]		85[b]		-[b]	
	S7	90[i]	110[a]				100[c]		110[a]	
	S8	85[i]	110[a]				75[c]		85[a]	
	S9						120[d]		95[a]	
	S10						120[d]		105[a]	
	S11						100[e]		95[b]	
	S12						145[e]		110[b]	
	S13						120[f]		110[c]	
	S14						120[f]		M[c]	
	S15						85[g]		110[d]	
	S16						110[g]		110[d]	
	S17								95[e]	
	S18								75[e]	
	S19								95[f]	
	S20								80[f]	
P_{ssm}		65	110	105	115	125	55	70	75	105
P_u		145	150	155	175	175	170	165	160	153
P_{ssm}/P_u		0.45	0.73	0.68	0.66	0.71	0.32	0.42	0.47	0.69
P_{ssm}/P_w		3.13	5.28	5.05	5.53	6.01	2.64	3.37	3.61	5.05

M represents a transducer malfunction.

Distance Between Monitored Strand and the Load Point

[a]0 in. [b]6 in. [c]12 in. [d]18 in. [e]24 in. [f]30 in. [g]36 in.
[h]42 in. [i]48 in. [j]72 in. [k]76 in. [l]78 in. [m]84 in. [n]96 in.

6.3. Composite Deck Slabs

6.3.1. Composite Behavior

For the precast concrete panels and the cast-in-place reinforced concrete slab to behave as a composite deck, relative movement between the two slab elements must not occur. As shown in Figs. 4.7 and 4.8, the top surface of the panels had longitudinal grooving to develop an interlock with the cast-in-place topping slab. The effectiveness of this grooving to obtain composite action was evaluated by inspecting core samples and by investigating the load versus slip behavior between the panels and the topping slab at various points within the deck span and at the ends of the panel span.

6.3.2. Core Samples

A visual inspection of the interface between the precast panels and the topping slab was accomplished by drilling 3 in. diameter core samples through selected locations in Specimen Nos. 3 and 4. These samples revealed that good bonding between the two concrete elements had taken place. Some of the cores, which were drilled through a slab reinforcing bar and a panel prestressing strand, showed that the concrete in both portions of the total slab thickness had enveloped the steel completely.

6.3.3. Interface-Slip Results

When composite interaction between two slab elements begins to deteriorate due to flexural loading, the initial distress will occur within the length of the span. As additional loading is applied, the propogation of the discontinuity between the strain at the top of the precast panel and the strain at the bottom of the topping slab will progress towards the supports in a wave-front type of action. If the strain discontinuity condition extends to the end of the slab, composite behavior between the two slab elements will be lost in this region of the deck, and physical movement between the topping slab and precast panel will occur at the end(s) of the span.

To detect the initiation of composite behavior deterioration, the strain condition at the interface between the precast panels and the reinforced concrete slab was investigated by analyzing the strain distribution through the total slab thickness. At several locations for each of the composite slab specimens, three strain gauges were positioned in vertical alignment. Strain gauges were mounted on the top and bottom surfaces of the precast panel and another strain gauge was attached to the top surface of the topping slab, as shown in Figs. 4.19 through 4.23 for Specimen Nos. 1 through 5, respectively. Unfortunately, many of the strain gauges which were glued to the top surface of the precast panels malfunctioned due to moisture penetration of the waterproofing barrier placed over the strain gauges and lead wire connections.

For those locations where a set of three vertically aligned strain gauges recorded reliable bending strains, a graph of the strain distribution through the depth of the slab could be drawn. If complete composite behavior existed, the three measured strain values would lie along a straight line. When a deterioration of composite interaction had begun, the three measured strains would not be co-linear.

The difference in the bending strains between the top of a precast panel and the bottom of the reinforced concrete slab was obtained by realizing that the curvature for both the panel and the topping slab has to be the same at a given cross section, if vertical separation between the two slab elements does not occur at the point of horizontal strain discontinuity. Therefore, for a given load application, a straight line connecting the measured concrete strains at the top and bottom surfaces of the precast panel must be parallel to a straight line constructed through the measured concrete strain at the top surface of the reinforced concrete slab. Knowing that the topping slab thickness was equal to the total slab thickness less the panel thickness, the strain at the bottom of the reinforced concrete slab was calculated. The numerical difference between the bending strains in the two slab elements at their common plane has been termed the interface-slip.

Figures 6.6, 6.7, 6.8, and 6.9 show representative load versus interface-slip relationships for an ultimate strength test on Specimen Nos. 1, 2, 5, and 5, respectively. Interface-slip at the monitored locations involving three properly functioning strain gauges did not occur during the service load or factored load tests. Since the calculated interface-slip amounts are not "precise" magnitudes, visually obtained, "best-fit", curves were drawn through the computed data points. Interface-slip was considered to have occurred when a significant change from the initial load versus slip behavior was observed. Theoretically, the initial load versus interface-slip relationship should be a vertical line. However, the strain calculations for the initial behavior produced an inclined line. This difference has been attributed to computational errors which were induced by the sensitivity of the calculations. A small error in a thickness measurement would produce large differences in computed strains. Therefore, even though the initial behavior was not represented by a vertical line in these figures, the initial linear relationship still represents a no-slip condition. The interface-slip can occur gradually as shown in Fig. 6.8 for the slip at Location I9 on Specimen No. 5, or the interface-slip can occur suddenly as illustrated in Fig. 6.6 by the slip at Location I3 on Specimen No. 1.

The magnitudes of the interface-slip can be small as shown by the abscissa values in the graphs. For Location I4 on Specimen No. 1 (Fig. 4.19) the magnitude of the interface-slip shown in Fig. 6.6 was less than 10 micro in./in. (0.000010 in./in.) when the initial break-down of composite behavior was considered to have begun.

Table 6.8 lists the interface-slip load, P_{is}, for a given location obtained from a graphical interpretation as to when slippage was initiated in the load versus interface-slip behavior for the ultimate load tests conducted on the five composite slab specimens. The interface-slip location (I1 through I16) refers to the strain gauge numbering designations shown in Figs. 4.19 through 4.23 for Specimen Nos. 1 through 5, respectively. A superscript shown in the table designates the lateral position of the interface gauge location with respect to the wheel load position. A dash (-) indicates that slippage at the interface between the topping slab and the precast panel did not occur at that

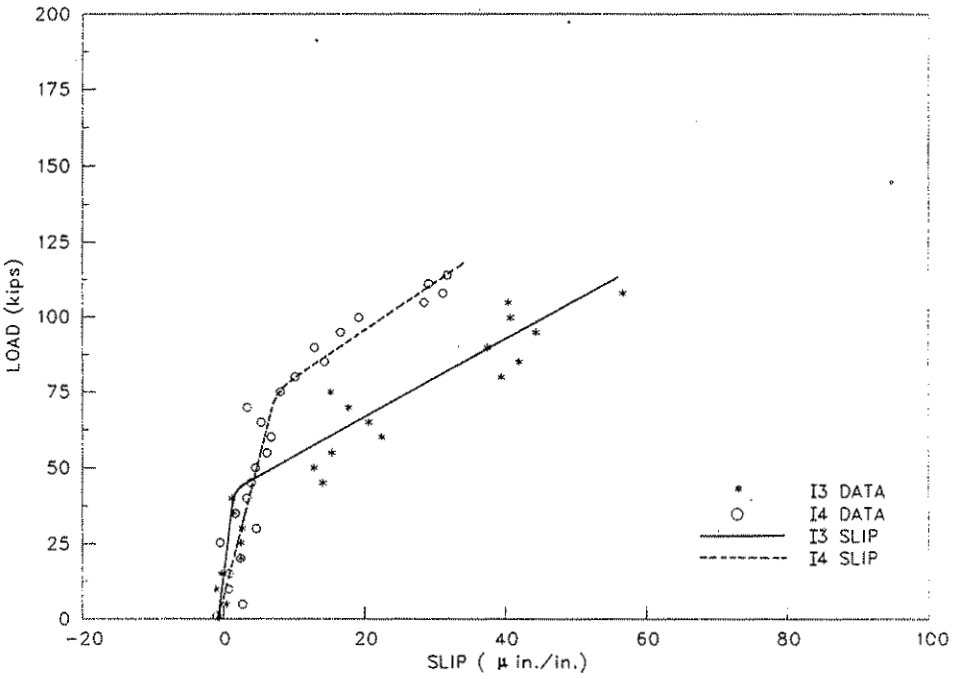

Figure 6.6. Interface-slip at I3 and I4 during Ultimate Test No. 1 on Specimen No. 1.

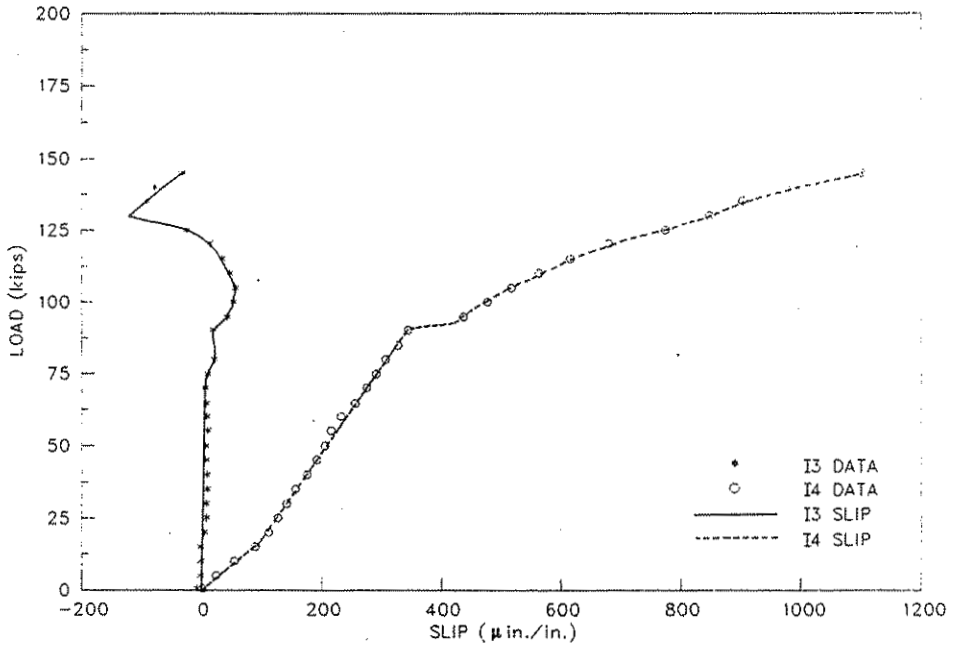

Figure 6.7. Interface - slip at I3 and I4 during Ultimate Load Test No. 1 on Specimen No. 2.

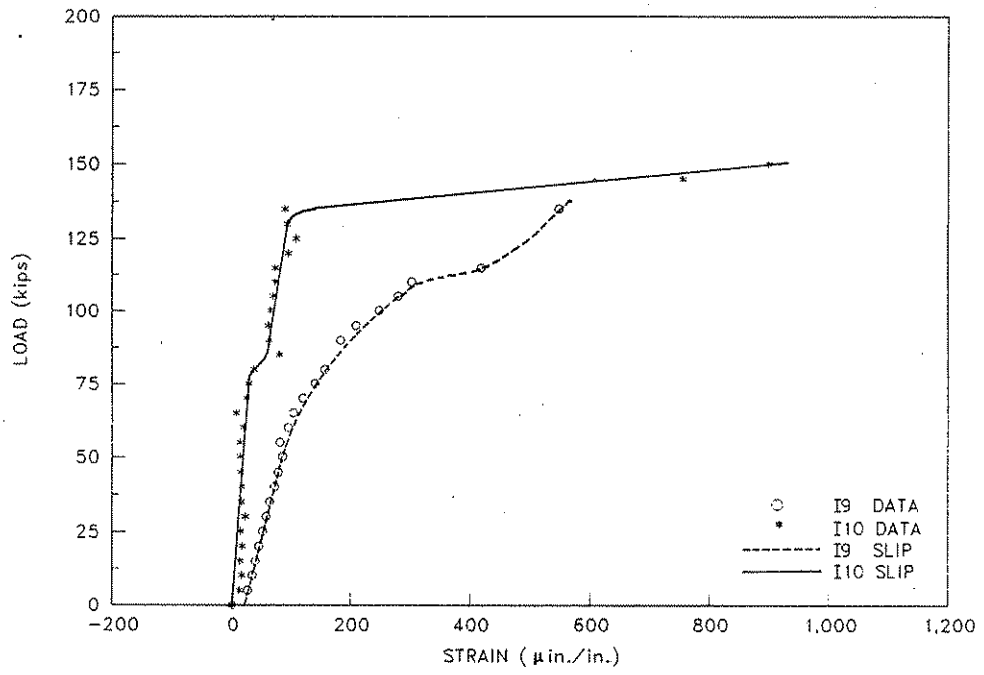

Figure 6.8. Interface-slip at I9 and I10 during Ultimate Test No. 1 on Specimen No. 5.

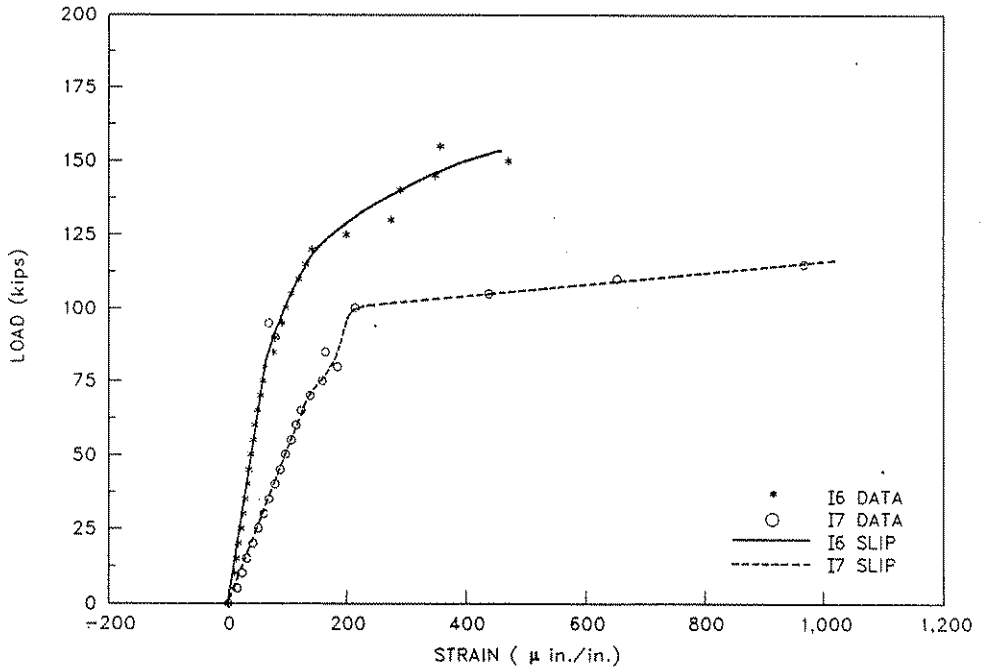

Figure 6.9. Interface-slip at I6 and I7 during Ultimate Strength Test No. 1 on Specimen No. 5.

Table 6.8. Interface-slip loads (kips).

Specimen No.		1	2		3		4		5	
Ultimate Test No.		1	1	2	1	2	1	2	1	2
Interface - Slip Location	I1	M[i]	M[i]	40[a]	M[g]		M[a]		-[k]	60[a]
	I2	85[f]	M[j]	90[h]	M[a]		M[a]		-[k]	55[a]
	I3	40[f]	70[h]		M[a]		M[a]		-[k]	60[a]
	I4	75[i]	90[a]		M[a]		M[e]		-[k]	70[a]
	I5		M[e]		M[e]		M[e]		-[k]	55[a]
	I6		105[e]		M[e]		M[g]		80[a]	
	I7						M[d]		75[a]	
	I8						M[b]		M[a]	
	I9								60[a]	
	I10								75[a]	
	I11								95[e]	
	I12								80[e]	
	I13								75[e]	
	I14								80[e]	
	I15								70[h]	
	I16								70[h]	
P_{ism}		40	70	40					60	55
P_u		145	150	155	175	175	170	165	160	153
P_{ism}/P_u		0.28	0.47	0.26					0.38	0.36
$P_{ism}P_w$		1.92	3.37	1.92					2.88	2.64

M represents a strain gauge or system malfunction.

Distance Between Measured Strain and the Load Point

[a]6 in. [b]7 in. [c]9 in. [d]11 in. [e]12 in. [f]18 in.
[g]24 in. [h]30 in. [i]54 in. [j]66 in. [k]72 in. [l]102 in.

location during the ultimate load test. The letter "M" shown in the table represents a strain gauge or system malfunction.

Listed at the bottom of Table 6.8 are the minimum load, P_{ism}, causing interface-slip at any of the monitored locations for the particular ultimate load test; the ultimate experimental load, P_u, for the slab; the ratio of P_{ism} to P_u; and the ratio of P_{ism} to the HS-20 AASHTO wheel load, P_w, including 30 percent impact. The maximum ratio of P_{ism} to P_u for Specimen Nos. 1, 2, and 5 was 0.47, which indicates that even after initial break-down of composite behavior had begun at some internal regions of the composite slab, a substantial reserve strength still existed for these slabs. The minimum ratio of P_{ism} to P_w for Specimen Nos. 1, 2, and 5 was 1.92, which indicates that interface-slip did not initiate in any of these slabs until a load equal to approximately two times the design load, P_w, had been placed on the slab. Since malfunctions occurred for the instrumentation associated with all of the interface-slip measurements for Specimen Nos. 3 and 4, conclusions regarding this type of slip can not be made for those specimens; however, similar results would have been expected.

6.3.4. Topping-Slip Results

As discussed in Sec. 6.3.3, once the interface-slip had progressed to an end of the span for a slab specimen, a relative movement between the precast panel and the reinforced concrete slab occurred at that end of the specimen. This relative displacement was termed topping-slip. Measurements of the relative horizontal movement between the two slab elements were taken at various locations along the ends of the span, as shown in Figs. 4.14 through 4.18 for Specimen Nos. 1 through 5, respectively.

To determine if topping-slip occurred, graphs of load versus slip were generated. As mentioned in the discussion on strand-slip (Sec. 6.2.4), data reduction of experimental results required elimination or adjustment of some of the scatter of the recorded measurements. After the data point pairs (load and slip amounts) were plotted, visually established, "best-fit" curves were drawn to represent the load versus topping-slip behavior. Measureable topping-slip was considered to have

occurred with the "best-fit" curve digressed from the initial vertical line that represented no topping-slip. Figures 6.10, 6.11, 6.12, and 6.13 show representative load versus topping-slip relationships for ultimate strength tests on Specimen Nos. 1, 2, 3, and 5, respectively. Topping-slip did not occur during the service or factored level load tests.

When topping-slip occurred, the movement was either gradual or sudden. Figure 6.13 illustrates both types of behavior for Specimen No. 5, during the ultimate strength test on the portion of the slab near the skewed diaphragm support. Topping-slip T4 occurred gradually, commencing at a load of about 105 kips; white, topping-slip T3 began more suddently at a load of about 85 kips. These movements were measured at opposite ends of the slab, as shown in Fig. 4.18. The initial magnitudes for the topping-slip were a few thousandths of an inch. When a slab specimen reached its ultimate load capacity, some of the topping-slip amounts were equal to about two-tenths of an inch.

Table 6.9 lists the load, P_{ts}, at which slippage between one of the precast panels and the reinforced concrete slab was obtained for each ultimate strength test on the five composite slab specimens. The topping-slip location (T1 through T6) refers to the displacement instrumentation designation shown in Figs. 4.14 through 4.18 for Specimen Nos. 1 through 5, respectively. The odd numbers for the topping-slip correspond to the north end of a specimen and the even numbers for the slip relate to the south end of a specimen. A superscript shown in the table refers to the location of the slip measurement with respect to the wheel load position. A dash (-) indicates that topping-slip did not occur at that particular location during the ultimate load test.

Listed at the bottom of Table 6.9 are the minimum load, P_{tsm}, causing relative movement between the two slab elements at any of the monitored locations along the ends of a specimen; the ultimate experimental load, P_u, for the slab; the ratio of P_{tsm} to P_u; and the ratio of P_{tsm} to the HS-20 AASHTO wheel load, P_w, including 30 percent impact. The maximum ratio of P_{tsm} to P_u for all of the slab specimens was 0.82, which indicates that even after a partial loss of composite behavior

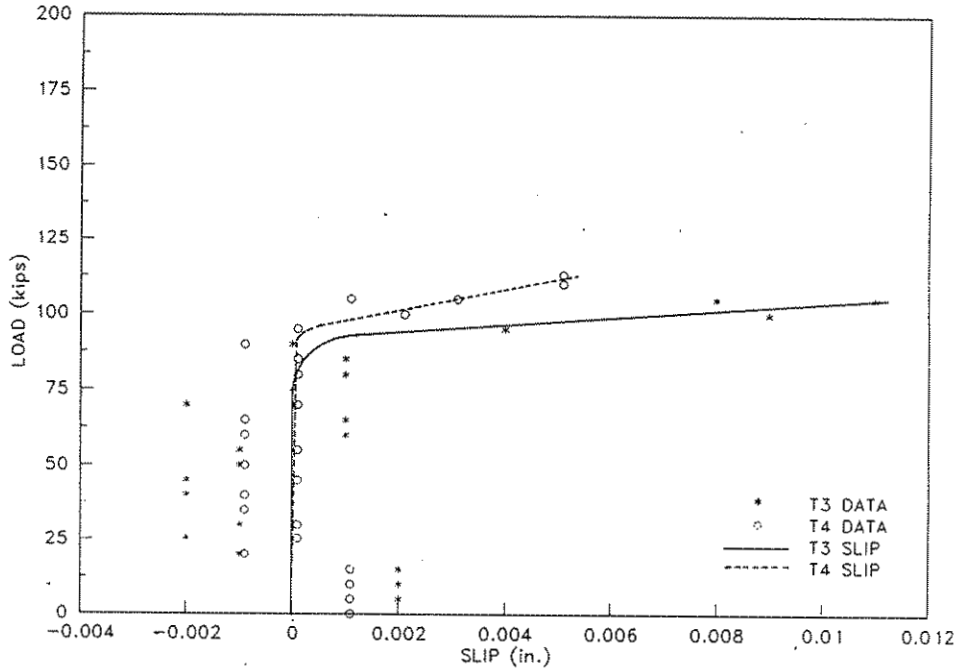

Figure 6.10. Topping-slip at T3 and T4 during Ultimate Load Test on Specimen No. 1.

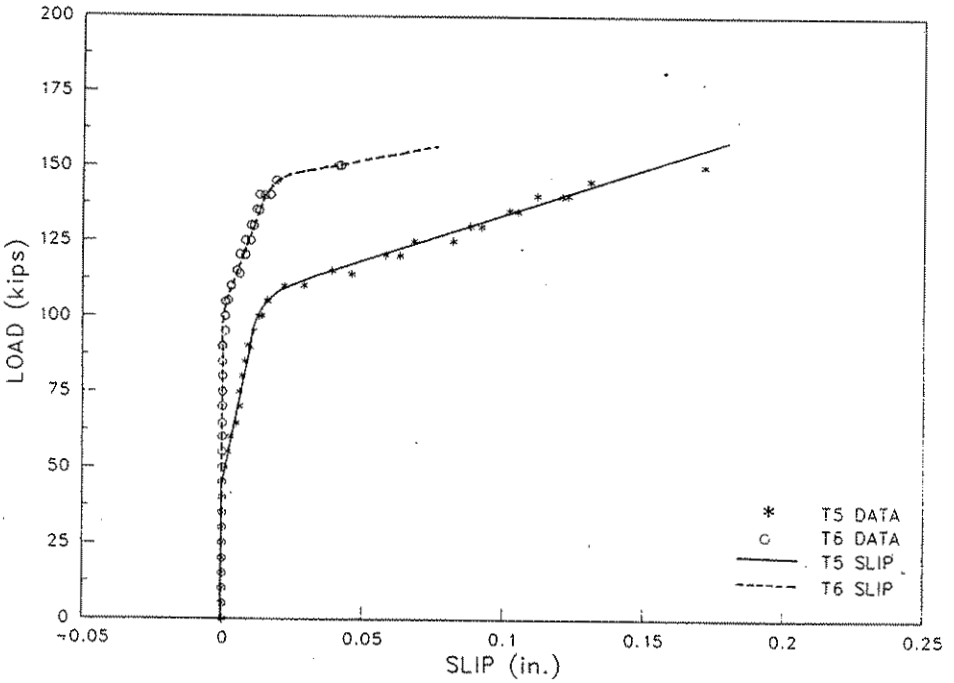

Figure 6.11. Topping-slip at T5 and T6 during Ultimate Strength Test No. 1 on Specimen No. 2.

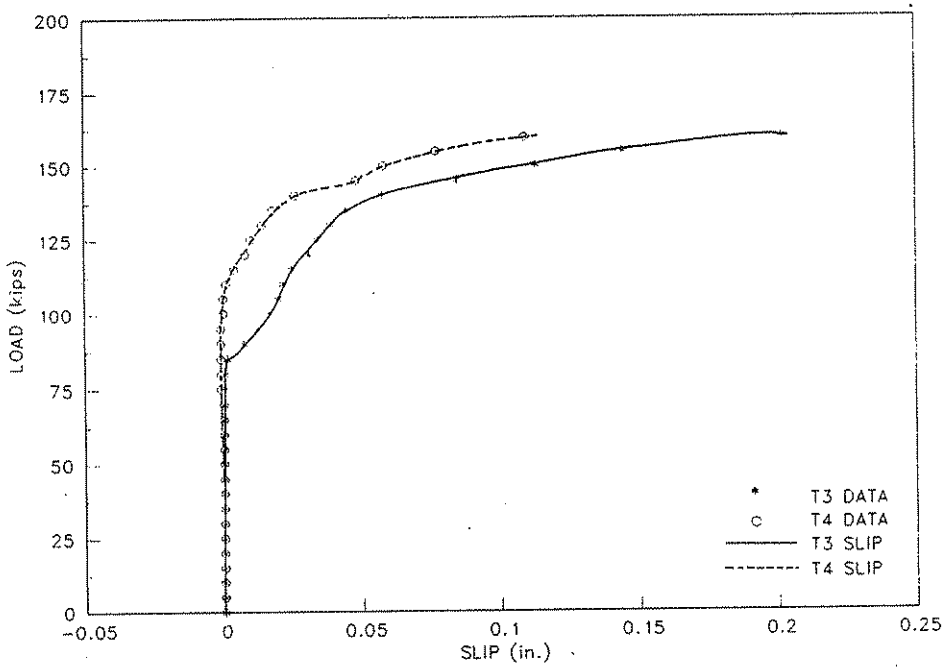

Figure 6.12. Topping-slip at T3 and T4 during Ultimate Test No. 1 on Specimen No. 3

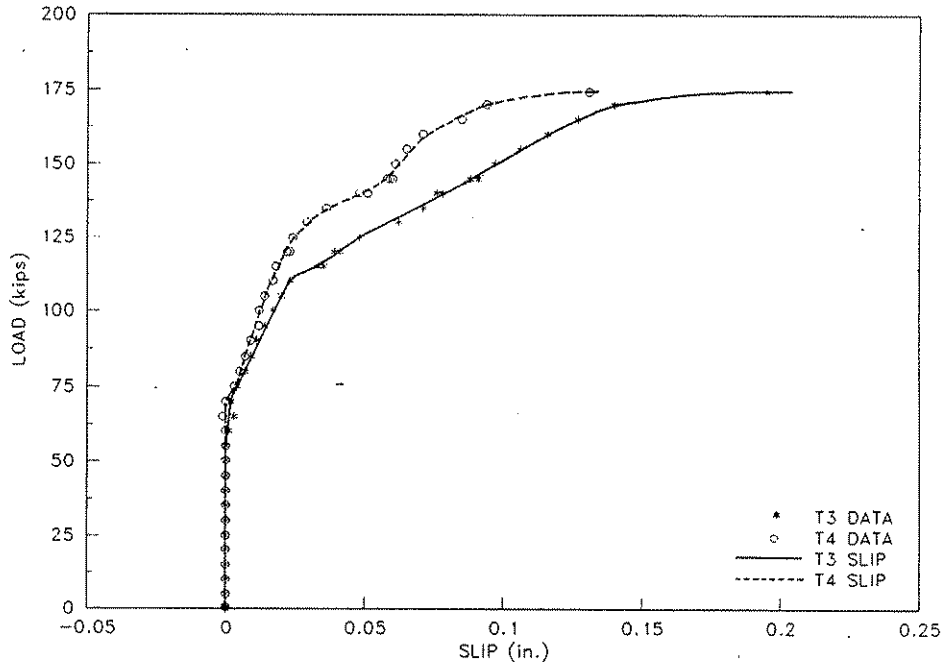

Figure 6.13. Topping-slip at T3 and T4 during Ultimate Test No. 1 on Specimen No. 5.

occurred a reasonable amount of slab strength still existed before a complete failure of this portion of the specimen was obtained. The minimum ratio of P_{tsin} to P_w for all of the slab specimens was 2.16, which indicates that a load of over two times the design wheel load, P_w, was required before topping-slip occurred.

Table 6.9. Topping-slip loads (kips).

Specimen No.		1	2		3		4		5	
Ultimate Test No.		1	1	2	1	2	1	2	1	2
Topping-Slip Location	T1	50[b]	-[f]	90[a]	-[e]	150[a]	-[d]	-[a]	-[c]	125[a]
	T2	85[b]	-[f]	M[a]	-[e]	90[a]	-[d]	85[a]	-[c]	-[a]
	T3	75[a]	-[b]	100[b]	60[a]		115[a]		85[a]	
	T4	90[a]	-[b]	-[b]	70[a]		-[a]		105[a]	
	T5	75[b]	45[a]							
	T6	80[b]	95[a]							
P_{tsm}		50	45	90	60	90	115	85	85	125
P_u		145	150	155	175	175	170	165	160	153
P_{tsm}/P_u		0.34	0.30	0.58	0.34	0.51	0.68	0.52	0.53	0.82
P_{tsm}/P_w		2.40	2.16	4.33	2.88	4.33	5.53	4.09	4.09	6.01

M represents a transducer malfunction.
[a]Measurement in line with load point.
[b]Measurement offset 48 in. from load point.
[c]Measurement offset 78 in. from load point.
[d]Measurement offset 84 in. from load point.
[e]Measurement offset 90 in. from load point.
[f]Measurement offset 96 in. from load point.

6.4. Load Versus Deflection Relationships

6.4.1. Service Level Loads

A measure of the stiffness of the composite slab specimens was obtained by establishing load versus deflection relationships for several load ranges. As discussed in Section 4.2.2., concentrated loads were placed at many locations on the top surface of the slab. The majority of the loads were confined to be within the service level load range of from zero to 20.8 kips. For this load range, the load versus deflection behavior for a single wheel load placed above the mid-width and midspan (Position No. 1A) of the east precast panel (Fig. 4.9) of Specimen No. 1 is shown in Fig. 6.14. The deflections are the average of the deflections measured on each side of the wheel footprint (Fig. 4.14). The graph shows both the experimental displacements and the deflections obtained from a finite element analysis, involving a model similar to the one shown in Fig. 5.3. The experimental results were adjusted to account for small vertical movements at the bearing ends of the slab. The displacement behavior was linear as can be observed from the figure and remained elastic throughout the entire load range. The correlation between the analytical solution for the load versus deflection behavior and the experimental deflection amounts was excellent, considering the potential test scatter associated with deflection measurements of concrete structures and the small magnitudes of deflections involved. The maximum deflection at the load point was about 0.012 in. when the 20.8 kip load was acting. This displacement represents about one-seven thousandth of the span length.

Similar load versus deflection relationships were established for other wheel load positions on all specimens. As anticipated, the finite element results showed greater divergence from the experimental results near the regions of a slab adjacent to and at the joint between the two precast panels and when the geometry of the slabs became more complex near a skewed diaphragm support condition.

Figure 6.15 shows the vertical deflections along the precast panel span for a single 20.8 kips wheel load applied over Position No. 1A (Fig. 4.9) of Specimen No. 1 for both the experimental and

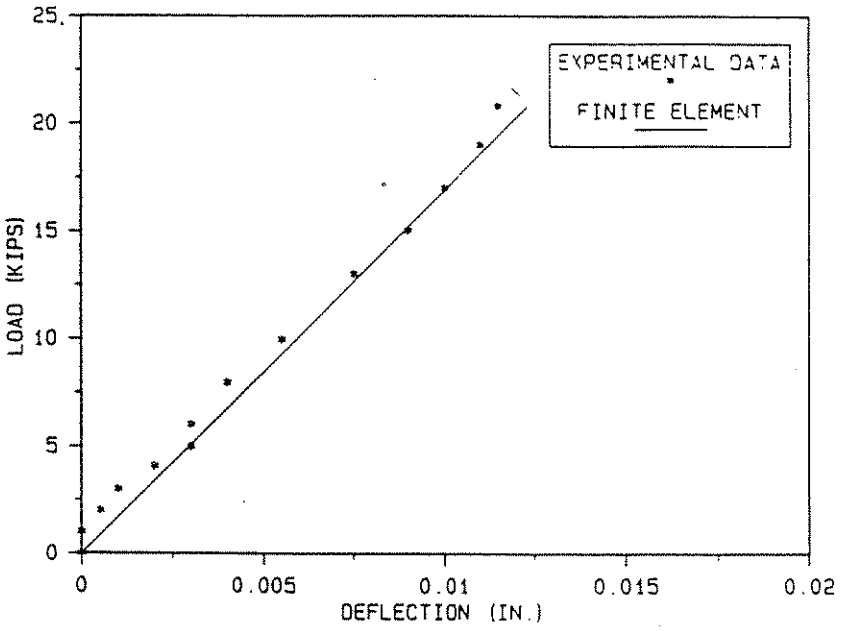

Figure 6.14. Load versus deflection for a single load at position No. 1A on Specimen No. 1.

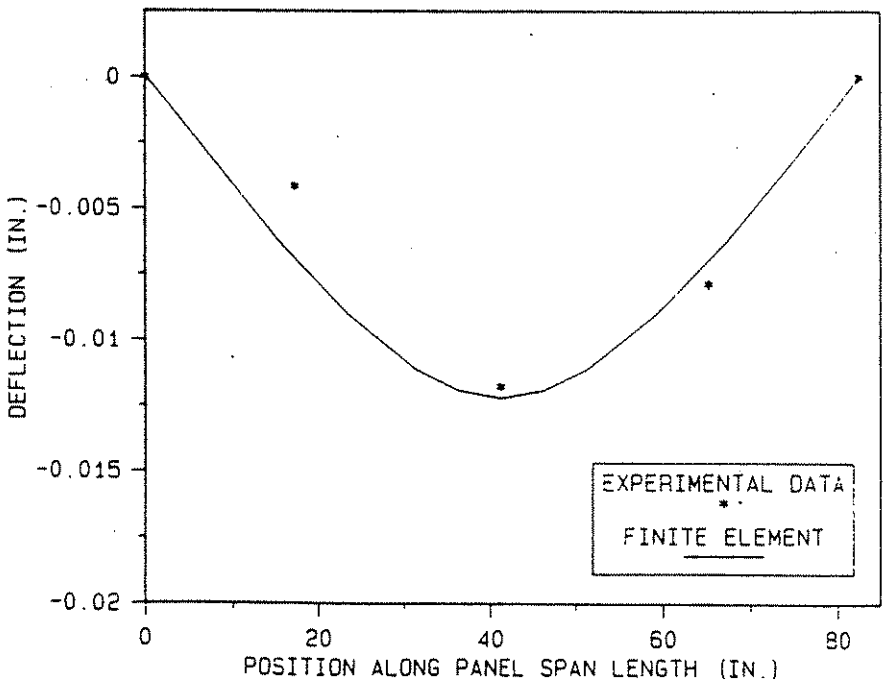

Figure 6.15. Deflections along the precast panel span for a single 20.8 kip load at No. 1A on Specimen No. 1.

finite element results. The midspan deflection corresponds to the maximum deflection shown in Fig. 6.14. As shown in Fig. 6.15, very good correlation occurred between the analytical and experimental results. For the other wheel load positions on this specimen and the other four specimens, similar results were obtained.

Double wheel loads spaced 4 ft. apart were also applied to the composite slab specimens. A four foot spacing was selected, since this is the minimum spacing to be considered by the AASHTO Specification [1] when two trucks are adjacent to each other. For the service level load range, each concentrated load had a minimum value of zero and a maximum magnitude equal to 20.8 kips. The loads were simultaneously applied through AASHTO footprints (8 in. by 20 in.). Figure 6.16 is a plot of the load versus the vertical deflection at the midspan for a double load at Position Nos. 3C on Specimen No. 3 (Fig. 4.11). The loads were located over the joint between the two precast panels. The analytical and experimental results for this load case are very similar to the results shown in Fig. 6.14 for a single load at the mid-width and midspan panel location on Specimen No. 1. The maximum midspan deflection of the composite slab for the double load condition was also equal to approximately 0.012 in. For the same load positions, the slab deflections along the panel span when the two loads were at their maximum magnitude of 20.8 kips each are shown in Fig. 6.17. Excellent correlation between the analytical and experimental results occurred.

6.4.2. Factored Level Loads

Specimen Nos. 4 and 5 were subjected to factored loads at selected locations on the slab surface as listed in Table 4.2. These two specimens experienced a load range of from zero to 48 kips. Load versus deflection relationships for two wheel load locations (Position Nos. 1D and 2E in Fig. 4.12) on Specimen No. 4 are shown in Figs. 6.18 and 6.19 and for one wheel load location (Position No. 1D in Fig. 4.13) on Specimen No. 5 is shown in Fig. 6.20. The slab deflections shown in these figures for the experimental results are the average of the deflections on each side of the load point. Figure 6.18 illustrates that the analytical model closely predicted the displacement behavior for the

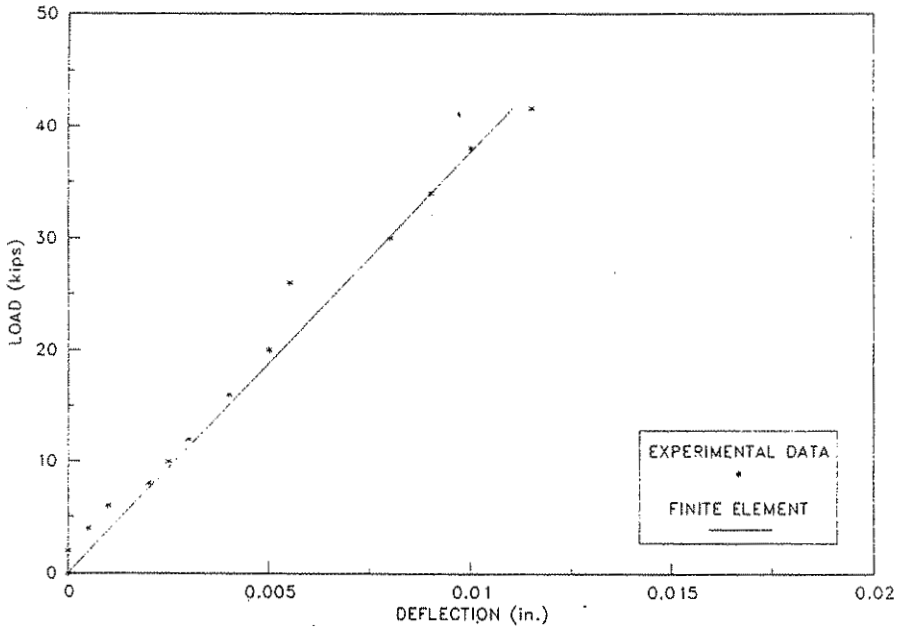

Figure 6.16. Load versus deflection for a double load at Position Nos. 3C on Specimen No. 3.

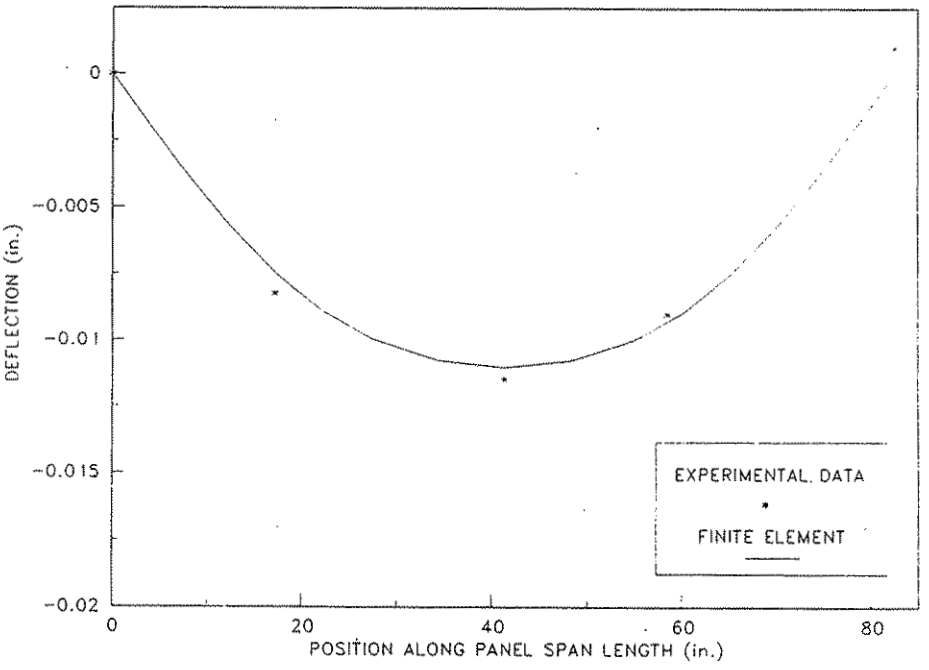

Figure 6.17. Deflections along the precast panel span for a double 20.8 kip load at Position Nos. 3C on Specimen No. 3.

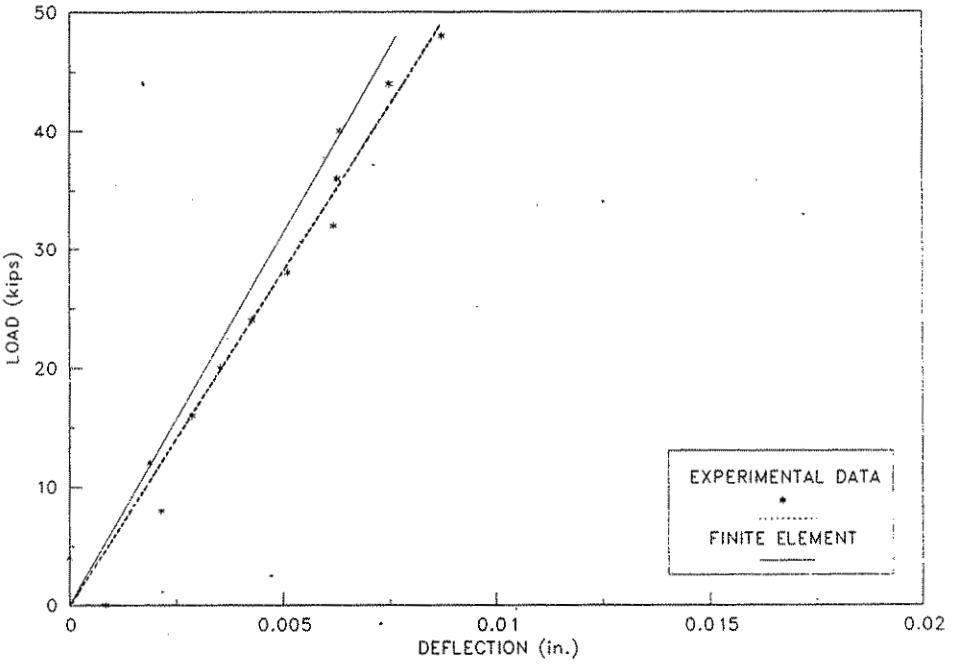

Figure 6.18. Load versus deflection for a single load at Position No. 1D on Specimen No. 4.

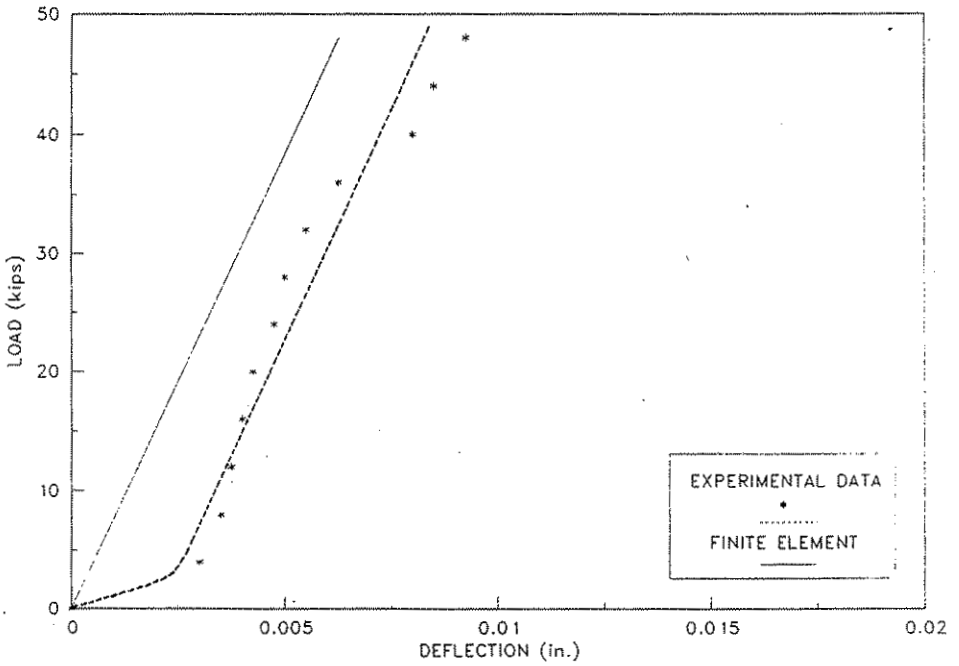

Figure 6.19. Load versus deflection for a single load at Position No. 2E on Specimen No. 4.

composite slab specimen when the load was incremented through the factored load range. The presence of the slab support along the skewed edge of the specimen significantly reduced the slab deflection from the amounts which occurred at locations not near a longitudinal edge support. Recall that a maximum deflection of 0.012 in. occurred for Specimen No. 1 when a service level load equal to 20.8 kips was applied over the mid-width and midspan of the east panel. Figure 6.18 shows that for the same load magnitude the deflection at Position No. 1D on Specimen No. 4 is about 0.0035 in. or approximately 30 percent of the previous amount of deflection.

The experimentally measured load versus deflection relationships shown in Figs. 6.19 and 6.20 as the dashed lines involves two distinct displacement behaviors. For low magnitudes of load (less than about 6 kips), the slab stiffness appears to be small; while for larger loads, the slab stiffness appears to have increased significantly. This anomaly was caused by a change in the slab support conditions as load was applied to Specimen Nos. 4 and 5 in the region of the slabs adjacent to the skewed support. Prior to placing any loads on a composite slab specimen, the corners of the slabs were observed to have lifted up off the concrete supports. Since the speicmens were not anchored to the supports, upward vertical movement was not restrained. This movement was attributed to the shrinkage of the concrete in the cast-in-place topping slab. The shrinkage was restrained along the bottom of the specimens by the precast panels, which had become composite with the topping slab. Since the concrete in the precast panels was substantially older than the concrete in the topping slabs, most of the panel shrinkage had already occurred prior to casting the topping slabs. The panel restraint caused the specimens to distort with a concave upward curvature, which caused the corners of the slabs to displace upwards. This effect was more pronounced at the acute corners of Specimen Nos. 4 and 5, representing the 30 and 40 degree skewed configurations, respectively. When low magnitudes of load were applied near this region of a composite slab specimen, the edges of the slab near the corners still were not bearing on the concrete supports. As the load was increased, these

slab edges eventually began to bear on the supports, which caused the apparent increase in the slab stiffness.

The finite element analysis did not model this uplift condition; therefore, the load versus deflection relationships shown in Figs. 6.19 and 6.20 for the analytical results involve a single straight line representing linearly elastic behavior. A comparison of the slopes of the load versus deflection relationships between the finite element solutions and the experimental results (above a load of about 10 kips) revealed that the analytical model closely matched the stiffness of the slab when the load was applied at Position No. 1D (Fig. 6.18) and 2E (Fig. 6.19) on Specimen No. 4, but underestimated the slab stiffness when the load was applied at Position No. 1D (Fig. 6.20) on Specimen No. 5.

An actual composite bridge deck should not experience the uplift conditions caused by shrinkage of the concrete in the topping slab, since the slab is anchored to the bridge girders and the abutment and pier diaphragms. Shrinkage of the concrete will still occur; therefore, with large skew angles, significant residual stresses will be induced into the bridge deck in these regions of the composite slabs.

Figure 6.21 shows the midspan deflections for Specimen No. 4 when a single 48 kips load was applied to Position No. 1C (Fig. 4.12). For this case and others (not shown), the finite element model realistically predicted the displacement behavior along the specimen length. The load point was located 132 in. from the left side of the graph, which placed the load about 5 in. to the right of the maximum displacement established by the analytical solution. The east end of the specimen (left side of the graph) was not supported; therefore, vertical movements at this point occurred. The west end of the specimen (right side of the graph) was supported by the modeled skewed abutment diaphragm; therefore, downward vertical movement was prevented at this point. As shown in the figure, the displacement magnitudes were quite small.

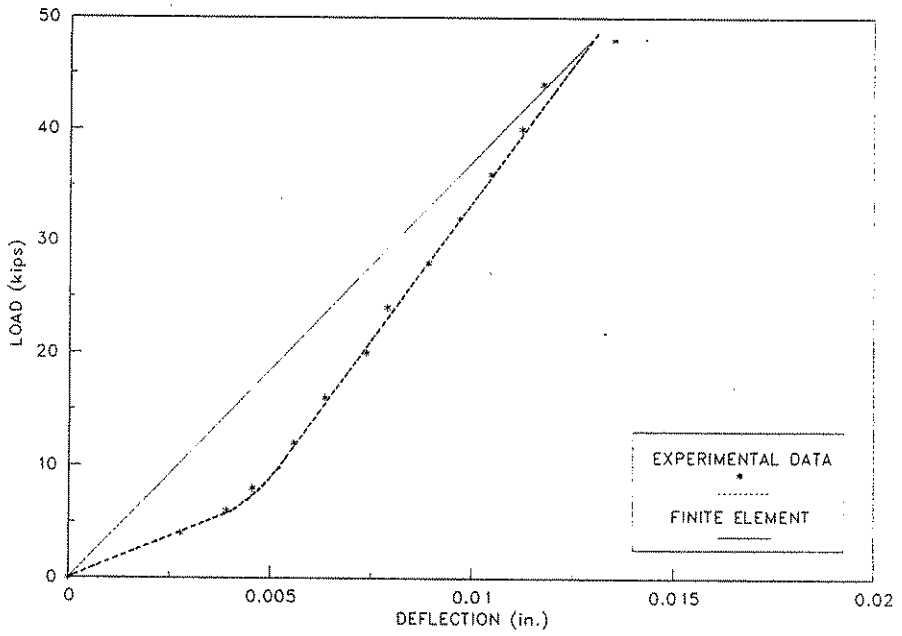

Figure 6.20. Load versus deflection for a single load at Position No. 1D on Specimen No. 5.

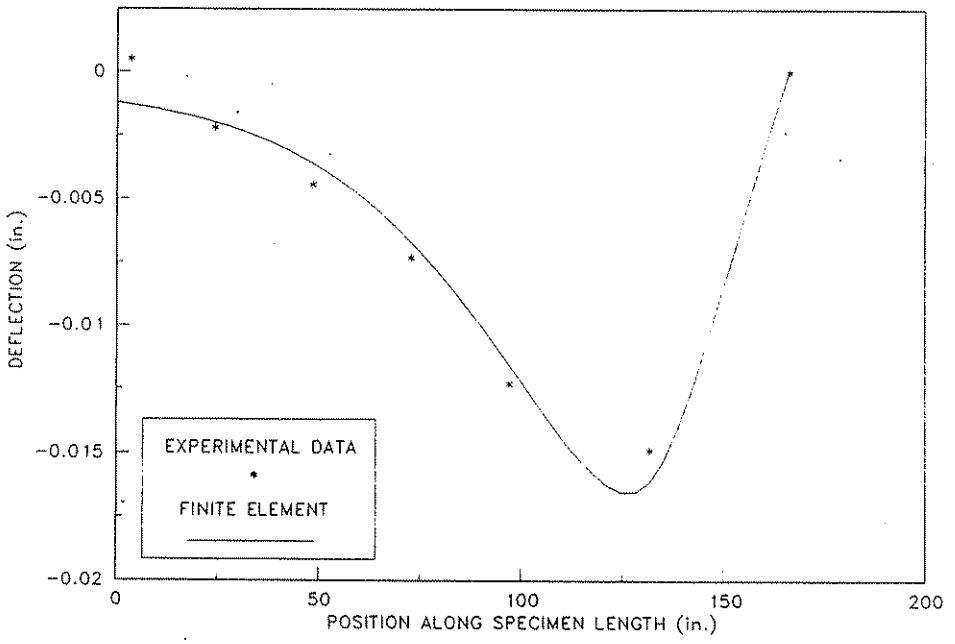

Figure 6.21. Midspan deflection along the specimen length for a single 48 kip load at Position No. 1C on Specimen No. 4.

6.4.3. Ultimate Loads

All of the specimens were subjected to loads which caused a failure of a portion of the composite slab. Figures 6.22 through 6.26 show the load versus deflection relationships obtained during the experimental testing of Specimen Nos. 1 through 5, respectively. The deflections shown are the average of the displacements on each side of the load footprint. In the key of each of the figures, the letter U refers to an ultimate load test, the prefix number represents the specimen number, and any suffix number refers to the ultimate strength test number. The position of the concentrated loads, referred to in the figure titles, corresponds to the wheel load positions shown in Figs. 4.9 through 4.13. Each of the figures show that the initial portion of the load versus deflection relationship is linear, and that each specimen was capable of resisting substantial increases in load after the limit of the elastic range had been obtained, as indicated by the continuously rising curve on the load versus displacement graphs. The failure of each specimen was sudden once the nominal strength of a slab was reached. The maximum elastic load, P_e; the load, $P_{0.1}$, which caused a deflection equal to 0.10 in. at the load point; the load, P_{cr}, corresponding to the first observed crack on the top surface of the slab; the ultimate experimental load, P_u; the maximum elastic deflection, Δ_e, at the load point and occurring at the load P_e; the maximum deflection, Δ_u, at the load point and occurring at the load, P_u; the ratio of P_u to P_e; the ratio of P_u to P_{cr}; and the ratio of Δ_u to Δ_e are listed in Table 6.10.

Except for Specimen No. 1, which had the load placed directly above the joint between the two precast panels, the ratio of P_u to P_e was at least equal to two. After the first crack was detected on the top surface of the composite slab, each specimen was able to resist a significant increase in load. Ratios of P_u to P_{cr} less than 1.75 occurred for Test Designations 1U, 2U1, 2U2, and 3U2.

Recall that Specimen No. 1 had the load over the panel joint, Specimen No. 2 was inadvertently cast about three-fourths of an inch too thin, and the second ultimate load test on Specimen No. 3 had the wheel footprint position close to one of the supports to induce a definite punching shear

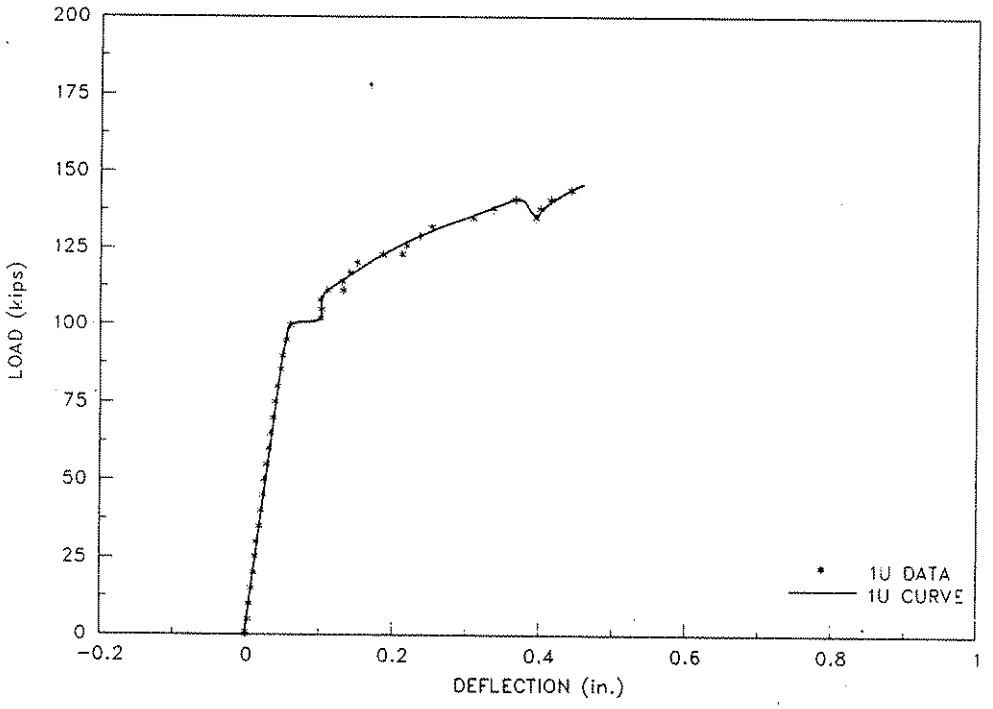

Figure 6.22. Load versus deflection for the Ultimate Lead Test on Specimen No. 1 (Load at Position No. 1C).

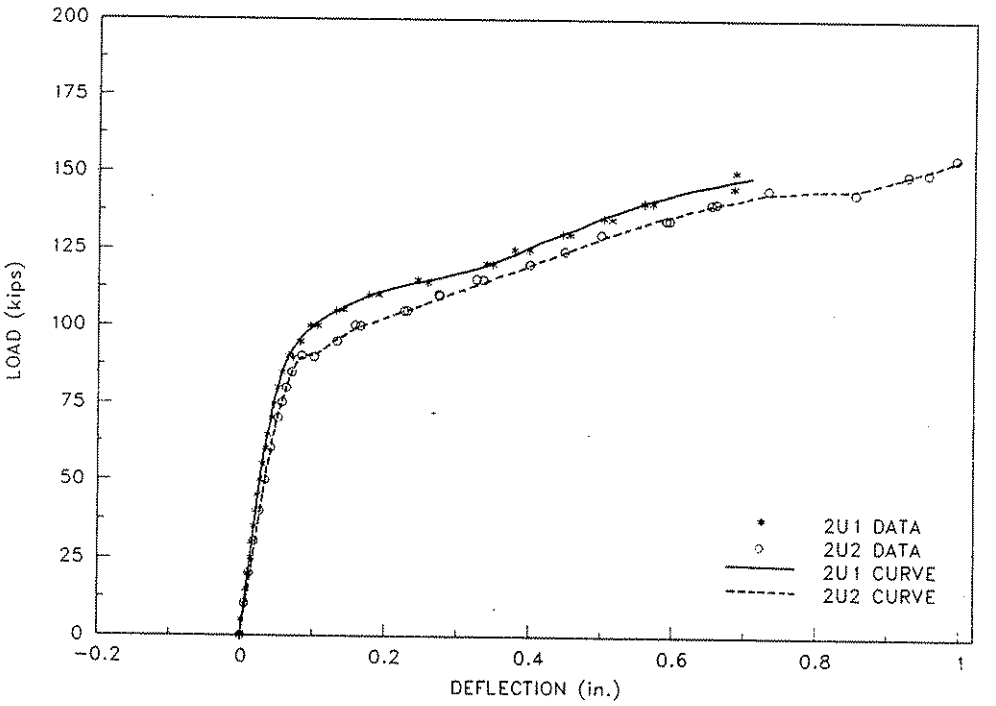

Figure 6.23. Load versus deflection for the Ultimate Load Tests on Specimen No. 2 (Load at Position Nos. 1D for 2U1 and at 1A for 2U2).

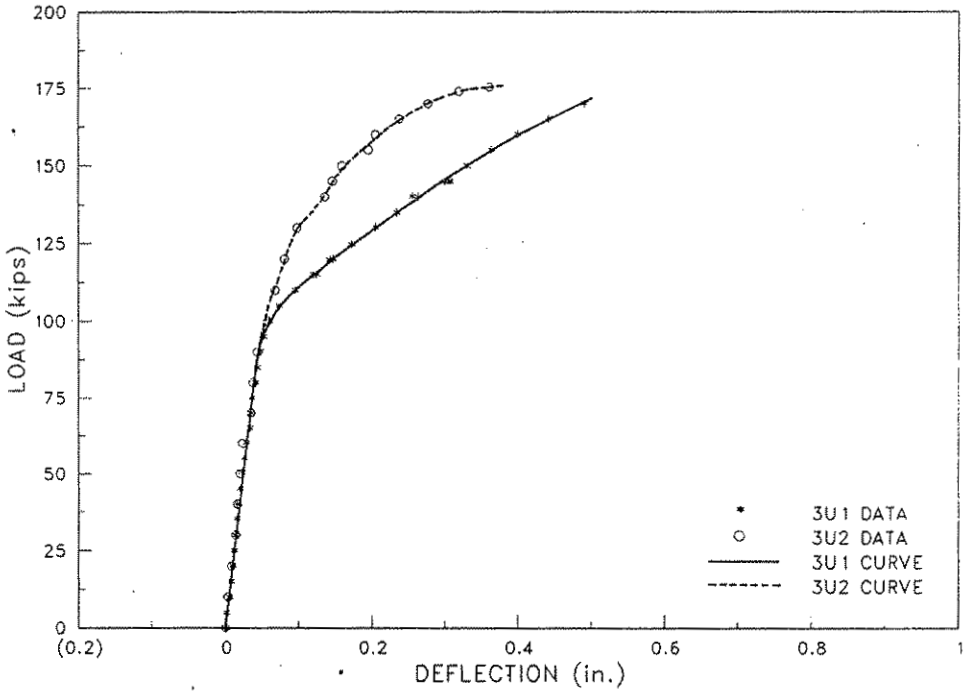

Figure 6.24. Load versus deflection for the Ultimate Load Tests on Specimen No. 3 (Load at Position Nos. 1E for 3U1 and 1.5 ft. above 1A for 3U2).

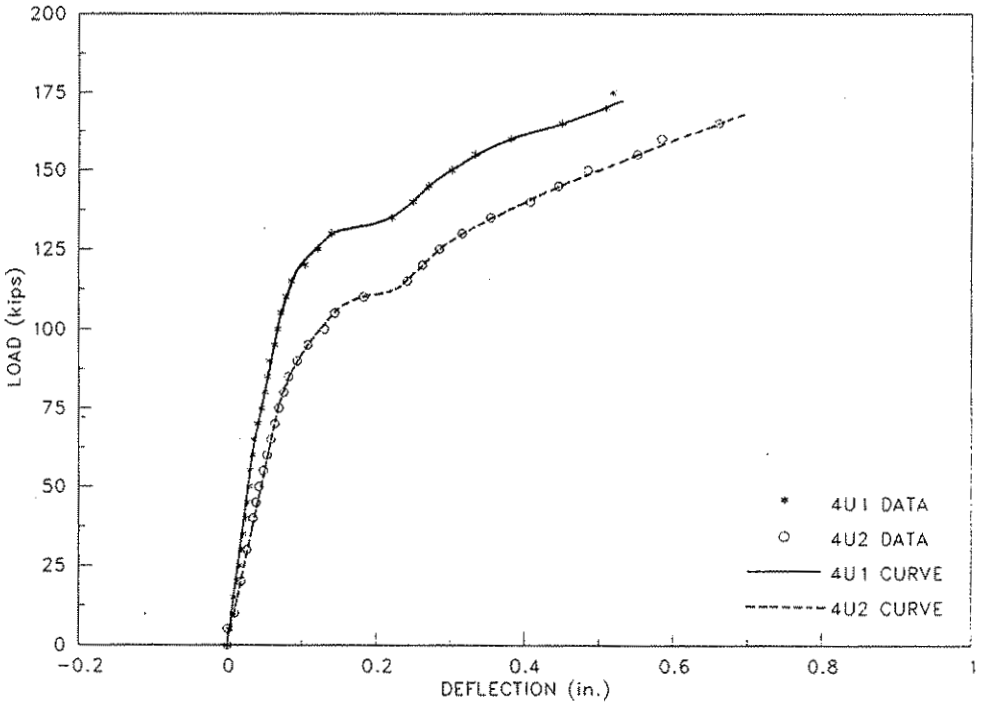

Figure 6.25. Load versus deflection for the Ultimate Load Tests on Specimen No.4 (Load at Position Nos. 1C for 4U1 and at 1A for 4U2).

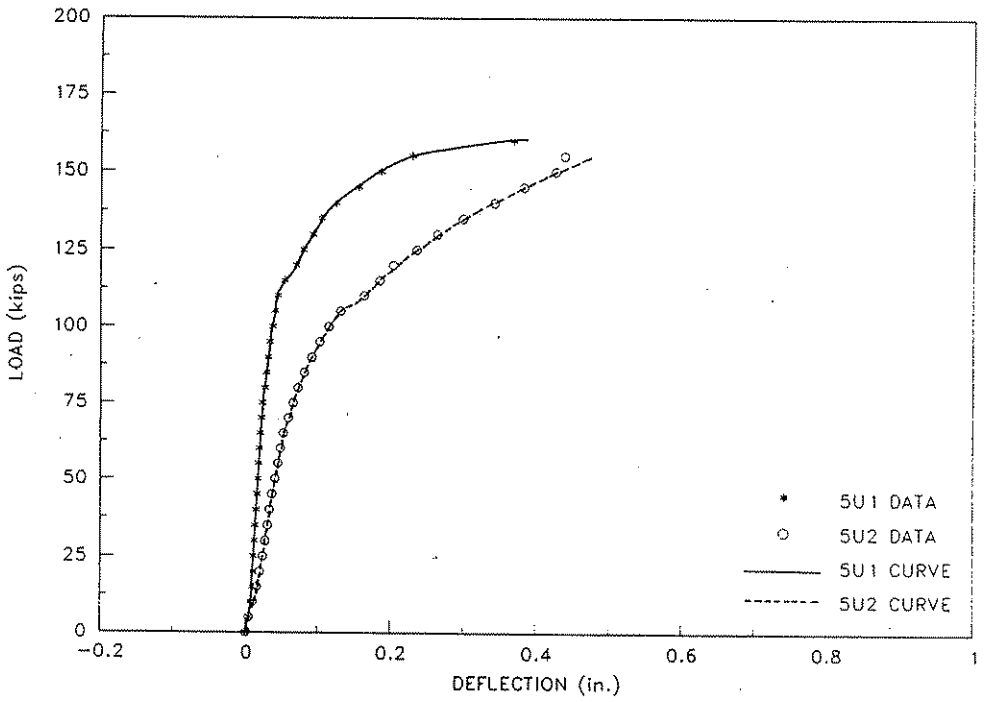

Figure 6.26. Load versus deflection for the Ultimate Load Tests on Specimen No. 5 (Load at Position Nos. 1D for 5U1 and 1.3 ft. above 1A for 5U2).

failure of the specimen. The second strength test on Specimen No. 3 produced the lowest ratio of P_u to P_{cr} equal to 1.35.

In a relative sense each composite slab specimen sustained a significant amount of inelastic deformation after the elastic limit had been obtained. The smallest ratios of Δ_u to Δ_e were equal to 9.1 and 9.2 for the specimens with Test Designations 5U2 and 3U2, respectively. Even though the ratios of Δ_u to Δ_e were large, the magnitudes of the maximum load point deflection which occurred just prior to the failure for the specimens were between about one-third of an inch and one inch.

Table 6.10. Load and deflection magnitudes for strength tests.

Test	P_e (kips)	$P_{0.1}$ (kips)	P_{cr} (kips)	P_u (kips)	Δ_e (in.)	Δ_u (in.)	P_u/P_e	P_u/P_{cr}	Δ_u/Δ_e
1U	90	100	105	145	0.046	0.459	1.61	1.38	10.0
2U1	65	100	90	150	0.035	0.710	2.31	1.67	20.3
2U2	70	90	90	155	0.050	1.000	2.21	1.72	20.0
3U1	85	110	90	175	0.041	0.518	2.06	1.94	12.6
3U2	85	130	130	175	0.041	0.379	2.06	1.35	9.2
4U1	65	120	80	170	0.038	0.511	2.62	2.13	13.4
4U2	70	95	70	165	0.065	0.679	2.36	2.36	10.4
5U1	70	130	70	160	0.023	0.385	2.29	2.29	16.7
5U2	65	95	85	153	0.052	0.475	2.35	1.80	9.1

6.5. Load Versus Strain Relationships

6.5.1. Service Level Loads

To determine whether the behavior of the composite slab specimens was affected by the joint between the precast panels, the distribution of the transverse midspan, flexural strains along the specimen length were investigated for various midspan wheel load positions. The strains were measured at the top of the cast-in-place slab and at the bottom of the precast panels in the direction

parallel to the panel span (transverse to the specimen length). The strain gauge locations are shown in Figs. 4.19 through 4.23 for Specimen Nos. 1 through 5, respectively.

For the maximum service level load of 20.8 kips, Figs. 6.27 and 6.28 show the experimental and finite element strain results for the transverse, midspan, strain distribution along the specimen length when a single wheel load was placed on Specimen No. 2 at Position Nos. 1C and 1E, respectively. Considering the experimental results, the measured strains at the top of the slab were slightly larger than the corresponding strains at the bottom of the precast panels, indicating that the neutral axis (axis of zero strain bending) occurred slightly below the mid-thickness of the composite slab. This relative location of the neutral axis is correct for the composite slabs, which had a larger modulus of elasticity for the concrete in the precast panels than for the concrete in the cast-in-place topping slab. The concrete properties for the panels and the cast-in-place slabs are listed in Table 6.1.

Figures 6.27 and 6.28 show that the transverse experimental strains appear to be continuous functions across the panel joint which was located at 96 in. from either end of the specimen. Therefore, the joint between the two precast panels did not appear to affect the service level load distribution along the length of the specimen. Similar results were obtained for other wheel load positions on Specimen No. 2 and for loads applied on the other four composite slab specimens.

The magnitude of the induced midspan, transverse strains were small when service level loads were applied to the specimens. For Specimen No. 1, the maximum, measured, experimental strain (not shown herein) at the top and bottom of the composite slab were equal to 84 x 10^{-6} in./in. and 82 x 10^{-6} in./in., respectively, when a 20.8 kip load was placed at Position No. 1A (Fig. 4.9). These strains were the largest recorded strains for the service load tests on Specimen No. 1. The lack of continuity of the slab at 4 ft. to the one side of the load position produced the larger strains. From Fig. 6.27, the maximum measured strain was equal to 67 x 10^{-6} in./in. As the loads were moved closer to the modeled abutment or pier diaphragm, the experimental, midspan, transverse strains decreased. Figure 6.28 shows a maximum measured strain of 55 x 10^{-6} in./in. due to the 20.8 kip

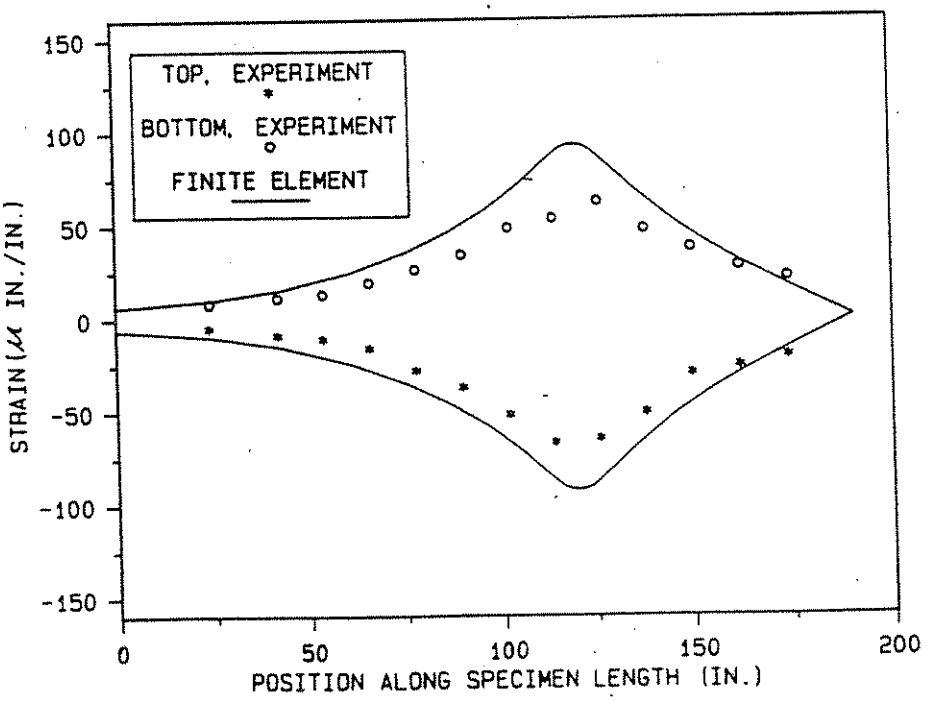

Figure 6.27. Midspan transverse strains along the specimen length for a single 20.8 kip load at Position No. 1C on Specimen No. 2.

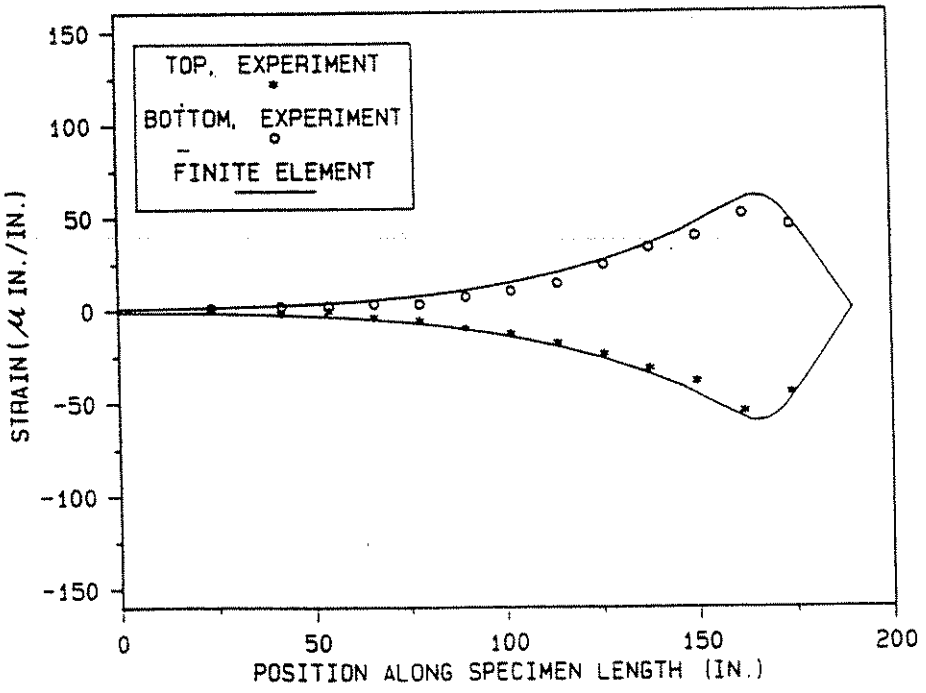

Figure 6.28. Midspan transverse strains along the specimen length for a single 20.8 kip load at Position No. 1E on Specimen No. 2.

load. Since the induced experimental strains were small, cracking of the concrete at the underside of the precast panels should not have occurred for any of the service level loads.

The finite element model, which idealized the composite slab as an isotropic slab, generally over estimated the midspan, transverse, slab strains, with the greatest divergence from the measured strain values occurring near the load point. However, the analytical model closely predicted the distribution pattern as can be seen from Figs. 6.27 and 6.28. Since the composite slab was uncracked for the service level load range, the simplified assumption of a homogeneous concrete slab remained valid.

Figure 6.29 shows the distribution of the bottom, midspan, transverse strains along the specimen length for Specimen No. 3, 4, and 5, when a maximum service level load of 20.8 kips was placed above or near the joint between the two precast panels. Specimen No. 5 was loaded 12 in. to the left of the panel joint. The numbers shown in the key for the figure refer to the skew angles of 15, 30, and 40 degrees for the three specimens. As shown in Table 4.1, the thickness of the slabs were approximately equal at the panel joint. The thicknesses were 8.62, 8.45, and 8.11 inches for Specimen Nos. 3, 4, and 5, respectively. Figure 6.29 shows that the finite element model reasonably predicted the behavior of the midspan, transverse strains. The figure also indicates that maximum transverse tensile strain near the load point is not significantly affected by the presence of the skewed support along the longitudinal edge of a trapezoidal-shaped precast panel.

Double wheel loads of up to 20.8 kips each were applied at a 4 ft. spacing to the composite slab specimens. Representative midspan, transverse strain distributions along the specimen length are shown in Figs. 6.30 and 6.31. These results correspond to loads placed at Position Nos. 3C and 3E, respectively, on Specimen No. 3, which involved the 15 degree skewed geometric condition. The two wheel loads were in alignment with the span of the precast panels; therefore, the loads occurred along the same transverse line with respect to the specimen length. For Fig. 6.30, both loads were above the precast panel joint. The relative position of the panel joint is 96 in. from the origin of the

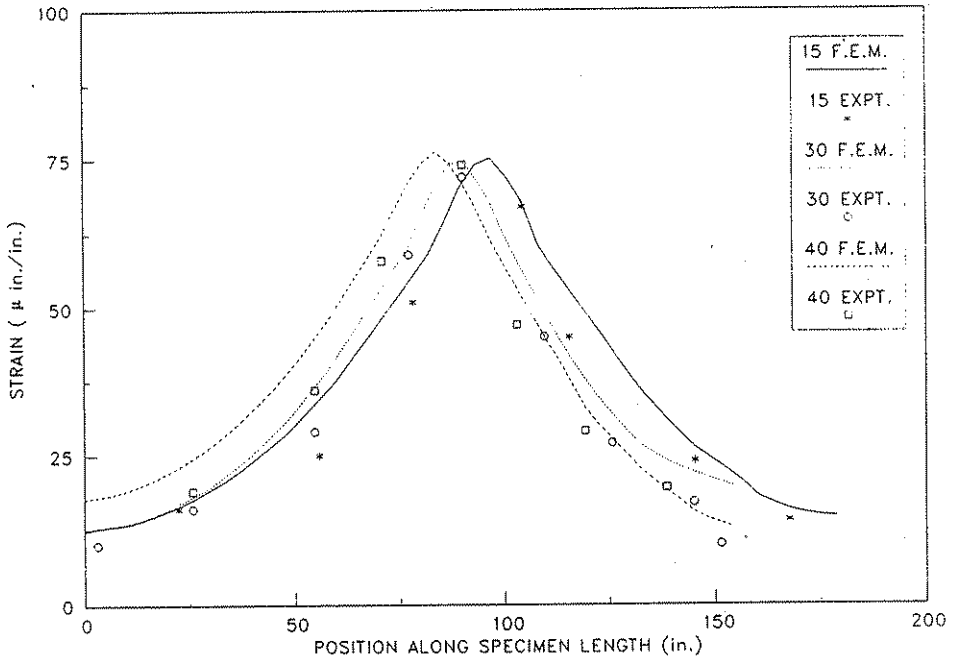

Figure 6.29. Bottom midspan transverse strains along the specimen length for a single 20.8 kip load applied near or above the panel joint on Specimen No. 3, 4, and 5.

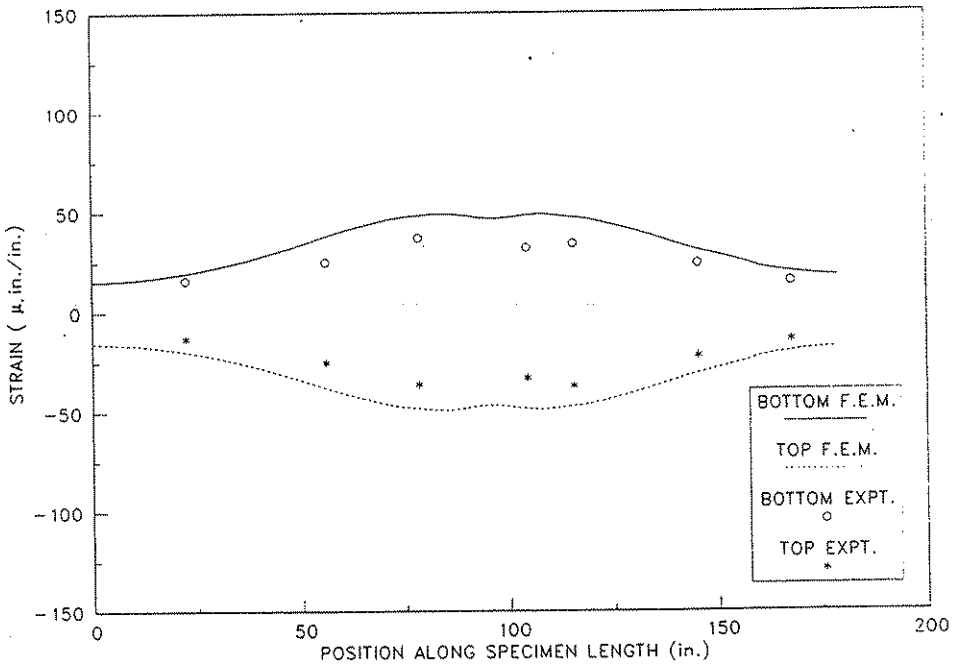

Figure 6.30. Midspan transverse strains along the specimen length for a double 20.8 kip load at Position Nos. 3C on Specimen No. 3.

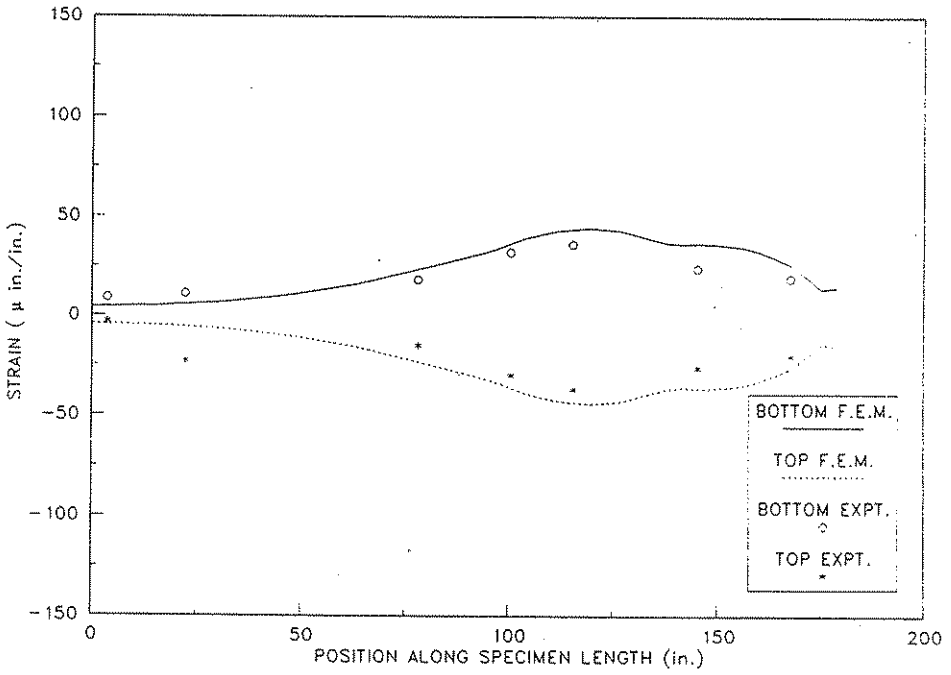

Figure 6.31. Midspan transverse strains along the specimen length for a double 20.8 kip load at Position Nos. 3E on Specimen No. 3.

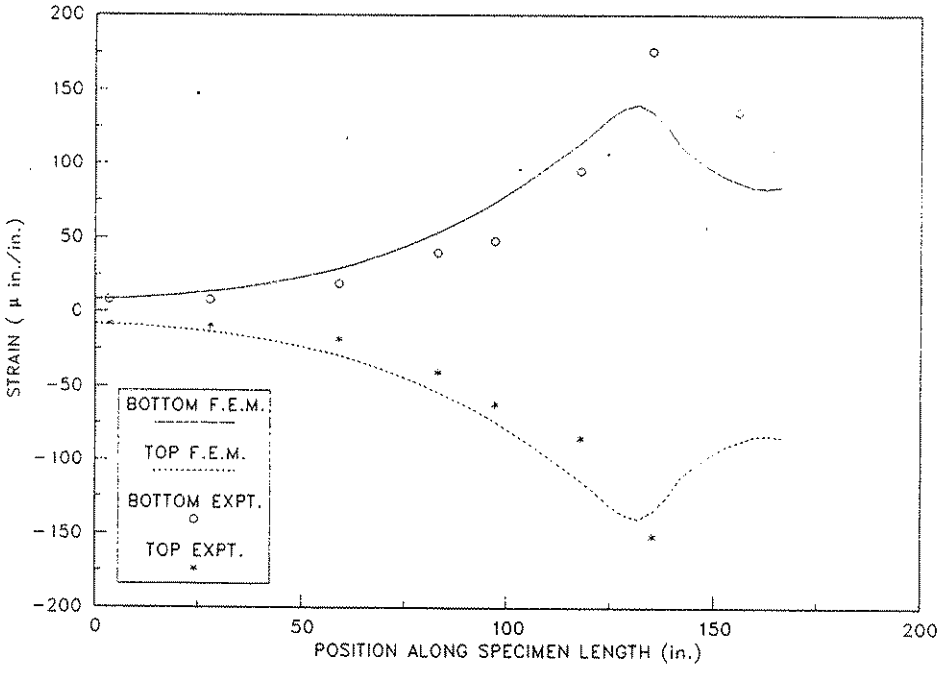

Figure 6.32. Midspan transverse strains along the specimen length for a single 48 kip load at Position No. 1C on Specimen No. 4.

graph. As indicated by both the experimental and analytical results, the maximum strain does not occur along the straight line joining the two loads, but was offset by about 16 in. to either side of that line. For loads applied at Position No. 3C on Specimen No. 3, the strains are basically symmetric with respect to the center of the specimen; therefore, the skewed support along the longitudinal edge of the west end of the specimen did not significantly influence the midspan, transverse strain distribution for this loading condition. Once again, the finite element solution predicted the general behavior of the strain distribution. However, the analytical solution overestimated the magnitude of the relatively low strains. Figure 6.31 shows that the distribution of strains becomes nonsymmetrical as the dual wheel loads approach the skewed abutment support. Since both loads were close to the ends of the span, the induced flexural strains in the transverse direction were quite small. Considering both locations (Position Nos. 3C and 3C) for the double loads, the maximum midspan, transverse strain due to the applied wheel loads was equal to 37 x 10^{-6} in./in.

6.5.2. Factored Level Loads

Factored wheel loads were applied to Specimen Nos. 4 and 5 at the positions listed in Table 4.1. The maximum magnitude of the factored load was 48 kips. To further investigate the effects of placing this maximum wheel load on the region of the composite slab near the modeled abutment or pier diaphragm, additional graphs of transverse strain along the length of the specimen were developed. Figures 6.32, 6.33, and 6.34 show the distribution of the midspan, transverse strain obtained by both experimental and analytical methods for Specimen No. 4, when the load was at Position Nos. 1C, 1D, and 2E, respectively, as shown in Fig. 4.12. These figures show a distinct change in behavior as the concentrated load was moved towards the modeled diaphragm support and into the acute corner of the slab. When the load was at Position No. 1C (Fig. 6.32), a maximum experimental strain of 178 x 10^{-6} in./in. occurred near the load point, and when the load was at Position 1D (Fig. 6.33) a maximum experimental strain of about 191 x 10^{-6} in./in. (extrapolated value) occurred near the edge of the slab. Recall that this edge of the slab was not monolithically cast or

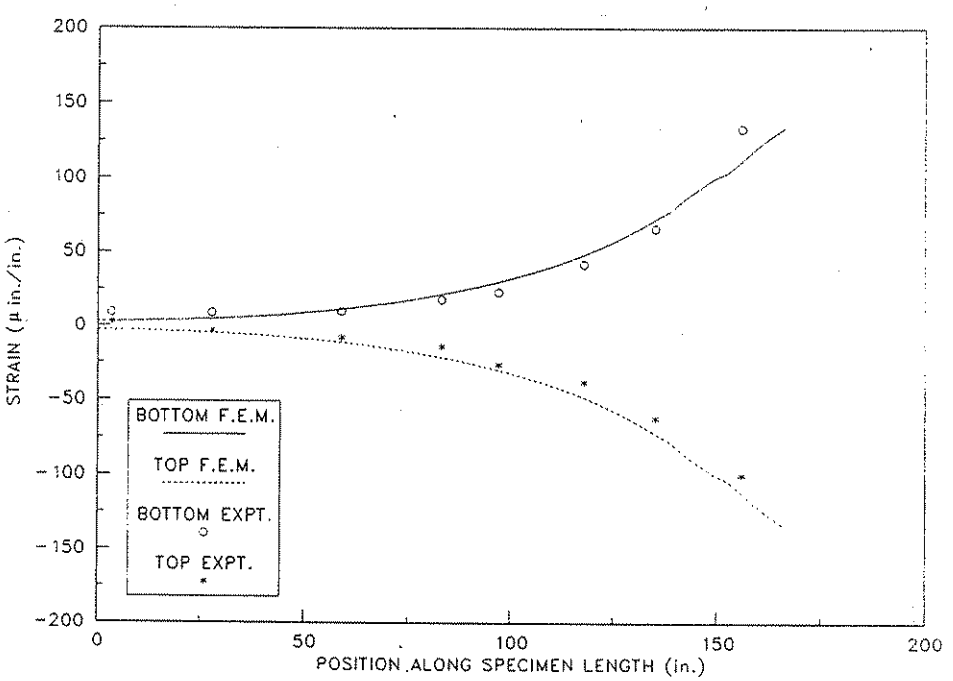

Figure 6.33. Midspan transverse strains along the specimen length for a single 48 kip load at Position No. 1D on Specimen No. 4.

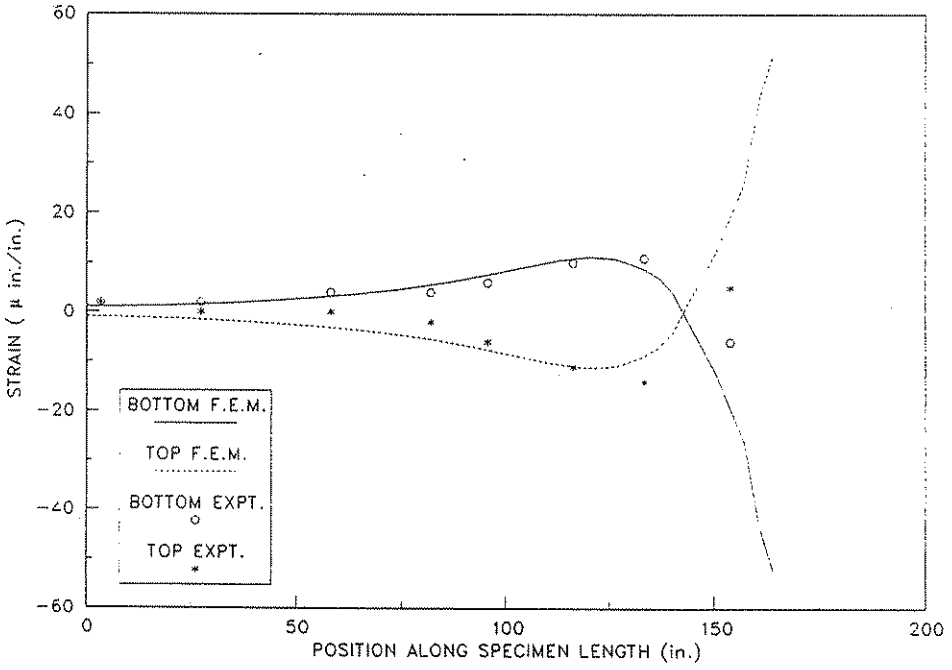

Figure 6.34. Midspan transverse strains along the specimen length for a single 48 kip load at Position No. 2E on Specimen No. 4.

tied to the modeled diaphragm. When the load was at Position No. 2E (Fig. 6.34), a moment reversal occurred as indicated by the sign change in the transverse strains. The maximum strain of 52×10^{-6} in./in. according to the analytical solution occurred near the edge of the slab. For this wheel load position, the measured, maximum, experimental strains were less than 15×10^{-6} in./in. Figures 6.32 through 6.34 show that the finite element solution predicted the distribution pattern for the midspan, transverse strains. At locations removed the point of load application, the analytically established strain magnitudes closely matched the experimentally measured strains, while near the load point, the analytical model did not predict strain magnitudes as accurately. This insensitivity was anticipated, since a simplified finite element model was selected. However, as shown in Fig. 6.34, the analytical model currently predicted that a moment reversal took place.

For the 40 degree skewed specimen configuration (Specimen No. 5), Figs. 6.35 and 6.36 show the midspan, transverse strain results when a single 48 kip load was applied at Position Nos. 1D and 1E, respectively (Fig. 4.13). The results shown in Figs. 6.35 and 6.36 are similar to those shown in Figs. 6.32 and 6.34, respectively, for the 30 degree skewed specimen configuration (Specimen No. 4).

When the 48 kip factored load was applied at Position 1A on Specimen No. 5, a maximum midspan, transverse, compressive strain (not shown) equal to 227×10^{-6} in./in. was measured at the top of the slab adjacent to the wheel load footprint, and a maximum transverse tensile strain, ε_t, equal to 225×10^{-6} in./in. was recorded at the bottom of the precast panel. These strains were larger than those obtained with the factored load applied at other positions on the specimen due to the discontinuous slab condition that occurred 4 ft. away from Position 1A (Fig. 4.13).

Even when a factored load equal to 48 kips was applied to Specimen Nos. 4 and 5, the strain distribution along the specimen length did not indicate any discontinuity at the joint between the two precast panels. Therefore, the topping slab adequately transferred vertical shear forces across the joint.

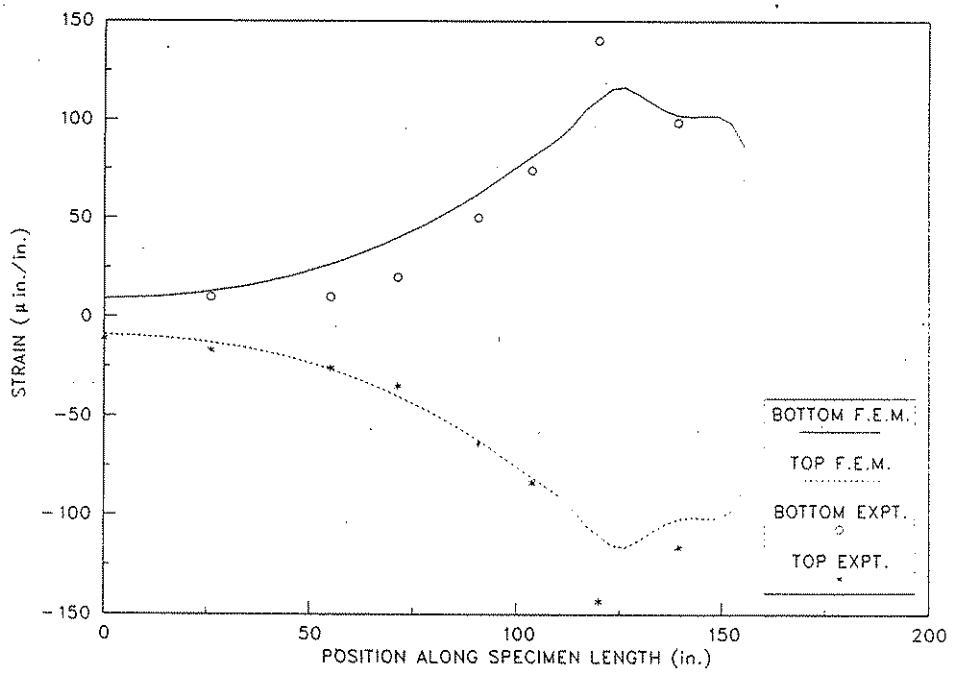

Figure 6.35. Midspan transverse strains along the specimen length for a single 48 kip load at Position No. 1D on Specimen No. 5.

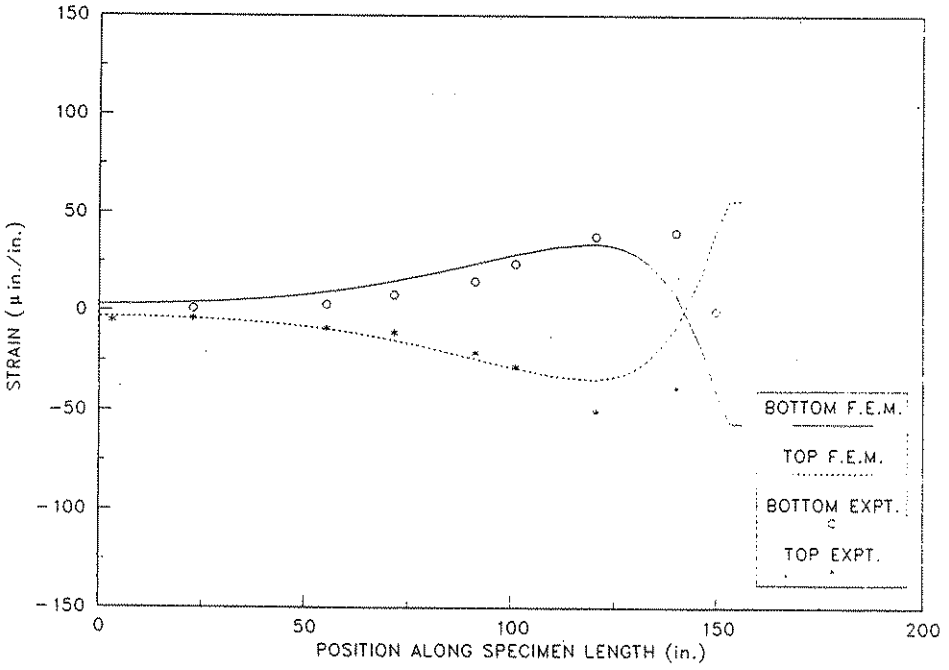

Figure 6.36. Midspan transverse strains along the specimen length for a single 48 kip load at Position No. 1E on Specimen No. 5.

Total tensile strains in excess of the strain associated with the modulus of rupture will produce cracking of the concrete. Before cracking at the bottom surface of a precast panel in the direction perpendicular to the panel span would occur, the maximum flexural tensile strain at the bottom of a panel, induced by the dead load of the precast panel and topping slab, superimposed live load (wheel load), and shrinkage of the concrete in the topping slab would have to exceed the sum of the precompression strain, caused by prestressing the panel, and the modulus of rupture strain. At locations not near the precast panel joints or near the skewed diaphragm support, an approximation for the tensile strain, ε_{cd}, at the bottom surface of a precast panel that is induced by the panel self-weight and the weight of the wet concrete of a topping slab is given by

$$\varepsilon_{cd} = \frac{3\, t\, l_p^2}{320\, t_p^2\, E_{cp}} \tag{6.3}$$

where, t = thickness of the composite slab, ℓ_p = span length of the precast panel, t_p = thickness of the precast panel, and E_{cp} = modulus of elasticity of the panel concrete. Substituting the numeric values for the parameters associated with Specimen No. 5 at Position No. 1A (Tables 4.1 and 6.1) into Eq. (6.3),

$$\varepsilon_{cd} = \frac{(3)(8.15)(6.58)^2}{(320)(2.50)^2(5{,}839)} = 91 \times 10^{-6}\ in./in.$$

A precompression strain, ε_{cp}, which is constant across the thickness of a precast panel and is induced by the effective strand prestress can be evaluated from

$$\varepsilon_{cp} = \frac{f_{se} A_s^*}{(t_p s - A_s^*)\, E_{cp}} \tag{6.4}$$

where, f_{se} = effective strand prestress from Eq. (5.1), A_s^* = cross-sectional area of a prestressing strand, and s = strand spacing. Substituting the appropriate values for the parameters for Specimen No. 5 into Eq. (6.4),

$$\varepsilon_{cp} = \frac{(172.4)(0.085)}{[(2.50)(6.0)-0.085](5,839)} = 168 \times 10^{-6}\ in./in.$$

The modulus of rupture strain, ε_{cr}, is given by

$$\varepsilon_{cr} = \frac{f_r}{E_{cp}} \tag{6.5}$$

where, f_r = modulus of rupture for the panel concrete at the time of testing. Evaluating Eq. (6.5) for Specimen No. 5 (Table 6.1),

$$\varepsilon_{cr} = \frac{925}{5,839,000} = 158 \times 10^{-6}\ in./in.$$

If the effects of shrinkage of the concrete in the topping slab are neglected, cracking of the bottom of the precast panel, in the direction perpendicular to the panel span, should not occur if the critical strain condition given by Eq. (6.6) is satisfied.

$$(\varepsilon_{cp} + \varepsilon_{cr}) > (\varepsilon_{cd} + \varepsilon_{l}) \tag{6.6}$$

For the 48 kip load at Position No. 1A on Specimen No. 5, evaluation of the strain condition produces

$$(168 + 158) \times 10^{-6} > (91 + 225) \times 10^{-6}$$

$$326 \times 10^{-6} > 316 \times 10^{-6}$$

Even though the strain condition is just satisfied, initial cracking in any direction at the bottom of the precast panel near the midspan may have occurred when the maximum factored load of 48 kips was placed at Position 1A, since the effect of the experimental tensile strains in the longitudinal direction due to the applied loads have not been considered and shrinkage effects were neglected. For the other factored positions, Eq. (6.6) would be satisfied for the strains in the direction perpendicular to the panel span, since the transverse strains induced by the superimposed live load were smaller for these cases. However, when the strains in both the longitudinal and transverse directions of the specimens due to all causes are considered, initial concrete cracking probably

occurred for the factored loading conditions. A more detailed investigation of the strains would be required to establish the degree and extent of concrete cracking.

6.6. Panel Bearing Conditions

As discussed in Section 4.1.1, the precast concrete panels were temporarily supported on 3/4 in. high x 1 in. wide continuous fiberboard strips during the construction of the bridge deck. To establish whether the concrete from the topping slab had flowed beneath the panels to provide the desired 2 1/2 in. width of solid bearing, the bearing areas were inspected during the demolision of the specimens. For those locations which were not at the block-outs, where monitoring of the prestressing strands for slip occurred, good bearing was generally provided. There were some isolated portions where the bearing was not complete; however, the amount of length of incomplete bearing was small compared to the 8 ft panel width. For adequate concrete bearing to be provided for the panels, sufficient vibration of the concrete during casting of the topping slab is necessary. The concrete vibrator should be drawn through the concrete along the ends of the panels.

An increase in the minimum height of temporary bearing would increase the probability that better permanent bearing would be obtained. The 3/4 in. thickness of the fiberboard strips, which were used in this research, was the same dimension as the maximum aggregate size in the D-57 concrete mix.

6.7. Limit Loads

6.7.1. Yield-Line Strengths Versus Test Results

An evaluation of the limit load for each probable collapse mechanism for each ultimate strength test was accomplished by substituting the appropriate nominal moment strengths from Table 5.4 and the yield-line dimensions from Table 5.3 into the appropriate limit load expression (Eqs. 5.24 through 5.30). The calculated collapse load for each ultimate strength test on Specimen Nos. 1 through 5

are given in Table 6.11. For a given ultimate load test, the minimum value of the yield-line limit load governs the slab capacity.

To establish whether a flexural mode of failure for a composite slab specimen potentially governed its strength, a comparison between the computed yield-line capacity and the experimental failure load shown in Table 6.11 was made. Realizing that test scatter associated with experimental work will always occur, a high probability for a flexural failure exists whenever the computed flexural strength is close to the tested strength. Also, to assist in determining whether a flexural failure mode occurred, a complete yield-line pattern must have been developed to physically subdivide the slab into a series of rigid plate elements, which are unrestrained from collapse. By observing the cracks on both the top and bottom surfaces of a slab and comparing these patterns with the generalized yield-line patterns shown in Fig. 5.7, conclusions were formulated as to whether a complete yield-line mechanism had been developed. Table 6.11 lists the results for the likelihood that a flexural failure may have occurred for each of the potential crack patterns selected. The presence of the joint between the two precast panels influenced the behavior of the composite slab specimens during the ultimate load tests.

For Specimen No. 1, yield-line Pattern B was not completely formed (Fig. 6.37), since a crack developed in the top surface of the slab directly above the joint between the two precast panels. A positive moment yield-line did not occur at this location as required for this pattern.

For the first ultimate load test on Specimen No. 2, yield-line Pattern D did not completely develop. As shown in Fig. 6.38a, the circumferential crack patterns which started at the edges of the slab and progressed towards the center had not met in the region between the load and the panel joint. A crack throughout the width of the specimen did occur directly above the panel joint at a load of about 90 kips. Considering the second ultimate load test on Specimen No. 2, yield-line Pattern E appears to have formed. The bottom slab surface shown in Fig. 6.39b had many cracks.

Table 6.11. Yield-line limit loads and experimental ultimate strengths.

Specimen No.	Ultimate Test No.	Crack Pattern Figure No.	Yield-Line Theory			P_u (kips)	$\frac{P_n}{P_u}$	Flexural Failure Mode
			Yield-Line Pattern[a]	Governing Eq. No.	P_n (kips)			
1	1	6.37[b]	A	5.1	207	145	1.43	No
		6.37	B	5.2	195[b]	145	1.34	No
2	1	6.38	C	5.3	198	150	1.32	No
			D	5.4	189[b]	150	1.26	No
	2	6.39	C	5.3	210	155	1.35	No
			D	5.4	191	155	1.23	No
			E	5.5	150[b]	155	0.97	Possibly
3	1	6.40	F	5.6	213[b]	175	1.22	No
	2	6.41	C	5.3	280	175	1.60	No
			D	5.4	242[b]	175	1.38	No
			E	5.5	269	175	1.54	No
4	1	6.42	F	5.6	241	170	1.42	No
			G	5.7	209[b]	170	1.23	No
	2	6.43	C	5.3	224	165	1.36	No
			D	5.4	201	165	1.22	No
			E	5.5	177[b]	165	1.07	Possibly
5	1	6.44	F	5.6	201[b]	160	1.26	No
			G	5.7	210	160	1.31	No
	2	6.45	C	5.3	241	153	1.58	No
			D	5.4	251	153	1.64	No
			E	5.5	182[b]	153	1.19	No

[a]Patterns shown in Fig. 5.7.
[b]Governs yield-line behavior.

Recall that a crack along the panel joint had formed during the ultimate load test on the adjacent panel. This crack was the negative moment yield-line shown in Fig. 5.7e.

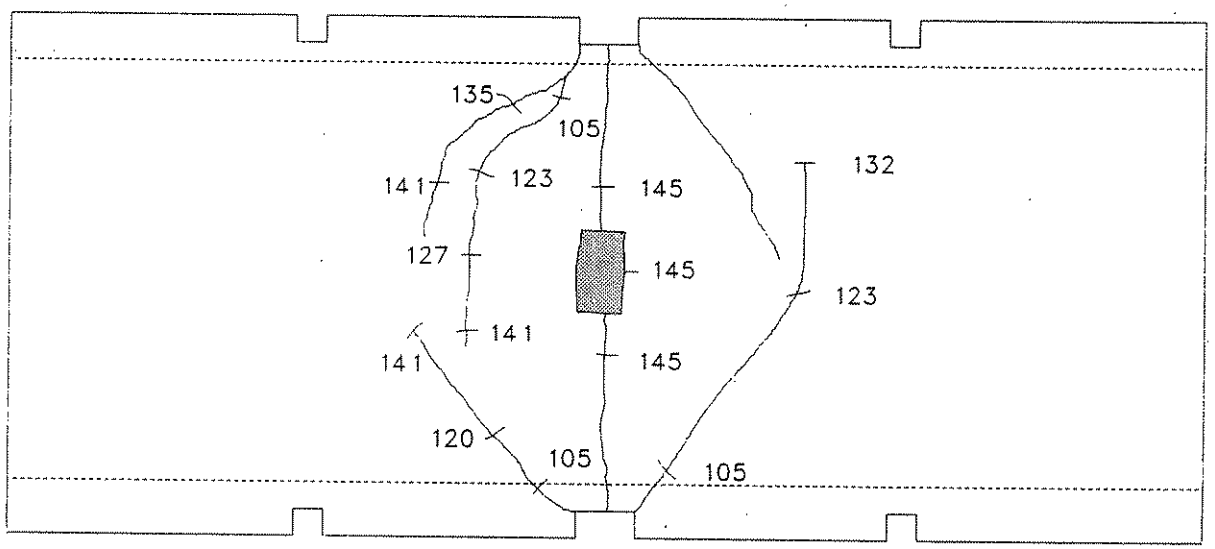

(a)

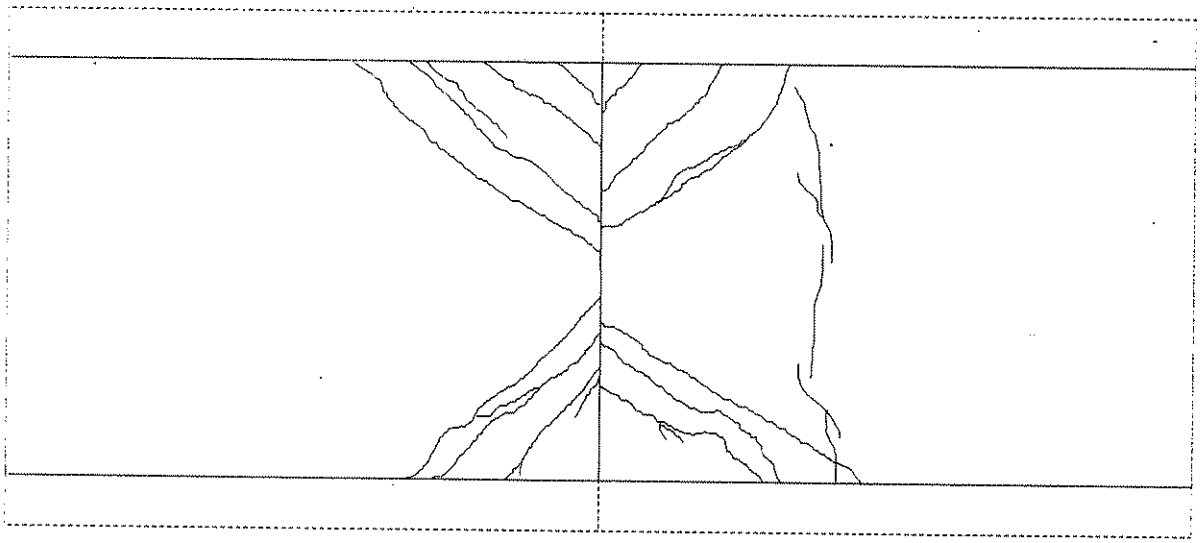

(b)

Figure 6.37. Crack patterns on Specimen No. 1 from Ultimate Load Test: (a) Top surface of slab, (b) Bottom surface of precast panels.

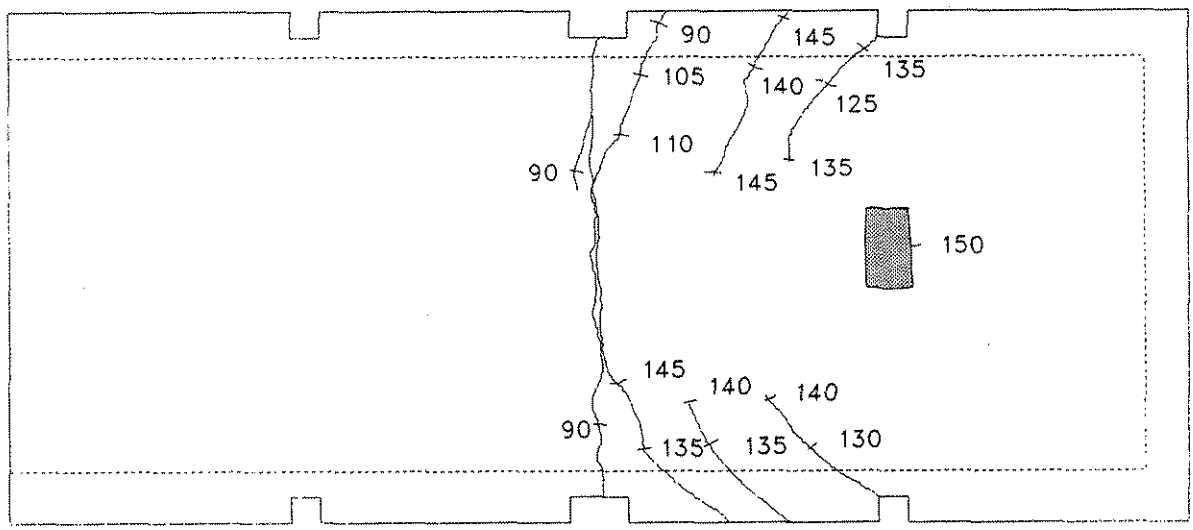

(a)

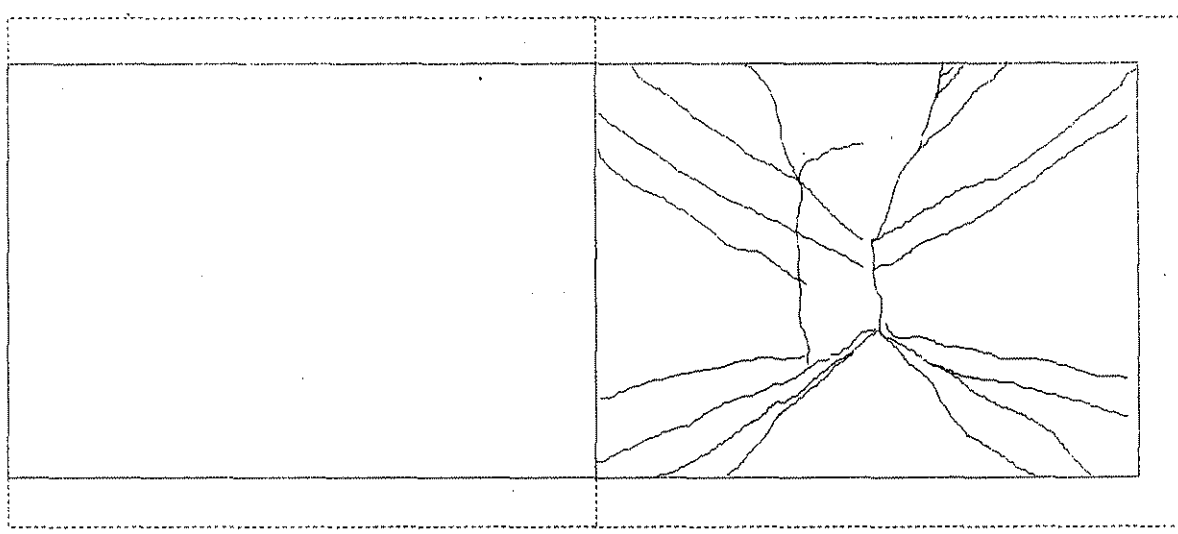

(b)

Figure 6.38. Crack patterns on Specimen No. 2 from Ultimate Test No. 1: (a) Top surface of slab, (b) Bottom surface of precast panel.

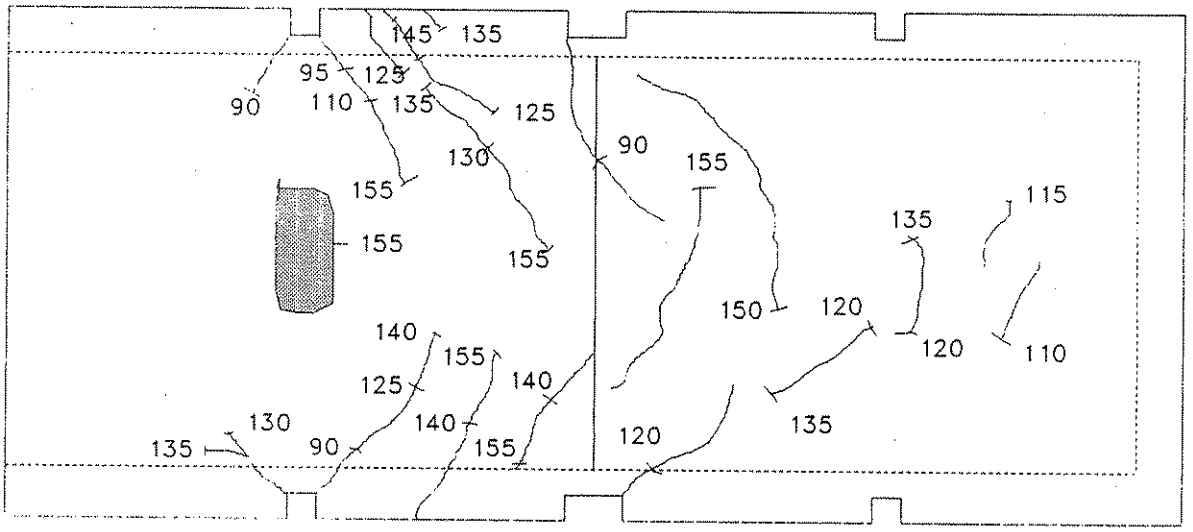

(a)

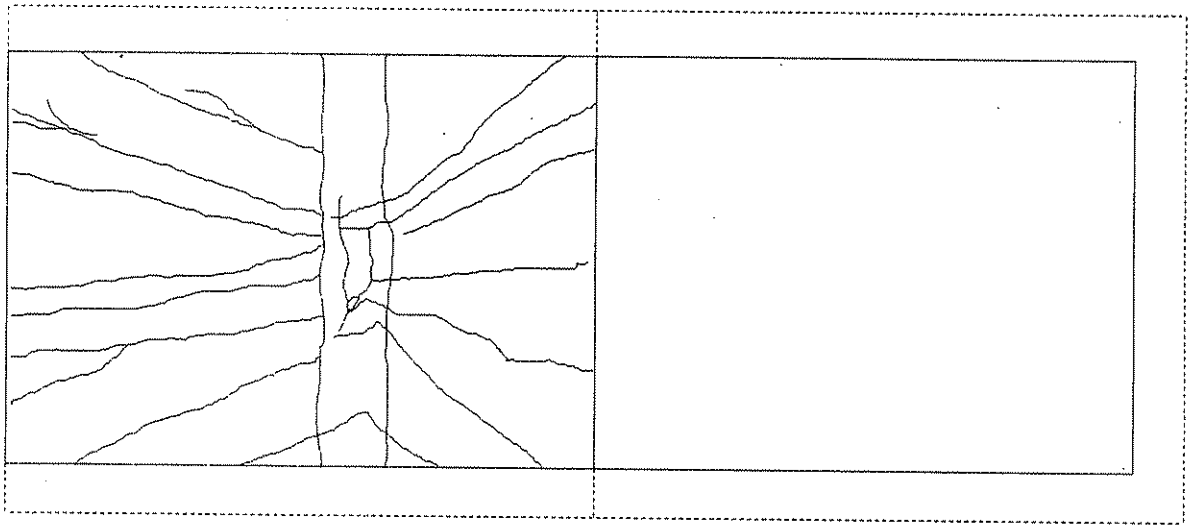

(b)

Figure 6.39. Crack patterns on Specimen No. 2 from Ultimate Test No. 2: (a) Top surface of slab, (b) Bottom surface of precast panel.

For the ultimate load test on the skewed panel of Specimen No. 3, yield-line Pattern F was almost formed. The positive moment yield-lines, located at the middle of the cracking band widths, appear to converge at the load point on the panel (g_4=0, in Fig. 5.7f). The negative moment yield-line near the panel joint (Fig. 6.40a) was formed between the 110 and 140 kip load levels. The second ultimate load test on Specimen No. 3 was conducted near the southern support to minimize the probability of a flexural failure and maximize the probability for a shear failure. The controlling yield-line pattern (Pattern D), shown in Fig. 5.7d represents the crack patterns shown in Fig. 6.41, had not completely formed.

For the first ultimate load test on Specimen No. 4, yield-line Pattern G (Fig. 5.7g) had almost formed. As shown in Fig. 6.42a, the negative moment yield-line, denoted by the curved crack in the top surface of the slab on the side of the load towards the panel joint, had formed along about half of the specimen width. The positive moment yield-lines obtained by observing the bottom surface of the slab (Fig. 6.42b) appeared to have formed. Considering the second ultimate load test on Specimen No. 4, Fig. 6.43, which show the crack patterns on the top and bottom surfaces of the specimen, indicate that the idealized yield-line Pattern E, shown in Fig. 5.7e, had possibly formed.

For the ultimate load test on the portion of the slab near the skewed diaphragm location of Specimen No. 5, the crack patterns on the bottom surface of the precast panel (Fig. 6.44b) indicate that a failure mechanism similar to yield-line Pattern F (Fig. 5.7f) had not completely formed. The resulting analytical limit load of 201 kips exceeded the ultimate load which the specimen resisted by 26 percent. The second ultimate test on Specimen No. 5 involved an offset load position from the midspan to reduce the possibility of a flexural failure and to increase the chances for a shear failure. The position of the load was not as close to the abutment support as a similar load arrangement was for Specimen No. 3. Yield-line Pattern E had not completely formed, since the horizontally orientated positive moment yield-line had not completely extended to the free edge of the slab, as can be noted by comparing Figs. 5.7e and 6.45b.

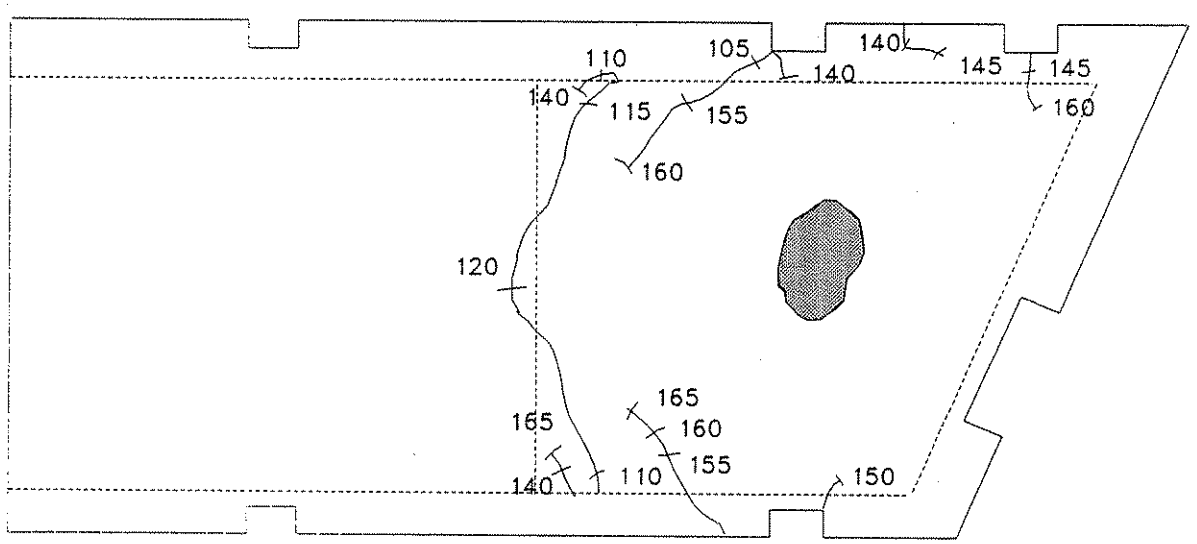

(a)

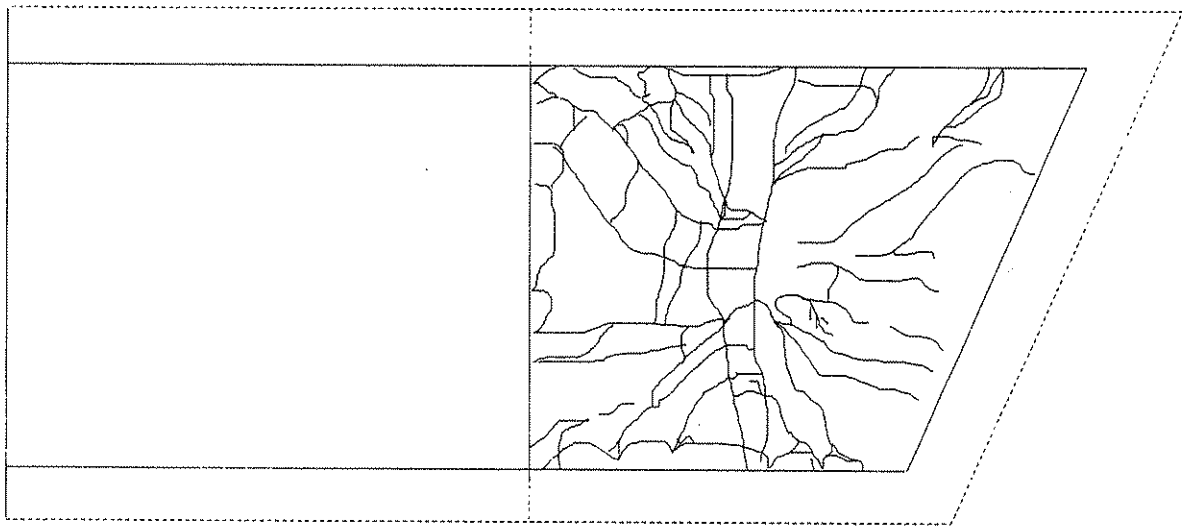

(b)

Figure 6.40. Crack patterns on Specimen No. 3 from Ultimate Test No. 1: (a) Top surface of slab, (b) Bottom surface of precast panel.

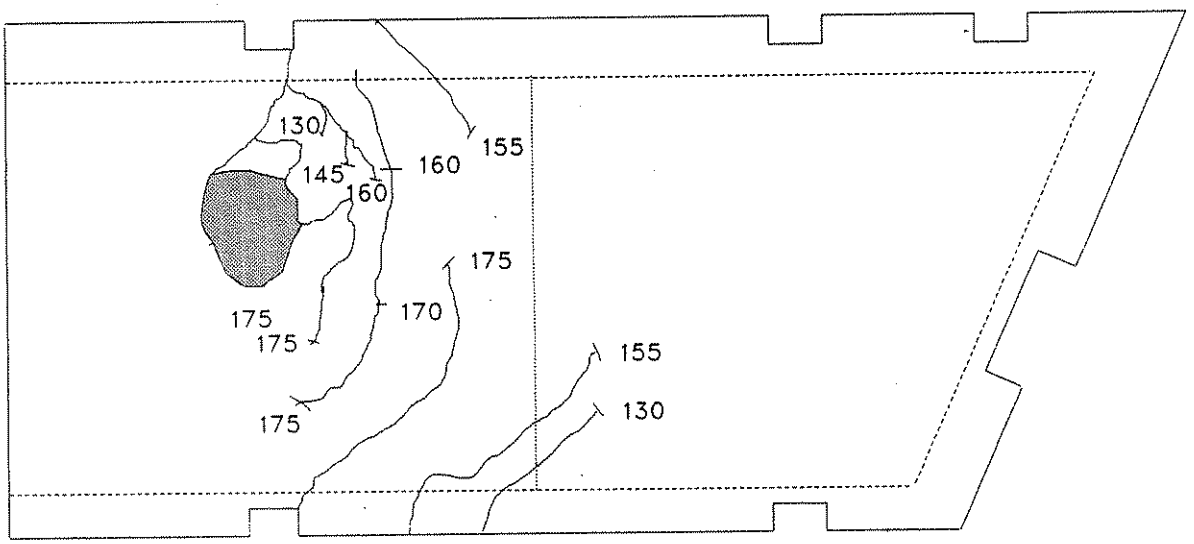

(a)

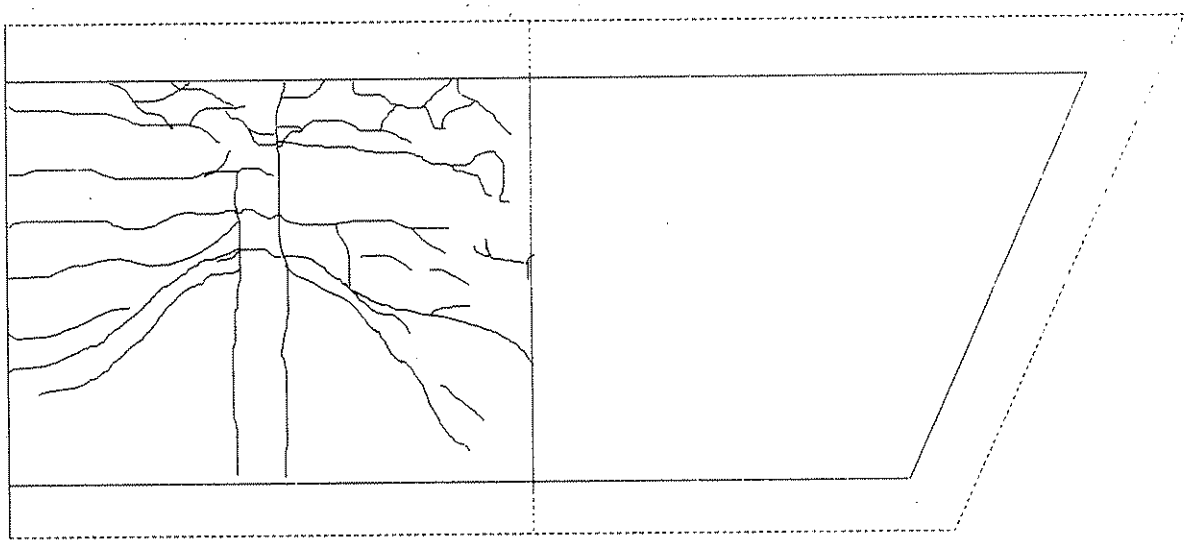

(b)

Figure 6.41. Crack patterns on Specimen No. 3 from Ultimate Test No. 2: (a) Top surface of slab, (b) Bottom surface of precast panel.

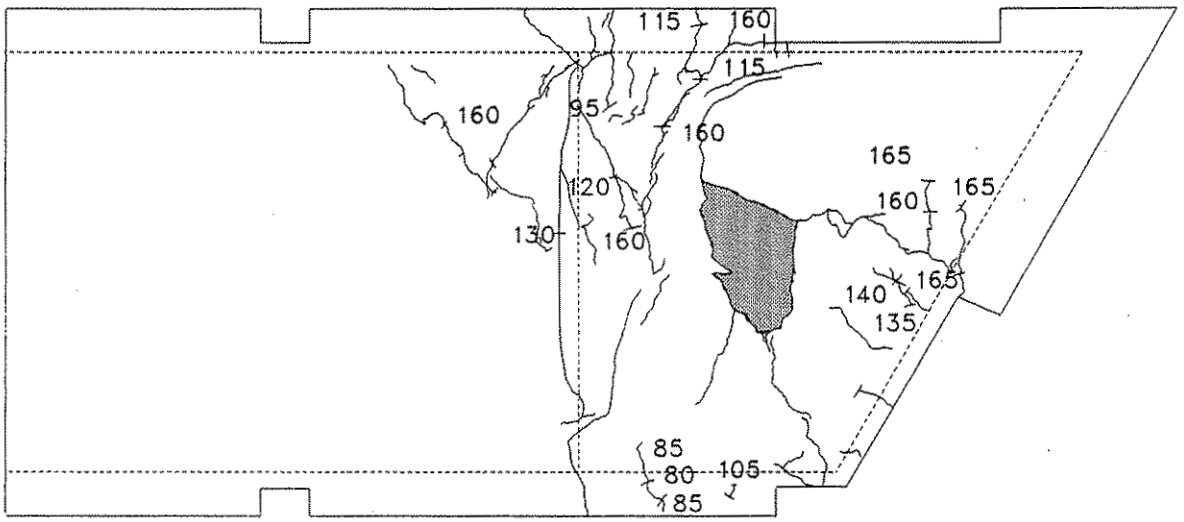

(a)

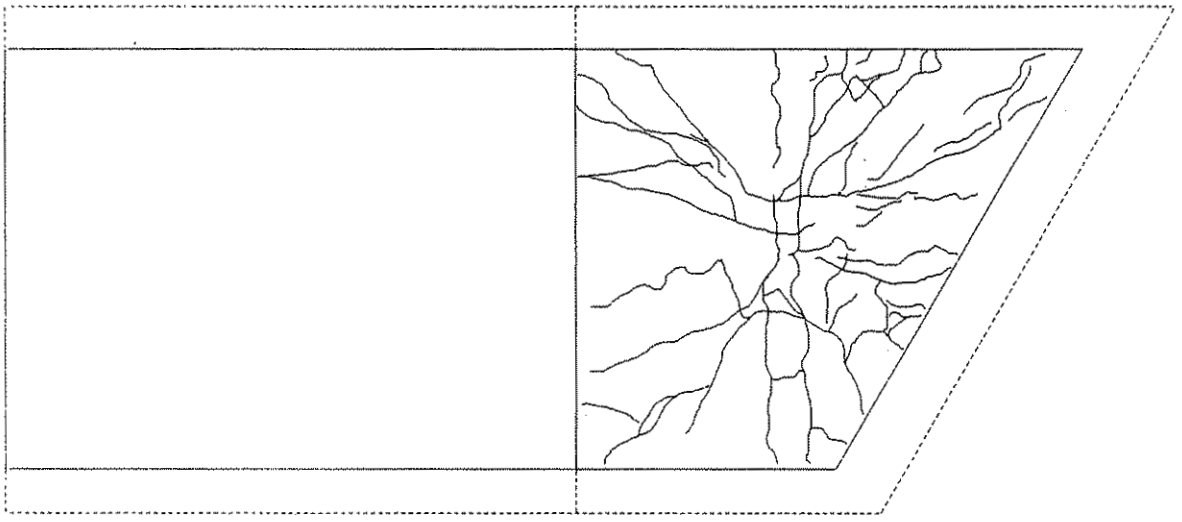

(b)

Figure 6.42. Crack patterns on Specimen No. 4 from Ultimate Test No. 1: (a) Top surface of slab, (b) Bottom surface of precast panel.

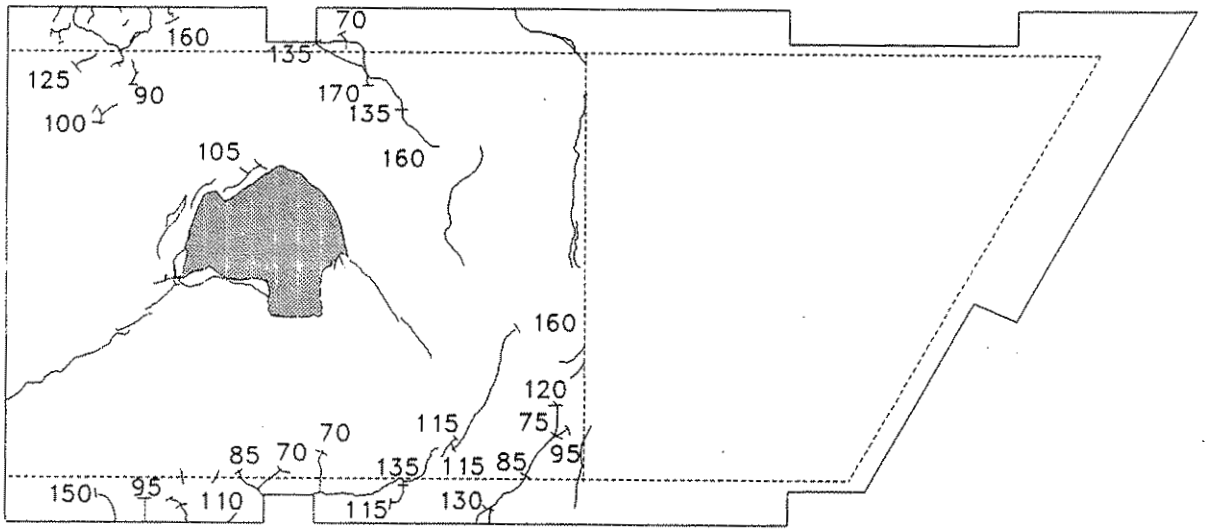

(a)

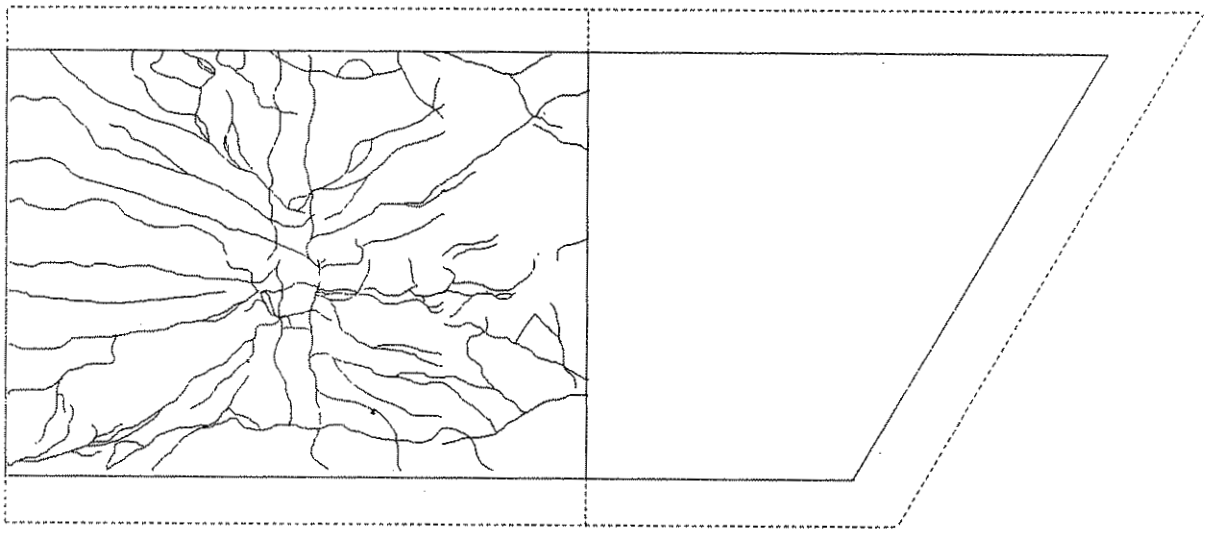

(b)

Figure 6.43. Crack patterns on Specimen No. 4 from Ultimate Test No. 2: (a) Top surface of slab, (b) Bottom surface of precast panel.

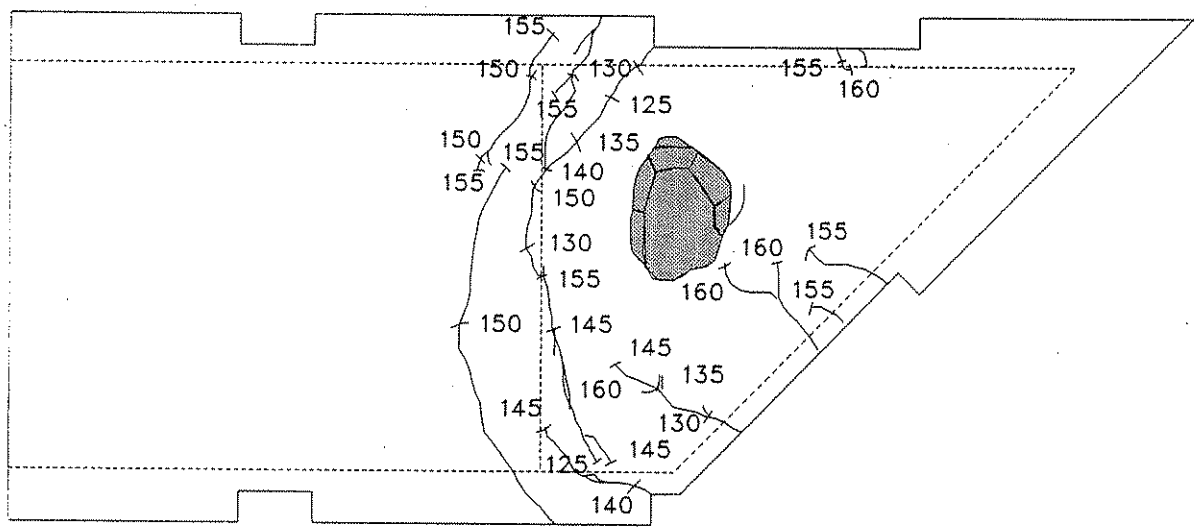

(a)

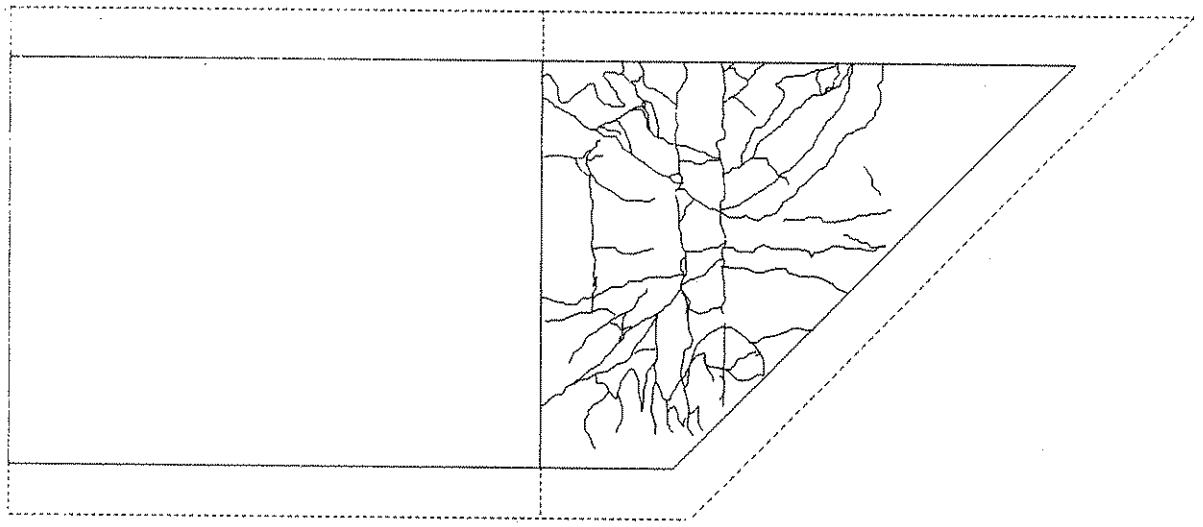

(b)

Figure 6.44. Crack patterns on Specimen No. 5 from Ultimate Test No. 1: (a) Top surface of slab, (b) Bottom surface of precast panel.

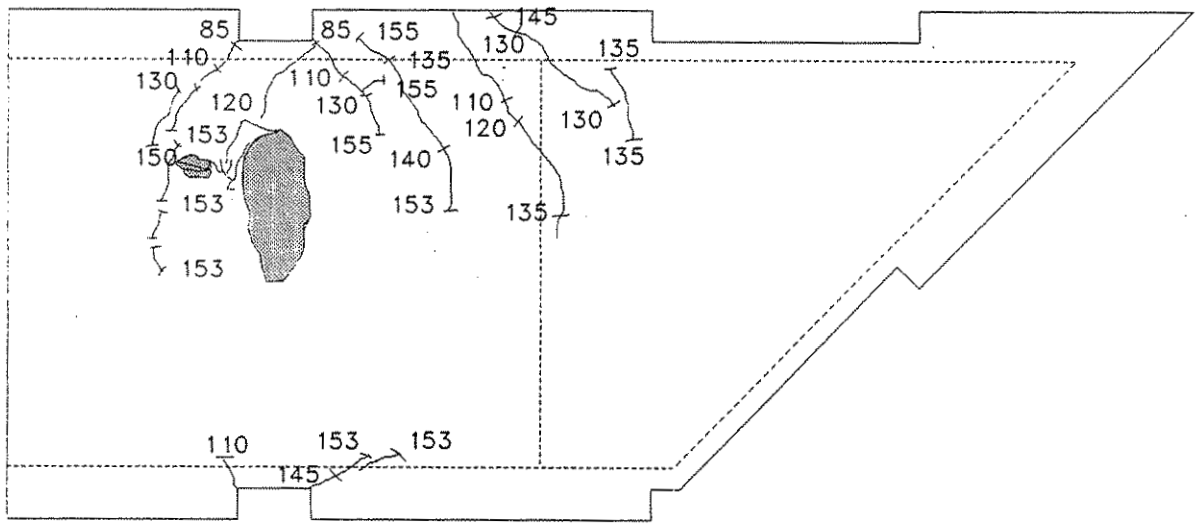

(a)

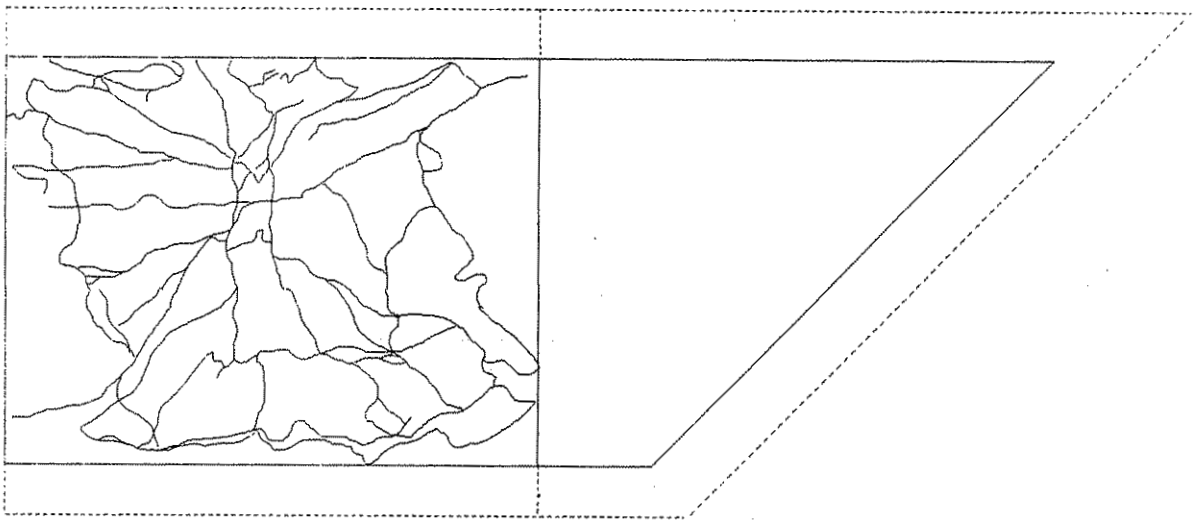

(b)

Figure 6.45. Crack patterns on Specimen No. 5 from Ultimate Test No. 2: (a) Top surface of slab, (b) Bottom surface of precast panel.

As Table 6.11 indicates, during only two of the ultimate load tests had a sufficient number of properly positioned cracks developed to form a potential yield-line pattern. These strength tests involved a wheel load position on the portion of the composite slab which was not adjacent to the modeled abutment or pier diaphragm for Specimen Nos. 2 and 4. If the failure in these two regions of the composite slab specimens was flexural, large inelastic rotations along the positive and negative moment yield-lines caused by yielding of the reinforcement or excessive tensile strains in the prestressing strands should have occurred. However, this type of deformation did not seem to have taken place, since the slab segments defined by the slab edges and yield-lines did not experience large rigid body rotations about the yield-lines or other axes of rotation. Therefore, the nominal strength of the composite slab specimens was probably not limited by the full flexural strength of the slabs had adequate strand development been provided.

6.7.2. Shear Strengths Versus Test Results

The nominal punching shear resistances calculated by the revised AASHTO model are listed in Table 6.12.

Even though a significant amount of test scatter can occur when the shear strength of reinforced concrete members is evaluated experimentally, a comparison of the calculated punching shear strength, P_a, and the ultimate experimental test load, P_u, for the composite slab specimens reveals remarkably good correlation. The close agreement indicates that for six of the tests, punching shear was probably the failure mode, and for the other three tests, punching shear may have been the failure mechanism. An indication that punching shear occurred for all of the specimen strength tests was noted by the observation that the wheel load footprint was depressed into the slab and large pieces of the bottom surface of the panel were split off when the ultimate load was reached.

Table 6.12. Punching shear limit loads and experimental ultimate strengths

Specimen No.	Ultimate Test No.	f'_c (psi)	Revised AASHTO				P_u (kips)	$\frac{P_n}{P_u}$	Shear Failure Mode
			β_c	b_o (in.)	d_p (in.)	P_n (kips)			
1	1	7,346	2.64	82.82	6.83	170	145	1.17	Yes
2	1	6,990	2.00	79.63	6.22	166	150	1.11	Yes
	2	7,596	2.00	79.79	6.26	174	155	1.12	Yes
3	1	7,186	2.00	82.91	7.04	198	175	1.13	Yes
	2	7,257	2.00	84.07	7.33	210	175	1.20	Yes
4	1	8,165	2.00	84.15	7.35	224	170	1.32	Possibly
	2	7,462	2.00	82.71	6.99	200	165	1.21	Possibly
5	1	7,229	2.00	81.47	6.68	185	160	1.15	Yes
	2	7,520	2.00	82.35	6.90	193	153	1.26	Possibly

6.8. Failure Mode and Reserve Strength

6.8.1. Method of Failure

The potential failure mechanisms for the composite slab, specimens were as follows:

1. Bond failure between the prestressing strands and the surrounding concrete in the precast panels, along the strand embedment length (Section 6.2).
2. Horizontal shear failure at the interface between the topping slab and the precast panels, resulting in the loss of composite behavior (Section 6.3).
3. Bearing failure at the panel supports (Section 6.6).
4. Flexural failure after a sufficient number of yield-lines had formed to produce a collapse mechanism (Section 6.7.1).
5. Punching shear failure around the wheel load footprint (Section 6.7.2).

Since the strength tests for the slab specimens involved a single concentrated load, the failure of the specimens involved a combination of some of the potential failure mechanisms previously

discussed. Considering the five failure modes listed, the only failure mechanism which was not observed for any of the specimens tested was a bearing failure at the panel supports. Due to the behavior of slab systems in general, a localized failure may not cause a complete collapse of the slab, since lateral continuity will distribute strains to adjacent portions of the slab. This behavior was observed for each of the specimens. For example, a bond failure for an individual prestressing strand located near the concentrated load was detected by strand-slip measurements at the end(s) of the strand well before the ultimate strength of the slab was reached.

The primary failure mechanism for the composite slab specimens was punching shear. Even though many flexural cracks propogated throughout the top surface of the topping slab and throughout the bottom surface of the precast panel(s) where the concentrated wheel load was applied, a complete yield-line mechanism was not formed for most specimens prior to failure of the deck. For the two instances where a yield-line mechanism had possibly formed, the required inelastic rotations about the yield-lines, that would induce large rigid body rotations of slab segments did not occur. The conclusion that punching shear was the primary failure mode for the composite slab specimens tested is in agreement with the findings by Fang et al [15].

6.8.2. Service Level and Nominal Strengths

A measure of safety (factor of safety) for any structure or structural element is given by the ratio of the nominal strength to the required service level strength. The nominal strength is the maximum anticipated strength based on geometric and material property parameters. The required service level strength is the required strength due to expected service level loads acting on the structure. For the AASHTO HS-20 truck loading, the service level wheel load is 16 kips without impact and 20.8 kips with a 30% impact load. When a 20.8 kip concentrated load was placed on the AASHTO wheel footprint (8 in. by 20 in.) at each of the designated positions on the surface of the specimens, the behavior of the deck remained elastic. Even when a factored load of three times the

standard HS-20 wheel load (48 kips) was applied to Specimen Nos. 3, 4, and 5, the deck behavior was still elastic.

The first concrete cracks, which were observed, appeared either along the edge(s) or on the top surface of the deck at a load of about 70 kips. This load magnitude was over three times the service level design load of 20.8 kips. For safety reasons, the propogation of cracks on the bottom surface of the concrete panels were not recorded until after the testing was completed. The smallest collapse load of 145 kips occurred when the concentrated test load was positioned directly over the joint between the two precast panels and at the mid-span of the slab for Specimen No. 1. This load was equal to almost seven times the service level design load. Specimen No. 3 resisted the largest ultimate load of 175 kips, which was over eight times the AASHTO wheel load including impact. Therefore, the range in the factor of safety for the composite slabs tested was from 6.97 to 8.41. Table 6.13 lists the ultimate test load, P_u, the load factor, L.F., and factor of safety, F.S., for each of the slab specimens.

Table 6.13. Load factors and factors of safety for the composite slab specimens.

Specimen No.	Ultimate Test No.	P_u (kips)	L.F.[a]	F.S.[b]
1	1	145	9.06	6.97
2	1	150	9.38	7.21
	2	155	9.69	7.45
3	1	175	10.94	8.41
	2	175	10.94	8.41
4	1	170	10.63	8.17
	2	165	10.31	7.93
5	1	160	10.00	7.69
	2	153	9.56	7.36

[a]L.F. = P_u/16.0
[b]F.S. = P_u/20.8

The load factor, L.F., is the ratio of the ultimate test load, P_u, to the standard AASHTO HS-20 wheel load (16.0 kips) without impact. The factor of safety, F.S., is the ratio of P_u to the design wheel load of 20.8 kips (standard AASHTO HS-20 wheel load with a 30% impact factor).

As shown by the magnitudes for the factor of safety listed in Table 6.13, the simply supported composite deck specimens, which were constructed and tested under laboratory conditions, had more than adequate strength. The skew angles of 15, 30, and 40 degrees for Specimen Nos. 3, 4, and 5, respectively, did not appear to affect the ultimate load resistance of the deck, when the ultimate wheel load was positioned at a selected point over each of the trapezoidal-shaped precast panels.

7. EPILOGUE

7.1. Summary

7.1.1. Overview

Precast prestressed concrete panels have been used in the construction of bridge decks for secondary roads in Iowa and for both primary and secondary roads in other states. The behavior of these deck types, in which the two bearing edges of the panels are parallel, have been investigated by previous researchers. When precast panels are specified at abutment and pier diaphragm locations, the end panels are supported along three edges. If a bridge involves a skew angle, the end panels will be trapezoidal in shape. These non-rectangular precast panels have prestressing strands with varying lengths; therefore, the strand embedment lengths are not constant within these panels. The lack of adequate development length for the strands in non-rectangular panels suggests that inadequate flexural strength could be possible when wheel loads are positioned over these panels.

The objective of this research project was to determine the behavior of precast prestressed concrete panels that the State of Iowa uses as permanent forms for both skewed and non-skewed reinforced concrete bridges at abutment and pier diaphragm locations. To accomplish this objective, a review of previous research related to bridge deck panels was completed, a survey of design agencies and precast concrete manufacturers was conducted, field inspections of three bridges constructed with precast concrete panels within the State of Iowa were performed, a finite element anlaysis of a trapezoidal shaped panel subjected to prestressing forces was completed, an experimental study to evaluate the prestress force developed in the panels at strand release was conducted, many finite element analyses of homogenous slabs used to model the composite slab specimens were performed, and an extensive experimental program which involved the testing of five full-scale composite bridge decks was conducted.

7.1.2. Surveys

A total of 121 questionnaires were sent to the 50 state departments of transportation, the District of Columbia, tollway authorities, two United States provinces, and eight Canadian provinces. This in depth survey contained 82 multiple choice questions which addressed general bridge geometry and conditions, general panel geometry and conditions, panel bearing details, prestressing strand description and conditions, design criteria, economy, experiences with panel useage, and panel details and specifications. Approximately 60 percent of the questionnaires were returned. Only 29 design agencies who returned the survey stated that they have designed or specified precast panels for permanent forms as the construction of bridge decks.

Another questionnaire was sent to 192 precast manufacturers who are members of the Prestressed Concrete Institute. This extensive survey also involved 82 multiple choice questions (some questions were identical with the ones contained on the questionnaire which was sent to the design agencies). The questions addressed relative background information about the precaster, general bridge panel geometry and conditions, bridge panel bearing conditions, prestressing strand conditions and description for bridge panels, design criteria, economy, inspection, experiences with panel useage, and panel details and specifications. Approximately 38 percent of the questionnaires were returned. Only 27 precasters who returned the survey stated that their company manufactures precast panels for bridge deck construction.

7.1.3. Bridge Deck Inspections

Three precast concrete girder bridges near the city of Eldora, Iowa in Hardin County were inspected. Two of the bridges have three spans and the other bridge is a single span structure. One of the three span bridges had been built with a 30 degree skew angle, while the other two bridges involved non-skewed construction. The multi-span bridges cross the Iowa River and the single span bridge crosses Pine Creek.

The inspections were performed to observe general geometrical relationships, construction details, and to note the visual condition of the bridges. Since each bridge involved water crossings and since the height beneath the bridges was substantial, the extent of the visual inspections was limited.

7.1.4. Finite Element Models

A finite element model, containing a single layer of 180 elements and 201 nodes, was developed to represent a trapezoidal-shaped panel, having a diagonal edge orientated to match a 40 degree skewed bridge condition. The mesh size was established to provide nodal points which occurred along the prestressing strands in an actual panel. Thin plate elements with isotropic properties were selected; therefore, the precast slab was modeled as a homogenous material with properties of the uncracked concrete in the panels. The prestressing strands were not included in the simple model. Forces were applied to the edge nodes of the finite element model to represent prestressing forces which were induced into the non-rectangular panel during strand detensioning. By comparing the analytically derived and experimentally measured concrete strains, the accuracy of the experimentally obtained initial strand transfer length was verified.

A large number of finite element models were generated to represent the full-scale composite slabs which were tested. A different model was developed for each wheel load position. Each model contained a single layer of between 200 and 470 thin isotropic plate elements and between 242 and 488 nodes. The precast panels and reinforced concrete portions of a deck were not modeled separately. Also, the reinforcement in both the panels and the topping slab was not included in the finite element models. For each experimental test performed, a finite element study was completed to obtain strains and displacements. The analytical results were compared with the experimental results.

7.1.5. Experimental Tests

The experimental program involved two aspects. The first experimental tests, which were conducted at the precast plant where the panels were cast, were performed to evaluate the initial strand transfer length. Prior to casting the concrete for the panels, polyester mold embedment strain gauges were wired between selected prestressing strands. After the concrete had cured, strain readings were taken before, during, and after the strands were cut. Knowing the stress in the prestressing strands from their elongation during tensioning and measuring the induced compressive strains in a panel after detensioning, the prestress remaining in the strands was calculated.

The second series of experimental tests involved the construction and testing of five full-scale composite bridge decks in the laboratory. Four of the specimens modeled conditions adjacent to an abutment or pier diaphragm with skew angles of 0, 15, 30, and 40 degrees. The other specimen represented a interior slab condition. Each of the slabs, which were simply supported on concrete abutments representing precast concrete bridge girders and reinforced concrete diaphragms, contained two precast concrete panels and a reinforced concrete cast-in-place topping slab. The construction details essentially followed the Iowa DOT standard bridge deck drawing involving the use of panel subdecks, except for the use of some sleeved prestressing strands. To prevent breakage of the triangular corner in a trapezoidal-shaped panel during strand detensioning, two, three, and four of the shortest strands were sleeved along their entire length for the panel adjacent to the modeled diaphragm having a bridge skew angle of 15, 30, and 40 degrees, respectively.

To establish the elastic behavior of the composite bridge slabs, both single and double loads incremented up to the standard AASHTO HS-20 wheel load with 30 percent impact were positioned at numerous locations on the slab surface. Particular attention was given to the region of the slab adjacent to the modeled diaphragm support condition. For the specimens containing a bridge skew angle of 30 and 40 degrees, a factored wheel load equal to three times the standard wheel load without impact was also applied at various locations within the region of the slab involving the

trapezoidal precast panel. This second load phase was instituted to investigate strand anchorage resistance for those prestressing strands which have shorter embedment lengths, due to the skew angle, than the lengths present in a rectangular shaped panel. After completing the service and factored level load tests, the ultimate strength (nominal resistance) of each composite slab was experimentally established by applying an incresing concentrated load over an area of approximately the same size as the AASHTO wheel load footprint, until a failure occurred. For Specimen No. 1, representing an interior composite slab condition, this load was placed at the midspan and directly above the transverse joint between the two precast panels. For Specimen Nos. 2, 3, 4, and 5, representing a composite slab adjacent to a abutment or pier diaphragm for a bridge with a skew angle of 0, 15, 30, and 40 degrees, respectively, this load was first positioned at or near the midspan and over the panel adjacent to the modeled diaphragm support. After the completion of this test, another strength test was performed on the portion of the slab containing the rectangular-shaped panel. For the second strength test, the load was placed along the mid-width of the panel and at the midspan for Specimen Nos. 2 and 4 and near the support for Specimen Nos. 3 and 5. These ultimate load tests provided information concerning both elastic and inelastic behavior of the composite slabs.

During all of the load tests, three types of displacements were monitored. The vertical deflections at many locations on the slab surface were measured with dial gauges. At both ends of selected prestressing strands, direct current displacement transducers were used to measure strand slippage. At selected locations along the supported slab edges, dial gauges were used to measure movement between the precast panel and the reinforced concrete topping slab.

To obtain experimental flexural strains, electrical resistance strain gauges were mounted at selected locations on the top surface of the reinforced concrete slab and on the top and bottom surfaces of the precast concrete panels. The majority of the strain gauges were orientated parallel to the panel span (transverse to the longitudinally modeled bridge girders). Some strain gauges were

aligned perpendicular to the panel span. The magnitudes of the flexural strains in the direction of the panel span provided information needed to evaluate the load distribution along the composite slab.

To resist the vertical loads applied to the composite slab specimens, a large structural steel frame was designed, fabricated and construction in the laboratory. The frame straddled the specimens and allowed loads to be applied anywhere on the top surface of the slab. Also, an instrumentation framework was fabricated and constructed to provide a stable platform for the dial gauges used to monitor the slab deflections.

7.2. Conclusions

7.2.1. Surveys

The design agencies' responses to their survey revealed that a significant amount of variation exists regarding the geometry for the precast panels, panel reinforcement, panel bearing details, and deck construction near abutment or pier diaphragms. Less variations amongst the design agencies exists with respect to design criteria. Considering some of the questions which drew a significant majority of the responses, the following list provides general trends in composite bridge deck construction:

- Panels are usually permitted on either primary or secondary roads.
- The maximum bridge skew angle for panels located adjacent to an abutment or pier diaphragms is not normally specified.
- Panels are usually supported by precast prestressed concrete girders.
- The maximum panel width normally used is 8 ft.
- The minimum panel thickness most frequently specified is either 3 or 3 1/2 in.
- Composite behavior between the precast panels and the cast-in-place reinforced concrete slab is usually accomplished by either a raked finish only or a raked finish with U-shaped bars or dowels. Composite action is applied in the bridge deck design.

- Non-rectangular shaped panels normally do not contain any additional reinforcement, other than the conventional rectangular panel reinforcement.
- For the precast panels, the concrete most frequently specified is normal-weight concrete with a 5000 psi compressive strength. The concrete contains air entrainment and does not contain corrosion inhibiting admixtures.
- The temporary bearing material, which supports the panels prior to casting of the topping slab, is usually fiberboard, neoprene, polystyrene, or a similar material.
- The permanent bearing material for the panels is normally a continuous mortar, grout, or concrete bed.
- The most common size of prestressing strand is 3/8 in. diameter, and the most common type of strand is ordinary stress-relieved.
- Usually, the strand positioning within a panel is concentric with the center of gravity of the panel and is uniformally spaced across the panel width.
- Strand extensions are specified very frequently; however, the extensions are not considered to be part of the strand development length.
- According to most design agencies that permit either rectangular or non-rectangular shaped panels, debonding some of the prestressing strands for a portion of their length is never done.
- Fatigue effects are rarely considered in the design of composite bridge decks.
- Continuity of the bridge deck across the girders was assumed by essentially all of the design agencies.

The validity of assuming complete continuity of the full-depth slab across the girders for negative moment strength may require additional investigation, considering that shrinkage cracking of the concrete cast between the ends of the panels may occur, particularly if strand extensions are not used or if the strand extensions do not overlap significantly. To resist the negative moment

within the composite slab at the girders, the design agencies use the top layer of reinforcement found in a conventional full-depth cast-in-place slab.

A significant number of design agencies, which had previously permitted the use of precast panel subdecks for bridge deck construction, have discontinued specifying panels even as an alternate to a full-depth cast-in-place slab. Problems with panel quality control, development of reflective cracks in the topping slabs, unknown economical benefits associated with composite bridge decks, completion of experimental programs, and specifically prohibiting use of panels on steel girder bridges were given as reasons for the change in agency policy. Many of the design agencies which have not specified precast panel subdecks provided explanations for their current position on bridge deck construction. Their comments implied that precast panels would not be permitted in bridge decks, until their agency has had an opportunity to evaluate any new information about deck performance, economics, serviceability, and future AASHTO guidance for design and until a demand for the product is generated by the construction industry. Even several of the agencies which permit or had permitted the use of precast panels had implied that evaluation of existing composite bridge decks will establish future applications of panels in bridge construction.

About 40 percent of the 29 design agencies, which have specified precast panels, responded that they could not really comment about specific problems encountered with panel usage, since they had not used panels often enough. The other 60 percent of the design agencies have experienced some cracking in the topping slab and panels of the composite decks; however, no agency classified the problems encountered as major. Twelve agencies categorized their problems associated with precast panels as moderate or significant, while 8 agencies classified the problems as minor to non-existent. The design agencies gave an average overall rating about midway between good and fair for precast panel usage.

The precasters' response to their survey showed that considerable variation exists regarding precast panel and prestressing strand geometries. Therefore, standardization does not exist for this

bridge panel product. About one-half of the panel manufacturers, who produce panels, perform a structural design for the panels. A comparison of some of the responses to the design questions which were identical on each questionnaire revealed that essentially consistant answers were provided by both the precast manufacturers and the design agencies.

Many of the precast concrete producers who have stopped producing panels or who never produced panels for bridge decks provided a variety of reasons for not casting panels. These reasons included the lack of demand for the product, production control can not meet the stringent tolerance limitations imposed by the design agencies, panel use is prohibited by the design agency, local contractors prefer to use cast-in-place slabs, deck panels are not economically feasible, and poor past performance by some manufacturers has caused a decline in panel use.

The precasters believe that the problems associated with precast panel usage are less severe than the design agencies implied. Fourteen panel producers classified any problems as minor to non-existent, four thought that the problems were moderate, and only one producer considered the problems to be major. As anticipated, the panel producers gave a higher overall rating for precast panel usage than the rating provided by design agencies. The average rating from the 24 panel producers was about midway between very good and good.

The responses by both design agencies and precast panel manufacturers to the questions on the surveys that addressed economy revealed that most design agencies and about one-half of the panel producers have not performed economical studies to determine whether panels are more economical than a full-depth cast-in-place slab. Therefore, most designers and precasters do not know if cost savings exist when composite slabs are constructed. When cost savings were estimated, only 3 out of 27 design agencies listed the savings as between zero and one dollar per square foot of deck area; while 8 out of 24 panel producers listed the savings as between zero and three dollars per square foot of deck area.

7.2.2. Bridge Deck Inspections

The general condition of the precast panels that were used in the three prestressed concrete girder bridges (Bridge Nos. 9066, 8401, and 7022) which were inspected appeared to be essentially the same. The similiarity in the visually evaluated condition of the panels is attributed to the fact that all three bridges have had about the same number of years of service and have been exposed to the same environmental conditions. Many of the panels, which were inspected from a close view, have single and sometimes multiple hairline cracks located directly below some of the prestressing strands within the center half of the panel width. These cracks usually extend along the entire panel length. Also, most of the observed panels have a slight discoloration (darker gray color) beneath essentially every strand within a panel. Some of the panels in Bridges Nos. 8401 and 7022 showed rust discoloration on the underside of panel directly beneath some strand locations. Two panels for Bridge No. 7022 show significant amounts of rust staining. One of the precast panels in Bridge No. 8401 was observed to have a diagonal crack at one of the panel corners.

The hairline cracks in bottom surface of the majority of the panels might be caused by shrinkage of the concrete in the topping slab, thermal expansion or contraction of the cast-in-place topping slab relative to the precast panels, and tensile strains along the bridge length induced by the wheel loads. Since a panel joint occurs at every 8 ft, strain relief perpendicular to the panel span is provided at each joint. Between the panel joints, the strain at the bottom surface of the panels increases towards the mid-width of the panels, until a crack forms when the modulus of rupture is exceeded. To establish the exact cause of these cracks, additional study would be necessary.

The cause for the rust discoloration and the possible cause for the concrete discoloration beneath the strands could be initial corrosion of the prestressing strands. The hairline cracks observed may allow moisture to penetrate through the concrete cover and reach the strands. Again, further study would be required to provide the proper explanation for the discolorations.

7.2.3. Analytical and Experimental Results

The initial transfer length for the prestress force in the strands was experimentally evaluated to be equal to approximately 28.5 in. This length compared reasonably well with the 24.4 in. length calculated from the modified ACI Code Commentary [3] expression and with the 30.3 in. length established by the equation proposed by Cousins et al [13]. Further studies of strand transfer lengths involving a finite element analysis of the trapezoidal-shaped panel, continuing a 40 degree skewed edge condition and subjected to prestressing forces obtained from the developed strand prestress versus embedment length relationship, produced concrete strains that closely matched the measured experimental strains.

The required development lengths for the 3/8 in. diameter, 270 ksi, 7-wire, prestressing strands, calculated from the expressions given by the AASHTO and ACI Specifications [1, 2], Cousins et al [13], and Zia and Mustafa [33], were longer than the embedment lengths available in the test specimens. Therefore, strand slippage should have resulted prior to obtaining the ultimate flexural strength of the composite slabs. Slippage of prestressing strands was recorded during all of the ultimate strength tests, except for one test when a transducer malfunction caused a loss of strand-slip measurements. For Specimen Nos. 1 through 5, the ultimate load tests revealed that slippage (strand-slip) between a prestressing strand and the surrounding concrete at the end of a precast panel occurred within a range of from 2.64 to 6.01 times the design load of 20.8 kips, (standard AASHTO wheel load with a 30 percent impact factor).

Composite behavior between the precast panels and the reinforced concrete topping slab is assumed to exist for conventional analyses of these types of bridge decks. For the service level wheel loads equal to 20.8 kips that were applied to all five specimens and for the factored level wheel loads equal to 48.0 kips that were applied to the fourth and fifth specimens (Specimen Nos. 1, 2, and 3 were not subjected to factored level wheel loads), movement (topping-slip) between the panels and the topping slab did not occur. Further verification that composite behavior existed at both service

and factored level loads for the specimens was obtained by comparing the deflection and strain results from the finite element analyses and from the experimental tests. Very good correlation for these parameters occurred between the analytical studies and the experimental tests.

For Specimen Nos. 1 through 5, the ultimate load tests revealed that the break-down of composite behavior as measured by the topping-slip occurred within a range of from 2.16 to 6.01 times the design load of 20.8 kips (standard AASHTO wheel load with 30 percent impact). Initial degradation of composite behavior was established by evaluation of the strain differences (interface-slip) between the top of a precast panel and the underside of the topping slab. Precise strain measurements were not possible due to a high degree of sensitivity caused by drift in strain readings for the strain gauges which were placed on the top of the precast panels and covered with concrete during casting the topping slab and by the accuracy of the thickness measurements for the panels and composite slab at the strain gauge locations. Considering a quantitative approach, interface-slip was believed to have occurred if a distinct shift in the behavior of load versus slip was observed. At those locations where reliable strain measurement were obtained, the ultimate load tests for Specimen Nos. 1, 2, and 5 revealed that the initial or localized break-down of composite behavior as measured by the interface-slip occurred within a range of from 1.92 to 3.37 times the design load of 20.8 kips (standard AASHTO wheel load with 30 percent impact). Instrumentation malfunctions involving the interface-slip monitoring devices caused erratic results for this parameter evaluation for Specimen Nos. 3 and 4.

The load versus deflection behavior of the composite slab specimens was linearly elastic for both the service level load range (0 to 20.8 kips) and the factored level load range (0 to 48 kips). The maximum slab deflections were quite small for both of these load ranges. Deflections of less than 0.012 in. were encountered for the majority of the tests on each specimen. Generally, the finite element predictions for the load versus deflection relationships were in close agreement with the experimental results. Comparisons of specific deflection magnitudes obtained analytically and

experimentally revealed that the finite element model provided reasonably accurate predictions of the slab deflections, considering the simple element types used in the analytical model.

As anticipated, the presence of the modeled abutment or pier diaphragm significantly reduced the slab deflections when loads were placed near the modeled diaphragm. For the 30 and 40 degree skewed diaphragm configurations, the load versus deflection behavior for loads placed above the trapezoidal-shaped precast panel showed two distinct behaviors due to uplift at the slab corners which had occurred prior to applying any wheel loads. The uplift was attributed to concrete shrinkage of the topping slab.

The ultimate load tests showed that the initial portion of the load versus deflection behavior was linear. The maximum elastic load, P_e, was 90 kips for the midspan strength test above the panel joint for Specimen No. 1. The minimum magnitude for P_e was 65 kips for the first strength tests on Specimen Nos. 2 and 4 and for the second strength test on Specimen No. 5. The minimum load for which the first crack was observed on the top surface of any of the five composite slabs was 70 kips. This load was over three times the design wheel load of 20.8 kips. For safety reasons, the underside of the specimens were not observed during testing of the specimens; therefore, conclusions as to when the first crack appeared on the bottom surface of the precast panels can not be made.

In a relative sense, each specimen experienced a significant amount of inelastic deformation after the elastic limit had been reached. Considering all of the strength tests conducted, the deflection at the load point just prior to failure of a given specimen was at least equal to nine times the maximum elastic deflection for the specimen. However, the magnitude of the maximum load point deflection was small, varying between about one-third of an inch to one inch.

During each strength test, the corners of the composite slabs displaced upwards by substantial amounts, causing significant lengths of the slab to lift off of the supports. This behavior is typical when slabs, which do not have hold-down devices, are subjected to concentrated loads. When uplift is prevented, special corner reinforcement is required in the slab to prevent cracking at the corners.

Investigation of the midspan, transverse, flexural strains revealed that the strains on the top of the slab were slightly larger than the strains on the bottom of the precast panels, since the concrete in the precast panels had a larger compressive strength than the concrete in the topping slabs. For the service and factored level load ranges, the maximum, experimentally measured, midspan, transverse strains were less than 85×10^{-6} in./in. and 230×10^{-6} in./in., respectively. For both of these load ranges, the distribution of the midspan transverse strains along the specimen length showed that the joint between the two precast panels did not appear to affect the performance of the composite slab. Therefore, the reinforced concrete topping slab adequately transferred vertical shear stresses across the joint.

For all of the service level load tests, the magnitude of any tensile strains in the bottom surface of the precast panels in the direction of the panel span were small enough that cracking of the precast concrete panels should not have occurred. The effect of the strand prestress and the high modulus of rupture strength fo the concrete used in the panels contributed significantly to the positive moment cracking strength of the composite slabs. For the factored load tests, initial concrete cracking may have occurred.

The finite element models accurately predicted the behavior for the midspan transverse strain distributions along the specimen length. At locations removed from the point of load application, the analytically established strain magnitudes closely matched the experimentally measured strains, while near the load point, the analytical model did not predict strain magnitudes as accurately.

The nominal flexural strength of the composite slab specimens was analytically evaluated by applying yield-line theory. To develop the full flexural strength of a slab specimen, a complete yield-line pattern would have to have formed to produce a collapse mechanism prior to any strand slippage. For most of the ultimate load tests, a complete yield-line pattern had not formed. Only two tests involved a cracking pattern at failure that entailed a sufficient number of intersecting positive and negative moment yield-lines and other axes of rotation to potentially produce a collapse

mechanism. These strength tests involved loads applied over the rectangular precast panel for Specimen Nos. 2 and 4; therefore, the load was not near the modeled abutment or pier diaphragm. However, even in these two instances, unrestrained plastic rotations along the yield-lines did not appear to have occurred, since the slab did not physically collapse as a mechanism involving rotations of rigid slab segments. Considering the nine ultimate load tests conducted on Specimen Nos. 1 through 5, the ratio of the nominal moment strength established by yield-line theory to the experimental failure load ranged between 0.97 and 1.38.

The punching shear strength of the composite slab specimens was established analytically by applying a revised AASHTO model for this type of behavior. Using the concrete strength for the weaker slab layer (the topping slab) and setting the effective depth of the composite slab equal to the distance from the top of the specimen to the centroid of the prestressing strands, the nominal shear strengths were calculated. A comparison of the computed punching shear strength to the ultimate test load for each specimen revealed close correlation. For all of the ultimate load tests, the range in the ratio of the nominal punching shear strength to the experimental failure load was between 1.11 and 1.32. The appearance of the failure surface around the wheel load footprint was essentially the same for all of the strength tests. The footprint was depressed through the plane of the top surface of the slab and the concrete cover on the prestressing strands located in a broad region below the footprint was factured and in some instances, spalled off. Based on the comparison between the analytical and experimental load strengths and on the appearance of the failure, punching shear was concluded to be the primary failure mechanism for the composite slab specimens.

The joint between the two precast panels did not appear to affect the behavior of the composite bridge decks when service or factored level loads were applied to the specimens. Therefore, longitudinal continuity (continuity perpendicular to the panel span) was maintained across the panel joint. However, when the strength tests were conducted on the specimens, the region of

the reinforced concrete topping slab above the joint between the two panels always developed a crack at large load magnitudes. As soon as this crack was completely formed, the flexural resistance of the composite slab was essentially confined to the portion of the deck containing the loaded panel.

A final evaluation of the strength of the tested composite bridge decks was accomplished by computing a load factor (the experimental failure load divided by the AASHTO wheel load without impact) and the factor of safety (the experimental failure load divided by the AASHTO wheel load with impact). Considering all of the strength tests conducted on the five composite slab specimens, the range in the load factor was from 9.06 to 10.94 and the range in the factor of safety was from 6.97 to 8.41. These factors indicate that the composite slabs tested had sufficient strength to resist the statically applied service level loads. The skew angles of 15, 30, and 40 degrees did not appear to affect the nominal strengths of the composite decks when the ultimate load was placed at a selected position on the portion of the slabs containing the trapezoidal-shaped precast panels.

7.3. Recommendations for Bridge Panels

7.3.1. Bridge Deck Inspections

Since concrete cracking in both precast prestressed panels and topping slabs has been reported in the literature and have been noted by both design agencies and precast producers in the surveys reported herein, and since concrete cracking, discolorations, and rust staining have been observed on the underside of many of the panels used in the three bridges visually inspected during this research project, an inspection program should be instituted to monitor the condition of all bridge decks constructed with precast panels. The first inspection for a bridge should establish the location and extent of all concrete cracks, discolorations beneath strands, and rust stains on each panel. This information should be documented on drawings for reference during subsequent bridge inspections to establish whether additional cracking or staining has occurred since the previous inspection. Particular attention should be given to those locations where rust stains are observed, since a possibility exists that strand corrosion caused by moisture penetration may be occurring.

7.3.2. Precast Panels for Bridge Subdecks

The results from the questionnaires sent to both the design agencies and the precast panel producers suggest that additional inspections during panel production and installation would be beneficial to provide better quality control of the product. Several precasters noted that to provide more economical panel designs, standardization for precast panels by the industry should be undertaken. Also, the surveys revealed that economical studies, which compare the overall cost associated with bridge decks constructed with precast panel subdecks to the costs (including soffit formwork) of full-depth cast-in-place bridge decks, have not really been conducted. Presently, the vast majority of both designers and panel producers do not know whether cost saving can be incurred by substituting a composite bridge deck for a conventional cast bridge deck. Based on the survey results, the following recommendations are made:

- Additional inspections should be conducted by both the design agencies and the panel producers. These additional inspections should cover all aspects of panel involvement from bed preparation through curing of the cast-in-place topping slab.
- Standardization of precast panels as a product should be instituted by the industry. Standardization might be best accomplished through the development of a specific AASHTO Specification covering the design, production, and installation of precast prestressed concrete panel subdecks. The Prestressed Concrete Institute has already published design recommendations [28,29,31].
- Comprehensive economical analyses should be conducted to determine if composite bridge decks should be specified instead of conventional full-depth bridge decks. Since all bridges are unique in some respect, a partial economical analysis can be accomplished by the alternate bid process. A complete economic study should include a life cycle cost analysis of both bridge deck types.

The inspections of three bridges, constructed with precast panels in Hardin County, Iowa, revealed that possible corrosion of some of the prestressing strands may be present. If the recommended inspections discussed in Section 7.3.1 show that premature reinforcement corrosion is occurring, the use of epoxy coated prestressing strands, welded wire fabric, and any supplemental reinforcement is recommended for future composite bridge decks. The effects of increased development lengths with epoxy coated prestressing strands and bar and wire reinforcements would have to be considered in the composite slab designs.

The strength performance of the five composite slab bridge decks which were constructed and tested during this research project was excellent. The ultimate static load strengths were substantially greater than a standard design wheel load of 20.8 kips. Even the loads which produced the first indications of distress in the specimens were significantly larger than the standard wheel load. A modeled bridge skew of up to 40 degrees did not appear to affect the static load strength of the composite deck system. Therefore, based on the static load strength information reported herein, the continued use of precast panels as subdecks in bridge deck construction is recommended.

7.4. Recommendations for Additional Research

Additional research into the behavior of composite bridge deck slabs constructed with precast prestressed concrete panels could include the following topics:

1. Continuity of composite slabs across bridge girders.
2. Continuity of composite slabs with abutment and pier diaphragms.
3. Panel prestress developed with epoxy coated prestressing strands.
4. Comparison of composite slab strengths for slabs constructed with panels containing uncoated prestressing strands and welded wire fabric and panels containing epoxy-coated prestressing strands and welded wire fabric.
5. Fatigue testing of composite slab segments.
6. Non-destructive field load tests of a composite bridge deck to monitor behavior.

7. Non-destructive evaluation of an existing composite slab bridge deck for potential reinforcement corrosion and integrity of composite behavior.
8. Effects of shrinkage of the concrete in the cast-in-place topping slab on the development of cracks in the composite slab.
9. Causes for concrete discoloration and cracking beneath the prestressing strands in the precast panels used in bridge deck construction.

8. REFERENCES

8.1. Cited References

1. AASHTO. *Standard Specifications for Highway Bridges.* 13th Edition. The American Association of State Highway and Transportation Officials, Washington, D.C., 1983, and Interim Specifications Bridges (Second Supplement) 1985.

2. ACI Committee 318. "Building Code Requirements for Reinforced Concrete." ACI Standard 318-89. American Concrete Institute, Detroit, Michigan, 1989.

3. ACI Committee 318. "Commentary on Building Code Requirements for Reinforced Concrete." ACI Standard 318-89. American Concrete Institute, Detroit, Michigan, (Printed with ACI-318 Code), 1989.

4. Barker, J. M. "Research, Application and Experience with Precast Prestressed Bridge Deck Panels." *PCI Journal,* 20, No. 6 (Nov-Dec. 1975): 66-85.

5. Barnoff, R. M. and Rainey, D. E. "Laboratory Test of Prestressed Concrete Deck Planks and Deck Plank Assemblies." *Research Project No. 71-8 An Experimental Prestressed Concrete Bridge Report No. 2.* The Pennsylvania Transportation Institute, The Pennsylvania State University, June 1974.

6. Barnoff, R. M., Orndorff, J. A., Jr., Harbaugh, R. B., Jr., and Rainey, D. E. "Full Scale Test of a Prestressed Bridge with Precast Deck Planks." *PCI Journal,* 22, No. 5 (Sept-Oct. 1977): 66-83.

7. Bieschke, L. A. and Klinger, R. E. "The Effect of Transverse Strand Extensions on the Behavior of Precast Prestressed Panel Bridges." *Research Report 303-1F.* Center for Transportation Research, Bureau of Engineering Research, The University of Texas at Austin, June 1982.

8. Buckner, C. D. and Turner, H.T. "Performance Test of Full Span Panel Form Bridges." Research Report No. 80-1C. Engineering Research Louisiana State University, Baton Rouge, Louisiana, 1981.

9. Buckner, C. Dale and Turner, H. T. "Performance of Full-Span Panel-Form Bridges Under Repetitive Loading." Transportation Research Record 903, Transportation Research Board, National Research Council: 45-52.

10. Callis, E. G., Fagundo, F. E., and Hays, C. O., Jr. "Study of Cracking of I-75 Composite Deck Bridge Over Peace River." *Research Report No. U49F Volume No. 1.* Department of Civil Engineering, College of Engineering, University of Florida, Gainesville, July 1982.

11. Cousins, Thomas E., Johnston, David W., and Zia, Paul. "Transfer Length of Epoxy-Coated Prestressing Strand." ACI Materials Journal, 87, No. 3 (May-June 1990):193-203.

12. Cousins, Thomas E., Johnson, David W., and Zia, Paul. "Development Length of Epoxy-Coated Prestressing Strand." ACI Materials Journal, 87, No. 4 (July-Aug. 1990): 309-318.

13. Cousins, Thomas E., Johnston, David W., and Zia, Paul. "Transfer and Development Length of Epoxy Coated and Uncoated Prestressing Strands." *PCI Journal*, 35, No. 4 (July-Aug. 1990): 92-103.

14. Fagundo, F. E., Tabatabai, H., Soongswang, K., Richardson, J. M., and Callis, E. G. "Precast Panel Composite Bridge Decks." Concrete International - Design and Construction, May 1985: 59-65.

15. Fang, I. K., Tsui, C. K. T., Burns, N. H., and Klingner, R. E. "Load Capacity of Isotropically Reinforced, Cast-in-Place and Precast Panel Bridge Decks." *PCI Journal*, 33, No. 4 (July-Aug. 1990):104-113.

16. Federal Highway Administration. "Prestressing Strand for Pretension Applications - Development Length Revisited." Memorandum to Regional Federal Highway Administrators, Direct Federal Administrator (HDF-1) from Chief, Bridge Division Office of Engineering, Oct. 26, 1988.

17. Hays, Clifford O., Jr., Fagundo, Fernando, E., and Callis, Eric C. "Study of Cracking of Composite Deck Bridge on I-75 Over Peace River." Transportation Research Record 903, Transportation Research Board, National Research Council: 35-44.

18. Iowa DOT. Standard Specifications for Highway and Bridge Construction. Series of 1984. Iowa Department of Transportation, Ames, IA, 1984.

19. Jones, H. L., and Furr, H. L. "Development Length of Strands in Prestressed Panel Subdeck." *Research Report No. 145-2.* Texas Transportation Institute, Texas A&M University, College Station, Texas, December 1970.

20. Jones, H. L., and Furr, H. L. "Study of In-Service Bridges Constructed with Prestressed Panel Sub-Decks." *Research Report 145-1*, Texas Transportation Institute, Texas A&M University, College Station, Texas, July 1970.

21. Kaar, P. H., and Hanson, N. W. "Bond Fatigue Test of Beams Simulating Pretensioned Concrete Crossties." *PCA Research and Development Bulletin*, 8, No. 6 (Oct. 1963): 1-11.

22. Kaar, P. H., LaFraugh, R. W., and Mass, M. A. "Influence of Concrete Strength on Strand Transfer Length." *PCI Journal*, 8, No. 6 (Oct. 1963): 47-67.

23. Klingner, Richard E. and Bieschke, Lee A. "Effects of Transverse Panel Strand Extensions on the Behavior of Precast Prestressed Panel Bridges." *PCI Journal*, 33, No. 1 (Jan-Feb. 1988): 68-88.

24. Kluge, R. W., and Sawyer, H. A. "Interacting Pretensioned Concrete Form Panels for Bridge Decks." *PCI Journal*, 20, No. 3 (May-June 1975): 34-61.

25. Lane, Susan N. "Status of Research on Development Length of Strand for Prestressed Concrete." Unpublished report. Federal Highway Administration, Office of engineering and Highway Operations Research and Development, Structures Division, May 1989.

26. Lin, T. Y. and Burns, N. H. *Design of Prestressed Concrete Structures*, 3rd Ed., John Wiley and Sons, New York, 1981.

27. Over, R. Stanton and Au, Tung, "Prestress Transfer Bond of Pretensioned Strands in Concrete," ACI Journal, Proceedings V.62, No. 11, Nov., 1965, pp. 1451-1459.

28. PCI Bridge Committee. "Tentative Design and Construction Specifications for Bridge Deck Panels." *PCI Journal*, 23, No. 1 (Jan-Feb. 1978): 32-39.

29. PCI Bridge Committee. "Precast Prestressed Concrete Bridge Deck Panels." *PCI Journal*, 32, No. 2 (Mar-Apr. 1987): 26-45.

30. PCI Bridge Producers Committee. Committee Correspondence to PCI Bridge Producer Members regarding Strand Development Length Actions from Dec. 1986 to Oct. 1988, from Scott E. Olson, Committee Chairman, Nov. 10, 1988.

31. Ross Bryan Associates, Inc. "Recommended Practice for Precast Prestressed Concrete Composite Bridge Deck Panels." *PCI Journal*, 20, No. 2 (March-April 1988): 67-109.

32. Wang, Chu-Kia and Salmon, Charles G., *Reinforced Concrete Design*, 4th Ed. Harper and Row, New York, 1985.

33. Zia, P. and Mostafa, T. "Development Length of Prestressing Strands." *PCI Journal*, 22, No. 5 (Sept-Oct. 1977): 54-65.

34. Zia, Paul, Preston, Kent H., Scott, Normal L., and Workman, Edwin B. "Estimating Prestress Losses." Concrete International-Design and Construction, Vol. 1, No. 6 (June 1979): 32-38.

8.2. References Not Cited

1. Ban, Shizuo, Muguruma, Hiroshi, and Morita, Shiro. "Study on Bond Characteristics of 7-Wire Strand at Prestress Transfer." Technical Report No. 67, Engineering Research Institute, Kyoto, Japan, March 1960: 1-14.

2. Brooks, Mark D., Gerstle, Kurt H., and Logan, Donald R. "Effect of Initial Strand Slip on the Strength of Hollow-Core Slabs." *PCI Journal*, 33, No. 1 (Jan-Feb. 1988): 90-111.

3. Janney, J. R. "Nature of Bond in Pre-Tensioned Prestressed Concrete." *ACI Journal*, 25, No. 9 (May 1954): 717-736.

4. Janney, J. R. "Report of Stress Transfer Length Studies on 270k Prestressing Strand." *PCI Journal*, 8, No. 1 (Feb. 1963): 41-45.

5. Martin, L. D. and Scott, N. L. "Development of Prestressing Strand in Pretensioned Members." *ACI Journal*, 73, No. 8 (Aug. 1976): 453-456.

6. Poston, Randall W., Breen, John E., and Carrasquillo, Ramon L. "Design of Transversely Prestressed Concrete Bridge Decks." *PCI Journal*, 34, No. 5 (Sept-Oct. 1989): 68-109.

7. Texas Transportation Institute. "Investigation to Determine Feasibility of Using In-Place Precast Prestressed Form Panels for Highway Bridge Decks." *PCI Journal*, 20, No. 3 (May-June 1975): 62-67.

9. ACKNOWLEDGEMENTS

The study presented in this final report was conducted by the Engineering Research Institute of Iowa State University and was sponsored by the Iowa Department of Transportation, Highway Division, through the Highway Research Advisory Board.

The author extends his sincere appreciation to William Lundquist and John Harkin from the Iowa Department of Transportation and Henry Gee formerly with the Iowa DOT for their support and assistance with the research work on precast prestressed concrete panel subdecks. The structural steel which was used to fabricate the large test frame and the aluminum posts and tubes which were used to construct the large instrumentation frame were provided by the Iowa Department of Transportation. Donald Henrich, general manager of Precast Concrete Operations, a Division of Wheeler Consolidated, Inc., in Iowa Falls, IA, provided the precast panels for the experimental testing program. For Don's assistance the author expresses his gratitude.

The author wishes to thank both Dr. Lowell Greimann for his participation and suggestions during the initial phases of the research and Douglas Wood, Structural Laboratory Supervisor, for his valuable assistance and contributions with the experimental program. Graduate students Arif Mahmood, who wrote the computer programs to compile the survey results, Roger Khoury, who assisted in tabulating the questionnaire results, and Bosedevarahatti T. Shivakumar, who helped to generate many of the figures in this report, are thanked for their efforts. Scott Keating, a graduate student, and Eric Schallert, an undergraduate student, performed the majority of the fabrication on the test and instrumentation frameworks. Undergraduate students David Bartels, Barbara Bellizzi, Paul Boring, Brian Corzine, Ronald Dehart, Bret Farmer, Craig Hawkinson, Jeffrey Heilstedt, Jonathan Lutz, Graig Neville, James Oppelt, William Quick, and Kyle Vogt also contributed significantly to the laboratory effort of this research project. For their help on the project, the author expresses his appreciation. The author wishes to thank Denise Wood, Structures Secretary, for typing this report.

10. APPENDIX A: DESIGN AGENCY QUESTIONNAIRE RESULTS

The number in the parentheses ( ) represents the number of design agencies having that particular answer. The notes within the braces [ ] are paraphrased comments from the respondents. An individual respondent's remarks are separated by a comma.

Part I. General Bridge Geometry and Conditions

1. Has your state or agency ever specified panels as stay-in-place formwork for cast in-place concrete bridge decks (including alternate designs)?
   (29) Yes [1962 bridge widening]
   (40) No Why? [Unconvinced on cost savings - question structural integrity - possible construction problems - difficulties with future deck rehabilitation, standard practice to use stay-in-place deck forms, No AASHTO Specification and no contractor requests, No precaster in area with panel beds, Satisfied with standard forming, Availability of epoxy coated strands, Panels can not be applied to our pertinent standard designs - Unfavorable reports involving panel seating, Use steel forms, Cantilevers must be formed, Unsatisfactory details, Local precaster could not show us that a cost savings exists with panels, cost savings do not justify panel use, Questionable benefit, No need or application, Fear of deck cracking along edges of panels - No successful performance report, Very satisfied with metal stay-in-place forms, No precaster promoting panels in the area, Lack of data and availability, History of performance reports not entirely satisfactory - No panel requests in our state - FHWA Region 10 has questioned serviceability of decks with panels and has recommended caution in their use, Potential cracking problems, Problems encountered by other states, Currently planning a project with panels, Need not expressed, Use SIP metal forms, Not applicable, Use orthotropic deck, Poor deck performance, Never proposed, Prefer removable forms, Not used in the area.]

2. Has your state or agency ever prohibited the use of or discontinued specifying panels for bridge deck construction after previously permitting panel usage?
   (12) Yes When? [2-Currently, 1978, 2-1982, Dec. 1984, 3-1985, 3-1986]
   Why? [Evaluating future usage, Use on steel bridges prohibited, Discontinued use on steel beam bridges - Concerns of excess differential beam deflection and deck cracking, Discontinued on primary route steel bridges, Deck cracks and spalding with composite design, Construction problems - Not cost effective - Design controversy, Strand slippage and excessive eccentricity, Poor panel quality control, Reflective cracking, Projects were experimental, One experimental project built in 1985 developed roadway cracks - Project is being monitored, No economical advantage, Concern about overall thickness and reflective cracks]
   (17) No [Prohibited for steel bridges, Not specified but will permit use if proposed by contractor as an alternate]

3. Is your state or agency currently using or specifying panels for bridge deck construction?
   (16) Yes [4 yrs ago, Contractor option on concrete bridges only, Not on horizontally cured steel bridges, None composite, Panels experimentally used on a single span 70" P/C I-girder structure in 1983 and in 1987 contractor option not exercised]

(13) No [1983 last project, Last project 4 years ago]

4. For approximately how many years (in total) has your state or agency specified panels for subdecks?
   (9) 0 to 2 years [27 years ago] (6) 2 to 5 years (7) 5 to 10 years
   (7) Over 10 years [Always contractor option except inside box girders, On a project by project basis]

5. For the last year during which panels were used in bridge deck construction, what percentage of bridge decks involved panels?
   (17) 0 to 10% (4) 10 to 25% (1) 25 to 50%
   (3) 50 to 75% (2) 75 to 100%

6. Roadway classification for bridge panel usage:
   (5) Primary roads only
   (0) Secondary roads only
   (21) Either primary or secondary roads
   (2) Other [Concrete bridges that cost less than 5 million dollars, special table for use]

7. Are panels permitted on bridges having a superelevation?
   (7) Always (17) Sometimes (3) Never

8. Maximum bridge skew for panels adjacent to abutments or pier diaphragms:
   (14) Not specified (2) 15 degree (3) 30 degree
   (0) 45 degree (4) Other [0,18,20,50 degree]
   (5) Panels not used at these locations

9. What type of panel support is provided for typical panels spanning perpendicular to the bridge span?
   (1) Panels are not used to span in this direction
   (16) Precast prestressed concrete girders only
   (3) Steel girders only
   (9) Either precast concrete or steel girders
   (3) Other [Occasionally P/C T-beam stems, With grout, C.I.P. superstructure only]

10. When panels are used adjacent to an abutment or pier, is the cast-in-place topping slab poured monolithic with the abutment and pier diaphragms?
    (1) Panels not used at these locations
    (10) Always (9) Sometimes (8) Never

11. Cast-in-place topping slab thickness to account for girder camber:
    (7) Variable thickness of the topping slab with constant permanent panel bearing thickness
    (15) Relatively constant topping slab thickness with variable permanent panel bearing thickness
    (3) Either of the above
    (0) Relatively constant top slab thickness with constant permanent panel bearing thickness
    (4) Other [For $\leq$ in. of camber vary slab cover over top bars and for > 1 in. of camber vary panel bearing thickness, Haunch on girder, Maximum of 1 in. increase in slab thickness and 1 1/4 in. to 1 3/4 in. variation in bearing material, Variable thickness of top slab and variable panel bearing thickness]

II. General Panel Geometry and Conditions

1. Maximum panel width used:
   (3) Not specified (5) 4 ft. (0) 6 ft.
   (18) 8 ft. [Discontinued due to excessive cracking during handling and transportation, For one project and have now switched to 4 ft]
   (0) 10 ft.
   (4) Other [9 ft, 7.5 ft, 9 ft, As required, 4 and 18 ft]

2. For non-rectangular shaped panels that occur at abutment and pier diaphragms in skewed bridges, what is the minimum length of a panel side?
   (8) Panels not permitted at these locations
   (5) Not specified
   (0) 0 ft. (triangular shaped panel)
   (5) 1 ft. (trapezoidal shaped panel)
   (2) 2 ft. (trapezoidal shaped panel)
   (9) Other [Unspecified, one-half the length of the opposite side, 1.5 ft, 2.25 ft, 3 @ 3 ft, 2 @ 3.25 ft]

3. Minimum panel thickness used:
   (1) Not specified (4) 2 1/2 in.
   (7) 3 in. [Started with 3 in. switched to 3 1/2 in.]
   (11) 3 1/2 in. (3) 4 in.
   (1) Other [Double bevel, 3 in. flange with 1/2 in. rib, 2 3/4 in.]

4. Minimum ratio of panel thickness to strand diameter
   (3) 9:1 (2) 8:1 (1) 7:1
   (2) 6:1 (13) Not specified
   (8) Other [10.67:1, 9.33:1, 7.33:1, 6.7:1, 4 @ 3/8 in. dia. strands]

5. Panel construction at skewed abutment or pier locations:
   (8) Panels not used at these locations
   (4) Panels sawn to match the skew only
   (2) Panels cast to match the skew only
   (12) Panels sawn or cast to match the skew
   (4) Other [Panels not used when skew > 15 deg., C.I.P. full depth, C.I.P. slab if skew > 30 deg., May also cast closure in place w/o panel]

6. Type of longitudinal panel joint (parallel to panel span):
   (1) Not specified (26) Butt joint (1) Other
   (0) Key joint (bulb key, rectangular key, etc)

7. Edge detail at end of panel (along bearing edge):
   (2) Not specified (18) Flat vertical face (2) Inclined or curved face
   (6) Other [2 @ 3/4 in. bevel on bottom, Bevel on bottom, 1/4 in. chamfer all around, Flat vertical face with 1 in. chamfer at bottom edge]

8. Top surface profile for the panels:
   (4) Not specified (21) Flat
   (2) Other [Bowing or camber limited, Keyed surface with 45° taped longitudinal panel edges]
   (1) Tapered at the longitudinal panel edges (panel thinner at edge than at mid-width)

9. What is the method used to develop bond between the panel and the cast-in-place slab?
   (0) Not specified
   (0) None (composite action not considered)
   (0) U-shape bars or dowels only
   (12) Raked finish only
   (12) U-shaped bars or dowels and raked finish only [With broom finish not raked]
   (0) Bonding agent only
   (0) Combination of above involving a bonding agent
   (5) Other [Continuous bent serpentine bars, Z-bars and brushing brooming or burlap drag, Roughened surface, Keyed surface 3 in.: 6 in.: 1 ft-6 in.: 6 in.: 6 in.: 3 in. symmetric about centerline, Broom finish]

10. What is the direction of the raked depression with respect to the panel span?
    (0) Raked depression not used
    (11) Not specified
    (8) Parallel to panel span
    (8) Transverse to panel span
    (1) Both parallel and transverse to panel span
    (0) Diagonal to panel span
    (0) Other

11. Minimum depth of raked finish depression
    (1) Raked depression not used
    (3) Not specified (9) 1/8 in. (0) 3/16 in.
    (12) 1/4 in. (3) Other [2 @ 1/16 in., 1/8 in. max., 1 in. key]

12. Minimum width of raked finish depression:
    (1) Not used (21) Not specified (3) 1/8 in.
    (0) 3/16 in. (0) 1/4 in.
    (3) Other [Scoring spaced 3/4 in. to 1 in., 1/16 in., 6 in. key width]

13. Transverse panel reinforcement along the entire panel length and perpendicular to the panel span:
    (1) Not used (15) R/C bar only (9) WWF only
    (0) Wire strands (1) Any of the above
    (6) Other [2 @ rebars or welded wire, No. 3 bars or wires, Rebars and/or WWF, WWF top and 4 - No. 3 bottom, Bars or wires, No. 3 bars or WWF, No. 3 rebar @ 12 in. o.c.]

14. Do the panel lifting hooks remain in place to be cast into the cast-in-place top slab?
    (2) Not used (21) Always (3) Sometimes
    (2) Never

15. What is the minimum age of the panels when the cast-in-place top slab is cast?
    (17) Not specified [When f'_c strength is reached]
    (3) Less than 2 weeks [May be cast when required strength has been reached]
    (3) Between 2 weeks and 4 weeks
    (5) 4 weeks and over

16. For non-rectangular panels, what type of additional reinforcement, other than the conventional rectangular panel reinforcemnent, is provided in the panel?
    (8) Non rectangular panels are not permitted
    (15) None (2) R/C bars only (0) Wire Strands
    (1) WWF only (0) Any of the above (1) Other [Unspecified]

17. Concrete weight for panels
    (0) Light weight (28) Normal weight (0) Both

18. Is air entrainment used in the panel concrete?
    (15) Always (7) Sometimes (5) Never

19. Are corrosion inhibithing admixtures used in the panel concrete?
    (2) Always (4) Sometimes (22) Never

Part III. Panel Bearing Details

1. Do the panels bear along the abutment or pier diaphragms for a non-skewed bridge?
    (4) Panels not used at these locations
    (10) Always (3) Sometimes (11) Never

2. Surface roughness of the girder at panel bearing location:
    (15) Smooth (5) Rough (8) Either

3. What is the minimum height of the temporary bearing material after it has compressed?
    (5) Temporary bearing material not used
    (10) Not specified (7) 1/2 in. (3) 1 in.
    (4) Other [Panels supported by either a mortar bed or metal angles - angles remain in place, $\pm$ 1/8 in., 1 1/2 in. fiberboard, Height of required fillet, Variable to compensate for camber]

4. What is the maximum height of the temporary bearing material after it has compressed?
    (5) Temporary bearing material not used
    (11) Not specified (1) 1 in. (6) 1 1/2 in.
    (2) 2 in.
    (4) Other [2 1/2 in. $\pm$ 1/8 in., Required fillet height, Variable to compensate for camber]

5. Temporary bearing material used to support panels:
    (4) Temporary bearing material not used
    (0) Not specified
    (19) Fiberboard, neoprene, polystyrene, or similar material only
    (4) Mortar, grout or concrete bed only

(1) Steel shims only
(0) Any of the above
(2) Other [High density expanded polystyrene foam, Timber strips]

6. Is the temporary bearing material removed after the permanent bearing is provided for the panels?
(5) Temporary bearing material not used
(1) Not specified (1) Always (3) Sometimes
(19) Never

7. Permanent bearing material used to support panels:
(1) Not specified
(7) Continous fiberboard, neoprene, polystyrene, or similar material only
(20) Continuous mortar, grout, or concrete bed only
(0) Steel shims at panel corner only
(1) Any of the above
(3) Other [Joint filler or polystyrene bedding material, C.I.P. concrete, Continuous epoxy adhesive filler cement]

8. What is the minimum length of permanent bearing parallel to the panel span
(3) Not specified (8) 1 1/2 in. (4) 2 in.
(1) 2 1/2 in.
(12) Other [2 @ 1 in., 1 1/4 in., 2 3/4 in., 3 @ 3 in., 3 $\pm$ 1/2 in., 2 @ Full length]

Part IV. Prestressing Strand Description and Conditions

1. Total diameter of the strand that is used most often:
(0) 1/4 in. (0) 5/16 in. (23) 3/8 in.
(2) 7/16 in. (3) 1/2 in. (0) Other

2. Type of strand (manufacturing process)
(12) Ordinary stress-relieved [250 k]
(6) Low relaxation
(9) Either ordinary stress-relieved or low relaxation
(1) Other [ASTM A-416]

3. Type of strands used:
(23) Standard (0) Super (1) Drawn
(0) Any of the above
(4) Other [High tensile strength, 270 k, M203, ASTM A-416]

4. Is the strands spacing across the width of the panel uniform?
(2) Not specified (24) Always (1) Sometimes
(1) Never

5. What is the location of the strand with respect to the panel center of gravity?
(3) Eccentric [Culverts] (23) Concentric [Bridges] (3) Either

6. Are strand extensions used?
(18) Always (2) Sometimes (8) Never

7. Minimum length of strand extension for a rectangular shaped panel:
   (8) Strand extensions not used (1) Not specified
   (9) 3 in. (3) 4 in. (3) 5 in.
   (1) 6 in. (3) Other [2, 9, 12 in.]

8. Are strand extensions considered for strand development length after the joint between the panel ends is cast?
   (6) Strand extensions not used (1) Always
   (1) Sometimes (20) Never

9. For a rectangular shaped panel, are some strands unbonded near the panels ends?
   (2) Always (0) Sometimes (26) Never

10. For a non-rectangular shaped panel, are some strands unbonded near the panel ends?
    (6) Only rectangular shaped panels are permitted
    (0) Always (0) Sometimes (21) Never

Part V. Design Criteria

1. Design AASHTO vehicle loading:
   (0) HS 15 (25) HS 20 (3) HS 25
   (0) Any of the above (0) Other

2. Panel concrete 28-days compressive strength
   (26) 5000 psi (1) 5500 psi (1) 6000 psi
   (0) Other

3. Minimum panel concrete compressive strength at release of prestress force:
   (2) 3000 psi (1) 3500 psi (24) 4000 psi
   (0) 4500 psi (1) Other [5000 psi]

4. What is the minimum concrete compressive stress at the panel center of gravity due to the prestressing force immediately after release (before losses), expressed in terms of the panel concrete strength, f'_{ct}, at the time of release?
   (17) Not specified (1) Less than 0.20 f'_{ct}
   (0) Between 0.20 and 0.30 f'_{ct} (2) Between 0.30 and 0.40 f'_{ct}
   (1) Between 0.40 and 0.50 f'_{ct} (6) Over 0.50 f'_{ct}

5. What method is used to establish the prestressing force in panels when the total strand embedment length is less than twice the required strand development length?
   (16) Not specified
   (9) Proportion prestress force based on the available embedment length to the required development length given in the AAHSTO Specification
   (1) Other [Assume full prestress at midspan]

6. Is a non-rectangular shaped panel considered to affect the prestress force in the strands?
   (9) Only rectangular shaped panels are permitted
   (4) Yes
   (13) No

7. Is additional steel provided in the panel ends to prevent splitting due to bond transfer?
   (2) Always (2) Sometimes (24) Never

8. What design criterion is applied to size the transverse panel reinforcment throughout the entire panel length?
   (1) Transverse panel reinforcment not used
   (10) Temperature and shrinkage requirements only
   (5) Wheel load distribution only
   (4) Both temperature and shrinkage requirements and wheel load distribution
   (7) Other [No. 3 @ 12", AASHTO Art. 9.23.2, 3 @ AASHTO Code, 2 @ 0.11 in.^{2}/ft]

9. Cast-in-place top slab concrete 28-day compressive strength:
   (9) 4000 psi (5) 4500 psi (1) 5000 psi
   (13) Other [2 @ 3000 psi, 3000 or 3500 psi, 3200 psi, 3250 psi, 3400 psi, 4 @ 3500 psi, 3 @ 3600 psi]

10. Are corrosion inhibition admixtures added to the cast-in-place top slab concrete?
    (1) Always (2) Sometimes (25) Never

11. Are epoxy coated rebars used in the cast-in-place top slab?
    (15) Always (7) Sometimes (5) Never

12. Minimum cast-in-place top slab thickness:
    (2) Not specified (1) 3 in. (6) 4 in.
    (8) 5 in. (1) 6 in. (2) 7 in.
    (8) Other [3 1/4 in., 3.4 in., 3 1/2 in., 4 @ 4 1/2 in., 5 1/2 in.]

13. Concrete weight for cast-in-place top slab:
    (0) Light-weight (28) Normal-weight
    (0) Either light-weight or normal-weight

14. Are any special precautions taken to minimize cracking in the top slab near the longitudinal panel joints (joints parallel to panel span)?
    (3) Always (3) Sometimes
    (21) Never [Except good vibration]

15. Are any special precautions taken to minimize cracking in the top slab near the transverse panel joints (joints at ends of panels)?
    (3) Always (2) Sometimes (23) Never

16. Degree of composite behavior between the panels and the cast-in-place slab:
    (27) Fully composite
    (1) Partially composite [Composite for live load]
    (0) None (composite behavior not considered)

17. Is the bridge deck designed as a continous span across the girders when panels are used?
    (24) Always (3) Sometimes [For live load] (1) Never

18. Is positive moment reinforcement (bottom steel) provided in the cast-in-place topping slab to achieve the continuity across the girders?
    (5) Always [Continuous for negative moment and simple for positive moment]
    (1) Sometimes (22) Never

19. Is any additional negative reinforcement (top steel) in the cast-in-place topping slab provided to obtain continuity across the girders, beside the normal negative moment reinforcement used in conventional full thickness cast-in-place decks, when panels are used?
    (1) Always (1) Sometimes (26) Never

20. Is any supplemental reinforcement provided in the cast-in-place topping slab provided to obtain continuity across the girders, beside the normal negative moment reinforcement used in conventional full thickness cast-in-place decks, when panels are used?
    (4) Always (5) Sometimes [0.25 $in.^2/ft$] (19) Never

21. Is two-way plate action considered in the design of the deck when the panels are supported along three edges?
    (10) Three edge panel support not permitted
    (1) Yes (16) No

22. Is fatique considered in the design of the deck when panels are used?
    (1) Yes (26) No

23. Effective slab width for wheel load distribution:
    (26) AASHTO Specification for full depth cast-in-place slabs (without panels)
    (1) Full panel width if less than the AAHSTO Specification
    (0) Other

24. Are torsional stresses caused by movements of curved and boxed shaped-steel girders considered in the deck when panels are used?
    (19) Panels not used with these girders
    (0) Yes (8) No

25. Are stresses caused by differential movements of long flexible steel girders considered in the deck design when panels are used?
    (13) Panels not used with steel girders
    (0) Yes (14) No

Part VI. Economy

1. Have cost effectiveness studies ever been performed to evaluate the economical advantages of using panels instead of full depth cast-in-place deck?
    (5) Yes (23) No

2. What are the approximate cost savings realized (including costs associated with construction time), when panels are used for subdecks on a typical bridge compared to a conventional full depth bridge deck?
    (18) Cost savings not known savings (6) No cost savings
    (3) \$0 - \$1.00/ft^2 of deck area (0) \$1.00 - \$2.00/ft^2 of deck area

(0) $2.00 - $3.00/ft² of deck area (0) $3.00 - $4.00/ft² of deck area
(0) Over $4.00/ft² of deck area

3. What was the basis used for the economy study?
   (19) Cost effectiveness studies have not been performed
   (3) Actual bids that included both a conventional cast-in-place slab and a panel system for the same bridge deck
   (1) Panel system substitution suggested (without actual bids) by the bridge constructor
   (1) Estimates, not actual bids
   (4) Other [Contractor substitute C.I.P. in lieu of P/C panels, Panels always bid as contractor option - selected about 95% of time, Actual bids on two bridges for both C.I.P. and panel system, Panels allowed as an alternate - savings assumed to be minimal]

Part VII. Experiences uith Panel Usage

1. Which of the following items of panel damage has your state or agency experienced more than just a few times or occasionally?
   (13) Can not really comment since we have not used panels often enough
   (8) Broken corners
   (9) Spalled or chipped edges
   (6) Cracking parallel to strands along a significant portion of the panel length
   (4) Cracking parallel to strands near the ends of the panel only
   (3) Cracking transverse to the strands near panel midspan
   (3) Diagonal cracks across panel surface
   (2) Strand slippage
   (7) Other [Random curing cracks, None reported, Some of the above occur during manufacturing but those panels are rejected, Cracked and spalled decks over panels, All have occurred but not regularly-acceptance per specification, Some occurrence of all of these but infrequently, Cracks at random in direction of strands which would leak water immediately when applied - these panels were replaced]

2. Which of the following items of panel irregularities has your state or agency experienced more than just a few times or occasionally?
   (13) Can not really comment since we have not used panels often enough
   (9) Panel dimensions (thickness, width, and/or length) did not meet specifications
   (7) Panel trueness (bow, horizontal alignment, and/or squareness) was beyond tolerances
   (3) Strand position (vertical, horizontal alignment, and/or extensions)
   (3) Panel surface finished improperly
   (5) Other [None reported, panels don't match beam camber, All have occurred but not regularly - acceptance per specification, No specific known irregularities]

3. Which of the following items related to the panel and cast-in-place topping slab installation has your state or agency experienced more than just a few times or occasionally?
   (12) Can not really comment since we have not used panels enough
   (4) Non-uniform panel support surfaces
   (4) Improper panel overlap on supports
   (5) Difficulty in leveling the panels
   (3) Difficulty in sealing the panel joints

(2) Air bleed slots at panel bearing allows mortar to drip from the structure
(1) Skewed panels were difficult to set properly
(5) Other [2 @ none of the above, Improper bed grout, Unknown - This is construction experience]

4. Which of the following items related to the performance of the panel and cast topping slab bridge deck have your state or agency experienced more than just a few times or occasionally?
(12) Can not really comment since we have not used panels often enough
(7) Reflective cracks in the top of the cast-in-place slab above the transverse panel joints
(7) Reflective cracks in the top of the cast-in-place slab above the longitudinal panel joints
(3) Cracks in the top of the cast-in-place slab that are not above the panel joints
(3) Cracks in the top of the cast-in-place slab at the abutment or pier diaphragms
(3) Cracks in the bottom of the panels parallel to the panel span
(1) Cracks in the bottom of the panels transverse to the panel span and near the midspan of the panel
(1) Strand slippage
(0) Some loss of composite behavior between panels and cast-in-place slab
(3) Apparent loss of panel bearing at some locations
(5) Other [3 @ none of the above, Cracks and spalls in C.I.P. slab parallel to and adjacent to the beam faces, All have occurred but not regularly - acceptance per specification]

5. How does your state or agency classify any problems associated with panel usage for bridge deck construction?
(12) Can not really comment since we have not used panels often enough
(1) Non-existent
(7) Minor
(6) Moderate
(6) Significant
(0) Major

6. Considering all aspects of manufacturing, transportation, erection, and performance of panels for bridge deck construction, how does your state or agency rate panel usage?
(11) Can not really comment since we have not used panels often enough
(1) Excellent
(3) Very good
(7) Good
(5) Fair
(5) Poor

7. Please feel free to expand on the experiences that your state or agency has had regarding any aspect of precast prestressed concrete panel subdeck manufacturing, transportation, storage, erection, casting of top slab, performance, maintenance, or economy, which have not been covered in the previous parts of the questionnaire. (Quotes are respondents' comments)

"Only used in one project to reduce construction time. We will be evaluating its cost effectiveness and performance. If satisfactory, we may institute a policy for panel use as an alternate to full cast in place slab."

"The use of stay-in-place panels is specified in the plans as an option. Contractors have not been selecting the panel option."

"The contractor has the option to redesign the full depth cast slab and use the deck panels on concrete bridges only."

"Continued use of panels will depend on maintenance problems encountered."

"Our limited experience in _____ indicates that contractors are not real excited about panels..."

"We have not used panels in quite awhile but we do have a few places that need to be observed. We are looking to use panels in more locations in the future."

"Their use has been discontinued."

"Deck panels used on only one job. This job is under construction."

"We question whether the laminated slab which results from use of panels is as durable as a full depth monolithic slab. We may be accepting an inferior product when panels are used."

"Quick and easy to erect but difficult to maintain deck grades due to variable I-beam camber."

"Since adopting and implementing our current standard drawings and special provisions in July 1985 we have had only very minor problems with deck panels. Continual inspection will be necessary to assure future results."

"Precast prestressed concrete panels were placed into our contracts by alternate bidding. It is believed that the contractors found it less economical than conventional construction. This type of construction would not be recommended, however, the system may have merit where the structure is straight with near right angle substructure units and a constant grade."

"We have improved deck panel useage and performance by revising our manufacturing and installation specifications."

"_____ has had good experience with the use of precast panels with very few problems. Overall, panel use has declined significantly over the years and is currently used on less than 10% of our projects."

"Have received panels from only one supplier, _____."

"Panels have separated from deck after 25 years. Even though separated, they are difficult to remove without damaging slab above."

11. APPENDIX B: PRECAST PANEL MANUFACTURE QUESTIONNAIRE RESULTS

The number in the parentheses ( ) represents the number of panel manufacturers having that particular answer. The notes within the brackets [ ] are paraphrased comments from the respondents. An individual respondent's remarks are separated by a comma.

Part. I. Background

1. Has your company ever produced panels as stay-in-place formwork for cast-in-place concrete bridge decks?.
   (27) Yes
   (45) No Why? [No bid opportunity, Not commonly used, No acceptance of product, Do not compete in bridge market, Contractor not interested, Local preference for C.I.P., Never been designed by local consultants, C.I.P. awarded over panels, Not economically feasible, Produce hollow core slabs only, Produce AASHTO Double Tees only, Depressed market, Not a profitable product, Do not do or want DOT work, Never successful in bidding during the 1970's - Product has been banned by DOT for many years, Product too hard to control and be a profitable item, Do not produce panels and over 25 years since the last bridge beams, Not used by DOT, We don't produce the I-girders, All decks have been full slab thickness, Too many producers for the market]

2. Has your company ever stopped producing panels as stay-in-place formwork for bridge deck construction?
   (8) Yes When? [1984, 1985, May 1986, 2 @ 1986, 1988, Over 10 years ago]
   Why? DOT discontinued use, DOT discontinued use due to panel cracking and poor quality, price too high compared to timber forming, state prohibited use, Tolerances, Change in design, No longer specified, No market and too high price, DOT stopped using S.I.P. panels]
   (19) No

3. Has your company produced or submitted a bid to produce panels for a bridge project within the last two years?
   (20) Yes (7) No [Last ones were made in Oct. 1986]

4. For approximately how many years (in total) has your company produced panels for subdecks?
   (5) 0 to 2 years (7) 2 to 5 years (10) 5 to 10 years
   (4) Over 10 years

5. List the agency that have specified panels or allowed for a panel alternative in bridge deck construction for which your companey was or would have been the panel producer or supplier?
   (26) State DOT's (1) Province DOT's
   (4) Tollway or turnpike authorities (6) Cities
   (9) Counties within states
   (4) Other [Forestry bridges, Port Authority, Private developers]

6. Is your company expected to perform or expected to hire an engineering consultant to perform the structural design of the panels as part of your contract for providing panels?
   (4) Always (9) Sometimes (14) Never

7. Before you cast panels, does your company verify the structural engineering design provided by a state or agency?
   (5) Always (12) Sometimes (9) Never

Part II. General Bridge Panel Conditions and Geometry

1. Maximum panel width cast:
   (5) 4 ft. (0) 6 ft. (19) 8 ft.
   (1) 10 ft. (2) Other [8.75 ft, 3.33 ft]

2. For non-rectangular shaped panels that occur at abutment and pier diaphragms in skewed bridges, what is the minimum length of a panel side?
   (6) Only rectangular panels are cast [Mostly saw cut in the field]
   (4) 0 ft. (triangular shaped panel)
   (3) 1 ft. (trapezoidal shaped panel)
   (7) 2 ft. (trapezoidal shaped panel)
   (6) Other (trapezoidal shaped panel cast) [1 ft, 2.83 ft, 3 @ 3 ft, 4 ft]

3. Panel length established by:
   (23) Distance between headers on the precast bed
   (5) Saw cutting panels from a continuous casting length
   (3) Other [3 @ spacing of bridge girders]

4. Minimum panel thickness cast:
   (6) 2 1/2 in. (8) 3 in. (12) 3 1/2 in.
   (2) 4 in. (1) Other [3 1/8 in. allowed]

5. Minimum ratio of panel thickness to strand diameter
   (15) Not specified [2 @ 3/8 dia. strands] (1) 9:1 (6) 8:1
   (3) 7:1 (1) 6:1
   (2) Other [8:1 for 3/8 in. dia. and 6:1 for 1/2 in. dia., 2 @ 6.67:1]

6. Panel construction at skewed abutment or pier locations:
   (3) Panels not used at these locations
   (3) Panels sawn to match the skew only
   (12) Panels cast to match the skew only
   (7) Panels can be either sawn or cast to match the skew
   (1) Other [N.A.]

7. Type of longitudinal panel joint (parallel to panel span):
   (23) Butt joint
   (0) Key joint (bulb key, rectangular key, etc)
   (5) Other [Vertical face with top edge chamfer, Double female key, Inclined butt joint, Shear key, 2 @ V-shaped joint]

8. Edge detail at end of panel (along bearing edge):
   (23) Flat vertical face
   (5) Inclined or curved face
   (2) Other [Strand extension, Bottom edge chamfer 1 1/2 in. vert. by 2 1/2 in. horiz. and top edge tooled]

9. Top surface profile for the panels:
   (26) Flat
   (2) Tapered at the longitudinal panel edges (panel thinner at edge than at mid-width)
   (0) Other

10. Top surface roughness and projections (not counting lifting hooks):
   (0) Smooth finish without bar projections
   (0) Smooth finish with U-shape bars or dowels
   (3) Broom finish without bar projections
   (1) Broom finish with U-shape bars or dowels
   (14) Raked finish without bar projections
   (17) Raked finish with U-shaped bars or dowels
   (2) Other [Grooved finish without bar projections, Screed vibratory finish]

11. What is the direction of the raked depression with respect to the panel span?
   (1) Raked depression not used
   (6) Parallel to panel span
   (17) Transverse to panel span
   (1) Both parallel and transverse to panel span
   (2) Diagonal to panel span
   (0) Other

12. Minimum depth of raked finish depression
   (1) Raked depression not used
   (2) 1/16 in. (12) 1/8 in. (2) 3/16 in.
   (10) 1/4 in. (1) Other [No minimum]

13. Minimum width of raked finish depression:
   (2) Raked depression not used
   (3) 1/16 in. (8) 1/8 in. (3) 3/16 in.
   (9) 1/4 in. (1) Other [Not specified]

14. Transverse panel reinforcement along the entire panel length and perpendicular to the panel span:
   (3) Transverse panel reinforcment not used
   (14) Reinforcing bars only. (13) WWF only
   (2) Prestressing strands only
   (3) Other [Reinforcing bars, WWF and reinforcement at panel ends, Varies with job]

15. Do the panel lifting hooks remain in place to be cast into the cast-in-place top slab?
   (3) Lifting hooks not used (19) Always
   (2) Unknown (4) Sometimes
   (0) Never

16. What is the minimum age of the panels when the cast-in-place top slab is cast?
(11) Unknown [Shipped at 28 days] (2) Less then 2 weeks
(8) Between 2 weeks and 4 weeks (5) 4 weeks and over

17. For non-rectangular panels, what type of additional reinforcement, other than the conventional rectangular panel reinforcemnent, is provided in the panel?
(6) Only rectangular panels without additional reinforcement are cast
(5) None (2) Prestressing strands only
(2) WWF only (1) Other [Varies with job]
(11) Reinforcing bars only [Extra No. 4 bars, 8 - No. 5 along future cutted skew location]

18. Concrete weight for panels
(3) Light-weight [2 @ 115 pcf, 120 pcf] (26) Normal-weight

19. Panel concrete admixtures:

Usage	Air Entrainment	Corrosion Inhibitors	Water Reducers	Strength Accelerators	Other
Always	(15)	(2)	(18)	(7)	(2)
Sometimes	(5)	(2)	(7)	(5)	(1)
Never	(6)	(18)	(1)	(11)	(3)

20. Maximum skew angle for casting non-rectangular panels to match the bridge skew for those panels adjacent to abutment or pier diaphragms:
(6) Only rectangular panels are cast
(2) 15 degree (3) 30 degree (4) 45 degree
(10) No maximum [Minimum edge length of 1 ft., No pointed corners]
(1) Other [As long as the ratio of the long to short panel end is 2 or less]

21. Panel concrete 28-days compressive strength
(22) 5000 psi (2) 5500 psi (3) 6000 psi
(2) Other [4500 psi (light-weight concrete]

22. Minimum panel concrete compressive strength at release of prestress force:
(4) 3000 psi (8) 3500 psi
(14) 4000 psi [For normal-weight] (2) 4500 psi
(1) Other [3750 psi (light-weight concrete) and 5000 psi (normal-weight concrete)]

23. Is additional steel provided in the panel ends to prevent splitting due to bond transfer?
(8) Always (8) Sometimes
(11) Never [But it should be]

Part III. Bridge Panel Bearing Details

1. Temporary bearing material used to support panels:
(2) Temporary bearing material not used
(3) Unknown
(18) Fiberboard, neoprene, polystyrene, or similar material only
(2) Mortar, grout or concrete bed only

(2) Steel shims only
(2) Other [None, External support]

2. Is the temporary bearing material removed after the permanent bearing is provided for the panels?
   (2) Temporary bearing material not used
   (5) Unknown (2) Always (1) Sometimes
   (16) Never

3. What is the minimum height of the temporary bearing material after it has compressed?
   (3) Temporary bearing material not used
   (9) Unknown [1 1/4 in. min. before compression] (3) 1/2 in. (7) 1 in.
   (2) 1 1/2 in. (2) Other [3/4 in., 1 1/4 in.]

4. What is the maximum height of the temporary bearing material after it has compressed?
   (3) Temporary bearing material not used
   (12) Unknown (2) 1 in. (5) 1 1/2 in.
   (1) 2 in. (3) Other [3 @ 3 in.]

5. Permanent bearing material used to support panels:
   (2) Unknown
   (5) Continous fiberboard, neoprene, polystyrene, or similar material only
   (8) Continuous mortar, grout, or concrete bed only
   (10) Cast-in-place concrete from pouring the top slab
   (0) Steel shims at panel corner only
   (2) Other [PVC pipe for 3 in. bearing and styrofoam for 4 in. bearing, Galvanized angle]

6. What is the minimum length of permanent bearing parallel to the panel span
   (3) Unknown (6) 1 in. (7) 1 1/2 in.
   (3) 2 in. (3) 2 1/2 in.
   (4) Other [1/2 in. 2 @ 3 in., Full length of panel]

Part IV. Prestressing Strand Conditions and Description for Bridge Panels

1. Total diameter of the strand that is used most often:
   (0) 1/4 in. (2) 5/16 in. (20) 3/8 in.
   (4) 7/16 in. [Light-weight concrete] (9) 1/2 in. [3/8 in. probably less splitting]
   (0) Other

2. Type of strand
   (16) Ordinary stress-relieved (14) Low-relaxation (1) Other

3. Is the strands spacing across the width of the panel uniform?
   (19) Always (6) Sometimes (2) Never

4. What is the location of the strand with respect to the panel center of gravity?
   (4) Eccentric (18) Concentric (4) Either

5. Are strand extensions used?
   (15) Always (8) Sometimes (5) Never

6. Minimum length of strand extension for a rectangular shaped panel:
   (6) Strand extensions not used
   (9) 3 in. (1) 4 in. (2) 5 in.
   (4) 6 in. (3) Other [Varies 3 in. to 6 in., 12 in., Varies]

7. For a rectangular shaped panel, are some strands unbonded near the panels ends?
   (0) Always (3) Sometimes [For a portion of the strands]
   (24) Never

8. What is the maximum length for debonding a strand, measured from each end of a rectangular shaped panel?
   (25) Debonding not done on rectangular shaped panels
   (1) 3 in. (0) 6 in. (1) Other

9. For a non-rectangular shaped cast panel, are some strands unbonded near the panel ends?
   (6) Only rectangular shaped panels are cast
   (0) Always (5) Sometimes (14) Never

10. What is the maximum length for debonding a strand, measured from each end or edge of a non-rectangular shaped cast panel?
    (6) Only rectangular shaped panels are cast
    (14) Debonding not done for non-rectangular panel
    (2) 3 in. (1) 6 in. (0) Other

11. Method used to measure the prestress force a strand:
    (1) Hydraulic pressure only (0) Strand elongation only
    (26) Hydraulic pressure and strand elongation (1) Electronic load cell on some strands
    (0) Other

12. What method is used to release the bridge panel prestressing strands?
    (20) Acetylene torches (6) Abrasive saw blades
    (3) Wire (bolt) cutters (2) Slow release of hydraulic pressure
    (0) Other

Part V. Design Criteria - Answer the questions in Part V only if your company performs a structural design for the panels; otherwise, skip to Part VI.

1. Design AASHTO vehicle loading:
   (0) HS 15 (10) HS 20 (1) HS 25
   (2) Other [MS-250 (metric), As specified]

2. What is the minimum concrete compressive stress at the panel center of gravity due to the prestressing force immediately after release (before losses), expressed in terms of the panel concrete strength, f'_{ci}, at the time of release?
   (8) Not specified (0) Less than 0.20 f'_{ci}
   (0) Between 0.20 and 0.30 f'_{ci} (0) Between 0.30 and 0.40 f'_{ci}
   (1) Between 0.40 and 0.50 f'_{ci} (1) Over 0.50 f'_{ci}

3. What method is used to establish the prestressing force in panels when the total strand embedment length is less than twice the required strand development length?
   (4) Not specified
   (6) Proportion prestress force based on the available embedment length to the required development length given in the AASHTO Specification [1.6 ℓ_d is used]
   (1) Other [Minimum panel length eliminates this problem]

4. Is a non-rectangular shaped panel considered to affect the prestress force in the strands?
   (3) Only rectangular shaped panels are permitted
   (2) Yes
   (4) No

5. What design criterion is applied to size the transverse panel reinforcment throughout the entire panel length?
   (2) Transverse, panel reinforcment not used
   (4) Temperature and shrinkage requirements only
   (0) Wheel load distribution only
   (0) Both temperature and shrinkage requirements and wheel load distribution
   (4) Other [AASHTO Design Specs., Project Specs., No. 3 @ 12 in. o.c. standard, No. 3 @ 12 in. o.c. or D5.5 @ 6 in.]

6. Cast-in-place topping slab concrete 28-day compressive strength:
   (1) 3500 psi (2) 4000 psi (4) 4500 psi
   (2) 5000 psi (2) Other [As specified, 3000 psi]

7. Minimum cast-in-place topping slab thickness:
   (2) Not specified (0) 3 in. (3) 4 in.
   (4) 5 in. (0) 6 in. (1) 7 in.
   (1) Other [Per state]

8. Concrete weight for cast-in-place topping slab:
   (1) Light-weight [115 pcf] (11) Normal-weight

9. Are any special precautions taken to minimize cracking in the topping slab near the longitudinal panel joints (joints parallel to panel span)?
   (1) Always (2) Sometimes (8) Never

10. Are any special precautions taken to minimize cracking in the topping slab near the transverse panel joints (joints at ends of panels)?
    (1) Always (1) Sometimes (9) Never

11. Degree of composite behavior between the panels and the cast-in-place slab:
    (10) Fully composite
    (0) Partially composite
    (1) None (composite behavior not considered)

12. Is the bridge deck designed as a continous span across the girders when panels are used?
    (6) Always (2) Sometimes (3) Never

13. Is positive moment reinforcement (bottom steel) provided in the cast-in-place topping slab to achieve the continuity across the girders?
(2) Always (3) Sometimes (5) Never

14. Is any additional negative reinforcement (top steel) in the cast-in-place topping slab provided to obtain continuity across the girders, beside the normal negative moment reinforcement used in conventional full thickness cast-in-place decks, when panels are used?
(0) Always (3) Sometimes (7) Never

15. Is any supplemental reinforcement provided in the cast-in-place topping slab provided to obtain continuity across the girders, beside the normal negative moment reinforcement used in conventional full thickness cast-in-place decks, when panels are used
(2) Always [No. 4 @ 9 in. o.c.] (1) Sometimes (6) Never

16. Is two-way plate action considered in the design of the deck when the panels are supported along three edges?
(2) Three edge panel support not permitted
(0) Yes (5) No

17. Is fatique considered in the design of the deck when panels are used?
(1) Yes (7) No

18. Effective slab width for wheel load distribution:
(7) AASHTO Specification for full depth cast-in-place slabs (without panels)
(1) Full panel width if less than the AASHTO Specification
(2) Other [State specifications, Don't know]

19. Are torsional stresses caused by movements of curved and boxed shaped-steel girders considered in the deck when panels are used?
(5) Panels not used with these girders (1) Yes (1) No

20. Are stresses caused by differential movements of long flexible steel girders considered in the deck design when panels are used?
(4) Panels not used with steel girders (0) Yes (2) No

Part VI. Economy

1. Have cost effectiveness studies ever been performed to evaluate the economical advantages of using panels instead of a full depth cast-in-place deck?
(11) Yes (12) No

2. What are the approximate cost savings realized (including costs associated with construction time), when panels are used for subdecks on a typical bridge compared to a conventional full depth bridge deck?
(15) Cost savings not known (1) No cost savings
(5) \$0 - \$1.00/ft^2 of deck area (2) \$1.00 - \$2.00/ft^2 of deck area
(1) \$2.00 - \$3.00/ft^2 of deck area (0) \$3.00 - \$4.00/ft^2 of deck area
(0) Over \$4.00/ft^2 of deck area

3. What was the basis used for the economy study?
   (10) Cost effectiveness studies have not been performed
   (5) Actual bids that included both a conventional cast-in-place slab and a panel system for the same bridge deck
   (2) Panel system substitution suggested (without actual bids) by the bridge contractor
   (4) Estimates, not actual bids
   (0) Other

Part VII. Inspection

1. Does the state or agency for which your company is casting panels have a representative at your plant to inspect the panel forms and strands before the panels are cast?
   (0) Not their responsibility
   (5) Sometimes
   (21) Always
   (0) Never

2. Does the state or agency for which your company is casting panels have a representative at your plant to observe strand detensioning, form stripping, and panel handling and storage?
   (1) Not their responsibility
   (6) Sometimes
   (19) Always
   (0) Never

3. Does your company send a representative to the bridge jobsite to inspect the panels after erection for cracks and proper bearing?
   (5) Not our responsibility
   (12) Sometimes
   (5) Always
   (4) Never

Part VIII. Experiences uith Panel Usage

1. Which of the following items of panel damage has your company directly experienced more than just a few times or occasionally?
   (4) Can not really comment since we have not used panels often enough
   (6) Have not experienced any problems [Not major problems]
   (8) Broken corners
   (9) Spalled or chipped edges
   (9) Cracking parallel to strands along a significant portion of the panel length [caused by lifting devices]
   (10) Cracking parallel to strands near the ends of the panel only
   (2) Cracking transverse to the strands near panel midspan
   (3) Diagonal cracks across panel surface
   (1) Strand slippage
   (4) Skewed panels are difficult to detension properly
   (1) Other [Problems not recurrent but do exist]

2. Which of the following items of panel irregularities has your company directly experienced more than just a few times or occasionally?
   (4) Can not really comment since we have not used panels often enough
   (10) Have not experienced any problems [Not major problems]

(4) Difficulty in maintaining panel dimensions (thickness, width, and/or length)
(4) Difficulty in maintaining panel trueness (bow, horizontal alignment, and/or squareness)
(3) Difficulty in maintaining strand position (vertical, horizontal, and/or extensions)
(2) Difficulty in maintaining panel surface finish
(1) Strands from some suppliers had an oily or graphite feel or coating
(1) Other [Difficulty with light-weight concrete strengths]

3. Which of the following items related to the panel and cast-in-place top slab installation has your company experienced more than just a few times or occasionally?
(4) Can not really comment since we have not cast panels enough
(5) Have not experienced any problems
(9) Can not really comment since we are not involved in panel erection
(1) Non-uniform panel support surfaces
(3) Improper panel overlap on supports
(2) Difficulty in leveling the panels
(0) Difficulty in maintaining a constant grout bed elevation
(2) Construction loads placed on untopped panels
(1) Difficulty in sealing the panel joints
(0) Air bleed slots at panel bearing allows mortar to drip from the structure
(3) Skewed panels were difficult to set properly [No experience with skewed panels]
(1) Other [We usually don't erect]

4. Which of the following items related to the performance of the panel and cast topping slab bridge deck have your company directly experienced more than just a few times or occasionally?
(3) Can not really comment since we have not cast panels often enough
(10) Have not experienced any problems [Not major problems]
(3) Reflective cracks in the top of the cast-in-place slab above longitudinal panel joint
(3) Reflective cracks in the top of the cast-in-place slab above the transverse panel joints
(2) Cracks in the top of the cast-in-place slab that are not above the panel joint
(0) Cracks in the top of the cast-in-place slab at the abutment or pier diaphragms
(0) Cracks in the bottom of the panels parallel to the panel span
(0) Cracks in the bottom of the panels transverse to the panel span and near the midspan of the panel
(0) Strand slippage
(0) Some loss of composite behavior between panels and cast-in-place slab
(0) Apparent loss of panel bearing at some locations
(2) Other [See states, Cannot comment since panels have not been in service long]

5. Which of the following shipping, handling, or storage related items, which your company believes might have caused or could have caused panel cracks to develop, has your company directly experienced more than just a few times or occasionally?
(4) Cannot really comment since we have not cast panels often enough
(9) Have not experienced any problems [Not major problems]
(5) Improper strapping or chaining of panels to truck beds
(1) Overstacking panels on truck beds
(1) Panel stacked on the rear end of trailers on long hauls
(10) Incorrect panel storage at bridge sites
(4) Stacking panels too high in storage stacks
(5) Settlement of cribbing in storage stacks

(8) Improper dunnage alignment for storage stacks
(1) Outside storage of panels over winter
(2) Improper forklift handling of panels
(5) Lifting an entire stack of panels at bridge sites
(1) Other [All of the above occur if you don't watch out]

6. Which of the following casting techniques has your company established to minimize problems in panel fabrication?
(4) Cannot really comment since we have not cast panels often enough
(4) Provided strand tie downs along prestress bed length
(10) Clean out header strand slots after each casting
(19) Allow for concrete preset prior to heat application for accelerated curing
(11) Instituted special strand cutting sequence
(14) Provided steel headers
(2) Allow strands to oxidize by exposure to the weather for a few days
(2) Increased concrete release strength above minimum specified
(4) Increased concrete ultimate strength above minimum specified
(13) Provided a reinforcing bar transverse to strand at panel ends
(0) Apply compressed air when stripping panels
(2) Cast panels inside a structure to avoid exposure to weather
(1) Other [Proprietary casting/stripping and handling techniques]

7. How does your company classify any problems associated with panel usage for bridge deck construction?
(4) Can not really comment since we have not cast panels often enough
(2) Non-existent
(12) Minor
(4) Moderate
(0) Significant
(1) Major

8. Considering all aspects of manufacturing, transportation, erection, and performance of panels for bridge deck construction, how does company rate panel usage?
(1) Can not really comment since we have not cast panels often enough
(7) Excellent
(7) Very good
(5) Good
(3) Fair
(2) Poor

9. Please feel free to expand on the experiences that your company has had regarding any aspect of precast prestressed concrete panel subdeck manufacturing, transportation, storage, erection, casting of top slab, performance, maintenance or economy, which may not have been covered in the previous parts of this questionnaire. (Quotes are respondents' comments)

"_____ Dept. of Trans. has discontinued use of plank since 1986. Prestressed Producers of _____ have been trying to reinstitute their use. Contractors VERY favorable to plank because of speed, $, and SAFETY. Due to regretable quality problems by some producers, _____ has proposed unobtainable specs. if plank is to be used. Example: 1) 1/32 in. tolerance on strand placement, 2) beds leveled to 1/16 in. in 20 ft, 3) "0" tolerance on slippage. _____ has

refused to consider 3 in. thick plank due to curent design constraints."

"Our DOT people are completely unrealistic by assuming that any water mark is a structural crack. Their ignorance is the only impediment to panel usage."

"Not an important product for our firm."

"We are not involved with work at jobsite or the long term performance problems of deck panels in general. We know of no problems with performance of our panels. Configurations of panels and their design meets the written (text) requirements of the DOT's for each project. (No standardization). We have used several different configurations at abutments and diaphragms and always had them approved. The very existence of panels as a product indicates how many precast concrete producers there are that do not know how to make money in this industry. It also indicates how easy it is the sell agency bureaucrats a bill of goods. Deck panels are a drain on the resources of any otherwise successful precasting operation. The problem with panels that still has not been solved in one area is the lack of standardization of the panel as a product and the lack of completion of engineering of the application of the product to the project. Producers have sold a product and a concept to DOT's and the DOT's have left the execution and any field problems to their inspection personnel and the bridge general contractor and his field superintendent. Had the product gone through the testing, revision and standardization process of other precast bridges products we would not be in this "no-win" war."

"Specifying agencies require unrealistic details and reinforcement, and call for difficult and expensive bearing/seating details."

"Most precastors do not erect bridge plank or design the bridge."

"Problems with standardization from one job to the next. Design not done by DOT in house and no consistency between different consultants. No criteria for acceptance of panels with any cracks, no matter what length or width."

"We have produced panels for only one project in _____. It was a DOT experimental project. Reflective cracks have shown through the deck above the main bridge girders where the panels are supported. Steel shims were used for temporary support of panels, contrary to specifications."

"Our P/C panel compete with metal stay-in-place forms. We cannot compete with price of metal stay-in-place."

"The precast soffit for stay-in-place forming of concrete bridge deck has been discontinued by _____."